CONTAIN Code Qualification Report/User Guide for Auditing Design Basis PWR Calculations

Jack Tills[1], Allen Notafrancesco[2], and Ken Murata[3]

August 2002

Office of
Nuclear Regulatory Research

SAFETY MARGINS AND SYSTEMS ANALYSIS BRANCH

[1] Jack Tills & Associates, Inc.

[2] USNRC, Office of Nuclear Regulatory Research

[3] Sandia National Laboratories, Modeling and Analysis Department, Org. 6421

CONTAIN Code Qualification Report/User Guide for Auditing Design Basis PWR Calculations

Jack Tills[1], Allen Notafrancesco[2], and Ken Murata[3]

August 2002

[1] Jack Tills & Associates, Inc.

[2] USNRC, Office of Nuclear Regulatory Research

[3] Sandia National Laboratories, Modeling and Analysis Department, Org. 6421

Table of Contents

Table of Contents (continued)

List of Figures

List of Figures(continued)

List of Figures(continued)

List of Figures(continued)

List of Figures(continued)

List of Figures(continued)

List of Figures(continued)

List of Tables

List of Tables (continued)

List of Tables (continued)

1 Introduction

1.1 Background

Current U.S. Nuclear Regulatory Commission (NRC) policy provides guidance to nuclear reactor licensees about what types of calculations need to be performed, and what calculational methods can be used to demonstrate the adequacy of their containment systems designs. A number of computer codes were developed in the time period 1960-1980 that embodied the NRC guidelines for Design Basis Accidents (DBAs). These codes, such as CONTEMPT-LT/028 (NUREG/CR-0255) and COMPARE (LA-NUREG-6488-MS) have been the principal calculational tools used by the NRC in reviewing license applications related to containment systems. Because licensing of new plants came to a standstill after that period, these codes, as well as NRC guidelines, have not been modified or updated significantly since then.

In the meantime, however, the NRC's research program following the TMI-2 accident has produced an abundance of technical information and scientific understanding about reactor accidents, applicable both to severe accidents and DBAs. Computer simulation codes are an important product of this research program, and in the containment area, the CONTAIN code [1] has been developed by Sandia National Laboratories for the NRC for studying conditions inside the containment building during and after postulated reactor accidents. It incorporates the best current understanding of all relevant phenomena, and has the most extensive validation basis of any code in its class.

CONTAIN can be used to model all types of domestic containments:

- the various pressurized water reactor (PWR) containments, including large dry, ice condenser and sub-atmospheric designs;
- the standard boiling water reactor (BWR) pressure suppression systems, including Mark I, II, and III configurations;
- the annular region of dual containment systems; and,
- advanced reactor designs (CONTAIN was used in NRC's review of the AP600).

The purpose of this document is to provide guidance on the use of CONTAIN to model the various PWR containments for performing DBA audit calculations. Specifically, CONTAIN can be used for pressure and temperature analysis of short-term transients to evaluate a) conservative containment loads, i.e., predict peak containment temperatures and pressures and b) minimum back pressures for emergency safety cooling system (ECCS) limit conditions. Long-term transients can be analyzed to determine a) depressurization time, b) safety equipment environments and c) the performance of engineering safety features (sprays and fan coolers) and other pressure control systems like ice condensers.

Included in this report are targeted comparisons with sample plant analysis cases and other analysis procedures to demonstrate the adequacy of the CONTAIN code to achieve its intended objectives. This qualification component is to demonstrate and establish a degree of "equivalency" with the existing licensing framework, e.g., as specified in the NRC Standard Review Plan. Thus, the calculated results tend to be bounding in nature or biased in a conservative manner.

It should be noted that, to the extent practicable, CONTAIN is a comprehensive containment analysis code which has been developed using a physics-based modeling approach consistent within a lumped parameter framework. Accordingly, user-defined parameters play a lesser role than with the older codes. However, the code does permit the user to perform sensitivity studies of containment response predictions using appropriate input parameters.

The CONTAIN code has been extensively assessed against a broad range of experimental programs. Therefore, CONTAIN can be used to pursue "best estimate" containment response predictions. However, that aspect is beyond the scope of this report. A report entitled "User Guidance on the CONTAIN Code for Advanced Light Water Reactors," SAND96-0947, is a good illustration of a "best-estimate plus uncertainty" containment analysis applied to the AP600 design.

Besides the underlying regulatory related guidelines which dictate the licensing based assumptions, the CONTAIN 2.0 Code Manual (NUREG/CR-6533) is the key reference document that is used and extensively cited in this effort. Another document that provides additional insight to form the basis of selected recommended parameters is entitled, "An Assessment of CONTAIN 2.0: A Focus on Containment Thermal-Hydraulics (Including Hydrogen Distributions)."[1]

Chapters 2, 3, and 4 of this report will cover, respectively, the large dry, sub-atmospheric, and ice condenser PWR containments. And Chapter 5 will address aspects related to secondary containment functional analysis. Each chapter will review the relevant phenomenology for DBA analysis and provide guidance on using CONTAIN. This guidance is intended to show how to prepare input decks that will produce CONTAIN calculations with an equivalent degree of conservatism to traditional approaches to DBA audit calculations. However, the experienced analyst will notice some differences between the CONTAIN treatments and traditional approaches. These differences derive primarily from the more consistent and more complete treatment of the applicable physics in CONTAIN, e.g., in the determination of condensation heat transfer to containment walls.

The appendices of this report provide a basic supporting foundation for Chapters 2, 3, 4 and 5. The specific support provided by the appendices is as follows:

---

[1] This CONTAIN assessment report will be referred to in the following text with the short-hand notation, CAR.

- Detailed comparisons of the CONTAIN and traditional PWR analytical approaches are provided in Appendices A and B.

- Detailed input-deck examples of the applications of CONTAIN for short-term analysis of a large dry containment is provided in Appendix C.

- A detailed input-deck example of a long-term analysis for a sub-atmospheric containment is provided in Appendix D.

- Detailed input examples of the application of CONTAIN for ice condenser PWR short and long-term analyses are provided in Appendix E. This Appendix also includes a demonstration secondary containment analysis using a generic ice condenser design.

- Formulas for comparing heat transfer coefficients for codes CONTEMPT and CONTAIN are presented in Appendix F.

- Methods for determining rate dependent values for CONTAIN output using the post-processing code POSTCON are discussed in Appendix G.

- Finally, Appendix H presents detailed results of CONTAIN calculations for DBA type ice condenser tests performed by Westinghouse during the early and mid 1970's. However, this Appendix has been *removed* from this report because it contained vendor proprietary information.

CONTAIN can be used for all containment types and for several different scenarios (e.g., both short-term and long-term events), without the need to perform supplemental calculations that were found to be required in previous approaches. The result is a more consistent and defensible calculational method, with increased confidence in the results because of the thoroughness of the validation base of CONTAIN. On the other hand, this dependence on CONTAIN means that it is important that the analyst understand how the various elements of the input deck control the calculational assumptions. Thus one important purpose of the discussions in Chapters 2-5 is to provide clear and understandable instructions on how to use CONTAIN for conservative DBA analysis. It should be noted that broader studies involving "best-estimate plus uncertainty" approaches would require the analyst to depend much more heavily on the CONTAIN 2.0 Code Manual.

1.2 Key Results and Accident Phases

Generally, a containment functional design evaluation includes calculations of the key containment loads, i.e., pressure and temperature effects, associated with a postulated large rupture of the primary or secondary coolant system piping. The focus of this report is to provide adequate guidance in performing containment pressure and temperature transient response calculations in order to obtain limiting conditions for auditing the licensing basis of the various

PWR containment systems. Other key values obtained from these types of analysis are peak pressure differentials, such as occurring between the lower and upper compartments in an ice condenser plant.

The qualitative nature of event sequence progression in PWR large dry and sub-atmospheric DBAs is similar for each of the containment types. A number of short-term events may be partitioned into phases, dependent on the blowdown characteristics and the actuation of various engineering safety features (sprays and fan coolers). Shown in Table 1-1 is the sequence of events for two accident types in a large dry PWR. For loss-of-coolant accidents (LOCAs), a two-phase steam/water injection in the lower containment region rapidly pressurizes the containment within 20-30 seconds. Following this initial pressurization a less severe injection of nearly pure steam continues the pressurization event while the engineering safety features are activated. These safety features retard the rate of pressurization somewhat until the steam injection rate is reduced to a level where a short-term pressure maximum is reached, usually within five minutes. In the case of secondary coolant system ruptures, such as main steam line breaks (MSLBs), steam is injected into the containment in a continuous, but declining rates. As with the LOCAs, safety features are activated during the injection which typically last less than a minute. The containment phases for the short-term analyses may be divided into a rapid and slow pressurization phase. The maximum containment loads occur during the slow pressurization phase.

In addition to a licensing requirement to establish maximum containment loads, there are other limiting conditions that involve a) the calculation of time to depressurize, as in the case of sub-atmospheric containments or b) minimum back pressure calculations to assess the limiting condition for ECCS operation. In the case of a sub-atmospheric containment, the licensee must show that a sub-atmospheric condition is reached within one hour after the accident. A sequence of events for a sub-atmospheric containment analysis is described in Table 1-2. Minimum back pressure analysis is a special case of the LOCA scenario (presented in Table 1-1) where assumptions are made to maximize containment atmospheric energy removal (passive and active) in order to calculate the minimum containment pressure that could occur during core reflood.

For the PWR pressure-suppression containments, a LOCA sequence of events may be described as shown in Table 1-3. This table shows the accident phases for both the short and long-term scenarios. Each scenario is characterized by a period of rapid pressurization. In the short-term scenario the pressurization is due to the blowdown injection; whereas, in the long-term scenario the pressurization is the result of the loss of pressure control when ice melt-out occurs.

1.3 Key Phenomena

Listed in Table 1-4 are key phenomena to be modeled to predict pressure and temperature responses in PWR containments. The phenomena are differentiated according to the containment accident phase. Both short and long-term accident scenarios are considered, covering a broad range of accident types. Accident phases where key results are to be determined

have been noted. The selection of phenomena is based mainly on Phenomena Identification and Ranking Tables (PIRTs) developed for DBAs and presented in the CAR for large dry containments, and in Appendix H for ice condenser containments. Key phenomena include those phenomena ranked either medium to high, or high. For a complete description of phenomenon definitions and ranking the reader is referred to these two reference documents.

1.4 Code Qualification

This report addresses qualification of the CONTAIN code for DBA application in two ways: 1) by equivalency to traditional analysis and 2) by confirmed conservatism derived from validated code exercises. First, the code is shown to provide "equivalency" to traditional codes, such as CONTEMPT or to other vendor codes that have been reviewed by the NRC in previous licensing applications (Westinghouse's TMD and LOTIC code, for example) as documented in various Final Safety Analysis Reports (FSARs). Establishment of a criterion for "equivalency" is based on the agreement between CONTAIN and these traditional analyses where bottom-line comparisons are stressed, i.e., for pressures and temperatures. A quantitative measure of equivalency has been set for key result comparisons; an "equivalent band" for results is within +/- 5% variation, e.g., calculated differences in pressure gauge. This 5% value represents a relatively negligible deviation for calculated comparisons. For example, in the case of maximum pressure increases for a short-term LOCA analysis, where CONTEMPT calculations represent the traditional results, the equivalent band is shown in Figure 1-1. Therefore, when we say that the CONTAIN results are "equivalent" to some other code result, it means that the CONTAIN results are within 5% of those results. In the following chapters, such an equivalency in terms of key results is investigated, noting what types of input are required to obtain this equivalency.

In Chapter 2, large dry containment pressure and temperature results for the short-term scenarios are presented for a CONTAIN analysis, and compared to similar CONTEMPT calculations. Appendix A might be consulted for detailed model comparisons for these codes. Additionally, the appendix presents some relevant comparisons of each code to experimental data for both integral (CVTR non-spray and spray tests) and separate effects tests (JAERI spray tests and Phebus FPT0 steam condensation test). Chapter 3 presents a sub-atmospheric analysis for a long-term scenario where a return to sub-atmospheric pressure is calculated. For this example application, the CONTAIN code results are compared to results given in the North Anna FSAR. Chapter 4 addresses both short and long-term containment pressure response following a LOCA in the Watts Bar ice condenser plant. Comparisons for the accident scenarios are between CONTAIN and TMD codes (short-term), and CONTAIN and LOTIC codes (long-term). Additionally, for the ice condenser application Appendix B is included, giving ice condenser modeling comparisons for the CONTAIN, COMPARE, and TMD codes.

Secondly, the qualification process addresses whether key phenomena, listed in Table 1-4, are appropriately modeled in the CONTAIN code to provide reasonably conservative results, independent of any other code comparisons. To demonstrate this aspect of the qualification, CONTAIN comparisons to an experimental database are cited and discussed in each chapter for

key phenomena modeling. In this regard, extensive reference is made to CONTAIN code assessments documented in "An Assessment of CONTAIN 2.0: A Focus on Containment Thermal-Hydraulics (Including Hydrogen Distributions)," and for ice condenser plants, in Appendix H, "CONTAIN Code Validation for Ice Condenser Plants: Waltz Mill Full-Scale, Short and Long-term Tests."

1.5 Code Guidance

Each of the following chapters presents a demonstration calculation for a specific containment type and accident scenario(s). The preparation of the input decks is discussed in the chapters and the commented input listings are included as appendices. Recommendations are made in each chapter to guide the user in selecting parameters that enable "equivalency" and/or conservative predictions of key results. Furthermore, by using any of these modeling or parametric recommendations, user directed code sensitivities can be pursued in an efficient manner. [The discussion of the demonstration calculations (including some sensitivity results) is mainly for guidance in input preparation and are not intended to be used as an analysis of specific containment accident events.]

1.6 Limitations

Because this report relies heavily on comparisons with traditional methods of analyses, there are some inherent limitations that such an approach imposes on the scope of the CONTAIN analyses. The main limitations imposed concerns nodalization and the effects of atmospheric stratification on both pressure and temperature results. In traditional DBA licensing applications that involves maximum or minimum pressure analyses, single compartment analyses are performed. As a result, the geometric descriptions of most containments found in FSARs are for single compartment analyses. And results are presented using single compartment codes like CONTEMPT, used for large dry containment analysis. In the case of pressure suppression containments (BWR or PWR ice condensers), multiple node analyses are performed but the nodalization is quite coarse, where a single compartment represents an entire region (wetwell or drywell for a BWR; lower compartment, ice condenser, or upper compartment for a PWR ice condenser). In many cases, the single compartment analyses, where it is assumed that the containment is characterized by a uniformly mixed volume, has been shown to be conservative for maximum pressure estimates based on comparisons of multiple and single compartment CONTAIN analyses of various scaled and configured containment experiments. For LOCAs where the break location is at a low elevation and the containment is relatively open, the degree of stratification is minimal and a single compartment analysis is appropriate even for long-term scenarios, as in the case of sub-atmospheric containments. Additionally, most containments are designed with spray pressure suppression systems that create a high level of turbulence when activated shortly after a pipe rupture. These sprays systems induce mixing currents within large open regions of the containment so that an assumption of a uniform atmosphere in the containment is reasonably accurate. Yet, in some cases we can anticipate transitory degrees of stratification, as in the case of an elevated secondary system break. However, within the context

of DBAs, these stratifications are also rapidly diminished by spray induced turbulence. In this report we limit our discussion of secondary system breaks to short-term scenarios where we are interested in pressure maximums; in these cases we believe the single cell results are conservative, based on numerous assessment studies.

Comparisons for maximum temperature profiles must be understood to represent the average maximum temperature inside containment. During short-term applications we have noted in our comparison studies of containment experiments that short-term average maximums are typically good approximations to local maximum temperatures.

Therefore, single compartment analyses are appropriate for limiting studies during DBAs where global results such as pressure maximums or minimums are concerned. Such analyses are less appropriate when assessments of local temperatures are required: although in the short-term, average maximum temperature calculated with single cell models typically bound local maximums. For a more complete discussion of the types of analyses and validations performed for containments where nodalization is important, the reader is referred to References 2 and 3.

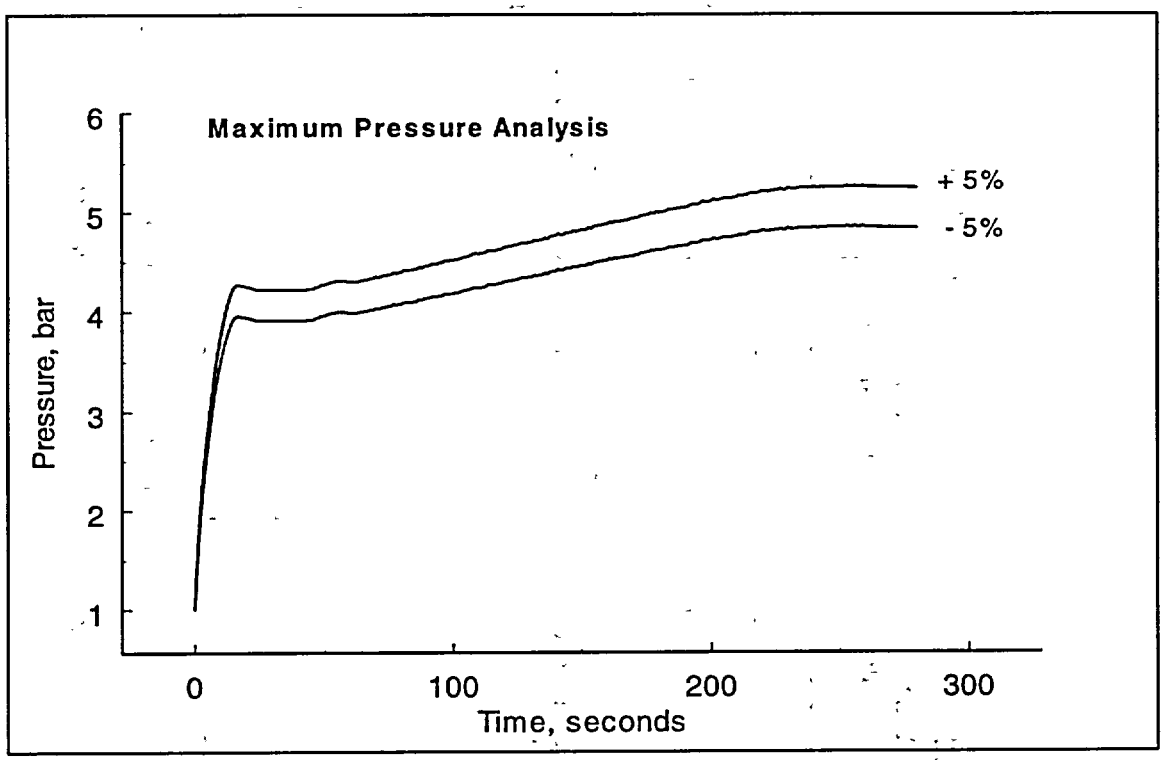

Figure 1-1 Equivalency band for the short-term maximum pressure analysis, based on CONTEMPT-LT/028 LOCA calculation for a large dry containment.

Table 1-1 Short-term accident phases for a large dry PWR containment					
Time period (approx.)	**Reactor Accident Phase**	**Containment Accident Phase**	**Source**	**Safety Features**	**Comment**
LOCA:					
0-25 sec.	RCS depressurization	Rapid pressurization	High pressure two-phase RCS water	None*	Flashing two-phase water expansion, emphasis on atmospheric thermodynamic processes
25-300 sec.	Core reflood/ post-reflood	Slow pressurization or depressurizatioin **	ECCS/RCS water and/or steam	Sprays and Fancoolers	Heat and mass transfers at spray drop and surface boundarys
MSLB:					
0-15 sec.	Secondary system depressurization	Rapid pressurization	High pressure steam	None	Single phase gas expansion, emphasis on atmospheric thermodynamic processes
15-60 sec.		Slow pressurization **		Sprays and Fancoolers	Heat and mass transfers at spray drop and surface boundarys

* Large variability in the safety feature initiation, but activation is usually begun after the RCS depressurization period.

** Maximum containment loads (pressure and temperature) or minimum back pressure occurs during this phase.

Table 1-2 Long-term accident phases for a sub-atmospheric PWR containment					
Time period (approx.)	**Reactor Accident Phase**	**Containment Accident Phase**	**Source**	**Safety Features**	**Comment**
LOCA:					
0-25 sec.	RCS depressurization	Rapid pressurization	High pressure two-phase RCS water	None	Flashing two-phase water expansion, emphasis on atmospheric thermodynamic processes
25-60 sec.	Core reflood / post-reflood	Slow pressurization or depressurization	ECCS/RCS water and/or steam		Heat and mass transfers surface boundarys
1 - 3 min.		Depressurization *		Quench sprays	Heat and mass transfer at spray drop and surface boundarys
3- 3600 min				Recirculation sprays	

* Period when sub-atmospheric pressure is re-established.

Table 1-3 Accident phases for a PWR ice condenser containments.					
Time period (approx.)	**Reactor Accident Phase**	**Containment Accident Phase**	**Source**	**Safety Features**	**Comment**
Short-term:					
0-3 sec.	RCS Depressurization	Rapid pressurization in lower compartment *	High pressure two-phase RCS water	Ice condenser	Flashing two-phase water expansion, emphasis on atmospheric thermodynamic processes and steam condensation
3-10 sec.		Upper compartment pressurization **			
Long-Term:					
30 - 600 sec.	Core reflood / post-reflood	Depressurization	ECCS/RCS water and/or steam	Ice condenser	Heat and mass transfer in condenser and on other containment surfaces
600 - 4000 sec.		Pressure control		Ice condenser and fans	Circulation of containment air/steam through ice condenser, condensation of steam in ice condenser
4000 - 4500 sec.		Rapid pressurization ***		Ice melt-out	Loss of pressure-suppression control
4500 sec. -		Slow depressurization		Sprays	Heat and mass transfer at spray drop and surface boundarys

* Maximum short-term pressure and pressure differential

** Maximum short-term upper compartment pressure

*** Maximum long-term containment pressure

Table 1-4 Key phenomena for determining pressure and temperature response in PWR containments		
Containment type	**Containment Accident Phase**	**Phenomena**
Large dry (short-term scenario)	Rapid pressurization	Multi-component gas compression; two-phase liquid expansion (LOCA), single-phase steam expansion (MSLB)
	Slow pressurization *	Free convective condensation on surfaces; structure heat conduction; spray droplet heat and mass transfer
Sub-atmospheric (long-term scenario)	Rapid pressurization	Multi-component gas compression; two-phase liquid expansion
	Slow pressurization	Free convective condensation on surfaces; structure heat conduction
	Depressurization *	Free convective condensation on surfaces; structure heat conduction; spray droplet heat and mass transfer; fancooler heat and mass transfer
Ice Condenser (short-term)	Rapid pressurization *	Multi-component gas compression; two-phase liquid expansion; entrainment/de-entrainment of blowdown water; liquid water carry over; forced convective condensation on ice film; ice film heat transfer
Ice Condenser (long-term)	Depressurization	Forced convective condensation on ice film; ice film heat transfer
	Pressure control	
	Rapid pressurization *	ice melt-out; multi-component gas compression; spray droplet heat and mass transfer
	Slow depressurization	free convective condensation on surfaces; spray droplet heat and mass transfer

* Accident phase where key results are determined

2 Large Dry Containment Analysis

In this section we discuss qualification and methods that can be used to model the DBA response of PWR large dry containments with CONTAIN [1]. Figure 2-1 depicts a typical large dry containment, showing the large and relatively open containment space within the reactor building. The open space above the operation deck, surrounding the steam generators, represents approximately 80% of the free volume within the building. Because of the relative openness of the containment design, DBA audit reviews have usually been performed using a single compartment model for the containment building. More detailed nodalizations of containments have been reserved for sub-compartment analyses, which are addressed in a separate report.

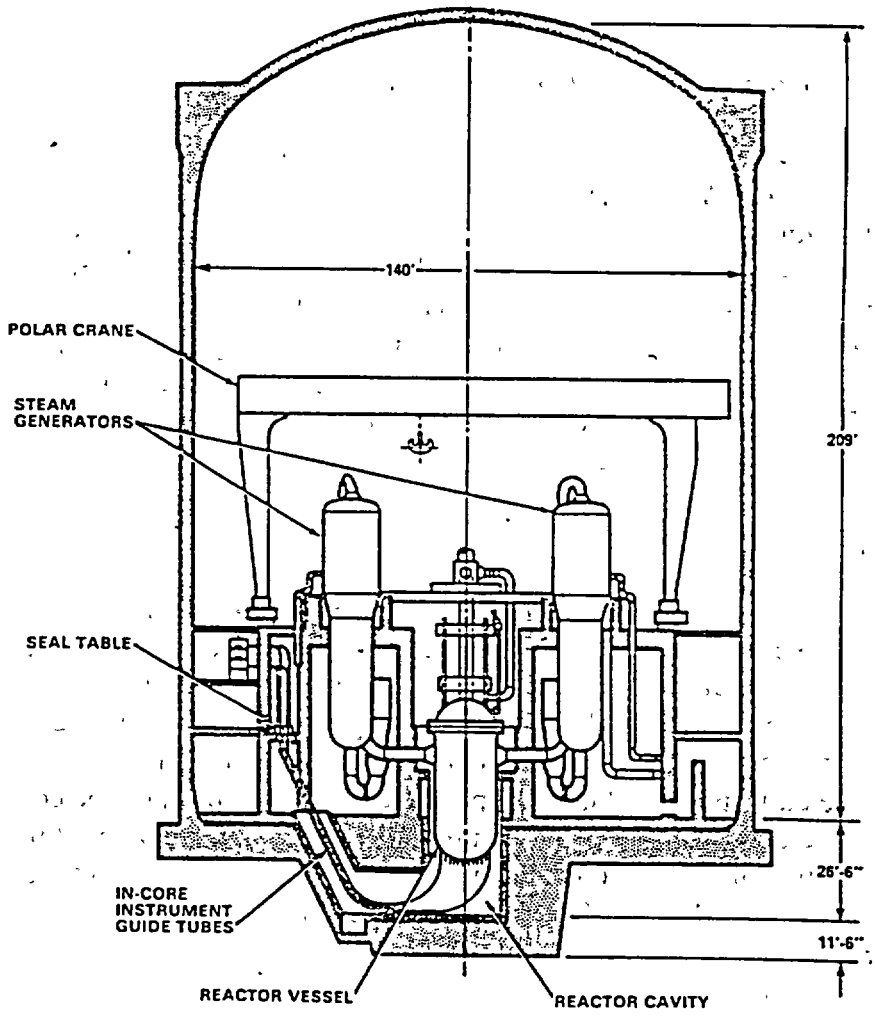

Figure 2-1 Typical large dry containment showing the openness of the large free volume above the lower compartments.

For the large dry containments, two types of short-term accident types are discussed and calculated in this section: (1) The LOCA scenario for demonstrating an evaluation of pressure and temperature during a two-phase water blowdown from the reactor primary cooling system, and (2) The MSLB scenario for demonstrating a similar evaluation for a single-phase water blowdown from the reactor secondary cooling system. These two types of accidents, discussed in Sections 2.1 and 2.2, include the actuation of engineering safety features, sprays and fan coolers, to mitigate the pressure and temperature increases during the slow pressurization phase of the accident. In the demonstration calculations for each accident type, the free volume and passive heat sinks are identical.[1] The analyses performed for these scenarios represent two types of assessments: (1) maximum containment loads analysis for each accident type; and, (2) a minimum back pressure analysis for a LOCA scenario. The discussion is structured according to the accident type.

2.1 LOCA Short-term Accident Analysis

In Section 2.1.1, we describe a LOCA short-term scenario, and in Section 2.1.2 we discuss the qualification of CONTAIN for predicting maximum containment loads, and in Section 2.1.3 we discuss qualification for performing minimum back pressure evaluations. Within the discussion section on maximum and minimum loads analysis, we present the recommended modeling and input preparations needed to ensure that CONTAIN will predict conservative results, and that predictions will be equivalent to traditional containment analyses using the NRC's containment analysis code, CONTEMPT. Detailed model comparisons between CONTAIN and CONTEMPT are given in Appendix A. CONTAIN and CONTEMPT inputs for demonstration calculations are listed in Appendix C.

2.1.1 LOCA Short-term Scenario

The LOCA scenario, summarized in Table 1-1, is initiated with a large break (typically, double-ended) rupture in either the cold or hot leg primary system coolant pipe attached to the reactor pressure vessel. A break in the primary coolant pipe is attended by a rapid depressurization of the reactor pressure vessel. The blowdown of the pressure vessel will release two-phase water at high pressure into the containment. High pressure liquid water will flash and subsequently condense in the atmosphere as liquid droplets that quickly deposit on the containment building floor. Hot, expanding steam will rapidly pressurize the containment building, and a portion of the hot steam will condense on colder containment structures. The rapid pressurization phase of the accident, which usually lasts 20-30 seconds, is responsible for most of the pressure and temperature rises that occur in the containment during a LOCA event. Because the process is so rapid, the pressurization is nearly adiabatic with the pressure and temperature increases limited through the accommodation of the blowdown steam in the large containment free volume.

---

[1] For demonstration purposes we used geometric modeling data based on the San Onofre large dry containment, as documented in a CONTEMPT input deck (see Appendix C).

Shortly after the rapid pressurization phase, a reflooding of the reactor vessel occurs as the emergency cooling system is activated. Accumulator water is injected and the coolant water is heated and steaming occurs: steam at a reduced rate (compared to the blowdown) is injected into the containment. The addition of the reflood steam source to the containment continues the pressurization process.

A signal to activate the engineering safety features, containment sprays and fan coolers, is initiated by the pressure increase in the containment. Times for initiation may range from a few seconds to tens of seconds. The safety features *actively* remove energy from the containment atmosphere by condensing out steam on spray droplets and on the condensing coils of the fan coolers. Additionally, during this extended slow pressurization period, large amounts of steam are condensing on relatively cold structures throughout the containment building. The removal of steam by condensation is a major contributing process, controlling the pressure and temperature maximums (or minimums in the case of a minimum pressure analysis) reached during the accident event. Shown in Table 1-4 are the key containment phenomena that occur in a LOCA type event. We focus our attention in these areas where modeling recommendations and input preparation guidelines are developed.

2.1.2 Maximum Containment Loads Analysis

2.1.2.1 Qualification

Shown in Figures 2-2 and 2-3 are the pressure and temperature responses calculated with CONTAIN and compared to results using the CONTEMPT code. Tabulated pressure and temperature maximums during the accident phases are given in Table 2-1. These results show that when the recommendations for short-term LOCA modeling and input preparation as discussed below are followed. The results will not only be consistent with traditional analysis methods, but even slightly more conservative with respect to a similar CONTEMPT code calculation, i.e., near the upper equivalency band. The sensitivity calculations shown in Figures 2-4 and 2-5 demonstrate that the key phenomena associated with a maximum pressure and temperature analysis is, for the slow pressurization phase, heat and mass transfer to passive heat sinks and the spray system pressure and temperature suppression. Qualification of the CONTAIN code, specifically for these phenomena are listed in Table 2-2, which gives a summary of key points concerning the qualification of CONTAIN for maximum containment load analyses.

Equivalency with respect to heat transfer during the rapid pressurization phase is an area that needs further discussion. In traditional containment analysis methods [4-7], it is common to specify an empirical correlation, i.e., the Tagami correlation to estimate steam condensation on structures during the rapid pressurization period when forced convective condensation is occurring. However, in a LOCA event, the rapid pressurization is of such short duration, forced convective condensation during this phase of the accident is relatively insignificant to a prediction of containment pressure and temperature shown in Figures 2-4 and 2-5. As noted in

Appendix A, the Tagami correlation is a non-scalable correlation, that must be regarded as a "best-estimate" model restricted to forced convective condensation in small-scale test facilities. Because the forced convective condensation phenomenon is relatively unimportant during the rapid pressurization phase, we qualified the CONTAIN code with a free convective condensation model.

We extend the use of free convective condensation modeling into the slow pressurization phase, realizing that this phase of an accident is characterized by natural circulation convection processes, and the free convective model is equivalent to the Uchida correlation used in the CONTEMPT calculation during this phase of the accident. Some added conservatism is interjected into the CONTAIN heat and mass transfer modeling, compared to the CONTEMPT model, by accounting for liquid film thermal resistance on the surface of passive heat sinks.

In the CONTAIN code, condensation phenomena, whether occurring on structure surfaces, spray droplet surfaces or fan cooler coils is determined using a heat and mass transfer analogy (HMT) methodology where steam diffuses through an air/steam boundary layer next to the condensing interface. This method for treating steam condensation in the presence of a noncondensible gas has been well documented and validated in the open literature [8, 9] and through CONTAIN code assessment [CAR], and other CONTAIN validations [10, 11]. For the prediction of short-term maximum pressure and temperature occurring during both the rapid and slow pressurization periods, the conservative nature of the calculation is assured though the use of a free convective algorithm that establishes the analogy between heat and mass transfer at a structure surface, and by assuming immediate and uniform mixing of steam and gases throughout the containment volume. With a single compartment model, the highest average air concentration and the largest resistance affecting steam transported to a liquid film interface is approximated. The conservatism of the CONTAIN code, as applied here for DBA type scenarios, has been verified through integral testing in the HDR and CVTR test facilities [CAR] where measured pressure and temperature during DBA two-phase injections have been compared to code results. The assessment of the HMT analogy method itself has been established in separate effects test analyses, and in large scale containment tests [CAR].

During the slow pressurization phase, in addition to the large removal of steam from condensation on structures, spray pressure suppression can also be important, as shown in Figures 2-4 and 2-5. In fact, one of main conservative aspects of the maximum containment loads analysis involves the assumption that only one train of spray systems is operable during the accident. For the spray processes, the CONTAIN code has been validated through separate effects (JAERI spray tests) and integral effects tests (CVTR spray tests) [CAR]. The test comparisons show that the code's spray modeling accurately predicts pressure suppression by spray sources in a containment atmosphere.

In the case of the fan coolers, which represent a less important phenomenon for maximum load analysis, there have been no validation tests of fan cooler modeling for pressure suppression. In this modeling area, it has been sufficient to indicate by model comparison that the CONTAIN fan

cooler model results are equivalent to the energy removal rates calculated by the CONTEMPT code.

All of the results shown in Figures 2-2 and 2-3 came from a single CONTAIN calculation. The input deck for this calculation is provided in Appendix C along with the set up inputs used for the CONTAIN fan cooler calibration (discussed in Section 2.1.2.3).

2.1.2.2 Modeling Recommendations for Maximum Containment Loads Analyses

As discussed in Chapter 1, there are only a few phenomena that affect key results for the large dry short-term scenarios. Shown in Table 2.3 are modeling recommendations for those phenomena, consistent with the code qualification criteria established here. In the following section on input preparation, these recommendations are discussed in terms of specific CONTAIN input.

We note that in the case of the fan cooler modeling, a user has the option in CONTAIN for choosing one of two models, the MARCH fan cooler or the mechanistic fan cooler model. We have chosen the mechanistic fan cooler option, because the model uses a method for treating energy and mass balances that is similar to the one implemented in the CONTEMPT model where condensed vapor mass is removed from the containment atmosphere. The MARCH fan cooler option on the other hand, while reproducing the energy removal rate with very good accuracy, does not remove condensed vapor mass from the atmosphere and therefore is not considered an equivalent model.

Phenomena that have a very small effect on pressure and temperature maximums are condensate film heat transfer and atmosphere to pool heat and mass transfer. For instance, a reduction of film thickness from the default (0.0005 meter) by a factor of 100 decreases the maximum over-pressure by less than ~ 1%, and the maximum temperature is decreased by less than ~ 1 degree. The presence or absence of atmosphere to pool heat and mass transfer has an even less effect on pressure and temperature. In modeling these phenomena, we chose to recommend the parameters affecting energy transfers that produce the more conservative pressure and temperature estimates, and these are reflected in the demonstration calculation.

In the case of spray modeling, we chose to use a spray droplet size that is consistent with measured distribution of droplets released from containment spray nozzles. Over-pressure maximums are relatively insensitive to spray droplet size; that is, a small increase in droplet size from 0.0005 meter in diameter to 0.0007 meter makes less than a 1% difference (increase) in the predicted over-pressure. Temperature maximums are slightly affected by small changes in spray modeling; for instance, an increase in spray droplet size, as noted, results in a ~ 3 degree increase in the maximum temperature. For consistency with the CONTEMPT spray modeling however, which assumes 100% spray efficiency, we chose the smaller spray droplet size (0.0005 meter) for the demonstration calculation that is still representative of a measured spray droplet distribution.

2.1.2.3 Input Preparation for Maximum Containment Loads Analyses

In this section we discuss the preparation of CONTAIN input for a large dry containment LOCA scenario for the demonstration plant.[2] Input preparation for this short-term scenario follows the general modeling recommendations discussed above to obtain a qualified CONTAIN calculation. These recommendations are linked to specific input parameters in Table 2-4. The LOCA demonstration problem in Appendix C may be consulted for detailed examples of implementation of the recommended modeling approach and input preparation. Some additional information regarding structural modeling and fan cooler input preparation are given below.

Structures. Shown in Table 2-5 are the structure data, and formatted in a form derived from the CONTEMPT input deck. The table shows the various thicknesses of the composite layers that comprise each structure type. Some structures are painted, and the thickness of the paint layer is also shown. Adapting this data to the CONTAIN structural input requires some pre-processing. First, paint thicknesses must be converted to paint resistance for input to CONTAIN using the "hpaint" parameter.[3] Secondly, the structure node thickness for the substrate material must be estimated for the structure nodalization scheme. We determine the node sizing for the structure by selecting a surface node thickness and adding additional nodes by following the general rule that adjacent nodes be kept to a thickness that is not more than a factor of two greater than the preceding node.

For determining the surface node thickness adjacent to the atmosphere we use a conservative criterion, where the surface node thickness is a fraction of the thermal diffusion length, δ. Table 2-6 lists some of the diffusion lengths for various time scales of interest. In the demonstration calculation we chose a time scale of interest of ~ 0.1 second, where the surface temperature changes by less than one degree. A reasonable surface node thicknesses for containment structures, based on this time scale of interest is:

- $\Delta x_s < 0.001$ meters, for steel;
- $\Delta x_s < 0.001$ meters, for stainless steel; and,
- $\Delta x_s < 0.0002$ meters, for concrete.

Since the coupling of structure heat conduction and atmospheric energy transfers to structures is explicit in the CONTAIN code, care must be taken to prevent surface node oscillations as a result of global time steps that are too large. For short-term calculations where the time steps are usually fractions of a second, temperature oscillations are generally not a concern, as shown in Table 2-7 .

---

[2] The specification for the demonstration plant is based on CONTEMPT input for San Onofre 2/3. Note that this plant was arbitrarily selected and is used for demonstration purposes only; actual plant related details may not be adequately reflected.

[3] hpaint = k/x, where k is thermal conductivity and x is paint thickness.

Fan cooler. Shown in Figure 2-6 are comparisons of the CONTEMPT fan cooler input specification compared to CONTAIN fan cooler energy removal rates based on the MARCH and mechanistic fan cooler modeling options used in CONTAIN. We have generated the CONTAIN curves using separate calculations for steady state fan cooler operation as a function of saturation temperature. These set up calculations are also listed in Appendix C. We note that the fan cooler temperature range during operation is between ~ 405 and 415 K. This range is best represented, in the case of the mechanistic fan cooler by the CONTAIN default fan cooler settings.

Table 2-1 Maximum pressure and temperatures for a short-term LOCA scenario in a large dry containment.

Accident Phase	Maximum Pressure, bar		Maximum Temperature, K	
	CONTEMPT	CONTAIN	CONTEMPT	CONTAIN
Rapid Pressurization	4.12	4.23	405	406
Slow Pressurization	5.07	5.17	415	417

Table 2-2 Summary of the CONTAIN qualification for short-term LOCA application					
Accident Phase	Modeling Area	CONTEMPT	CONTAIN	Comments	Reference
Rapid pressurization	geometric nodalization	Single cell	Single cell	For short-term pressurization phases, single cell nodalizations are shown to give conservative estimates of containment loads	[CAR*, p. 4-52, 4-80, 4-109]
	free volume	fixed free volume	free volume reduce by water pool volume	Displacement of free volume air by pool water is a physical reality. Including displacement represents a slight conservatism with respect to the CONTEMPT model.	N/A
	two-phase water injection	temperature flash modeling, with dropout of condensed liquid water	temperature flash modeling, with dropout of condensed liquid water	Thermal equilibrium, homogeneous mixing of injection mass with containment atmosphere is equivalent to the CONTEMPT temperature flash model. The thermal equilibrium assumption is conservative. Dropout of condensed water during a two-phase injection is conservative, based on integral test comparisons.	[CAR, p. 4-52, 4-53]
	heat and mass transfer to passive heat sinks	Tagami correlation	free convective condensation by HMT analogy	Tagami correlation is a non-scalable attempt to account for forced convective condensation during rapid steam injections. Free convective condensation by the HMT analogy has been shown to be a conservative method for estimating energy transfers during blowdown periods.	See Appendix A for discussion on Tagami correlation; conservatism of free convective condensation [CAR, p. 4-51, p. 4-73, p. 4-109]
	heat and mass transfer to pool surface	not modeled	not modeled	Excluding heat and mass transfer to the pool is an equivalent choice, and conservative	See Appendix A

* CAR is the CONTAIN Assessment Report which is a short-hand designation for a NRC informal report – "An Assessment of CONTAIN 2.0: A Focus on Containment Thermal Hydraulics (Including Hydrogen Distributions)," March 1999.

Table 2-2 Summary of the CONTAIN qualification for short-term LOCA application (continued)					
Accident Phase	Modeling Area	CONTEMPT	CONTAIN	Comments	Reference
Slow pressurization	heat and mass transfer to passive heat sinks	Uchida correlation	free convective condensation by HMT analogy	Both Uchida and the HMT analogy model are methods for treating free convective condensation. The two methods are nearly equivalent for single cell models.	See Appendix A
	heat and mass transfer to pool surface	not modeled	not modeled	Excluding heat and mass transfer to the pool is equivalent to the CONTEMPT model input and conservative.	
	spray pressure suppression	100% spray efficiency model	condensation on spray droplet using HMT analogy method	Both models give similar results as verified through separate effects test comparisons	
	fan cooler pressure suppression	tabular input: temperature verses total energy removed; condensed vapor removed from atmosphere	mechanistic fan cooler model using the HMT analogy method	Both models are equivalent (within 10%) in terms of total energy and vapor mass removal rates within the operating range of fan coolers during accidents	

Table 2.3 General modeling recommendations for a CONTAIN qualified short-term LOCA calculation in a large dry containment.	
Phenomena	**Modeling Recommendation**
Multi-component gas compression	Nodalize the containment as a single compartment
Two-phase liquid expansion	Use a temperature flash method for liquid expansion, dropout unflashed liquid from atmosphere
Convective condensation	Use a *free* convective heat transfer correlation for the HMT modeling
Structure heat transfer	Account for liquid film and paint resistance for surfaces; include any steel-liner-to-concrete air gaps at constant, full width
Spray droplet heat and mass transfer	Use a mass mean spray droplet size for the injected spray droplet diameter
Fan cooler heat and mass transfer	Use mechanistic fan cooler model, calibrated to the operation environment during accident

Table 2-4 Input guidance for modeling a short-term LOCA calculation in a large dry containment.		
Input Section/Block	**Parameter(s)**	**Comment**
Global:		
Nodalization	ncells = 1	Single cell nodalization for equivalency and conservatism
Material properties	user defined properties	density, thermal conductivity, and specific heat capacity for air, stainless steel, steel, and concrete are set for equivalency
Timesteps	~ 0.01 seconds	set to give accurate results for the time scale of interest (fractions of second)
Flow	DROPOUT	dropout condensed liquid water in atmosphere for equivalency and conservatism
Upper Cell:		
Geometry	gasvol	free volume equivalency
Atmosphere initial conditions and sources	ATMOS block; SOURCE block	pressure, and temperature equivalency (saturated conditions for conservatism); external source for temperature flash equivalency
ESF (sprays)	SPRAY block input	spray droplet diameter set to mass mean diameter of spray nozzle distribution, released at full height: spdiam = 0.0005 meters; sphite = 50 meters
ESF (fan coolers)	FANCOOL block input	Use keyword CONDENSE for mechanistic fan cooler model; set time to activate using SOURCE option with coolant mass = 123.1 kg/s and temperature = 300 K.
Structures	STRUC block input	fully implicit algorithm (default); free convection (default); maximum liquid film thickness (default); paint resistence set for equivalency; no thermal radiation; air gaps of constant thickness; initial condition for equivalency; surface node thickness as fraction of diffusion length (see text)
Lower Cell:		
Low-cell	HT-TRAN on on on off off	All condensed water dropped from atmosphere, spray removal, and condensate overflow from structures are diverted to pool (equivalency); pool-to-atmosphere heat and mass transfer set to ~ zero (equivalency); free volume displacement by pool water mass.

Table 2-5 Passive heat sinks used for the large dry PWR containment demonstration calculation (see CONTEMPT input deck, Appendix C).

Struc #	description	area, m2	material*	compound	rt. boundary, m	thickness,m	hpaint(W/m2-K)
1	dome&cylinder	7399.48	1	—	2 29e-04	2.29e-04	743.6
			2	fe2	6.58e-03	6.35e-03	
			5	air	7.11e-03	5.30e-04	
			3	conc2	1.60e-01	1.52e-01	
			3	conc2	1.29e+00	1.13e+00	
2	basmats	1341.88	1	—	2.38e-04	2.38e-04	715.0
			3	conc2	1.53e-01	1.52e-01	
			3	conc2	3.26e+00	3.13e+00	
3	rc wall below 15ft	147.71	1	—	5 85e-04	5.85e-04	290.5
			3	conc2	1.53e-01	1.52e-01	
			3	conc2	1.22e+00	1.07e+00	
4	misc rc walls	432.92	1	—	5.85e-04	5.85e-04	290 5
			3	conc2	1.53e-01	1.52e-01	
			3	conc2	1.22e+00	1.07e+00	
5	lined refueling canal	854.70	4	ss2	4.76e-03	4.76e-03	
			5	air	4.77e-03	1.07e-05	
			3	conc2	1.52e-01	1.48e-01	
6	interior conc.	3899.67	1	—	5.85e-04	5.85e-04	290 5
			3	conc2	1.53e-01	1.52e-01	
			3	conc2	5 24e-01	3.71e-01	

Table 2-5 Passive heat sinks used for the large dry PWR containment demonstration calculation. (cont.)

Struc #	description	area, m2	material*	compound	rt. boundary, m	thickness,m	hpaint(W/m2-K)
7	gfloor slabs	2159 05	1	—	4.27e-05	4.27e-05	3983 8
			2	fe2	1.63e-03	1.59e-03	
			5	air	2.16e-03	5.30e-04	
			3	conc2	1.55e-01	1.52e-01	
			3	conc2	4.59e-01	3 05e-01	
8	lifting devices	5322.00	1	—	3.81e-04	3.81e-04	446 2
			2	fe2	1.31e-02	1.27e-02	
9	misc. steel, t>2.5in	47.94	1	—	1.52e-04	1.52e-04	1115.5
			2	fe2	9.47e-02	9.46e-02	
10	misc. steel 1<t<2.5	809.92	1	—	1.92e-04	1.92e-04	885 3
			2	fe2	5 30e-02	5.29e-02	
11	misc steel 0.5<t<1	6010 13	1	—	2 05e-04	2.05e-04	827.5
			2	fe2	1.18e-02	1.16e-02	
12	misc. steel t<0 5	9189.24	1	—	1.85e-04	1.85e-04	920 4
			2	fe2	3.91e-03	3.73e-03	
13	electrical equip	3497.21	2	fe2	1.65e-03	1.65e-03	
14	misc. ss	2234.11	4	ss2	5.32e-03	5.32e-03	
15	wall stiffeners	147.81	1	—	2 29e-04	2.29e-04	743 6
			2	fe2	2.03e-01	2 03e-01	
			5	air	2 04e-01	5.30e-04	

* CONTEMPT material designation, material #1 represents paint

Table 2-6. Material diffusion lengths for various time constants.						
Material	time scale, Δt					
	0.001	0.01	0.1	1	10	100
paint	2.27e-05	7.18e-05	2.27e-04	7.18e-04	2.27e-03	7.18e-03
steel	2.19e-04	6.91e-04	2.19e-03	6.91e-03	2.19e-02	6.91e-02
stainless steel	1.38e-04	4.37e-04	1.38e-03	4.37e-03	1.38e-02	4.37e-02
concrete	5.25e-05	1.66e-04	5.25e-04	1.66e-03	5.25e-03	1.66e-02

Table 2-7. Maximum cell time-step to prevent surface temperature oscillations.				
Material	Compound	$\Delta t_{oscillation}$		
		h=1500 W/m^2-K	h=800	h=400
paint	---	0.10	0.36	1.45
steel	fe2	69.64	244.81	979.26
stainless steel	ss2	27.85	97.92	391.69
concrete	conc2	1.24	4.35	17.41

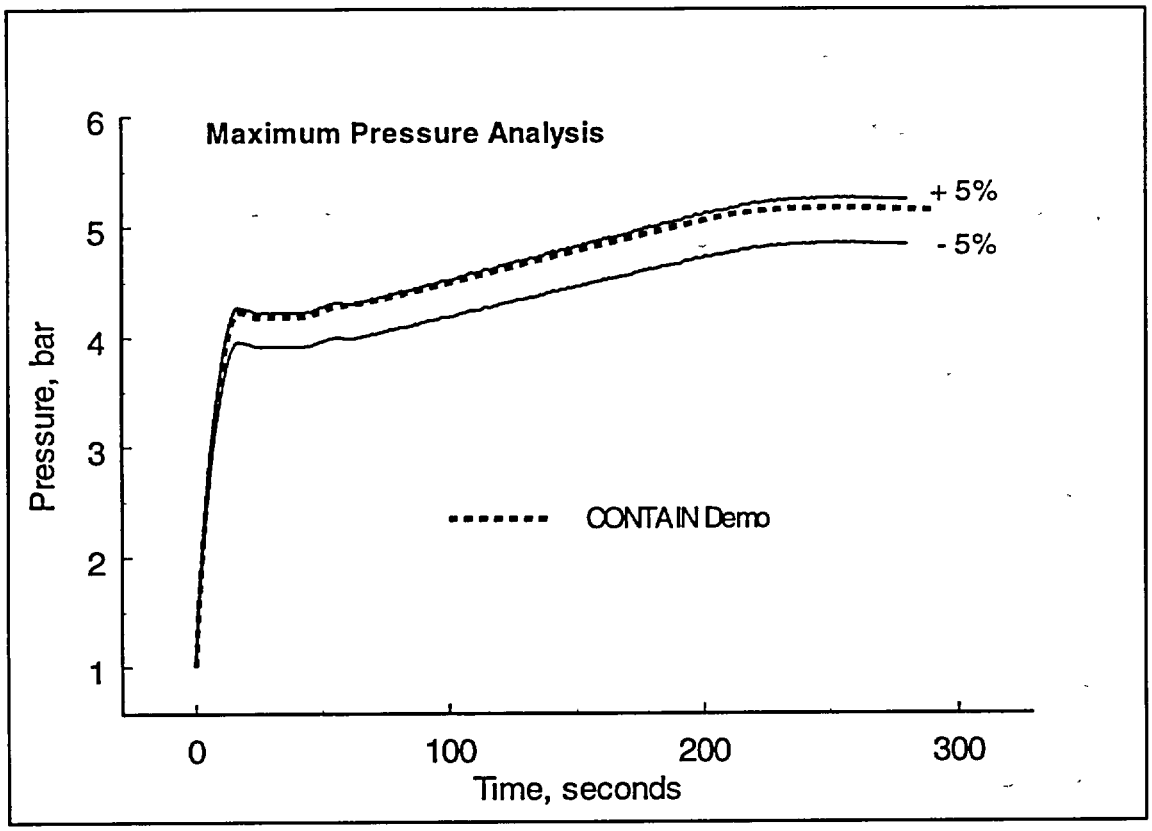

Figure 2-2 CONTAIN pressure calculation for a demonstration of a maximum pressure analysis for a short-term LOCA scenario in a large dry containment. Equivalency bands of +/- 5% are based on a CONTEMPT demonstration calculation.

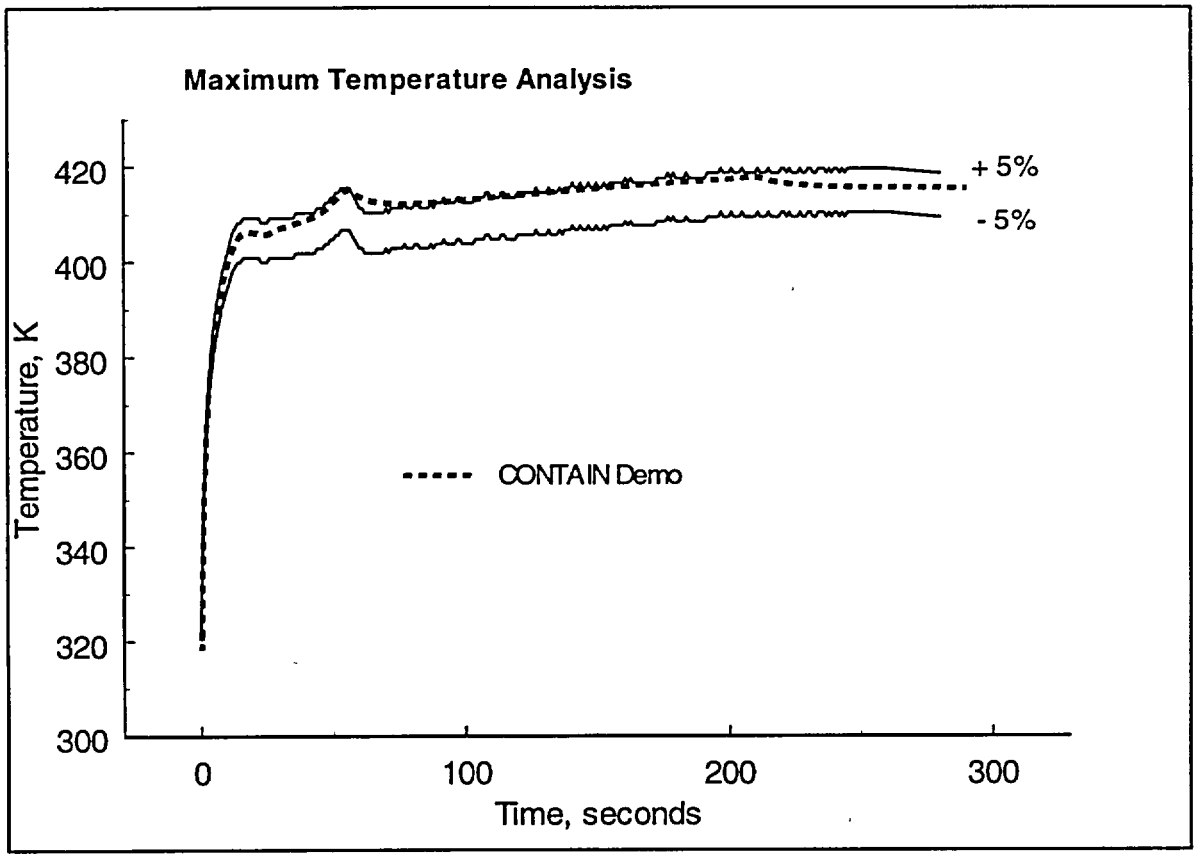

Figure 2-3 CONTAIN atmospheric temperature calculation for a demonstration of a maximum temperature analysis for a short-term LOCA scenario in a large dry containment. Equivalency bands of +/- 5% are based on a CONTEMPT demonstration calculation.

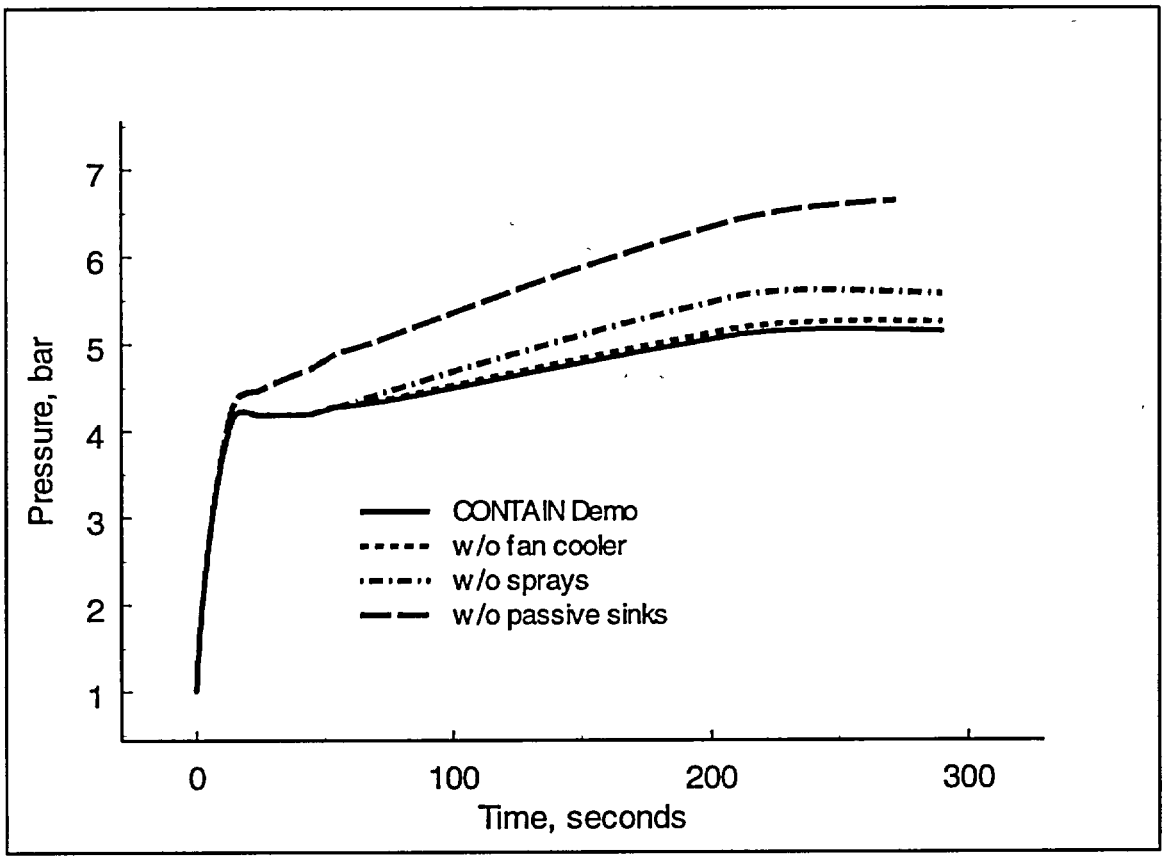

Figure 2-4 CONTAIN sensitivity calculations for the maximum pressure during a short-term LOCA scenario in a large dry containment.

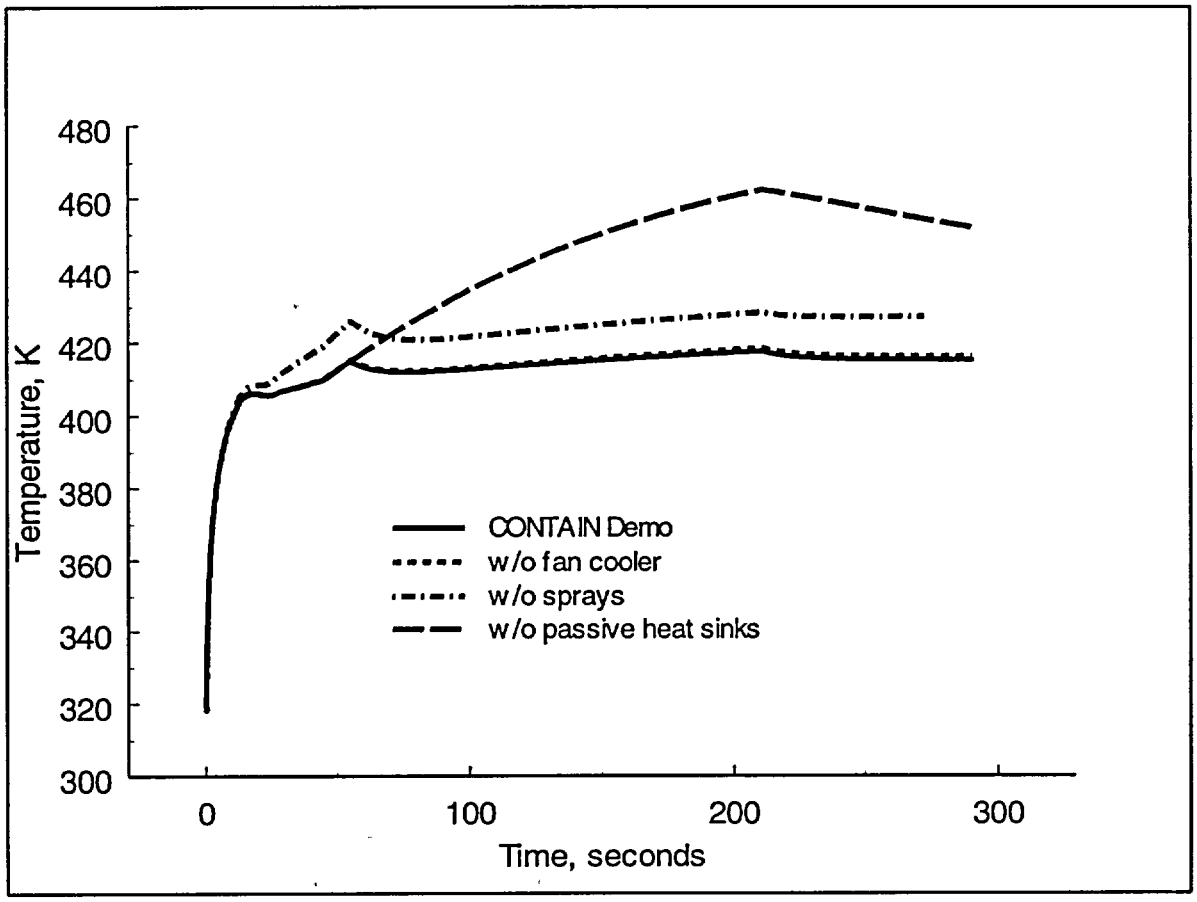

Figure 2-5 CONTAIN sensitivity calculations for the maximum atmospheric temperature during a short-term LOCA scenario in a large dry containment.

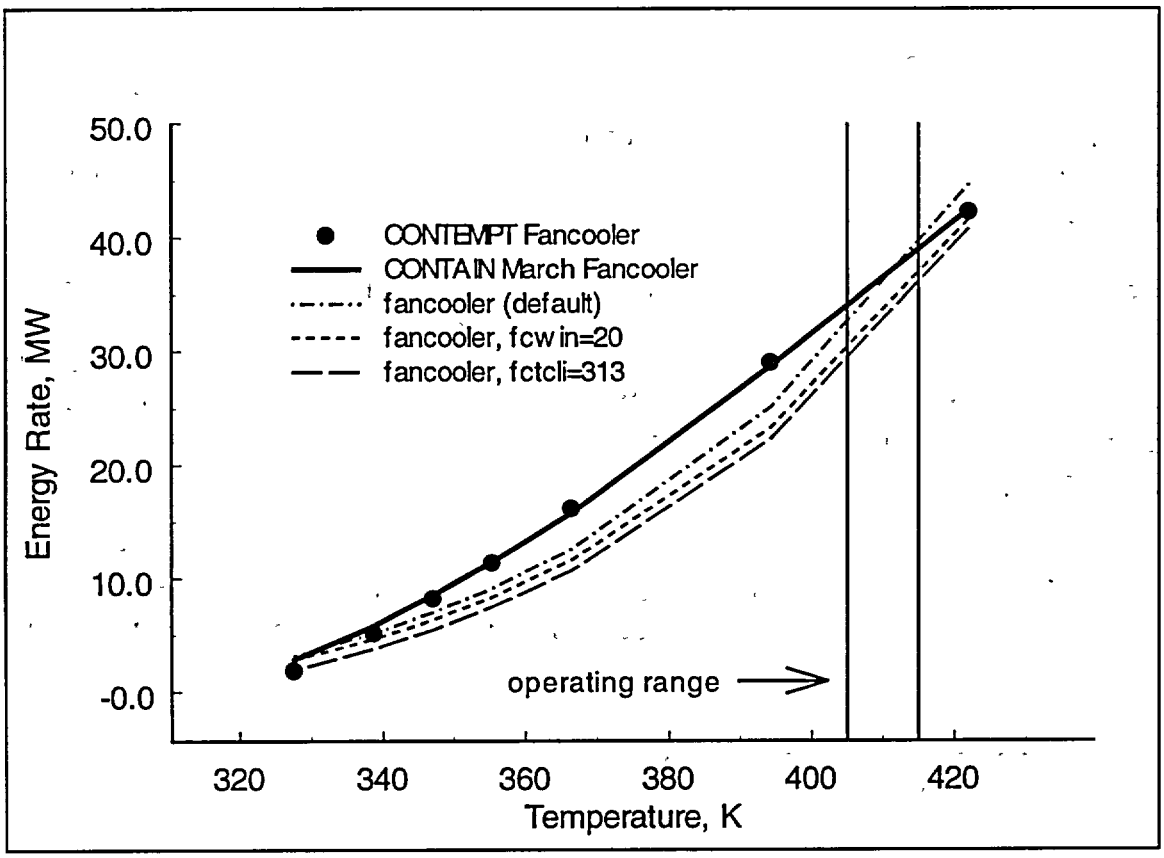

Figure 2-6 Calibration of the CONTAIN MARCH and mechanistic fan cooler models to the CONTEMPT fan cooler performance data. Parameters fcwin and fctcli relate to the volumetric air/steam flow through the cooler and the coolant water inlet temperature, respectively. The MARCH fan cooler input parameters are given in the input set up for the CONTAIN fan cooler calibration decks, listed in Appendix C.

2.1.3 Minimum Containment Pressure Analysis

Following a LOCA in a PWR plant, the emergency core cooling system (ECCS) will supply water to the reactor vessel to reflood the vessel and cool the reactor core. For PWR plants, reflooding is dependent on the containment pressure. Core reflood increases as the containment pressure increases. Therefore, a minimum containment pressure analysis is warranted in order to assess the minimum ECCS performance for reactor core cooling.

Performing the minimum containment pressure analysis is a direct counterpart to the maximum containment loads analysis discussed in the previous sub-section. In this case, however, assumptions are made that would result in a minimum pressure prediction. A number of these assumptions are discussed in the SRP for "Minimum Containment Pressure Analysis for Emergency Core Cooling System Performance Capability Studies."[4] The assumptions of significant importance are:

1) Initial conditions for pressure, temperature, and humidity are selected to provide minimum pressure under operating conditions; additionally, initial temperatures of passive heat sinks are assumed to be at the low point of the range for containment temperatures.

2) All engineered safety features (sprays and fan coolers) are assumed to be in operation, and functioning at maximum allowed capacity.

3) Heat and mass transfers to passive heat sinks are maximized to account for forced convection during the rapid pressurization phase of the short-term scenario.

The first two requirements are readily met through simple modifications to a code's input for initial conditions and operation parameters for the engineered safety features. The last requirement however needs further discussion.

For the rapid and slow pressurization/depressurization phase in a containment accident, traditional minimum pressure analysis recommends that:

1) during the vessel depressurization phase, i.e., blowdown period, we should assume a linear increase in the condensing transfer coefficient from $h_{cond} = 45$ Watts/m^2-K to a peak value four times the Tagami correlation at the end of the reactor depressurization period;

2) during the slow pressurization/depressurization phase in a containment accident, characterized by low turbulence in the containment atmosphere, we should assume a condensing transfer coefficient that is 20% greater than what would be predicted using the Uchida heat transfer coefficient data; and,

---

[4] Standard Review Plan, NUREG-0800, Rev. 2 , July 1981 – Branch Technical Position CSB 6-1, "Minimum Containment Pressure Model for PWR ECCS Performance Evaluation."

3) during the transition phase between the end of the vessel depressurization phase and reflood and long-term post-blowdown period, a reasonably conservative exponential transition in the condensing transfer coefficient should be assumed.

Another assumption often used for minimum pressure analysis involves the elimination of any resistance to energy transfer between adjoining materials in passive heat sinks, i.e., no air gaps or interface resistance should be modeled.

In the following sub-sections, we have adopted the intent of these assumptions into a CONTAIN calculation for minimum pressure analysis, and show that the CONTAIN results are equivalent to traditional methods by comparing to CONTEMPT code results.

2.1.3.1 Qualification

Shown in Figure 2-7 is the CONTAIN results for a minimum containment pressure prediction in relation to an equivalency band calculated with the CONTEMPT code. The CONTEMPT calculation demonstrates the effect of the key assumptions recommended above for minimum pressure analysis.

We note that the validation of CONTAIN for performing minimum pressure analysis rests mainly on the realization that the conservative assumptions regarding ESFs can be incorporated into the calculation through appropriate input, i.e., through spray and fan cooler input parameters that allow these components to operate a maximum capacity. The most important ESF component for this analysis is the containment spray system, as shown in Figure 2-8. In the case of the spray system, we have validated spray modeling in both separate effects and integral test studies. In Appendix A, we have compared CONTAIN and CONTEMPT spray pressure suppression calculations with data. In those comparisons, we have concluded that while the CONTAIN results are in very good agreement with measured pressure responses, the CONTEMPT model tends to reduce pressure more rapidly than the data indicates. However, our interest in the conservative modeling of sprays, as noted in the SRP, is in relation to assumptions regarding maximum allowed capacity, as opposed to conservative modeling of spray phenomena. Therefore, a validated model for spray pressure suppression is acceptable for minimum pressure analyses.

The relative importance of heat transfer to passive heat sinks is also shown in Figure 2-8. We used the forced convective modeling in CONTAIN to bound the heat transfer coefficient as implemented in CONTEMPT for our qualification analysis. For the CONTAIN demonstration calculation, we assumed a forced velocity profile as shown in Figure 2-9 for each heat sink. The bounding aspect of this calculation is indicated in a comparison plot of coefficients, Figure 2-10, where CONTAIN coefficients are compared with the coefficients calculated in CONTEMPT using the Tagami correlation with a multiple factor of four, as suggested in the SRP for minimum pressure analyses. To present a common basis for comparisons, we have derived for each code the heat transfer coefficients from a total energy transfer equation,

$$h = \frac{Q}{A\left(T_{gas} - T_s\right)}, \qquad 2\text{-}1$$

where Q is the total energy transfer to a structure surface having an area A, T_{gas} is the atmosphere gas temperature, and T_s is the surface temperature as would be measured experimentally.[5] In the heat transfer coefficient plot, the depression of the CONTEMPT coefficients (based on a 4 X Tagami correlation) is an outcome of the high degree of superheating that occurs for this calculation during the early rapid pressurization, Figure 2-11, and the method by which condensation heat transfer is modeled in CONTEMPT under superheated conditions, i.e., when $T_{gas} > T_{sat}, T_{gas} \rightarrow T_{sat}$, where T_{sat} is the saturation temperature of the atmosphere. Figure 2-10 shows that the CONTAIN coefficients provide a substantial margin of conservatism compared to the CONTEMPT coefficients during the rapid pressurization phase of the containment accident. However, from the pressure plot, we see that this degree of conservatism translates into a very small pressure effect. In fact, even if a free convective correlation is used in CONTAIN (neglecting the forced convective effects during the rapid pressurization phase), the increase in pressure is well within the equivalency band established for this scenario type, as shown in Figure 2-12.

Because the injection process is of key importance to the estimation of peak pressure at the end of the RCS depressurization phase, the minimum pressure analysis implicitly includes assumptions regarding the injection source and method of modeling the partitioning of that source injection.[6] Shown in Figure 2-13 is the injection source used for the minimum pressure LOCA analysis. This source differs from the previous injection source used in the maximum containment load analysis mainly in that the reflood water source is a lower quality two-phase fluid, which is conservative for the minimum pressure analysis during the reflood phase. What is important to a conservative estimate for minimum pressure analysis is therefore the method used to model low quality injections during both the rapid and slow depressurization accident phases.

Shown in Figure 2-14 are the pressurization profiles for two common treatments of two-phase injections into containments. These treatments, referred to as temperature and pressure flash, are discussed in Appendix A in some detail. We simply note here that the pressure flash model which expands a two-phase fluid to a constant containment pressure, putting unflashed liquid into the containment sump directly, is the most conservative modeling option for a minimum pressure analysis. The pressure prediction in Figure 2-7 for CONTAIN includes the CONTEMPT equivalency band that has been determined using a pressure flash model.

---

[5] T_s is the temperature at the surface of the painted substrate. It is not the temperature of the paint surface.

[6] See Appendix K of the CONTEMPT-LT/028 code manual [6].

Presented in Table 2-8 is a summary of some of the main items that address how the CONTAIN code is qualified for minimum pressure analysis application.

2.1.3.2 Modeling Recommendations for Minimum Pressure Analysis

Shown in Table 2-9 are the modeling recommendations for performing minimum pressure analyses.

2.1.3.3 Input Preparation for Minimum Pressure Analysis

Table 2-10 gives a summary of the input preparation for a minimum pressure analysis. We inject the two-phase steam into the containment using the SRVSOR input block to implement a pressure flash expansion method. Input preparation for the ESFs is according to what input reproduces spray and fan cooler maximum cooling capacity. The passive heat transfer input is prepared to meet or exceed the conservatism represented by the recommendations (short and long term) for heat transfer coefficients described in the SRP for minimum pressure analysis. Some guidance regarding ESF and passive heat sink input are discussed below.

ESF. In the case of the spray system, the maximum capacity is specified through the maximum spray water injection rate with the lowest spray water temperature allowed by design specification. For the fan coolers, the user must adjust the mechanistic fan cooler effective area across one row of tubes, fcefar, to provide a reasonable match to the maximum capacity cooling rate. Some iteration may be required to meet these specifications. We have noted that the fan cooler capacity during the short-term scenario is relatively constant at ~ 250 MW removed by vapor condensation. In the CONTAIN plot file, we output the fan cooler capacity as "qfan" using the POSTCON input:

```
...
340 && timestep
type=stepsize vector=dt endcurve
...
810
engname=fan type=envmssor vector=fenv endcurve
...
mix
vector qfan = fenv/dt
```

We adjust the "fcefar" parameter to converge on the maximum cooling capacity specification, noting that the containment temperature range during fan cooler operation is approximately 10 to 15 degrees. The fan cooler capacity is set to agree with the cooler specifications within this range.

Passive Heat Transfer. In the demonstration calculation, we assumed a forced velocity profile to bound the heat transfer coefficients calculated with the CONTEMPT code, by applying the following methods:

1) During the rapid pressurization phase, we apply a forced convective profile as shown in Figure 2-9. Depending on the time to depressurize the reactor vessel, the length of the velocity plateau will be extended or shorten, accordingly. We use a maximum velocity of 5 m/s.

2) During the slow pressurization/depressurization phase, we allow the forced convective velocity to go to zero (over a 5 second period) so that free convective condensation dominates the late time passive heat removal process. A heat and mass transfer coefficient multiplier of 1.2 is applied using the "hmxmul" input parameter to satisfy the SRP recommendation for an increased natural convection condensation of 20% for periods after the rapid pressurization phase.

Alternatively, we may select a forced velocity profile that simply bounds a multiple of the Tagami coefficient during the rapid pressurization phase, as suggested in the SRP. In this case, we apply a forced convective profile as shown in Figure 2-15, where the ramp up occurs during the rapid pressurization phase, and the ramp down is over a 5 second span following this phase. Depending on the time to depressurize the reactor vessel, the length of the ramp up period will be extended or shorten, accordingly. We use a maximum velocity of 15 m/s and check that the calculated coefficients bound, for example, four times the Tagami coefficient (assumed saturation conditions). Shown in Figure 2-16 are comparisons of heat transfer coefficients for the demonstration case with a 5 m/s plateau profile and the ramp profile along with the recommended four times the Tagami coefficient, corrected for a paint layering. (See Appendix F for the formulas that convert empirical correlations to coefficients defined on the basis of Eq. 2-1.) The CONTAIN pressure profile using this alternative guideline for structure heat and mass transfer input preparation is plotted in Figure 2-17. We note that the CONTAIN results using the ramped velocity profile, as with simpler velocity plateau, remains within the equivalency band based on the CONTEMPT demonstration calculation.

Table 2-8 Summary of the CONTAIN qualification for short-term LOCA application for minimum pressure analysis.					
Accident Phase	Modeling Area	CONTEMPT	CONTAIN	Comments	Reference
Rapid pressurization	geometric nodalization	single cell	single cell	equivalent to other traditional analyses.	N/A
	free volume	fixed free volume	free volume reduced by water pool volume	displacement of free volume air by pool is reality.	N/A
	two-phase water injection	pressure flash modeling	pressure flash modeling	conservative model for two-phase water injections	[Appendix K of CONTEMPT/LT Manual, Ref. 6]
	heat and mass transfer to passive heat sinks	4 X Tagami correlation for rapid pressurization phase	forced convective condensation by HMT analogy during rapid pressurization phase	CONTAIN forced convective model used to bound 4 X Tagami correlation	See Appendix A for discussion on Tagami correlation; conservatism of free convective condensation [CAR, p. 4-51, p. 4-73, p. 4-109]
	heat and mass transfer to pool surface	not modeled	not modeled	Not modeling heat and mass transfer to pool is equivalent and conservative	See Appendix A

* CAR is the CONTAIN Assessment Report which is a short-hand designation for a NRC informal report – "An Assessment of CONTAIN 2.0: A Focus on Containment Thermal Hydraulics (Including Hydrogen Distributions)," March 1999.

Table 2-8 Summary of the CONTAIN qualification for short-term LOCA application for minimum pressure analysis (continued)

Accident Phase	Modeling Area	CONTEMPT	CONTAIN	Comments	Reference
Slow pressurization	heat and mass transfer to passive heat sinks	Uchida correlation	free convective condensation by HMT analogy	Both Uchida and the HMT analogy modeling method for treating free convective condensation. The two methods are nearly equivalent for single cell models.	See Appendix A
	heat and mass transfer to pool surface	not modeled	not modeled	Not modeling heat and mass transfer to pool is equivalent to CONTEMPT input	
	spray pressure suppression	100% spray efficiency model	condensation on spray droplet using HMT analogy method	Both models give similar trends as verified through separate effects test comparisons, however, the CONTEMPT results tend to show a greater pressure suppression effect than measured	
	fan cooler pressure suppression	tabular input: temperature verses total energy removed; condensed vapor removed from atmosphere	mechanistic fan cooler model using the HMT analogy method	Both models are shown to be near equivalent (within 10%) in terms of total energy and vapor mass removal rates within the operating range of fan coolers during accidents	

Table 2.9 General modeling recommendations for a qualified CONTAIN short-term LOCA calculation used for minimum pressure analysis.	
Phenomena	**Modeling Recommendation**
Multi-component gas compression	Nodalize the containment as a single compartment
Two-phase liquid expansion	Use a pressure flash method for liquid expansion, dropout unflashed liquid from atmosphere
Convective condensation	Use a *forced* convective heat transfer correlation for the HMT modeling during the rapid pressurization phase, free convective modeling during the slow pressurization phase
Structure heat transfer	Minimize liquid film thickness on structure; eliminate air gaps between liner and concrete walls; assume all walls are available for atmosphere-to-structure heat transfer
Spray droplet heat and mass transfer	Use a spray droplet diameter that is less than the spray mass mean diameter, 0.0001 m
Fan cooler heat and mass transfer	Use mechanistic fan cooler model

Table 2-10 Input guidance for modeling a short-term LOCA calculation in a large dry containment for minimum pressure analysis.		
Input Section/Block	**Parameter(s)**	**Comment**
Global:		
Nodalization	ncells = 1	single cell nodalization for equivalency
Material properties	user defined properties	density, thermal conductivity, and specific heat capacity for air, stainless steel, steel, and concrete are set for equivalency
Timesteps	~ 0.01 seconds	set to give accurate results for the time scale of interest (fractions of second)
Flow	dropout option	dropout condensed liquid water in atmosphere for equivalency
Upper Cell:		
Geometry	gasvol	free volume equivalency
Atmosphere initial conditions and sources	ATMOS block; SRV block	pressure and temperature, and humidity equivalency; pressure flash modeling using SRV source input block
ESF (sprays)	SPRAY block input	spray droplet diameter set to maximize spray-atmosphere heat and mass transfer, released at full height: spdiam = 0.0001 meters; sphite = 50 meters
ESF (fan coolers)	FANCOOL block input	Use keyword CONDENSE for mechanistic fan cooler model; set time to activate using SOURCE option with coolant mass = 380 kg/s and temperature = 283 K; fcepar to set for equivalent fan cooler vapor energy extraction.
Structures	STRUC block input	fully implicit algorithm (default); forced convection during rapid pressurization phase using ramp velocity, relax to free convection within 5 seconds; hmxmul=1.2; minimum liquid film thickness (0.000005m); paint resistance set for equivalency; no thermal radiation; no air gaps; initial condition for equivalency; surface node thickness as fraction of diffusion length; characteristic length of structures set to 1 m.
Lower Cell:		
Low-cell	HT-TRAN on on on off off	All condensed water dropped from atmosphere, spray removal, and condensate overflow from structures are diverted to pool; pool-to-atmosphere heat and mass transfer set to ~ none (equivalency); free volume displacement by pool water.

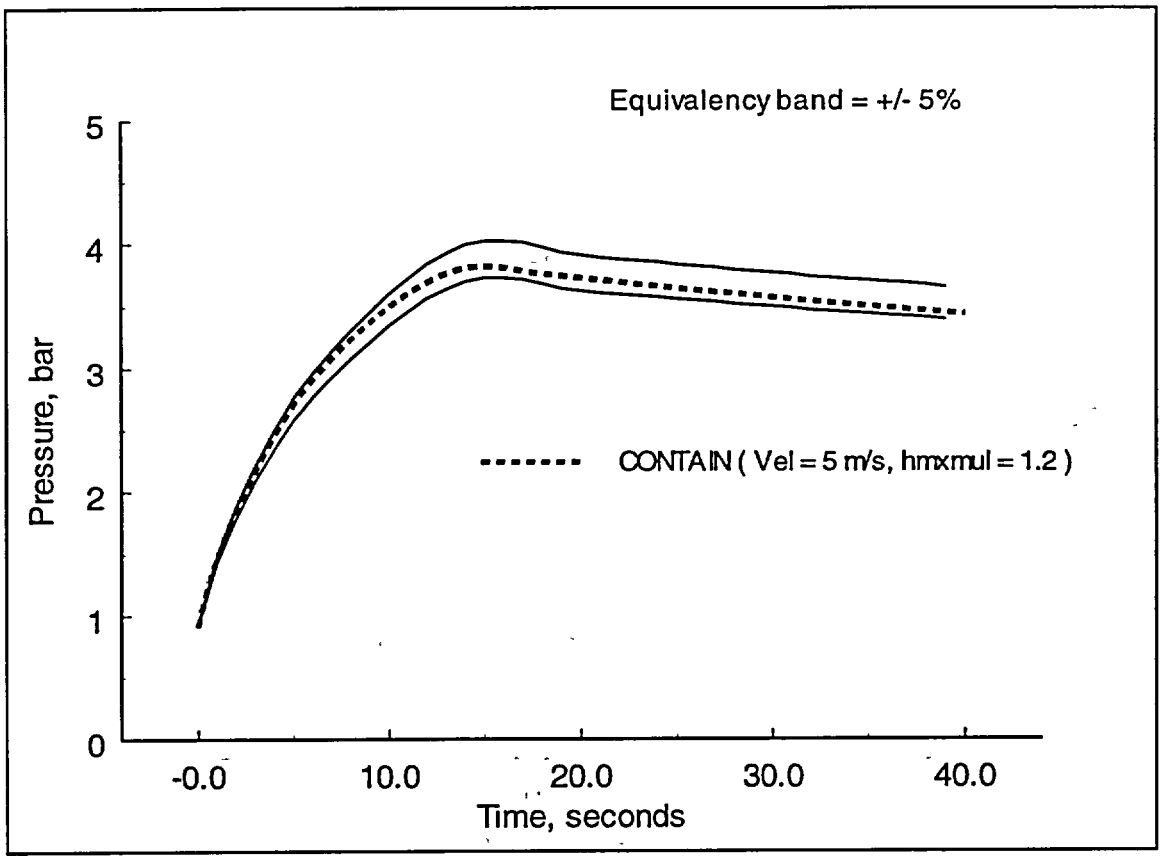

Figure 2-7 CONTAIN pressure prediction for a minimum pressure analysis, showing the equivalency with a CONTEMPT code calculation.

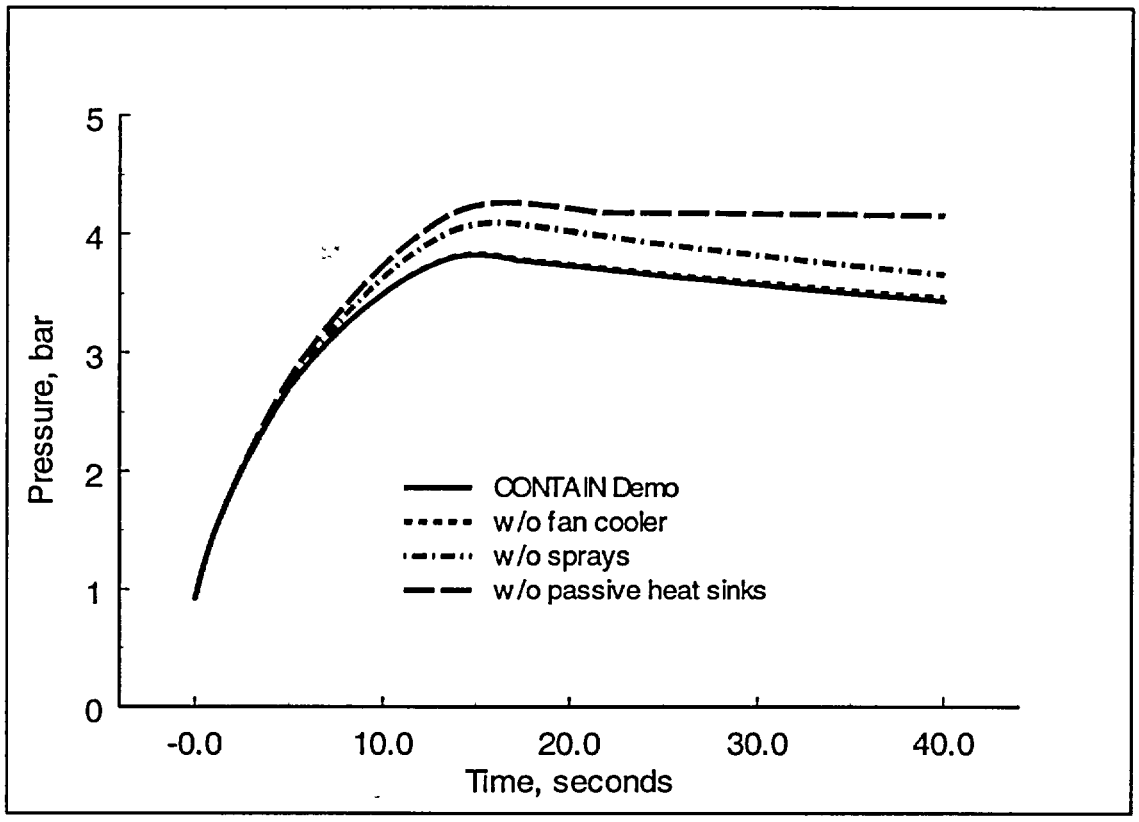

Figure 2-8 Pressure sensitivity to active and passive energy removal for a minimum pressure analysis.

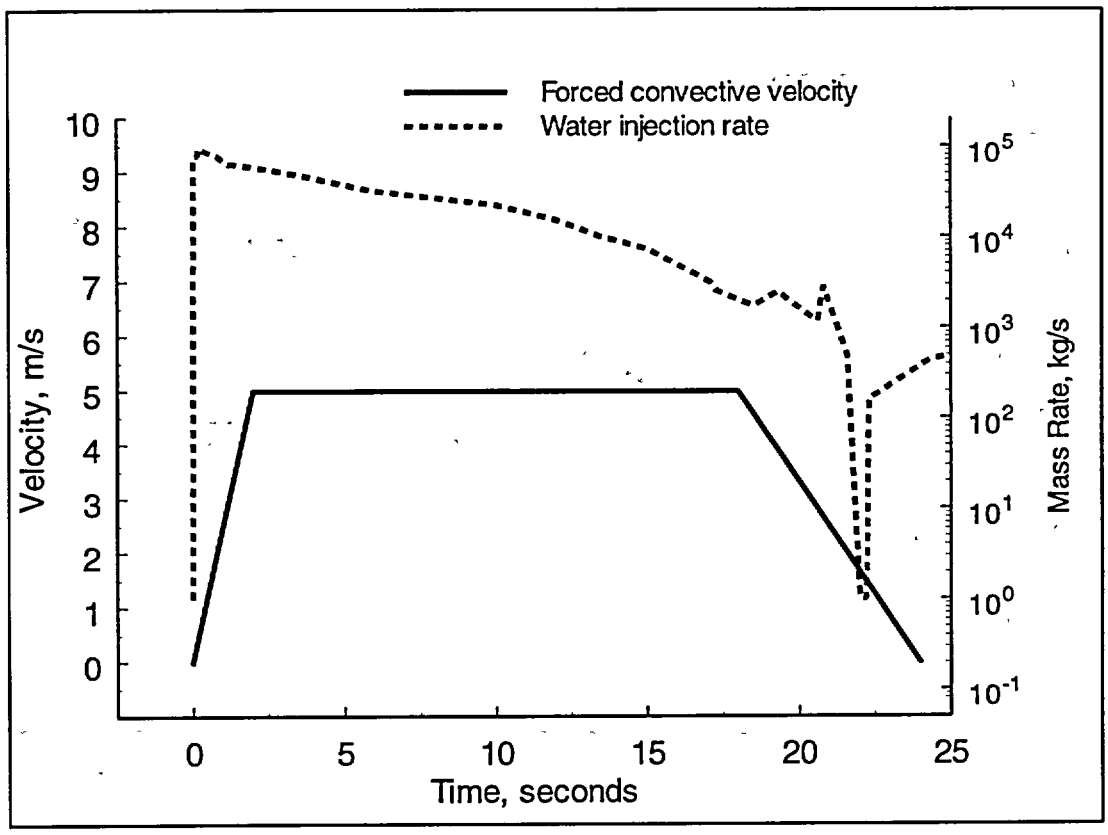

Figure 2-9 CONTAIN forced velocity profile used for qualification in a minimum pressure analysis.

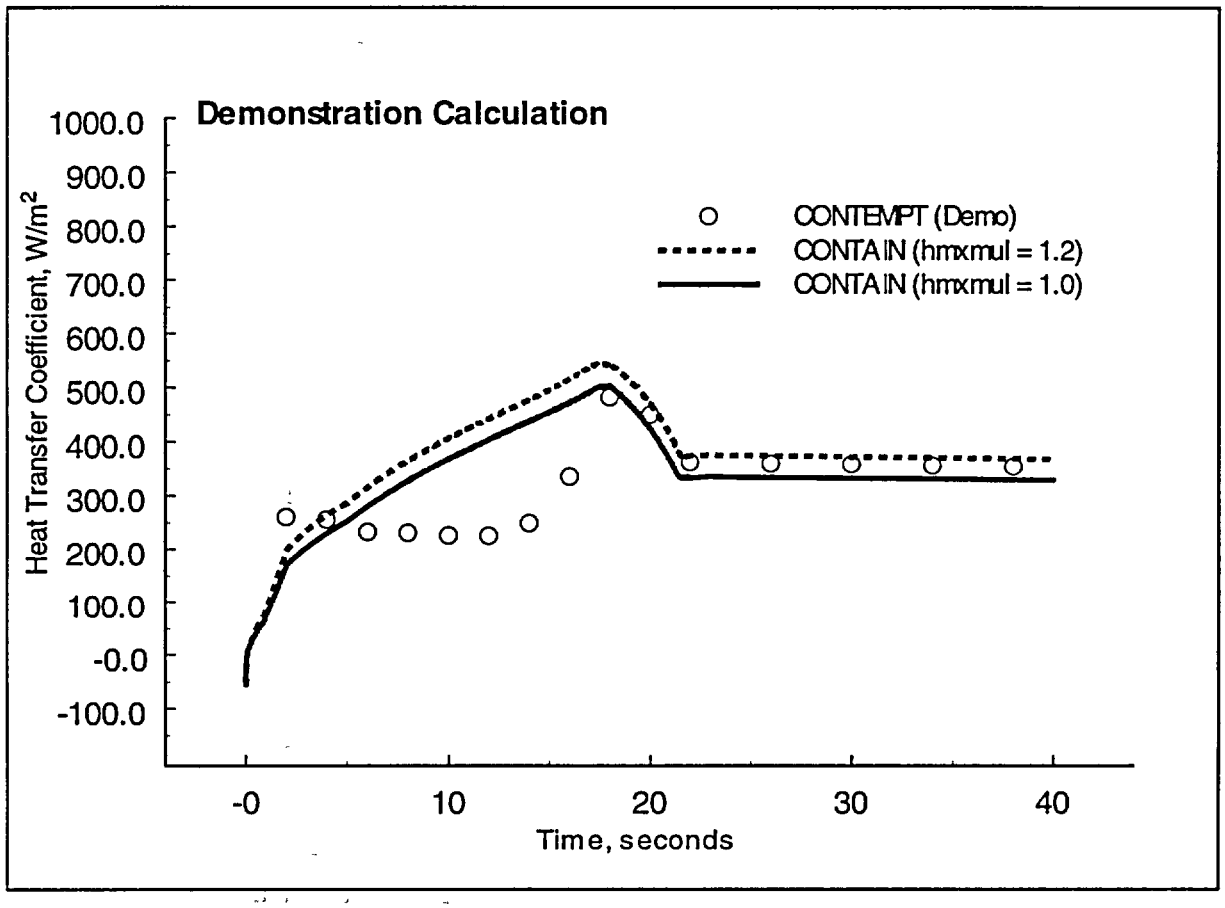

Figure 2-10 Comparison of CONTAIN and CONTEMPT heat transfer coefficients for the minimum pressure analysis, showing the bounding aspect of the CONTAIN results obtained by using a forced velocity profile.

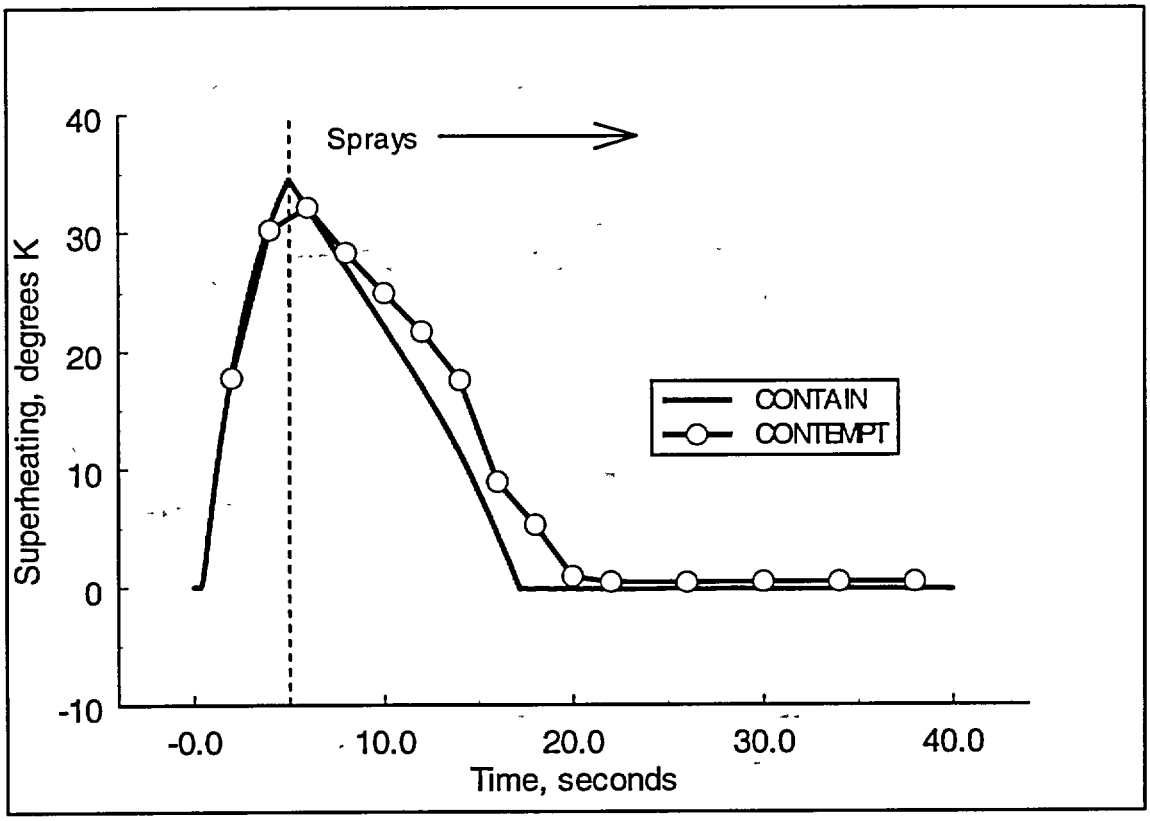

Figure 2-11 Prediction of superheating in the demonstration calculation for minimum pressure analysis.

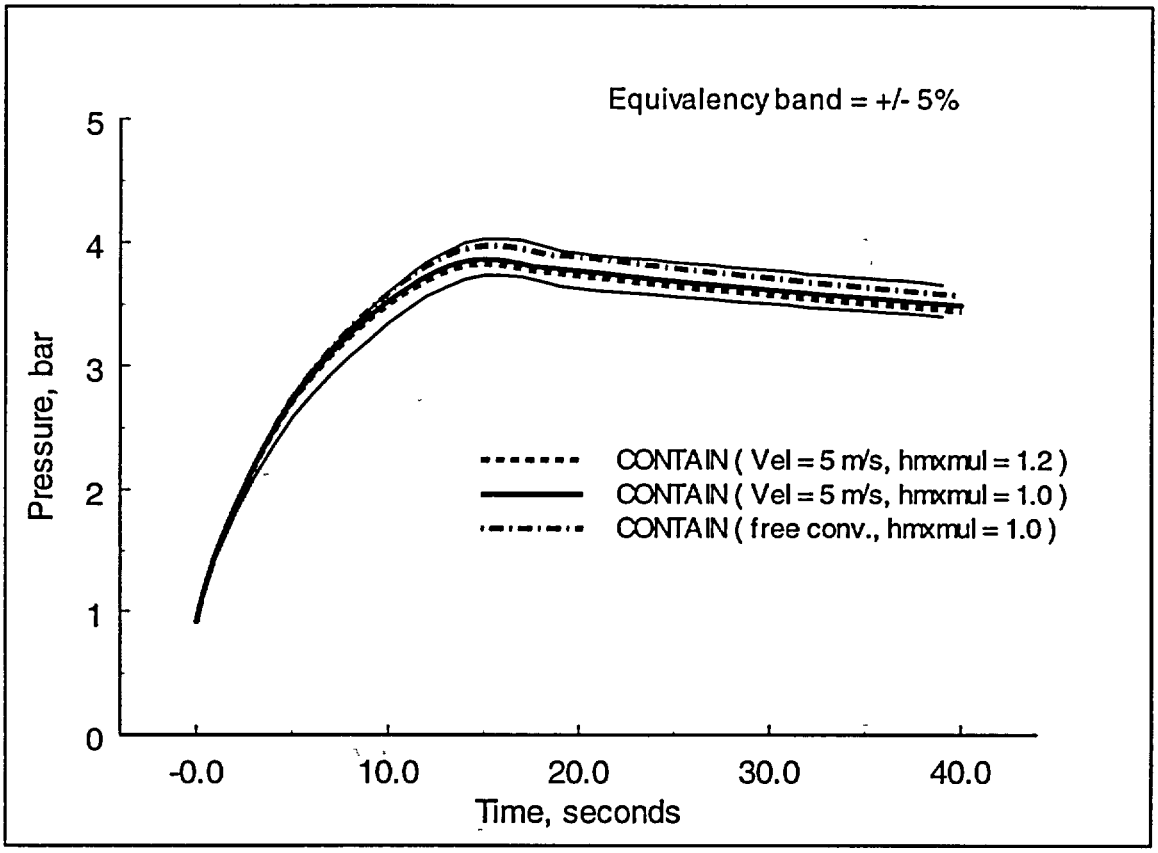

Figure 2-12 Pressure sensitivity to forced and free convective condensation for the minimum pressure analysis.

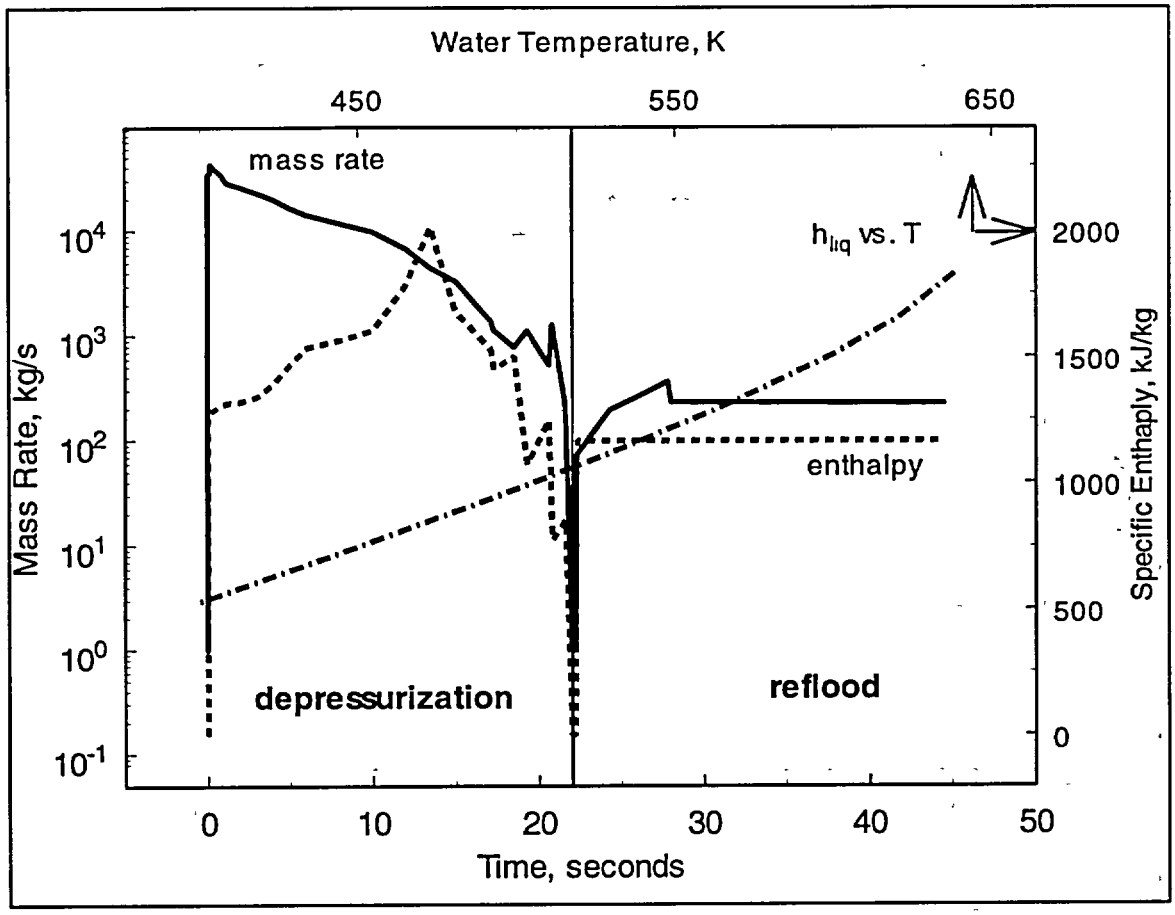

Figure 2-13 Water injection source for the minimum pressure demonstration calculation. The relatively low enthalpy of the injection during the depressurization and reflood phases indicates that the water is injected into the containment as a two-phase water source during both phases.

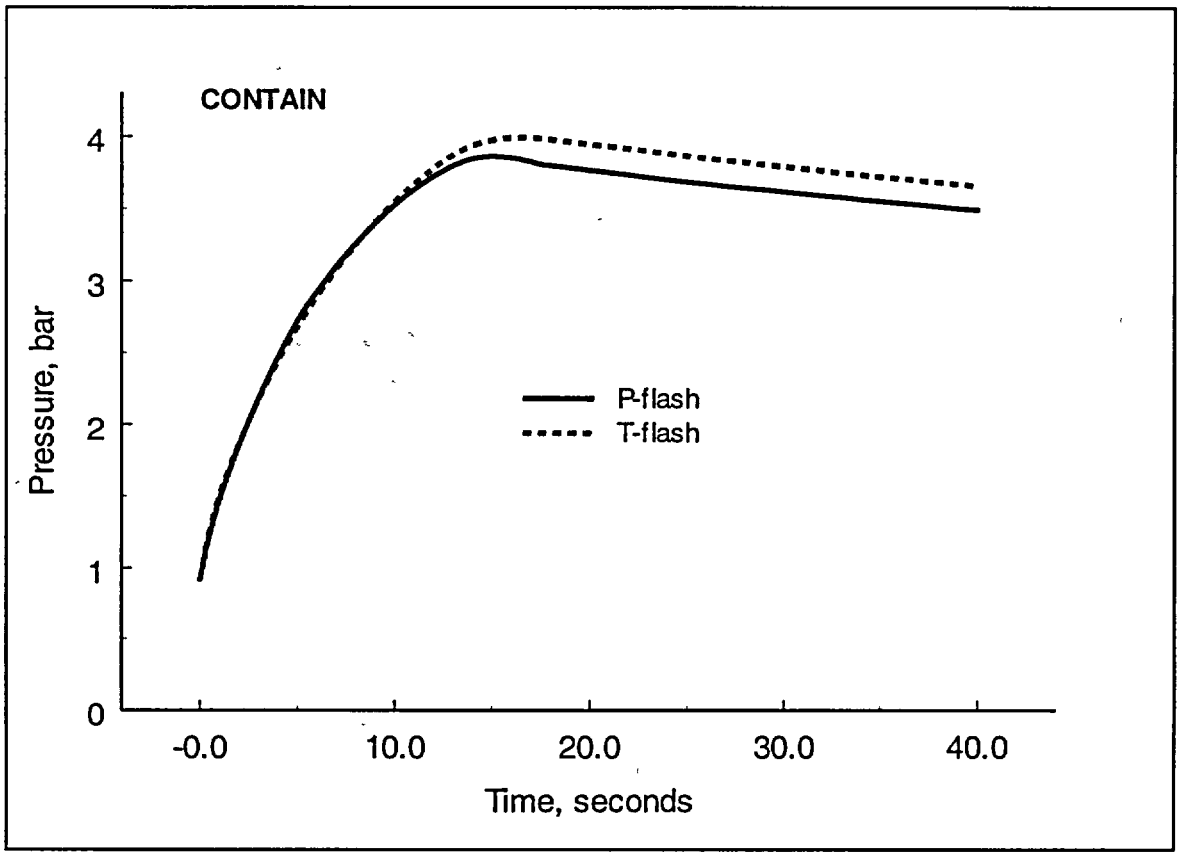

Figure 2-14 Comparison of pressure and temperature flash methods for treating the expansion of two-phase water injections in the CONTAIN code. The pressure flash method is activated by using the CONTAIN safety relief valve source input (SRVSOR), while the temperature flash method is implemented by using the external atmospheric source input tables (SOURCE).

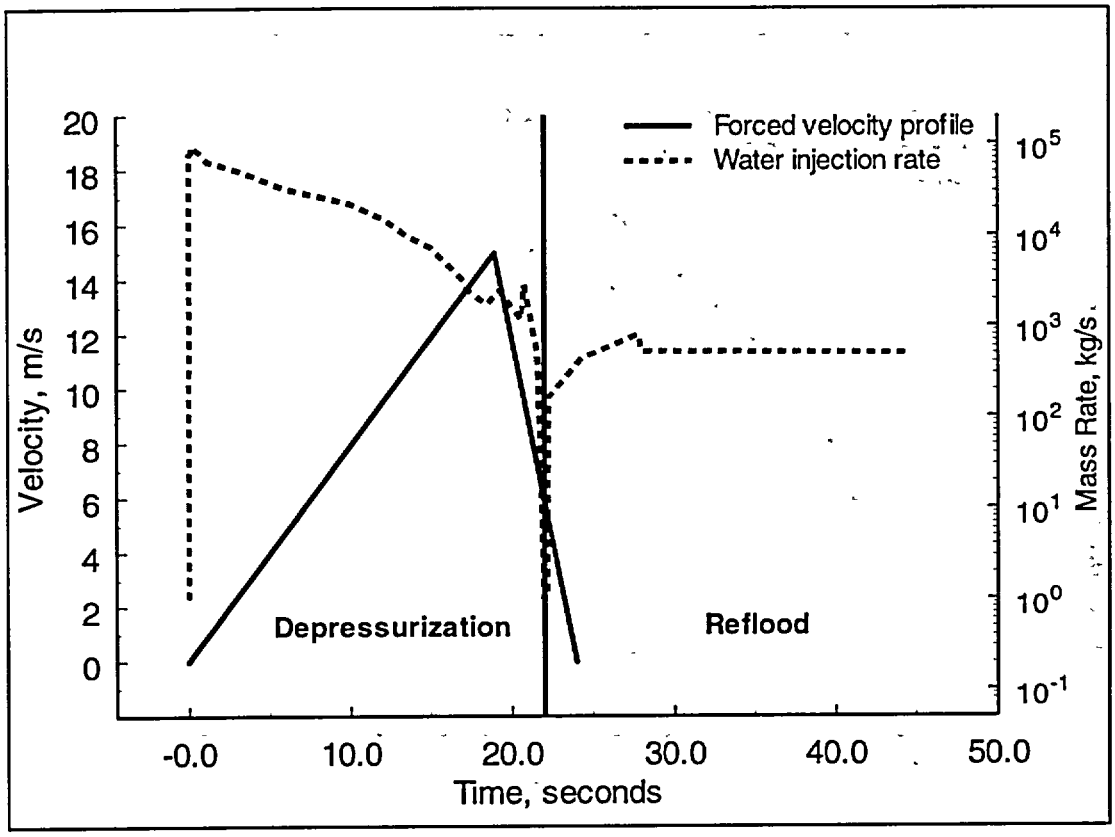

Figure 2-15 Forced velocity profile to simulate the 4 X Tagami coefficient as recommended in the USNRC's SRP for minimum pressure analysis.

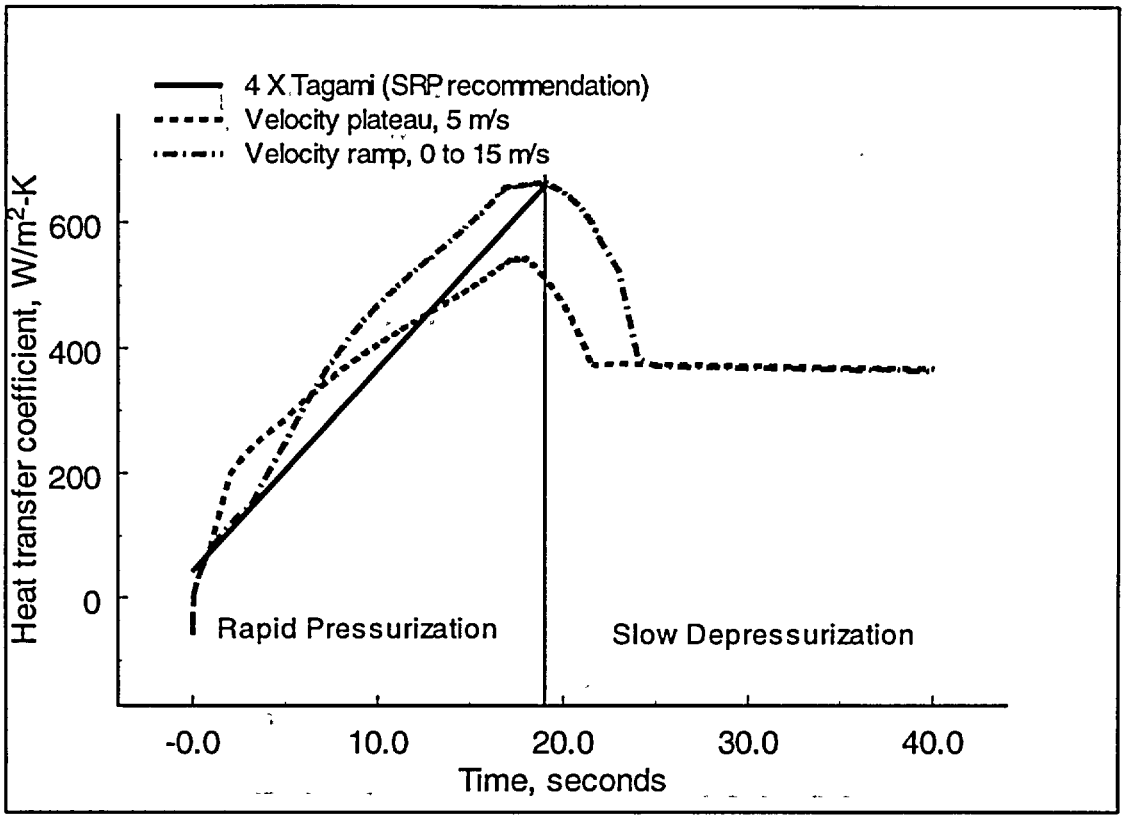

Figure 2-16 Comparison of heat transfer coefficients derived from the CONTAIN code where the forced velocity profiles are used during the rapid pressurization phase of a containment accident.

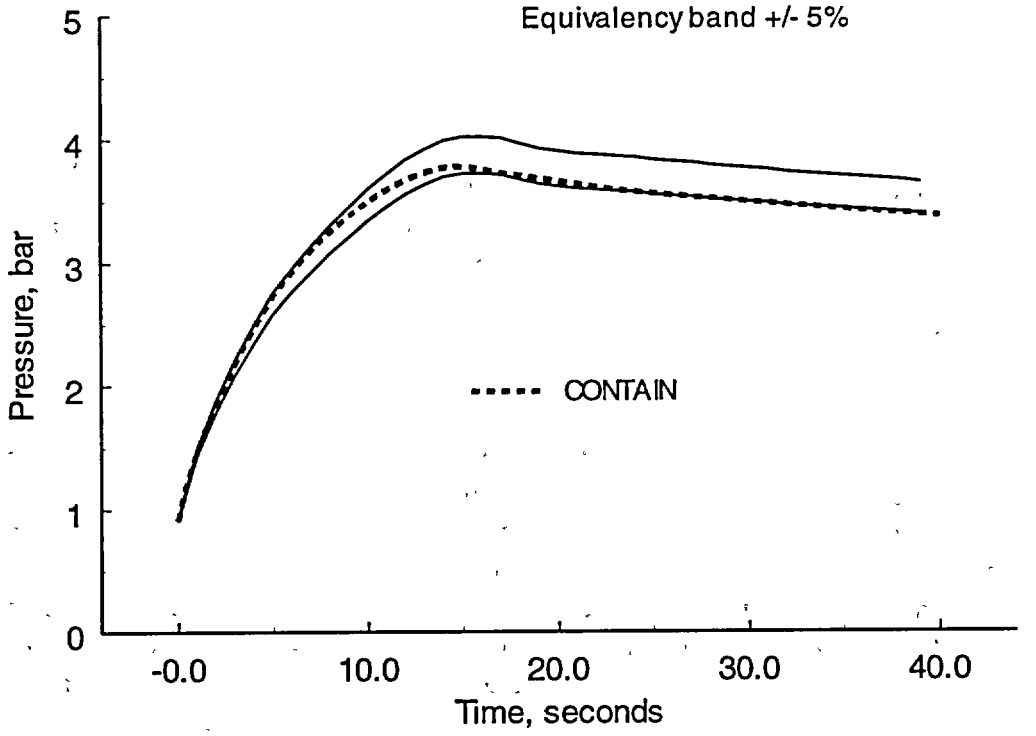

Figure 2-17 CONTAIN pressure prediction for a minimum pressure analysis using a ramped forced velocity profile and a multiplier of 1.2 (hmxmul = 1.2) to approximate the SRP recommended "4 X Tagami" coefficient during the rapid pressurization phase of a containment accident.

2.2 MSLB Short-term Accident Analysis

In Section 2.2.1, we describe a MSLB short-term scenario, and in Section 2.2.2, we discuss the qualification of CONTAIN for predicting maximum containment loads. In Sections 2.2.3 and 2.2.4 are recommended modeling and input preparation needed to ensure that CONTAIN will predict conservative results equivalent to traditional containment analyses using the NRC's containment analysis code, CONTEMPT. Detailed model comparisons between CONTAIN and CONTEMPT are given in Appendix A. CONTAIN and CONTEMPT input for the MSLB demonstration calculations presented in this section are listed in Appendix C.

2.2.1 MSLB Short-term Scenario

The MSLB scenario, summarized in Table 1-1, is initiated with a break in the secondary cooling system, i.e., the main steam line connected to the steam generator. A break in the secondary cooling system can occur in a region above the operation deck, and therefore is typically at an elevated location compared to a break associated with the primary system. The blowdown of the secondary system is limited by the inventory of steam contained within the system. High pressure steam is released from the break and will rapidly pressurize the containment. The injection is characterized as single phase superheated steam, with an injection duration of approximately a minute. As the hot steam expands to pressurize the containment atmosphere, some of the steam will condense on colder containment structures. Because the early blowdown process is so rapid, the pressurization during this phase is nearly adiabatic with the pressure and temperature rises limited through the accommodation of the blowdown steam in the large containment free volume.

Following an initial rapid pressure rise, the pressurization process is controlled or suppressed by energy removed through active and passive methods. The active measures are the engineered system features; containment sprays and fan coolers that activate upon signals generated during the rapid pressurization phase. Maximum containment loads are determined, in part, by assuming a single failure criterion for ESF availability, e.g., one spray train and one fan cooler pair are available. Passive energy removal is realized by condensation of steam on the containment walls and miscellaneous steel structures.

2.2.2 Qualification

Shown in Figures 2-18 and 2-19 are the pressure and temperature responses calculated with CONTAIN and compared to results using the CONTEMPT code. These results show that when the recommendations for short-term MSLB modeling and input preparation as discussed below are followed the CONTAIN results will be slightly less conservative than a traditional calculation approach, just below the equivalency band for temperature. In Figure 2-18, the pressurization is divided into a rapid and slow pressurization/depressurization phase. Unlike the LOCA pressurization where the injection discontinuity clearly divides each phase, the MSLB injection is

continuous and there is no obvious division of phases. We have divided the pressurization curve for the MSLB based on the time at which an adiabatic pressure calculation departs from the CONTAIN pressurization by more than 5%. In this way we may contrast periods where passive and active energy removal models are significant to predicted maximum pressures.

Unlike the LOCA demonstration case, the equivalency of the MSLB calculation is marginal. The reasons for this seemly inconsistency between the CONTAIN modeling and traditional methods are the result of a twofold disparity between code modeling during conditions of high superheat:

3) The CONTEMPT code uses an empirical correlation (Uchida) based on experiments in saturated air/steam atmospheres for determining passive energy removal by heat sinks under atmospheric superheated conditions for the demonstration calculation. In an attempt to adjust the modeling approach to a superheated atmosphere, an ad hoc method of using the saturated temperature instead of the gas temperature in the structure energy transfer equation, $Q = h_{Uchida} A(T_{sat} - T_s)$, is implemented. In contrast, the CONTAIN code uses a physically-based modeling methodology that treats both saturated and superheated atmospheric conditions within the mechanistic framework of the modeling.

4) The CONTEMPT code uses the Uchida empirical correlation for determining the total passive energy removal by heat sinks. This modeling approach must be adjusted by parametric input to parse the total energy transfer between condensation or latent energy transfer and sensible heat transfer to structure surfaces. In a highly superheated atmosphere the ratio of sensible to condensation energy transfer can significantly affect atmospheric temperatures while having a relatively minor affect on pressures. CONTAIN on the other hand explicitly models condensation and sensible energy transfers to structures using a physically-based modeling methodology that has been validated in separate effects testing.

In the CONTAIN code assessment report [CAR], the code is applied and assessed for a separate effects test, Phebus FPT0, where free convection condensation occurs in a superheated air/steam atmospheric environment. The assessment has shown the validity of the CONTAIN condensation modeling approach during superheated conditions. In Appendix A, the CONTAIN and CONTEMPT codes are compared for this same separate effects test. The comparisons, obtained using CONTEMPT in modeling approach similar to that used in the MSLB scenario show that the CONTEMPT code predicts higher gas temperatures than measured or calculated by the CONTAIN code -- consistent with the trend observed here for the MSLB scenario. We can demonstrate for the MSLB scenario the rationale that explains the lower pressure and temperature results predicted by CONTAIN, as compared to a similar CONTEMPT calculation in an identical manner as described in Appendix A for the Phebus test.

The explanation begins with a realization in this scenario that the differences between these codes occur in the degree of superheating, Figure 2-20. During this time, the dominant atmospheric energy removal process is energy transfer to passive heat sinks, as shown in Figure

2-21. Shown in Figure 2-22 is a comparison of each code's derived heat transfer coefficient for the containment shell.[7] From this figure we see that there is a divergency in the coefficients during the period of significant superheating, and a convergence during the time when saturation conditions are approached. The convergency effect is expected since the Uchida correlation and CONTAIN free convective condensation modeling method are shown to give similar results for saturated air/steam mixtures when the initial air pressure is ~ 1bar (see Appendix A). Shown in Figure 2-23 is the total energy transfer to the containment shell predicted by each code. In this comparison, the CONTAIN total energy removal rate during the pressurization phases, when superheating is increasing, is greater than that predicted by CONTEMPT using the ad hoc method of substituting saturation temperature for gas temperature in the equation for total energy transfer. This discrepancy in total energy rates explains most of the variation in temperature and pressure between the codes. The parametric assumption in CONTEMPT regarding the ratio of sensible to total energy transfer is another potential aspect to the dissimilarity in containment loads, specifically gas temperature.

Shown in Figure 2-24 is the comparison of sensible to total energy removal rates for the combined passive heat sinks in the demonstration calculation as determined by CONTAIN and parametrically set in the CONTEMPT calculation.[8] We see that there is a significant variation during the rapid pressurization period as superheated steam is first injected into the containment; the CONTAIN results show a much higher initial ratio of sensible to total energy transfer. However, by the time the rapid pressurization phase is finished there is convergence between the ratio assumed in CONTEMPT and that calculated in the CONTAIN code. There is a sensitivity to various assumptions for treating sensible heat transfer in superheated air/steam environments, as indicated in Table 2-11 at the time of ~ maximum degree of superheating. However, because the difference in the actual ratios occurs only early in the pressurization when energy removal is minor compared to the injection energy, the modeling variation between CONTAIN and CONTEMPT for this phenomenon is not considered an important issue. Therefore, we associate the major variation between the CONTEMPT and CONTAIN results due to the ad hoc method used in the former for approximating convective condensation during superheated conditions.

In light of the above discussion that explains why CONTAIN calculations for the maximum containment loads during a MSLB may be somewhat lower than a traditional calculation due to

---

[7] $h = \frac{Q}{A\left(T_{gas} - T_s\right)}$, where the atmospheric temperature T_{gas} is the gas temperature, and the surface temperature T_s is the surface temperature of the structure substrate (steel).

[8] The selection of a revaporization of 8% in the CONTEMPT code input here is specified by regulatory guidelines for performing MSLB containment analyses, and whose justification is apparently based on studies involving best estimate fitting of CONTEMPT code results to the CVTR test #3 pressure and temperature results subsequent to a steam injection.

the contrasting modeling approaches for treating condensation in superheated conditions, we establish the qualification of the CONTAIN code based on the following statements:

- The CONTAIN modeling approach is a mechanistic method that explicitly accounts for key phenomena involved in the energy removal processes that determine maximum containment loads.

- The CONTAIN passive energy modeling methods have been validated for the type of superheated conditions that are anticipated in MSLB scenarios.

Presented in Table 2-12 is a summary of the key points concerning the qualification of the CONTAIN code for performing MSLB maximum containment loads analysis.

2.2.3 Modeling Recommendation for Maximum Containment Loads Analyses

As discussed in the above section on qualification and mentioned in Table 1.1, the maximum containment loads analysis for a MSLB is dependent on a few phenomena. Presented in Table 2-13 are modeling recommendations for those phenomena, consistent with the code qualification discussion presented.

As with the LOCA maximum containment loads modeling recommendations, we chose a single cell nodalization scheme. Although we have noted in our assessment work on the CONTAIN code that multiple nodalizations may be required to predict loads for situations where steam injections are elevated, as may be the case for a MSLB when compared to the lower elevated LOCA scenario, we also note here that those assessment conclusions were based on relatively long-term periods after which stratification of the containment atmosphere had time to develop. In the case for maximum containment loads prediction in the short-term, our assessment of near prototypical containment tests, e.g., CVTR and HDR testing programs, indicate that a single cell nodalization represents a conservative modeling approach providing that free convective condensation models are implemented.

We have recognized that the maximum temperature predictions during MSLBs are sensitive to the assumptions regarding sensible heat transfer modeling. We regard convective sensible heat transfer, as modeled in CONTAIN, to be an integral component of the overall validated HMT analogy modeling approach used in the code. Therefore, we recommend applying the convective models in the default mode where sensible heat transfer by convection is modeled. In the case of sensible heat transfer by radiation, this model as with the convective model, can affect predicted temperatures. However, the implicit validation that we have realized in the case of convection through the use of the HMT analogy methodology is not present for the thermal radiation modeling and input preparation required in the model. Therefore, it is recommended that thermal radiation modeling be omitted in the input preparation. As noted in Table 2-11, excluding radiation modeling has a very small effect on containment pressure. Other phenomena that have a very small effect on pressure and temperature maximums are condensate film heat transfer and

atmosphere to pool heat and mass transfer. For instance, a reduction of film thickness from the default (0.0005 meters) by a factor of 100 decreases the maximum over-pressure by less than ~ 1%, and the maximum temperature is decreased by less than ~ 1 degree. The presence or absence of atmosphere to pool heat and mass transfer has an even less effect on pressure and temperature. In modeling these phenomena, we chose to recommend the parameters that produce the more conservative pressure and temperature estimates.

For the MSLB scenario, maximum pressure and temperatures occur prior to spray actuation. Therefore, small variations in the spray modeling, such as in the spray droplet size, have a negligible affect on maximum containment loads.

2.2.4 Input Preparation for Maximum Containment Loads Analyses

In this section we discuss the preparation of CONTAIN input for a large dry containment MSLB scenario for a demonstration plant.[9] Input preparation for this short-term scenario follows the general modeling recommendations discussed above to obtain a qualified CONTAIN calculation for a MSLB scenario. These recommendations are translated into specific input parameters in Table 2-14. The CONTAIN MSLB demonstration problem in Appendix C may be consulted for detailed examples of implementation of the recommended modeling approach and input preparation.

For specific input preparation pertaining to the passive heat sinks and the mechanistic fan cooler modeling, the user is referred to the discussions in Section 2.1.2.3.

[9] The specification for the demonstration plant is based on CONTEMPT input for San Onofre 2/3. Note that this plant was arbitrarily selected and is used for demonstration purposes only; actual plant related details may not be adequately reflected.

Table 2-11 Temperature and pressure sensitivity for a MSLB scenario to various modeling options for sensible heat transfer (time = 30 seconds).			
Case	**Comment**	**Temperature, K**	**Pressure, bar**
1	CONTEMPT, sensible factor = 0.08*	480 [472 – 488]**	3.96 [3.81 – 4.11]**
2	CONTAIN Demo, convection only	470	3.88
3	CONTAIN, no sensible heat	480	3.95
4	CONTAIN, convection and thermal radiation	463	3.84

* CONTEMPT input parameter, FAC (0.92)
** Equivalency band, +/- 5%

Table 2-12 Summary of the CONTAIN qualification for short-term MSLB application					
Accident Phase	Modeling Area	CONTEMPT	CONTAIN	Comments	Reference
Rapid pressurization	geometric nodalization	Single cell	Single cell	For short-term pressurization phases, single cell nodalizations are shown to give conservative estimates of containment pressure loads	[CAR*, p. 4-105, 4-109]
	free volume	fixed free volume	free volume reduce by water pool volume	Displacement of free volume air by pool water is a physical reality. Including displacement represents a slight conservatism with respect to the CONTEMPT model.	N/A
	single-phase steam injection	thermal equilibrium modeling, with dropout of condensed liquid water	temperature flash modeling, with dropout of condensed liquid water	Thermal equilibrium, homogeneous mixing of injection mass with containment atmosphere is equivalent to the CONTEMPT temperature flash model. The thermal equilibrium assumption is conservative. Dropout of condensed water during a two-phase injection is conservative, based on integral test comparisons.	[CAR, p. 3-63, 4-105, 4-109]
	heat and mass transfer to passive heat sinks	Uchida correlation	free convective condensation by HMT analogy	The CONTAIN HMT analogy modeling for free convective condensation is a similar method for determining total energy transfers in processes dominated by condensation. Free convective condensation by the HMT analogy has been shown to be a conservative method for estimating energy transfers during blowdown periods.	See Appendix A for discussion on Uchida correlation; conservatism of free convective condensation [CAR, p. 4-109]
	heat and mass transfer to pool surface	not modeled	not modeled	Excluding heat and mass transfer to the pool is an equivalent choice, and conservative	See Appendix A

* CAR is the CONTAIN Assessment Report which is a short-hand designation for a NRC informal report – "An Assessment of CONTAIN 2.0: A Focus on Containment Thermal Hydraulics (Including Hydrogen Distributions)," March 1999.

Table 2-12 Summary of the CONTAIN qualification for short-term MSLB application (continued)					
Accident Phase	Modeling Area	CONTEMPT	CONTAIN	Comments	Reference
Slow pressurization	heat and mass transfer to passive heat sinks	Uchida correlation	free convective condensation by HMT analogy	Both Uchida and the HMT analogy model are methods for treating free convective condensation. The two methods are nearly equivalent for single cell models.	See Appendix A
	heat and mass transfer to pool surface	not modeled	not modeled	Excluding heat and mass transfer to the pool is equivalent to the CONTEMPT model input and conservative.	
	spray pressure suppression	100% spray efficiency model	condensation on spray droplet using HMT analogy method	Both models give similar results as verified through separate effects test comparisons	
	fan cooler pressure suppression	tabular input: temperature versus total energy removed; condensed vapor removed from atmosphere	mechanistic fan cooler model using the HMT analogy method	Both models are equivalent (within 10%) in terms of total energy and vapor mass removal rates within the operating range of fan coolers during accidents	

Table 2.13 General modeling recommendations for a qualified CONTAIN short-term MSLB calculation in a large dry containment.	
Phenomena	**Modeling Recommendation**
Multi-component gas compression	Nodalize the containment as a single compartment
Single-phase steam expansion	Use a thermal equilibrium method for steam expansion, dropout condensed liquid from atmosphere
Convective condensation	Use a *free* convective heat transfer correlation for the HMT modeling
Structure heat transfer	Account for liquid film and paint resistance for surfaces; include any steel-liner-to-concrete air gaps at constant, full width
Spray droplet heat and mass transfer	Use a mass mean spray droplet size for the injected spray droplet diameter
Fan cooler heat and mass transfer	Use mechanistic fan cooler model, calibrated to the operation environment during accident

Table 2-14 Input guidance for modeling a short-term MSLB calculation in a large dry containment.		
Input Section/Block	**Parameter(s)**	**Comment**
Global:		
Nodalization	ncells = 1	Single cell nodalization for equivalency and conservatism
Material properties	user defined properties	density, thermal conductivity, and specific heat capacity for air, stainless steel, steel, and concrete are set for equivalency
Timesteps	~ 0.01 seconds	set to give accurate results for the time scale of interest (fractions of second)
Flow	DROPOUT	dropout condensed liquid water in atmosphere for equivalency and conservatism
Upper Cell:		
Geometry	gasvol	free volume equivalency
Atmosphere initial conditions and sources	ATMOS block; SOURCE block	pressure, and temperature equivalency (saturated conditions for conservatism); external source for temperature flash equivalency
ESF (sprays)	SPRAY block input	spray droplet diameter set to mass mean diameter of spray nozzle distribution, released at full height: spdiam = 0.0005-0.0007 meters; sphite = 50 meters
ESF (fan coolers)	FANCOOL block input	Use keyword CONDENSE for mechanistic fan cooler model; set time to activate using SOURCE option with coolant mass kg/s and temperature set to default values; adjust energy removal rate using parameter "fcefar."
Structures	STRUC block input	fully implicit algorithm (default); free convection (default); maximum liquid film thickness (default); paint resistance set for equivalency; no thermal radiation; air gaps of constant thickness; initial temperature condition for equivalency; surface node thickness as fraction of diffusion length (see Section 2.1.2.3)
Lower Cell:		
Low-cell	HT-TRAN on on on off off	All condensed water dropped from atmosphere, spray removal, and condensate overflow from structures are diverted to pool (equivalency); pool-to-atmosphere heat and mass transfer set to zero (equivalency); free volume displacement by pool water mass.

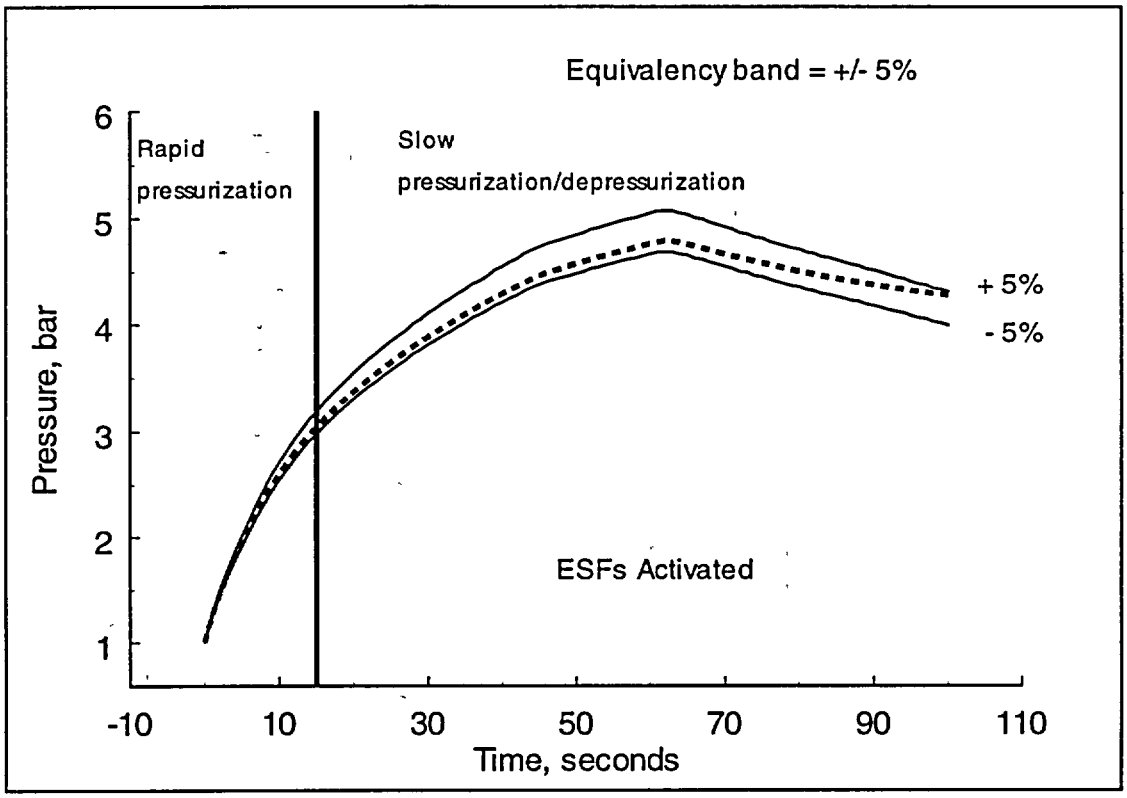

Figure 2-18 CONTAIN pressure calculation for a demonstration of a maximum pressure analysis for a short-term MSLB scenario in a large dry containment. Equivalency bands of +/- 5% are based on a CONTEMPT demonstration calculation.

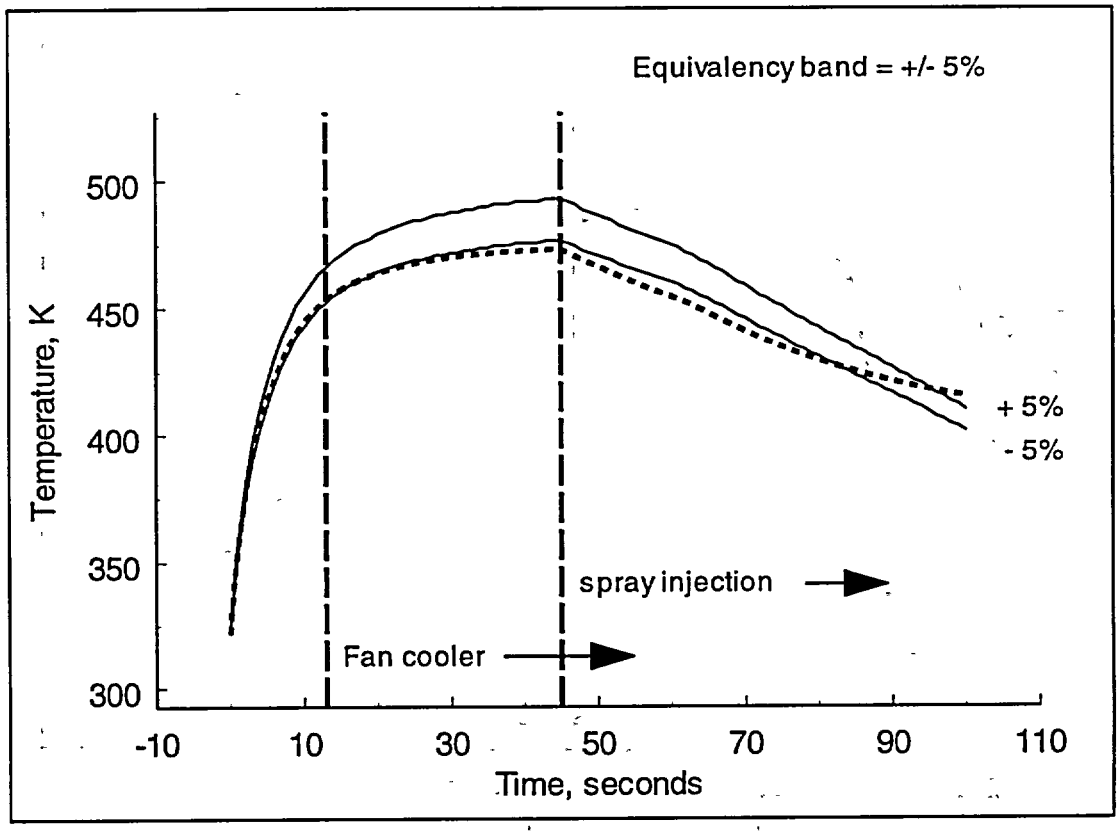

Figure 2-19 CONTAIN atmospheric temperature calculation for a demonstration of a maximum temperature analysis for a short-term MSLB scenario in a large dry containment. Equivalency bands of +/- 5% are based on a CONTEMPT demonstration calculation.

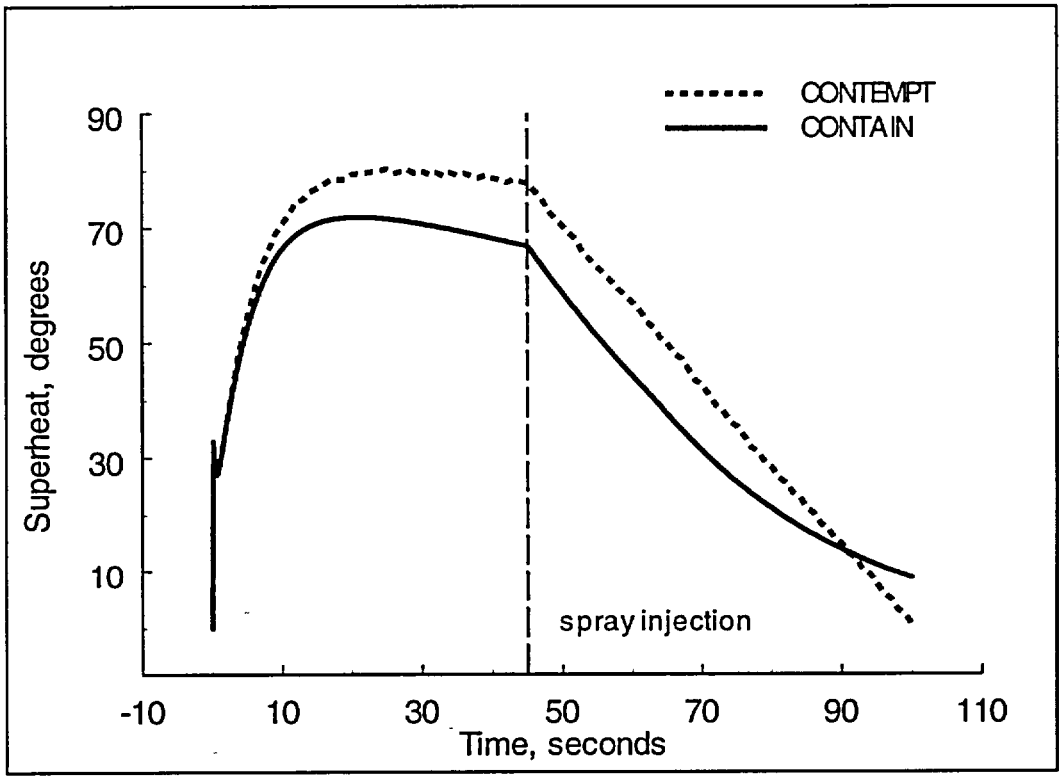

Figure 2-20 Comparison of superheating during a MSLB demonstration calculation in a large dry containment.

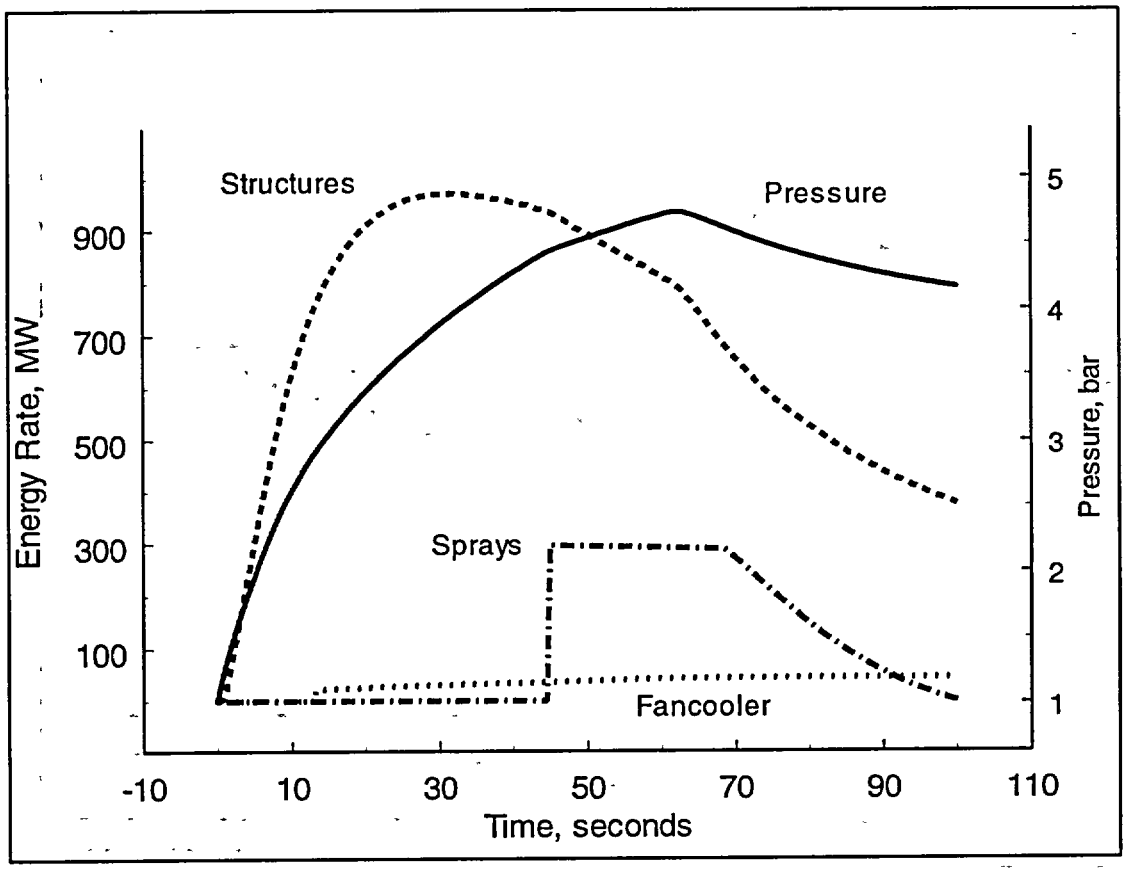

Figure 2-21 CONTAIN calculated partitioning of energy removal during a MSLB demonstration calculation for a large dry containment.

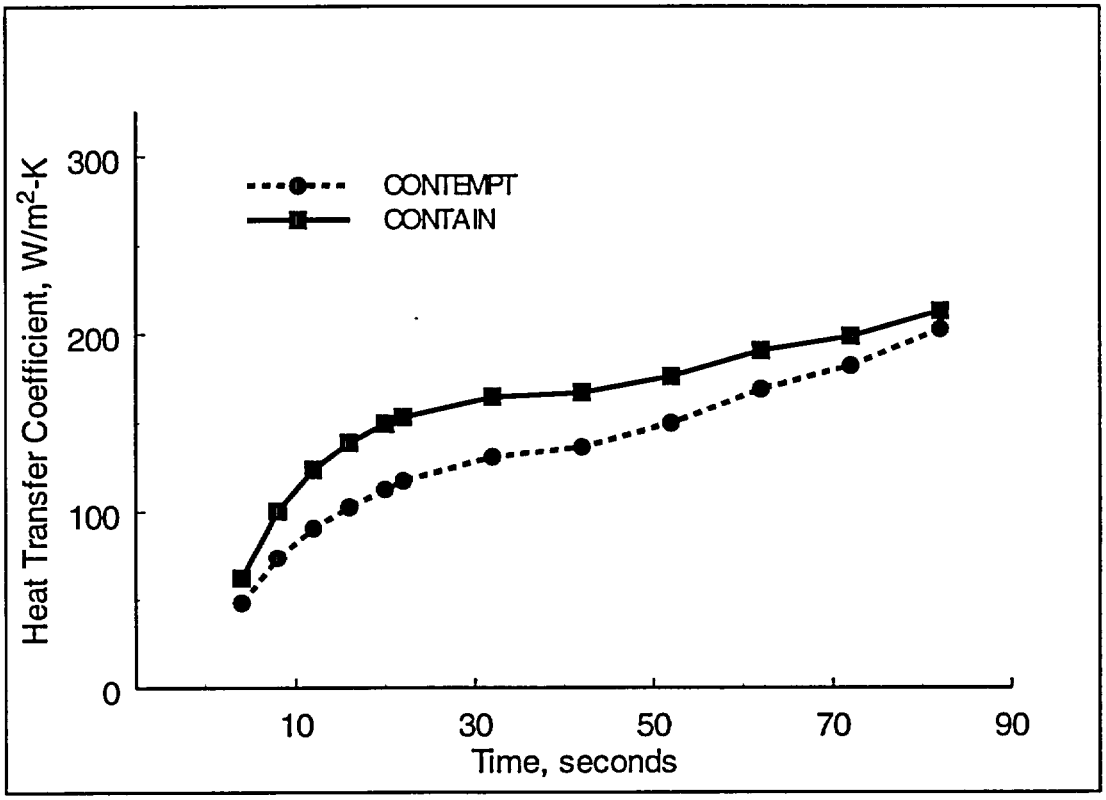

Figure 2-22 Comparison of heat transfer coefficients for the containment shell during a MSLB demonstration calculation in a large dry containment.

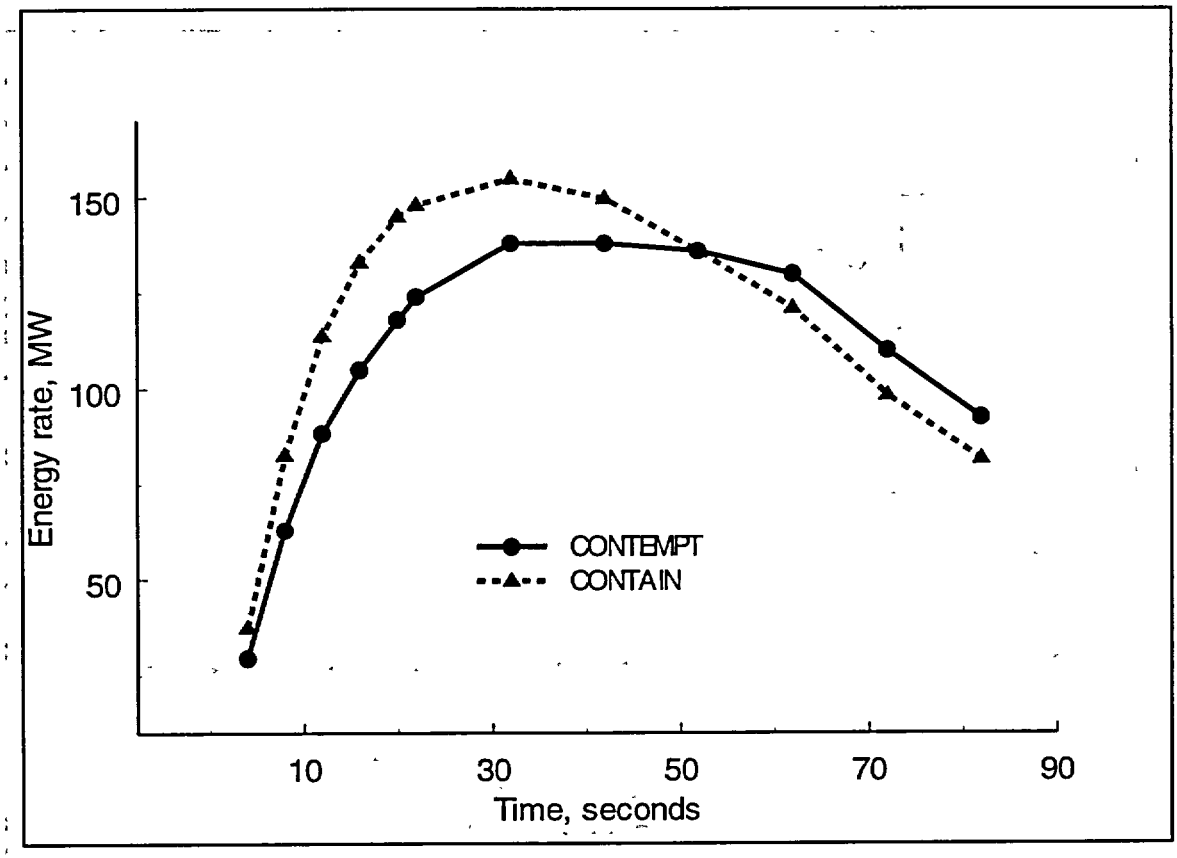

Figure 2-23 Comparison of energy transfer rates to the containment shell during a MSLB demonstration calculation in a large dry containment.

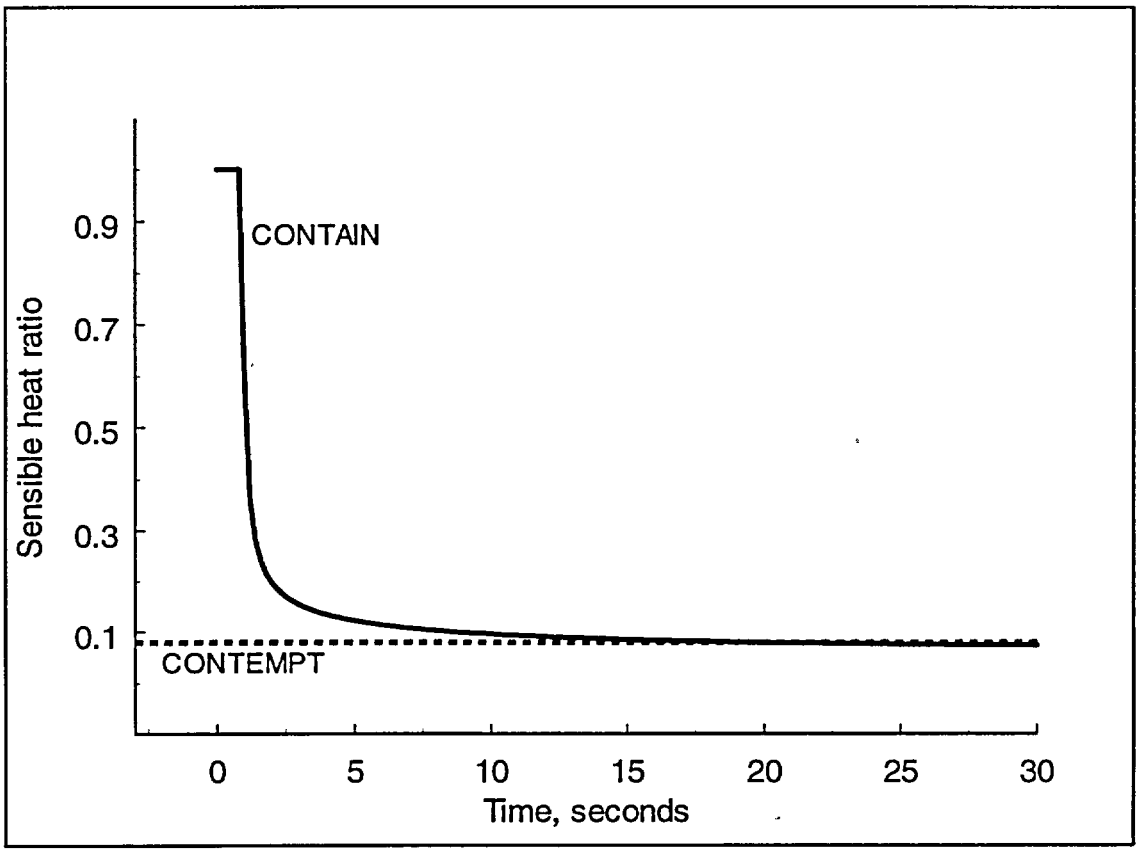

Figure 2-24 Comparison of sensible heat ratio for passive heat sinks during a MSLB demonstration calculation for a large dry containment. The sensible heat ratio is the ratio of energy transferred by sensible heat transfer processes to the total energy transfers to structures. In this figure, the sensible heat calculated in the CONTAIN calculation is from convective heat transfer; whereas, the CONTEMPT value is a set via input using the parameter, FAC (1-FAC is often referred to as the revaporization factor).

3 Subatmospheric Containment Analysis

In this section we discuss qualification and methods that can be used to model the DBA response of a PWR subatmospheric containment with CONTAIN [1]. Figure 3-1 depicts a typical subatmospheric containment. Subatmospheric containments are variations on the large dry containments; they differ in that the normal operating conditions are at subatmospheric pressure. The reduced operating pressure permits these containments to be constructed with a free volume that is 20-30% less than the large dry containments.

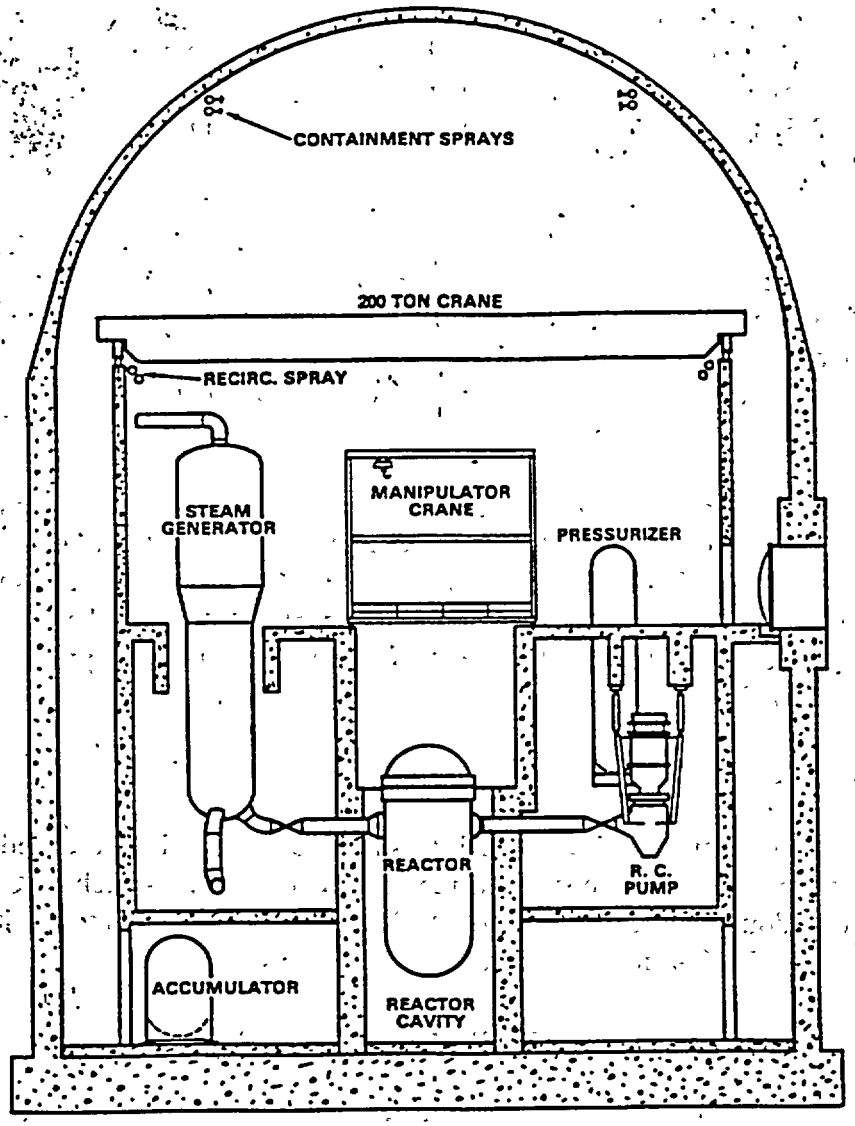

Figure 3-1 Typical subatmospheric containment showing the approximate locations of the quench and recirculation sprays used to depressurize the containment after a LOCA.

Additionally, these containments are equipped with a containment depressurization system. The integrity of the containment is maintained by the depressurization system which includes a:

- quench spray (QS) subsystem, and a
- recirculation spray (RS) subsystem.

These engineering safety systems (ESFs) are capable of cooling and depressurizing the containment to subatmospheric pressure within an hour following a loss-of-coolant accident (LOCA), as specified in the SRP. The recirculation spray system can maintain the subatmospheric pressure inside the containment for periods exceeding one hour. Shown in Figures 3-2 and 3-3 are examples of the circuit schematics for quench and recirculation spray subsystems [12].

As in the case of the large dry containments, the location of the primary system pipe rupture is at a low elevation within the containment, and therefore most of the containment free volume will be, to a good approximation, uniformly mixed soon after the pipe break occurs. The uniform mixture is also maintained through turbulent currents set up by the quench and recirculation sprays. As a result of the uniform mixing, DBA containment analyses are performed using a single compartment model for the containment building.

In Section 3.1, we describe a LOCA long-term (times > one hour) scenario, and in Section 3.2 we discuss the qualification of CONTAIN for predicting the time to return to subatmospheric conditions following a LOCA. Sections 3.3 and 3.4 present recommendations for modeling and input preparations for performing a long-term subatmospheric analysis that may be used for DBA audit reviews. The CONTAIN input for the demonstration calculations presented in this chapter is listed in Appendix D.

3.1 LOCA Long-term Scenario

The LOCA scenario, summarized in Table 1-1, is initiated with a double-ended rupture (DER) in a reactor coolant pipe on the pump suction side of the coolant pipe – such a LOCA is referred to as a pump-suction double-ended rupture (PSDER). Minimum ESFs that are activated to limit the consequences of this LOCA in the containment are the following:

- one out of two trains of the containment QS subsystem; and,
- one out of two trains of the containment RS subsystem (i.e., one inside recirculation spray pump, and one casing cooling pump).

For the demonstration calculation, minimum service water temperature conditions for the containment are assumed as shown in Table 3-1. Shown in Table 3-2 is the accident chronology for a PSDER, which is the limiting case for containment depressurization [12].

A LOCA such as the PSDER proceeds initially like the LOCA event in the large dry containment reviewed in Chapter 2. The rapid pressurization phase of the accident progresses in a manner essentially identical to the short-term LOCA in the large dry containment; the phase begins with the pipe rupture and extends to the time when the reactor vessel depressurizes (~ 20 seconds). Because the blowdown or depressurization injection represents such a significant energy source to the containment over a short time period, this portion of the accident is characterized as a pseudo adiabatic pressurization phase where maximum pressures and temperatures in the containment are reached.

Shortly after the reactor vessel depressurization, the emergency core cooling system and the spray subsystems activate. During this slow depressurization phase, the containment pressure declines from its maximum pressure to subatmospheric pressure. The QS and RS subsystems are required to affect this decline within regulatory guidelines, and the RS subsystem must continue to operate in order to maintain the containment at subatmospheric conditions.

In the demonstration calculation we emphasize the modeling aspects of the slow depressurization phase of the containment accident, showing how the CONTAIN code is utilized to predict a return to subatmospheric conditions following a PSDER accident. For a comparison to the traditional calculation approach, we make use of pressure calculations presented in the North Anna FSAR for a PSDER accident, following the accident chronology listed in Table 3-2.

3.2 Qualification

Shown in Figure 3-4 is the containment pressure response calculated with CONTAIN and compared to results obtained using the LOCTIC computer code.[1] These results show that the pressure results calculated with CONTAIN and reported in the North Anna FSAR are very similar, with both results indicating a return to subatmospheric *beginning* at 3000 to 3200 seconds. The predicted approach to subatmospheric pressure is shown in Figure 3-5.

We show in Figure 3-6 the sensitivity of the containment pressure profile to various assumptions regarding energy removal process (QS, RS, and passive heat transfer) in the containment. These sensitivity cases indicate, for this scenario, the following:

- Among the spray systems, the recirculating spray system is the more important depressurization system (due the higher spray flow rate capacity).
- Passive heat transfer is important for determining maximum pressure, but is relatively unimportant for predicting the time at which pressure returns to subatmospheric conditions (rapid depressurization without the moderating effect of heat structures).

---

[1] The LOCTIC computer code was used to obtain the results reported in the North Anna FSAR.

These conclusions regarding relative importance of energy removal mechanisms means that special attention should be directed at spray modeling qualification. As noted in the previous chapter, the CONTAIN spray model has been validated through both integral and separate effects testing. For long-term pressure suppression by sprays, the separate effects tests conducted by JAERI are especially pertinent to the subatmospheric qualification. Shown in Figure 3-7 is an example of the type of agreement that has been demonstrated with the CONTAIN spray model for long-term pressure suppression. Additional details on the assessment of the CONTAIN spray modeling via experimental comparisons can be found in the CAR.

Presented in Table 3-3 are the summary points for the qualification of CONTAIN for subatmospheric containment analysis.

3.3 Modeling Recommendations

The model recommendations for the subatmospheric containment analysis, where the return to subatmospheric pressure following a LOCA is a focus of the analysis, are developed in a manner that ensures conservative estimates of the containment pressure profile, and therefore the longest time to return to subatmospheric conditions. As in the previous chapter dealing with maximum containment loads during a LOCA, we adopt here those same model recommendations for the rapid pressurization phase of the subatmospheric LOCA; the most important recommendation here being the use of free convective condensation.

During the core reflood or slow pressurization/depressurization containment accident phase, we note especially that the injection of water into the containment is characterized as water entering from each side of the pipe rupture. For one injection path, path no. 1 which is on the steam generator side of the break, the blowdown water enters as high pressure two-phase water and the reflood water enters the containment as single-phase steam, as shown in Figure 3-8. Whereas, on the other side of the break, which is on the pump-side, the blowdown water also enters as high pressure two-phase water but the reflood water enters through path no. 2 as colder liquid water, Figure 3-9. We model the vessel water injection sources in the CONTAIN code by using an external atmospheric source option to treat the blowdown or depressurization injections for both path no. 1 and 2 and the reflood injection for path no. 1. The reflood source for path no. 2 injection source is modeled using the safety relief valve model activated through the SRVSOR keyword. The SRV source options do not allow the injected water to come into thermal equilibrium with the containment atmosphere as modeled with the external atmospheric source option. In the SRV-modeled source, the water expands during a time step against a constant pressure in the containment. Whatever water does not flash in the process is diverted directly to the containment sump, i.e., it is not mixed with the containment atmosphere. As a result, the containment atmosphere is not fictitiously cooled by assumed mixing of injected cold water. Shown in Figures 3-10 and 3-11 are comparisons of the containment pressure profiles predicted using various assumptions regarding the treatment of reflood water from path no. 2. The thermal equilibrium mixing of path no. 2 reflood water with the atmosphere, in the case where the external atmospheric source (Source) is used, results in a more rapid reduction of the

containment pressure in comparison to a case where the SRVSOR option is chosen. It is therefore recommended that the SRVSOR option be utilized to model reflood water from the pump-side break to prevent too rapid depressurization of the subatmospheric containment and a non-conservative estimate of a return to subatmospheric conditions.

The conservative aspects of the quench and recirculation spray subsystems are determined in this demonstration calculations through the conservative boundary conditions specification for those systems, i.e., one of two subsystems activated.

A summary of the modeling recommendations for the subatmospheric containment analysis is presented in Table 3-4.

3.4 Input Preparation

In this section we discuss the preparation of CONTAIN input for a subatmospheric containment long-term analysis where the focus is on the estimate of the time to return to subatmospheric conditions subsequent to a LOCA event. Input preparation for this long-term scenario follows the general modeling recommendations discussed in the previous section that assures a qualified CONTAIN calculation. These recommendations are linked to specific input parameters in Table 3-5. The subatmospheric demonstration problem in Appendix D may be consulted for detailed examples of the implementation of the recommended modeling approach and input preparation. Some additional information regarding the quench and recirculation spray and accumulator gas input preparation is provided in this section.

Quench Spray Input Preparation.

As indicated in Figure 3-2, the quench spray system draws water directly from the reactor water storage tank (RWST). A quench spray flow rate versus pressure curve is used to estimate the variation of flow rates as the containment pressure varies. We note that the QS vs. pressure curve is a linear function of pressure – at the high pressure (QS start) the spray rate is 113 kg/s and it increases to 132 kg/s at a low pressure (~ 1.3 bar). The CONTAIN code is limited to spray water input tables where the flow rate is given as a function of time. Since the pressure profile curve, Figure 3-12 is nearly linear with time, and slightly concave, we assume a linear variation in spray flow rates also with time, beginning at the high pressure flow rate and increasing to the flow for low pressure conditions. Because the assumed pressure profile is above the calculated profile, selecting flow rates that vary linearly with time in this manner (from start to stop) results in QS flow rates that are slightly lower than what may actually be the case, and therefore slightly conservative. The flow rate variation due to pressure variation, admittedly, is rather small, showing a 17% increase from high to low pressure. As a consequence, the effect of QS flow variation on the depressurization rate is also small as shown in Figure 3-13 where the depressurization using two bounding cases – constant QS flow rates at the high and low pressure values (113 and 132 kg/s) – are compared. The choice to model the QS flow variation in the approximate manner as described is a recommendation that gives near equivalency with other DBA code modeling.

Recirculation Spray Input Preparation.

The one recirculation spray subsystem that is operational during the subatmospheric long-term scenario consists of a system where one inside (sump pump) and one outside (casing pump) pumping circuits are available. Table 3-6 shows the operation characteristics of this system. In the following discussion, beginning with the inside containment system, we show how to initiate the start of the spray system through the use of tank and pump input, where the tank input is used to effectively delay the starting time of the recirculation pump. Heat exchanger input is described for both subsystems. For the outside containment system that includes the addition of external chill water into the pumping circuit, we show how a "dummy" cell may be used as a mixing cell for sump and chill water that is pumped to the spray nozzles.

The CONTAIN recirculation input is made up of a number of engineered safety components: tank (TANK), pump (PUMP), and heat exchanger (HEX). Pumping of sump water begins only after tank water is exhausted. The tank would typically refer to the RWST that feeds the quench spray system, for example. Because the QS is modeled in the demonstration calculation with a variable flow rate, the TANK input is not used for this subsystem; rather, the quench spray is modeled as a separate spray subsystem with an external water source table. However, the recirculation spray subsystems are separately modeled using TANK, PUMP, and HEX input. In the case of both the inside and outside spray systems, the tank component input is used to set the time that the recirculation pumping of sump water begins. A very small amount of tank water with an even smaller flow rate is set to exhaust the tank inventory at the time when the recirculation pumps are to start.

Heat exchanger input for the RS subsystems are determined simply by using the exchanger specification and the shell type exchanger input provided in the CONTAIN ESF component input. In the demonstration problem, the exchanger effective heat transfer area and overall heat transfer coefficient are combined as the cooler thermal conductance (coefficient x area), so that the inputted heat transfer coefficient is the overall thermal conductance for the total heat exchanger surface area and the surface area inputted is unity.

The addition of chill water to the recirculation circuit for the outside pumps poses a special problem of mixing two streams of water prior entering the exchanger and spray nozzles. To mix these two streams, a "dummy" CONTAIN cell is created with a sump. Into the mixing sump, water from the containment sump is flowing at a rate equal to the total pumping rate minus the chill water addition rate. The method for flowing the sump water into the mixing cell is through the use of an engineering vent (pool type) that links the containment cell to the mixing cell. The engineering vent is opened when the recirculation sprays start. Chill water is added to the mixing cell using a LOW-CELL external source table, at a rate and temperature specified for the chill water subsystem. Finally, the outside pump component is directed through input in the engineered safety feature ENGINEER block to use the mixing cell sump water as the source water for the spray system.

One additional note regarding sump water transfers: safety injection pumps are modeled by transferring sump water to a "holding" cell using, again, an engineering vent (pool type) input between the containment and "holding" cell. This method of input allows for excess water to be removed from the containment sump when the safety injection pumps are turned on.

Nitrogen Accumulators.

The accumulators in the subatmospheric plant are driven by nitrogen gas. To account for this gas mass in the containment atmosphere inventory of gases, an additional atmospheric external source input is included in the CONTAIN deck. The nitrogen gas inventory is determined from the accumulator gas volume, pressure, and temperature prior to release into the containment. A release rate is then calculated based on the gas inventory and the specified time to empty the accumulators.

Table 3-1 Reactor containment initial conditions for the demonstration calculation – minimum service water temperature conditions [Ref. 12].	
Component	**Initial Condition**
Service water temperature (K)	274.8
Refueling water storage tank (RWST) temperature (K)	283.2
Atmosphere temperature (K)	322
Water vapor partial pressure (kPa)	11.6
Air partial pressure (kPa)	82.7

Table 3-2 Accident chronology for a pump suction double-ended rupture (PSDER) LOCA [Ref. 12].	
Time, second	**Event**
0.0	Accident occurs
2.2	Containment depressurization actuation signal
18.4	First containment peak pressure occurs
20.8	End of reactor depressurization; core reflooding begins; safety injection pumps become effective
42.0	Accumulators empty
62.5	Quench spray subsystem and casing cooling become effective
253.4	Core reflooding ends; post-reflood frothing begins
304.0	Recirculation spray system becomes effective
1595.8	Post-reflood frothing ends
3370.0	Containment pressure becomes subatmospheric

Table 3-3 Summary of the CONTAIN qualification for long-term LOCA calculations in a subatmospheric containment.				
Accident Phase	Modeling Area	CONTAIN	Comments	Reference
Rapid pressurization	geometric nodalization	Single cell	For short-term pressurization phases, single cell nodalizations are shown to give conservative estimates of containment loads.	[CAR*, pp. 4-52, 4-80, 4-109]
	free volume	free volume reduce by water pool volume	Reduction of free volume by water pool represents a realistic modeling approach that is also conservative with respect to maximum containment loads.	N/A
	two-phase water injection	temperature flash modeling, with dropout of condensed liquid water	The thermal equilibrium (temperature flash) assumption is conservative. Dropout of condensed water during a two-phase injection is conservative, based on integral test comparisons.	[CAR, pp. 4-52, 4-53]
	heat and mass transfer to passive heat sinks	free convective condensation by HMT analogy	Free convective condensation by the HMT analogy has been shown to be a conservative method for estimating energy transfers during blowdown periods.	conservatism of free convective condensation [CAR, pp. 4-51, 4-73, 4-109]

* CAR is the CONTAIN Assessment Report which is a short-hand designation for a NRC informal report – "An Assessment of CONTAIN 2.0: A Focus on Containment Thermal Hydraulics (Including Hydrogen Distributions)," March 1999.

Table 3-3 Summary of the CONTAIN qualification for long-term LOCA calculations in a subatmospheric containment (cont.).				
Accident Phase	Modeling Area	CONTAIN	Comments	Reference
Slow pressurization/ depressurization	geometric nodalization	single cell	Low elevation of injection and presence of sprays produce a well mixed containment atmosphere that can be adequately approximated with a single compartment.	CAR [pp. 3-34,3-60,3-67,4-15]
	free volume	free volume reduce by water pool volume	Reduction of free volume by water pool represents a realistic modeling approach that is also conservative with respect to maximum containment loads.	N/A
	two-phase liquid water expansion	pressure flash method for pump-side water injection	Pressure flash method for injecting relatively cool liquid water is conservative; method compares favorably with FSAR.	N/A
	nitrogen gas injection from accumulators	single-phase gas injection	Addition equivalent to the method used in the FSAR.	N/A
	heat and mass transfer to passive heat sinks	free convective condensation by HMT analogy	The HMT analogy model has been validated in the large-scale HDR and AP600 containment testing programs where long-term pressure depressurization by passive heat transfer was a dominant process for atmospheric energy removal.	CAR [pp. 3-55,3-60] Ref [11]
	heat and mass transfer to pool surface	modeled	Addition of pool with heat and mass transfer represents a conservative model approach since evaporation of the hot sump water will slightly retard the depressurization rate.	CAR [p. 4-22]
	spray pressure suppression	condensation on spray droplet using HMT analogy method	Spray model has been validated using the separate effects and integral tests.	CAR [pp. 3-33,3-64,4-15]

Table 3-4 General modeling recommendations for a CONTAIN qualified long-term LOCA calculation in a subatmospheric containment.	
Phenomena	**Modeling Recommendation**
Multi-component gas compression	Nodalize the containment as a single compartment
Two-phase liquid expansion (reactor vessel depressurization)	Use a temperature flash method for liquid expansion (atmospheric SOURCE table), dropout unflashed liquid from atmosphere
Two-phase liquid expansion (reflood and post-reflood)	Use a pressure flash method for liquid expansion from the pump-side break having a low specific enthalpy (SRVSOR)
Single-phase gas injection from nitrogen driven accumulators	User external atmosphere source table for a nitrogen compound
Convective condensation	Use a *free* convective heat transfer correlation for the HMT modeling
Structure heat transfer	Account for liquid film and paint resistance for surfaces; include any steel-liner-to-concrete air gaps at constant, full width
Sump	Include sump atmosphere/pool surface heat and mass transfer
Spray droplet heat and mass transfer	Use a mass mean spray droplet size for the injected spray droplet diameter (~ 0.0005 m)
Quench spray (QS)	Use tank depletion to determine start of QS; source table for mass flow rate using a variable rate to model pressure dependence of spray rate; heat exchanger modeled
Recirculation spray (RS)	Use tank depletion to determine start of RS; add mixing cell to provide proper water temperature for outside pump subsystem; heat exchanger modeled

Table 3-5 Input guidance for modeling a long-term LOCA calculation in a subatmospheric containment.		
Input Section/Block	**Parameter(s)**	**Comment**
Global:		
Nodalization	ncells = 3	containment modeled as single cell for conservatism during the rapid pressurization phase, and as a good approximation for slow depressurization phase; mixing cell for outside RS pump subsystem; "dummy" cell for safety injection pumping of excess sump water
Material properties	user defined properties	density, thermal conductivity, and specific heat capacity for air, stainless steel, steel, and concrete are set for equivalency
Timesteps	~ 0.0 - 0.05 seconds during rapid pressurization; 0.1- 2 seconds during slow depressurization	variable set to give accurate results for the time scale of interest during each accident phase
Flow	DROPOUT; engineering vents (pool type) for pumping containment sump water to mixing cell and "dummy" holding cell	dropout condensed liquid water in atmosphere for equivalency and conservatism; vents are opened to start flow; use "vmflow" to specify pump rate
Upper Cell: (containment cell)		
Geometry	gasvol	given free volume
Atmosphere initial conditions and sources	ATMOS block; SOURCE block	pressure, and temperature equivalency (saturated conditions for conservatism); external sources for temperature flash during two-phase blowdown phase and for steam during the reflood phase; nitrogen gas injection during accumulator injection period
Safety relief valve source	SRVSOR block	external source for pressure flash of low enthalpy water injected from the pump-side of pipe rupture during the reflood phase

Table 3-5 Input guidance for modeling a long-term LOCA calculation in a subatmospheric containment (cont.).		
Quench spray (QS)	SPRAY block input	spray droplet diameter set to mass mean diameter of spray nozzle distribution, released at full height: spdiam = 0.0005 meters; sphite = 30-40 meters; external source table (based on QS flow rate vs. pressure curve); hex input based on exchanger thermal conductance, shell water flow rate, and inlet temperature.
Recirculation spray (inside)	SPRAY block input	spray droplet diameter set to mass mean diameter of spray nozzle distribution, released at full height: spdiam = 0.0005 meters; sphite = 25-30 meters; tank input with dummy small inventory and rate to set time to start recirculation pump; pump input at specified flow rate from sump; hex input based on exchanger thermal conductance, shell water flow rate, and inlet temperature.
Recirculation spray (outside)	SPRAY block input	spray droplet diameter set to mass mean diameter of spray nozzle distribution, released at full height: spdiam = 0.0005 meters; sphite = 25-30 meters; tank input with dummy small inventory and rate to set time to start recirculation pump; pump from mixing cell sump at the specified flow rate; hex input based on exchanger thermal conductance, shell water flow rate, and inlet temperature.
Structures	STRUC block input	fully implicit algorithm (default); free convection (default); maximum liquid film thickness (default); paint resistence set for equivalency; no thermal radiation; air gaps of constant thickness (if specified); initial condition for equivalency; surface node thickness as fraction of diffusion length (see Section 2.1.2.3)
Lower cell: (containment cell)		
Low-cell	surface area: geometry = basemat surface area	All condensed water dropped from atmosphere, spray removal, and condensate overflow from structures are diverted to pool; free volume displacement by pool water mass (default); pool/atmosphere heat and mass transfer; basemat/pool heat transfer.

Table 3-5 Input guidance for modeling a long-term LOCA calculation in a subatmospheric containment (cont.).		
Upper cell: (mixing cell)		
Geometry	gasvol	set to large value – 1.0×10^6 m^3
Atmosphere/pool interaction	ht-tran off off off off off	no interaction between atmosphere and pool
Lower cell: (mixing cell)		
Low-cell	Pool SOURCE	chill water addition to outside RS subsystem at specified rate and temperature
Upper cell: (holding cell)		
Geometry	gasvol	set to large value – 1.0×10^6 m^3
Lower cell: (holding cell)		
Low-cell	geometry	"dummy pool input" (see Appendix D)

Table 3-6 Recirculation spray subsystem conditions used for the subatmospheric demonstration calculation.		
Description	**Outside containment**	**Inside containment**
Recirculation spray pump (shell side) flow rate (kg/s)	230.4**	209
Service water (tube side) flow rate (kg/s)	285	285
Service water (tube side) inlet temperature (K)*	275	275
Recirculation spray cooler thermal conductance (UA) Watts/K	1.9239×10^6	1.8712×10^6

* minimum service water temperature
** includes 48.1 kg/s of chilled water addition at 283.1 K

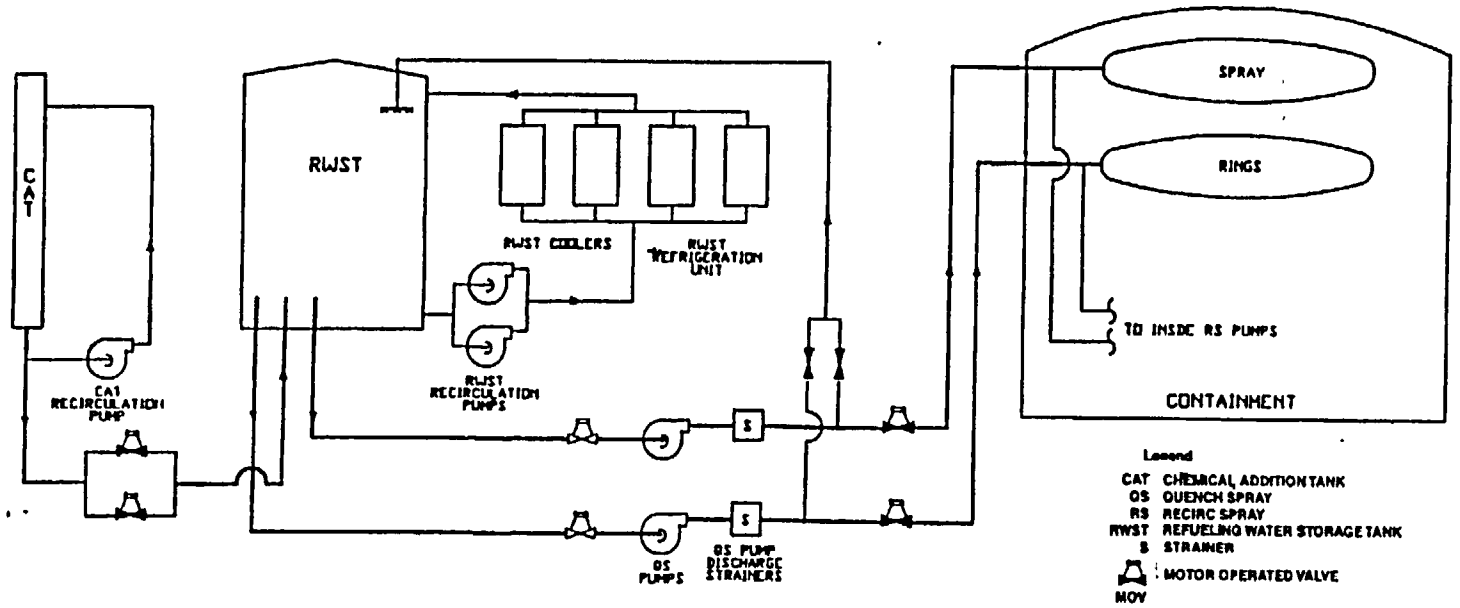

Figure 3-2 Quench Spray Subsystem

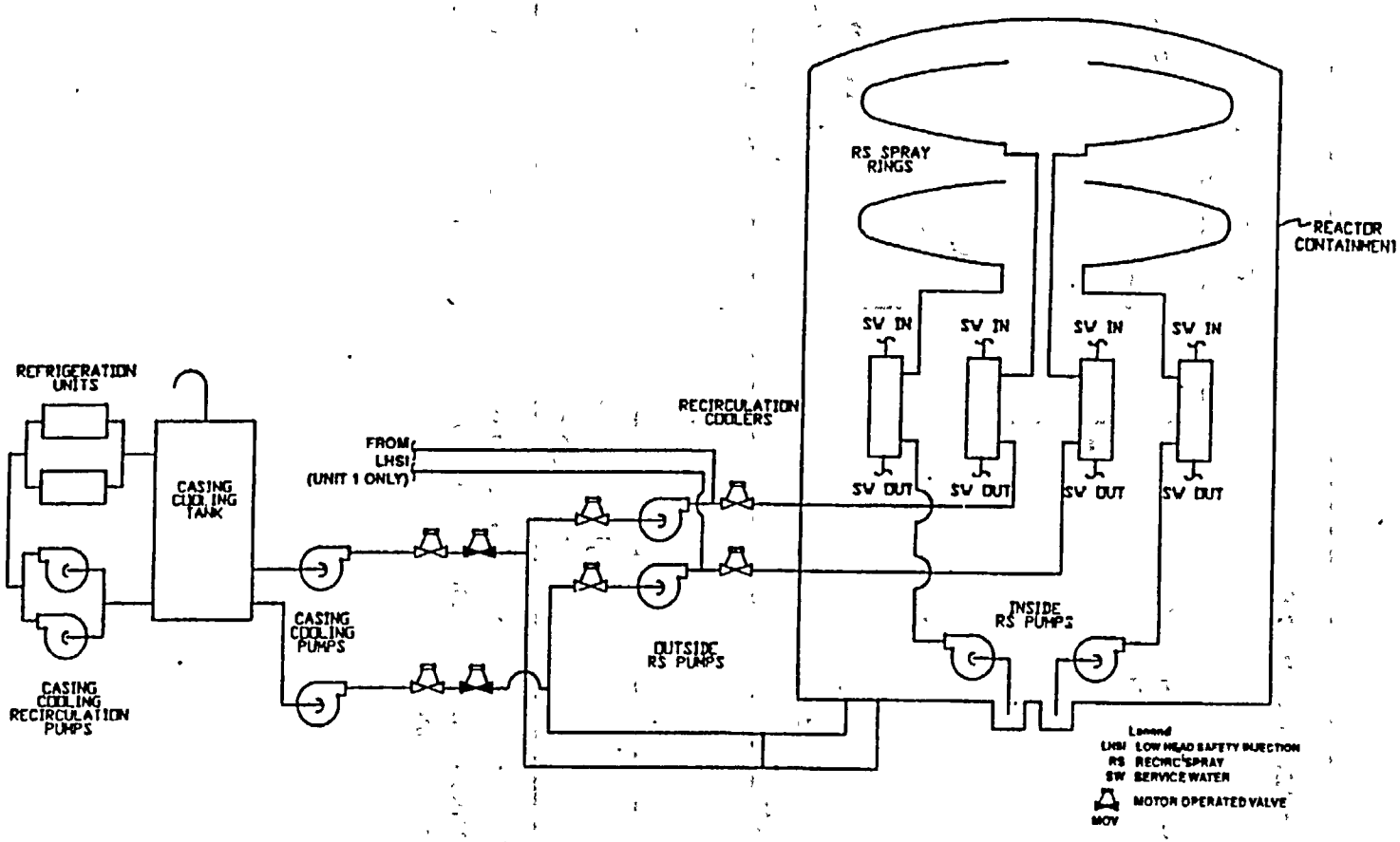

Figure 3-3 Recirculation Spray Subsystem

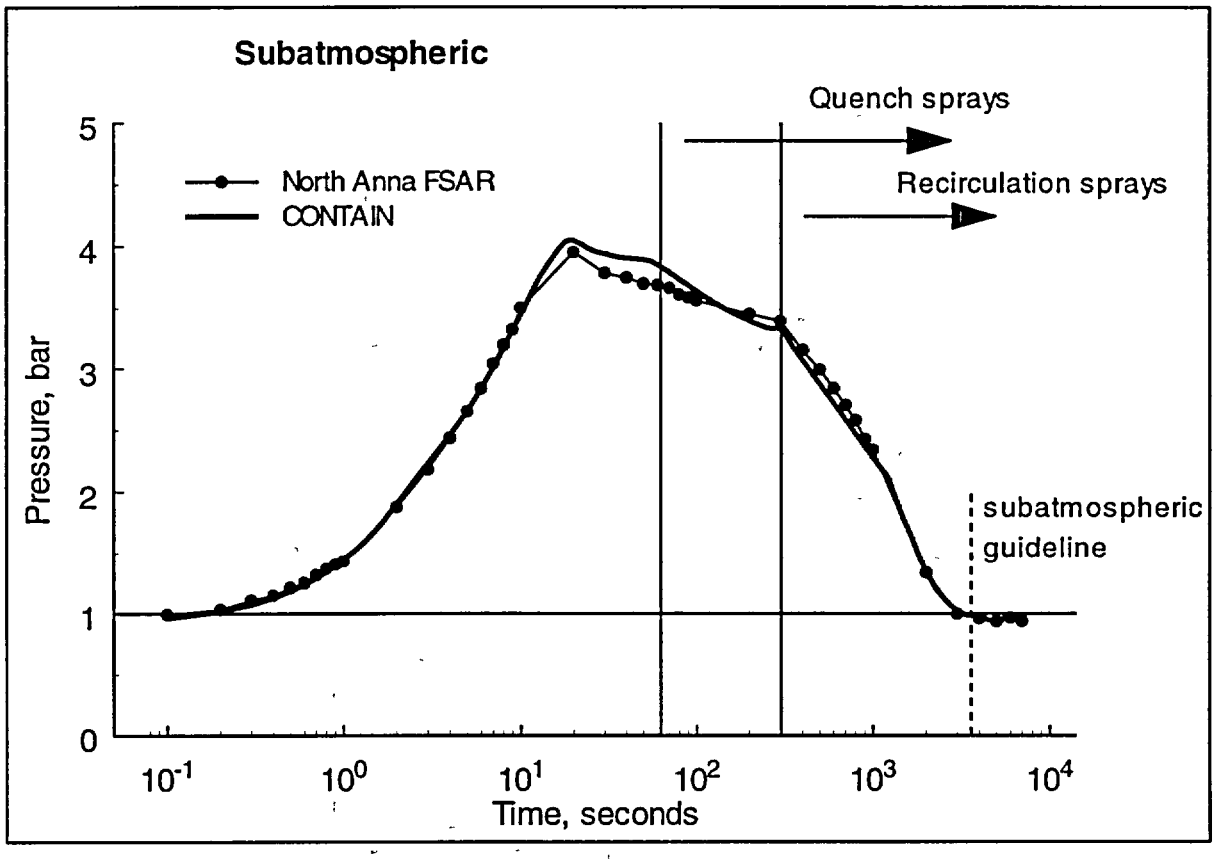

Figure 3-4 Pressure comparisons for a subatmospheric containment analysis for a PSDER scenario, showing that subatmospheric conditions are recovered in less than 3600 seconds.

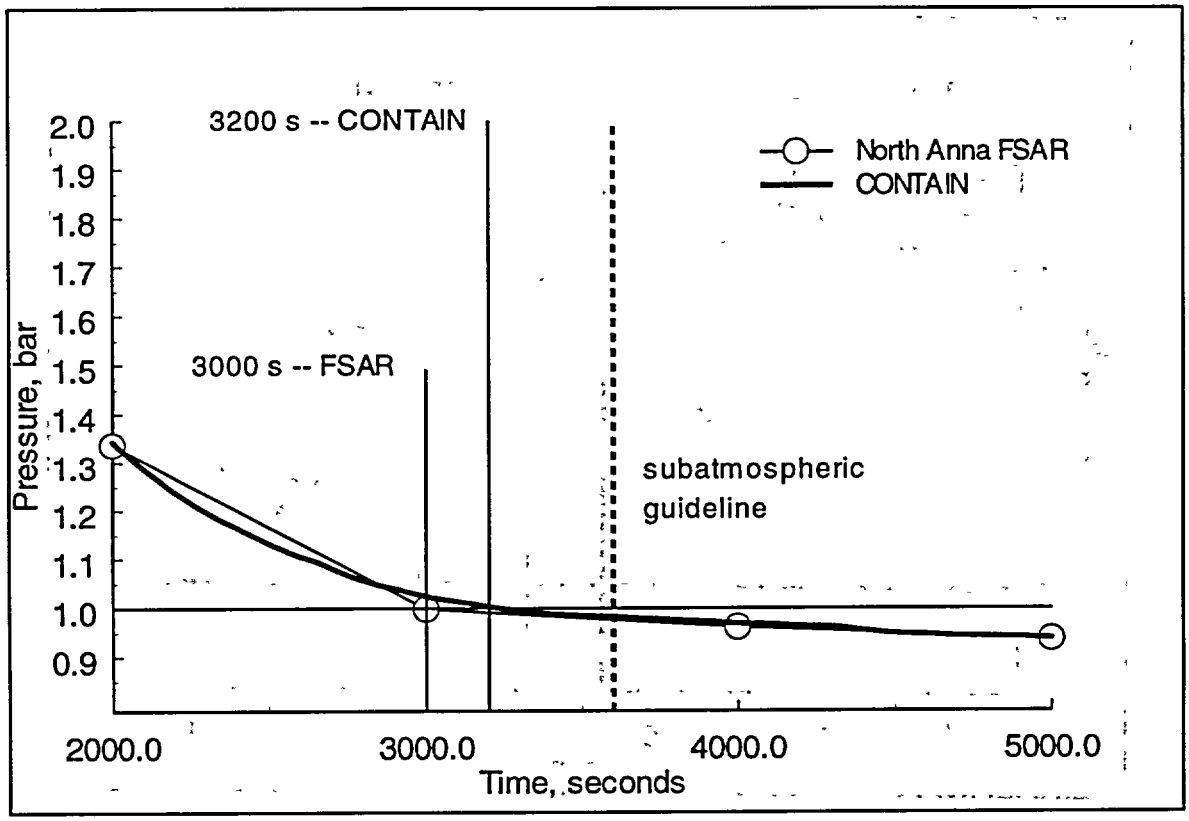

Figure 3-5 Pressure comparison showing the pressure profiles in a time window near the point of return to subatmospheric conditions for the PSDER scenario.

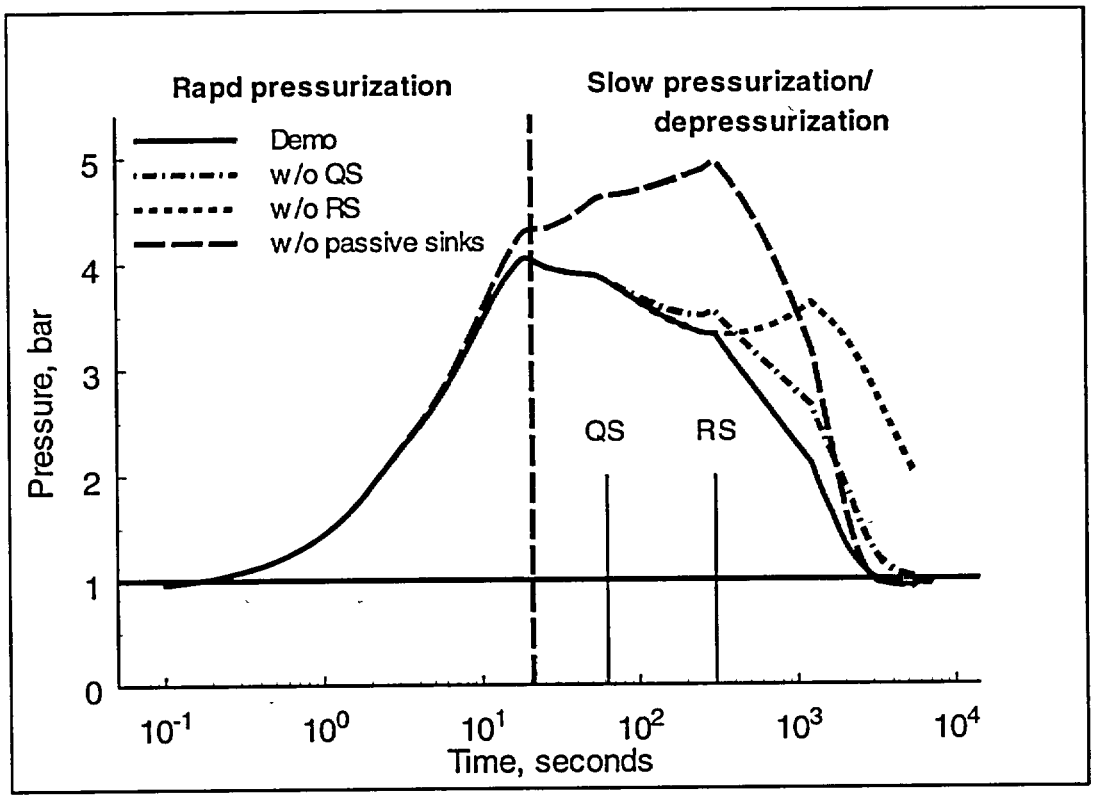

Figure 3-6 CONTAIN pressure profile for the PSDER scenario showing the effects of various energy removal processes on the pressure predictions.

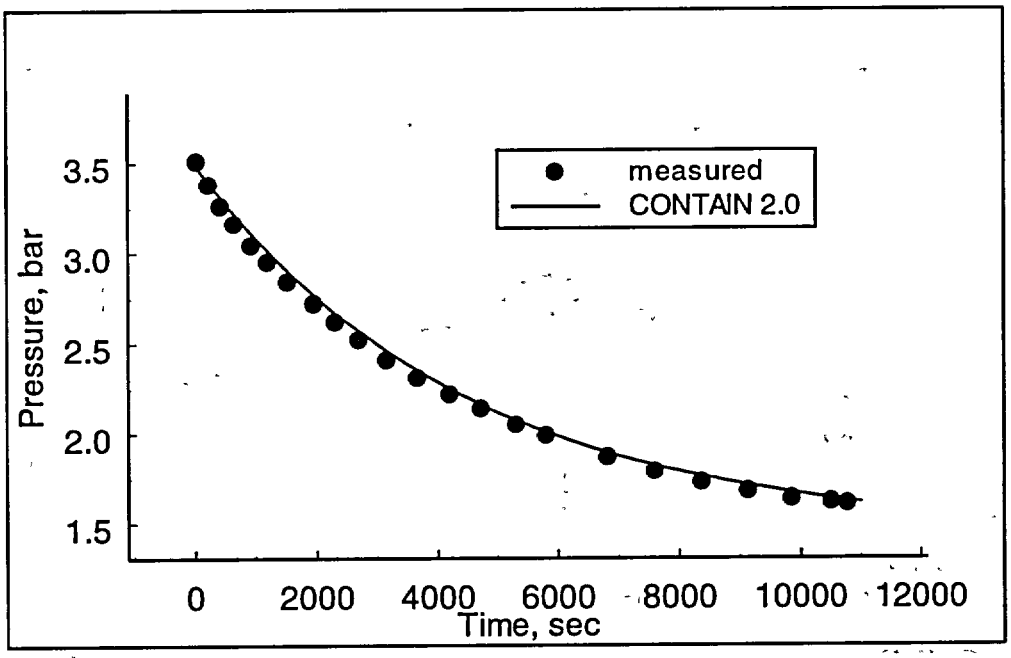

Figure 3-7 Comparison of measured and calculated pressure suppression for JAERI test PHS-6 (single nozzle spray) [CAR, p. 3-50].

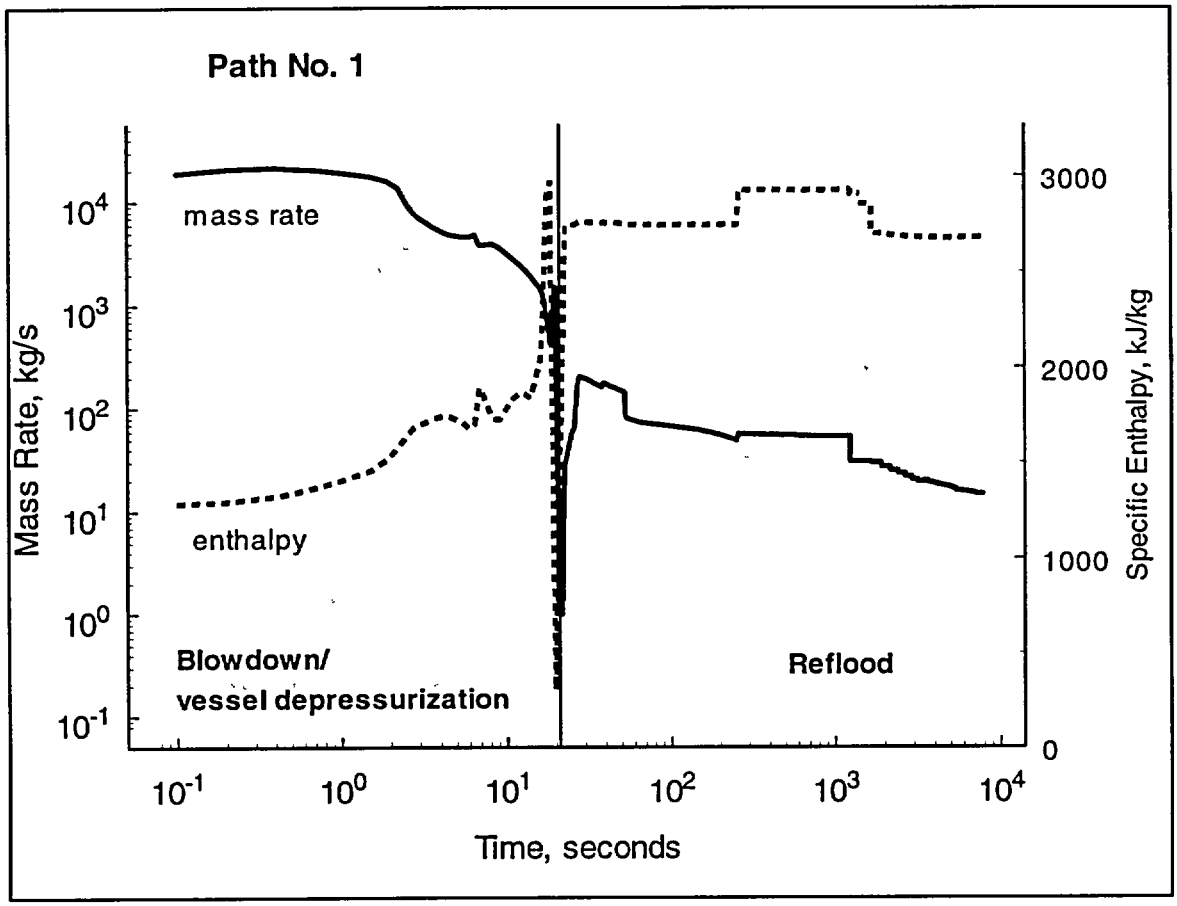

Figure 3-8 Water injection into containment for a PSDER scenario; path no. 1 is on the steam generator side of the double-ended pipe rupture.

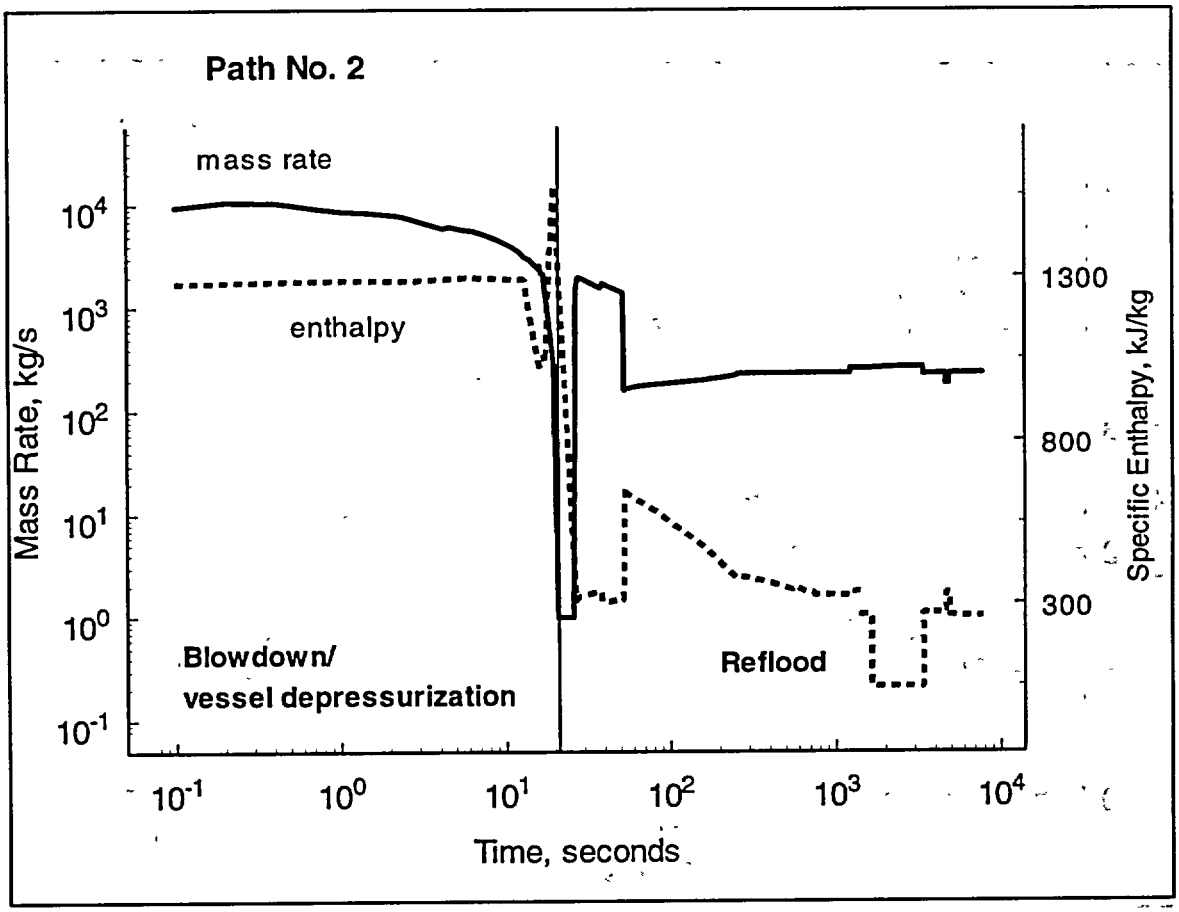

Figure 3-9 Water injection into containment for a PSDER scenario; path no. 2 is on the pump-side of the double-ended pipe rupture.

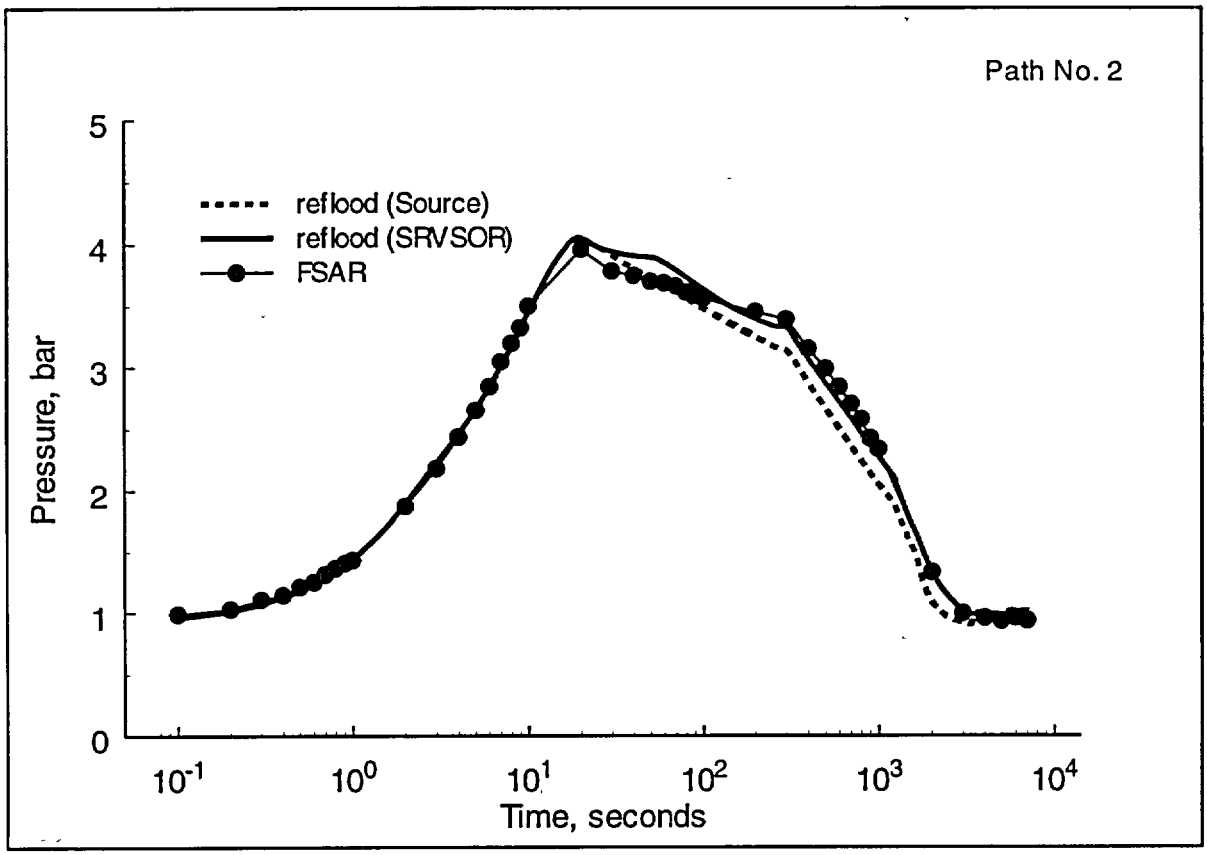

Figure 3-10 CONTAIN and FSAR pressure profile comparisons for a PSDER scenario, showing the effect of different modeling methods for treating the pump-side reflood water injection into the containment.

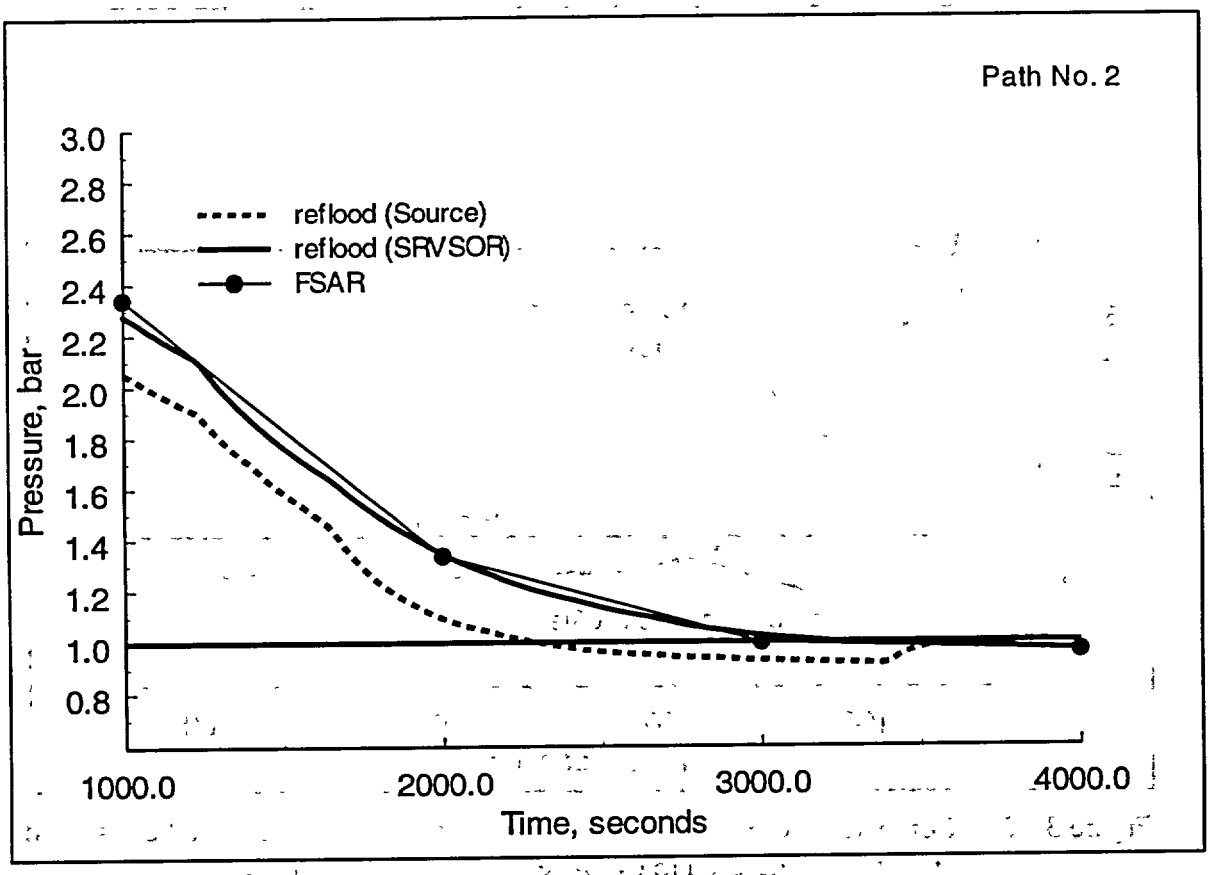

Figure 3-11 CONTAIN and FSAR pressure profiles in the time region where the pressure returns to subatmospheric conditions. The CONTAIN results show the effect of two modeling approaches for treating the injection of pump-side water during the reflood phase of a PSDER accident.

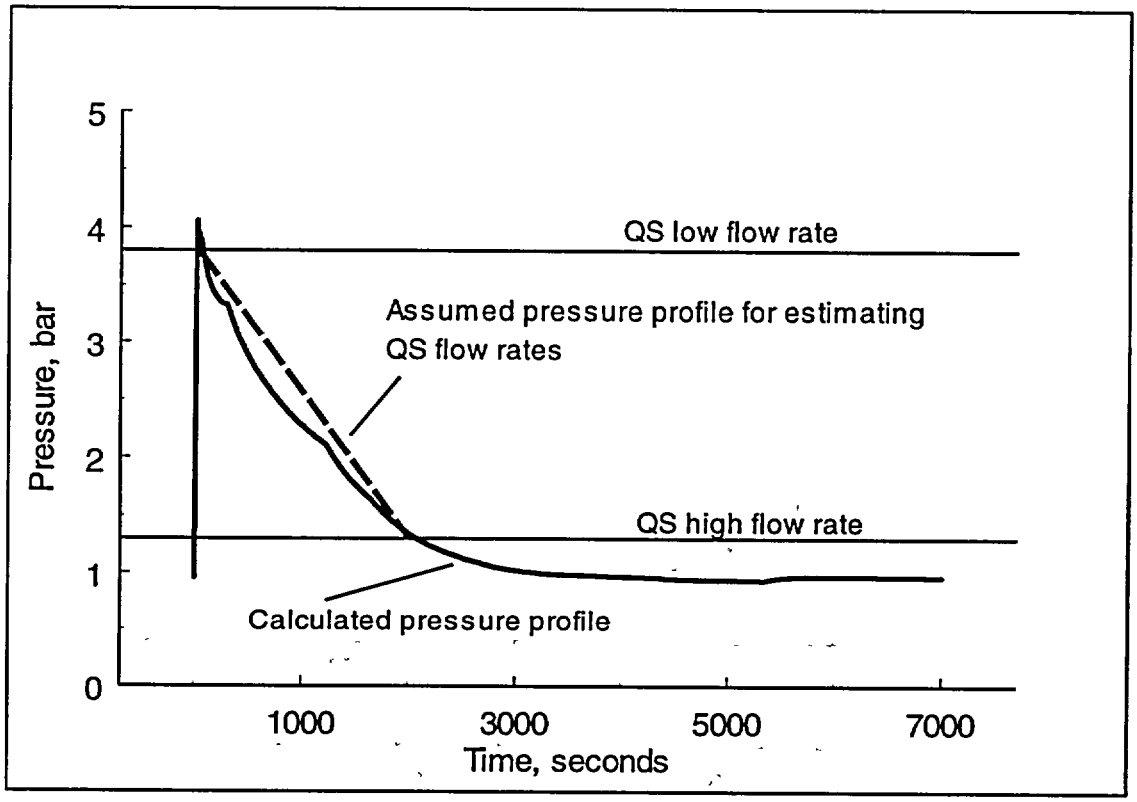

Figure 3-12 Comparison of CONTAIN calculated pressure profile with the assumed pressure profile used to estimate the quench spray flow rate as a function of pressure.

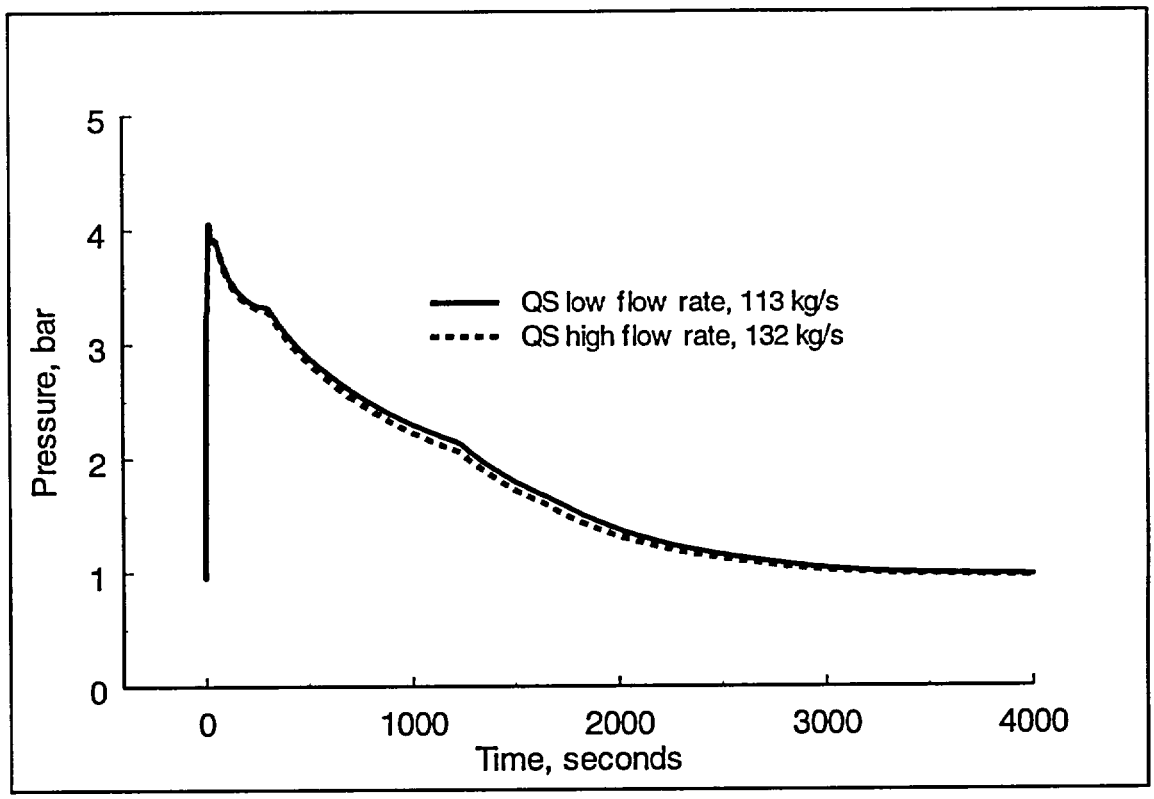

Figure 3-13 CONTAIN calculated pressure profiles for a PSDER scenario, showing the effect of bounding quench spray flow rates on depressurization.

4 Ice Condenser Containment Analysis

In this chapter we discuss qualification and methods that can be used to model DBA response of a PWR ice condenser containment with CONTAIN [1]. Figure 4-1 depicts a typical ice condenser containment. A representation of the containment lower compartment and ice condenser are shown in Figures 4-2 and 4-3, respectively. Ice condenser containments make use of large columns of ice to condense steam from the containment atmosphere following a large pipe rupture in the reactor coolant or secondary coolant system located in the lower compartment.

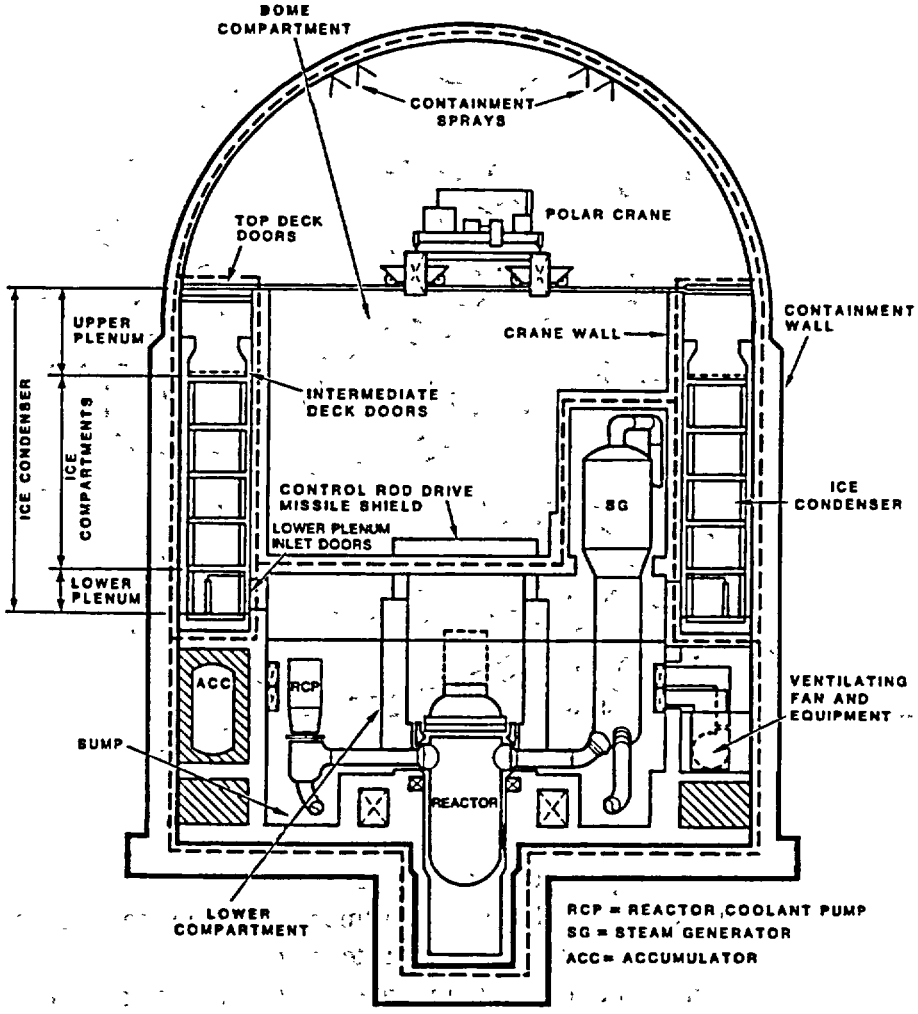

Figure 4-1 Typical PWR ice condenser containment showing the three regional divisions of the containment: lower compartment, ice condenser, and dome or upper compartment.

Rapid condensation of steam provides a method for limiting the maximum short-term pressure increases in the containment as lower compartment steam, driven by the pressurization, is removed from air/steam inflows to the condenser region. A simple sketch of this pressure-suppression process is shown in Figure 4-4. Long-term pressure control is maintained similarly through a continuous removal of steam that has been generated by decay heating of vessel water. In these long-term scenarios, a directed air/steam inflow to the ice condenser is produced by use of deck fans. Additional margins for pressure control are designed into the containment by including containment sprays (quench and recirculating sump spray subsystems), as indicated in Figure 4-5. The sprays may be positioned, in some designs, in both upper and lower compartment regions.

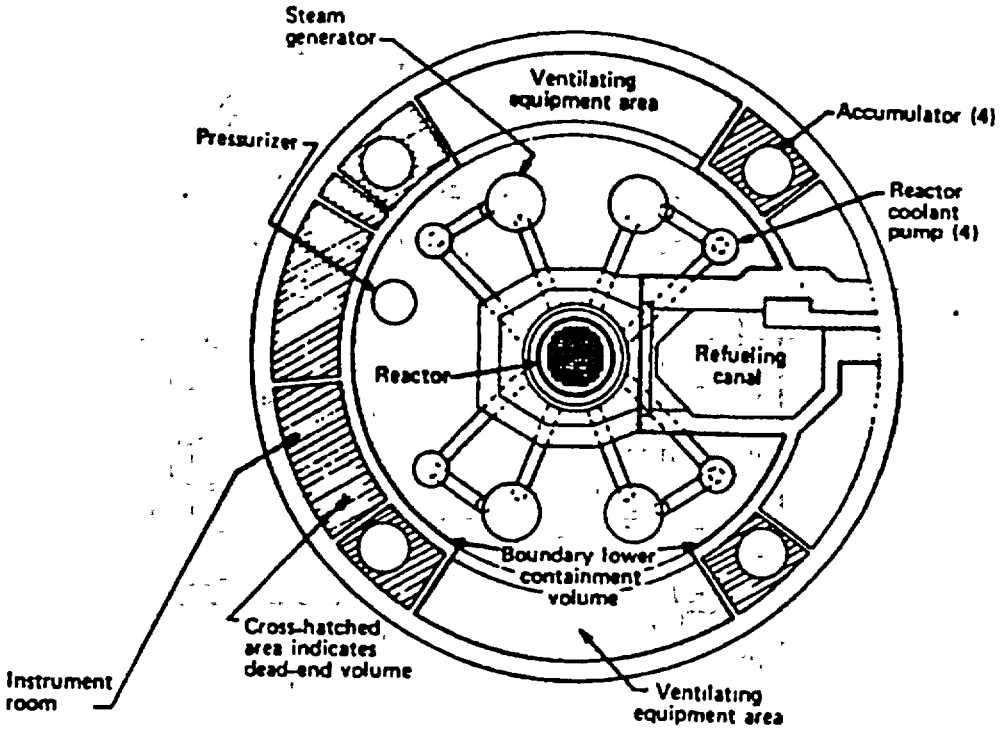

Figure 4-2 Lower compartment of a typical PWR ice condenser showing the two subregions of this compartment: the open region contains the reactor pump and piping, and steam generators; dead-ended regions contain the instrumentation and other engineering safety features.

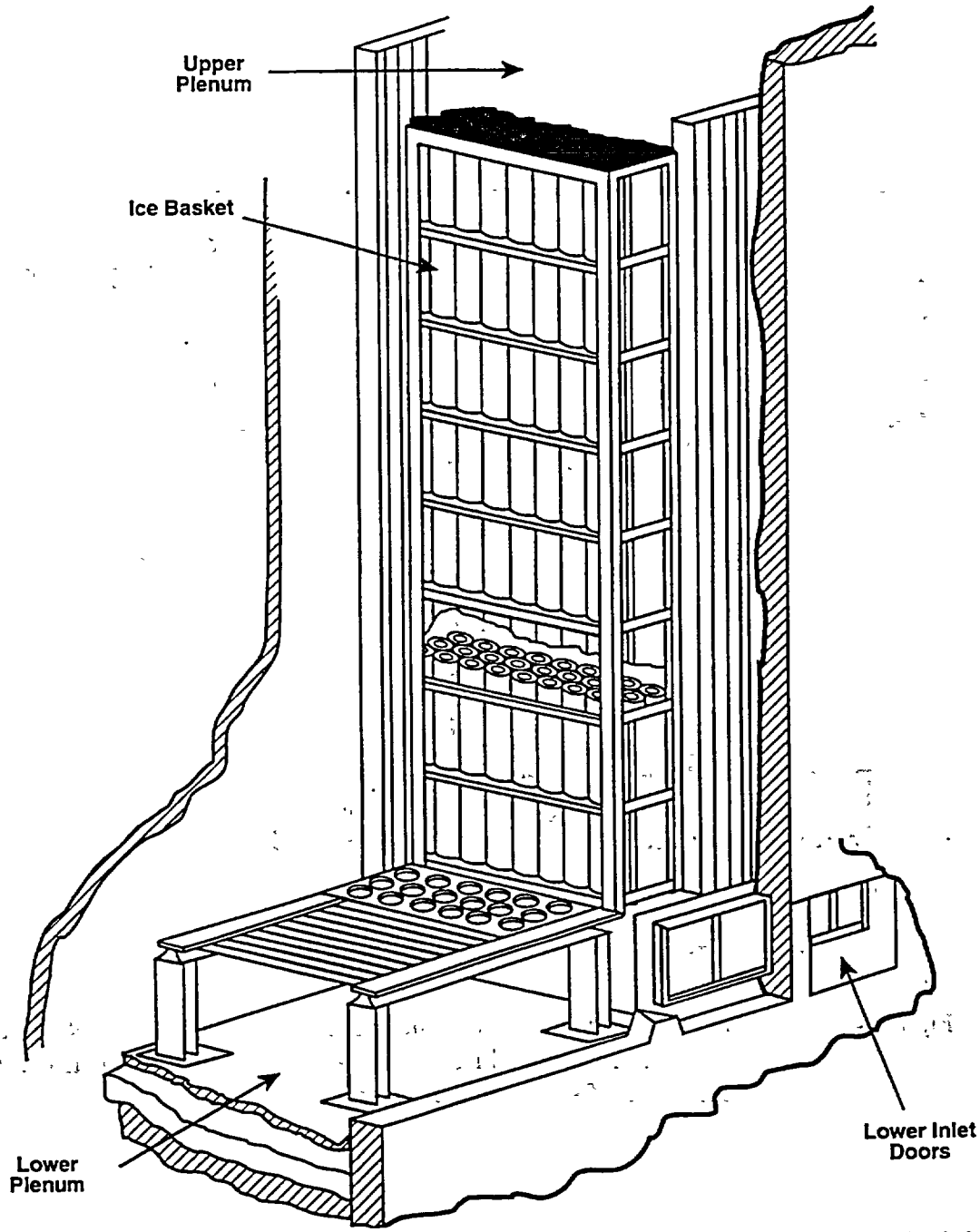

Figure 4-3 Cross-sectional sketch of a typical PWR ice condenser showing the inlet doors, lower plenum, ice bed with ice baskets, and upper plenum.

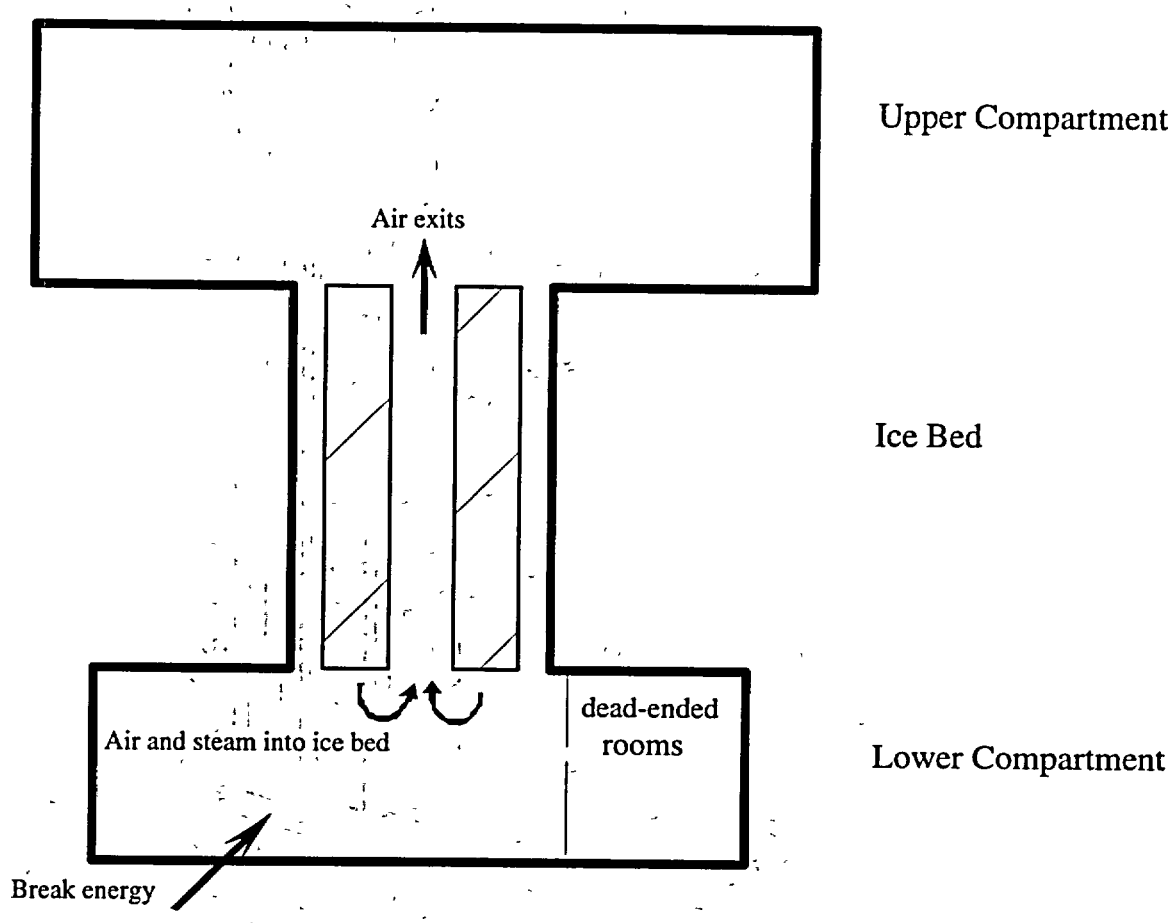

Figure 4-4 Sketch showing the pressure-suppression control for a PWR ice condenser where steam is removed from the lower compartment injection by condensation of steam on ice surfaces.

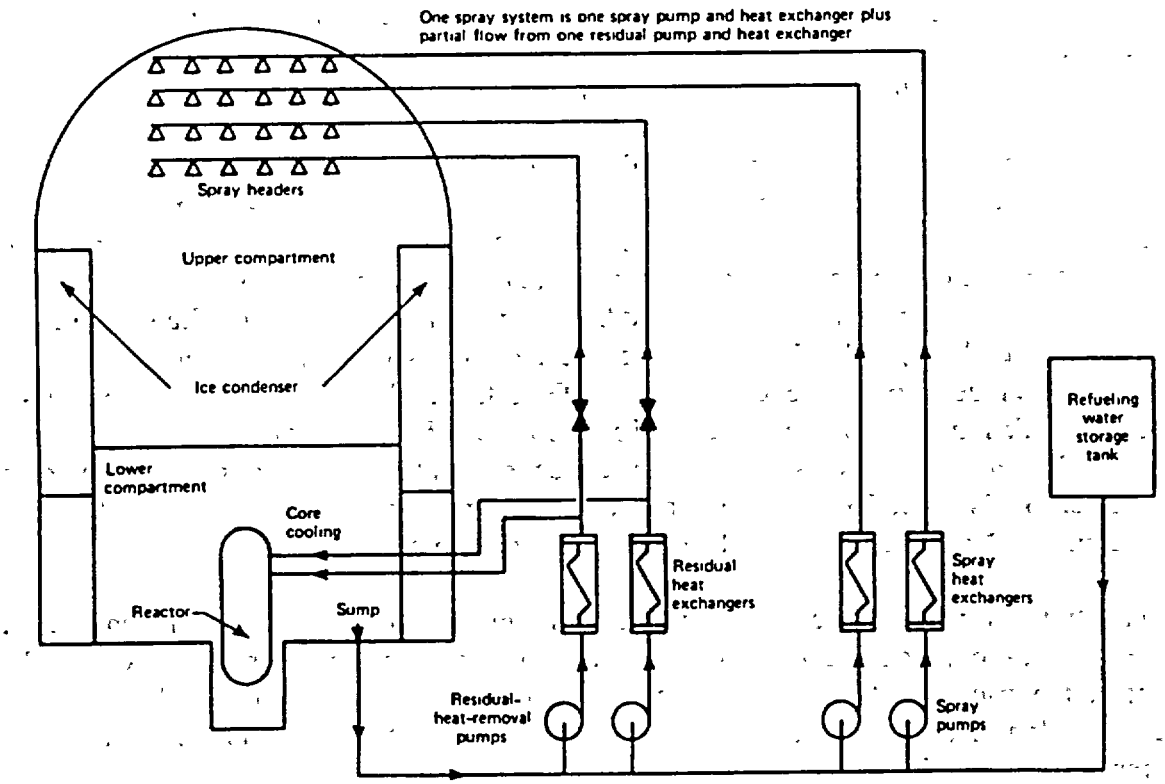

Figure 4-5 Typical layout of containment quench and recirculation spray subsystems for a PWR ice condenser containment.

With pressure-suppression capability, ice condenser containments are designed with a smaller total free volume and lower design pressure than large dry containments. The load analysis for these containments focuses on the assessment of pressure-suppression performance, where maximum pressures and pressure differentials that developed during pipe rupture events are evaluated. Pressure control, as steam is continuously generated during the post-blowdown time period, must be verified during the ice melting phase and after ice melt out.

As a result of the compartmentalization that is designed into the containment for pressure-suppression enablement, ice condenser containments require multiple-cell modeling methods, and therefore represent a more complex geometrical setup than used for either large dry or subatmospheric containments. Some of the more difficult aspects associated with modeling pressure-suppression containments are addressed in an assessment report featuring the CONTAIN code applied to Westinghouse's scaled prototypical type ice condenser tests. This report, which describes these tests and the CONTAIN validation for ice condensers, has therefore been included in this report as an appendix (Appendix H), and may be consulted to illuminate some of the modeling issues unique to ice condenser containments. In the following discussion, we refer to this appendix to support various modeling recommendations and input preparation guidelines. [Note that Appendix H is *not* in this version of the report]

In Section 4-1, we describe a short-term LOCA scenario for a demonstration plant, and discuss the qualification, model recommendations, and input preparation when using CONTAIN. We extend the discussion to a long-term demonstration analysis in section 4.2, where we describe an example long-term scenario, the CONTAIN qualification, model recommendations, and input preparation guidelines.

4.1 LOCA Short-term Accident Analysis

In the short-term accident analysis, we used the Watts Bar Nuclear Plant Final Safety Analysis Report [13] to obtain specific information for our demonstration calculation; this consists mostly of information on the geometrical arrangement of the containment and specific blowdown source data. We compare CONTAIN results to the TMD code [14] calculations, as reported in the FSAR, to support our conclusions regarding qualification where a degree of equivalency is sought, and refer to the CONTAIN validation efforts (Appendix H) to show qualification based on CONTAIN performance studies.

4.1.1 LOCA Short-term Scenario

The LOCA short-term scenario is initiated by a double-ended rupture in either a hot or cold leg of the reactor primary coolant piping. In the scenario selected for a demonstration calculation, a rupture is assumed to occur in the cold leg. During the reactor coolant system depressurization, a release of high pressure, subcooled water pressurizes the lower compartment of the reactor containment. Shown in Figure 4-6 is the mass and energy release for a typical cold leg pipe rupture. As the lower compartment pressure increases, the lower plenum doors rapidly swing open allowing inflow to the ice condenser lower plenum. Flow continues from the lower plenum

to the ice bed, and then from the ice bed into the upper plenum through intermediate doors on the top of the ice bed. Finally the flow enters the upper compartment through the top ice condenser doors. Lower compartment maximum pressurization occurs within a ~ 2 seconds after a pipe rupture for a design-basis LOCA.

Because the break injection is subcooled, the blowdown generates a two-phase steam/liquid stream exiting the lower compartment. During this early portion of the blowdown, unflashed water will be partly entrained into the highly turbulent flow in the lower compartment that enters the ice condenser. This portion of air/steam/liquid that enters the condenser also exits into the upper compartment, but most of the steam content of the flow stream is removed by condensation onto ice surfaces. Additionally, a fraction of the lower compartment air (trapped in the lower compartment dead-ended regions) remains in the compartment and is not available for transport to the upper compartment. Total air transported into the upper compartment pressurizes that compartment mainly as a result of air accumulation. Temperature increases in the upper compartment are therefore at a minimum.

4.1.2 Qualification

In qualifying the CONTAIN code for ice condenser containment analysis, we explore issues of equivalency and validation. For addressing equivalency, we approach the qualification by comparing the CONTAIN calculations to TMD code results for calculating pressurization and the pressure differentials across the operation deck; TMD code results are obtained from the Watts Bar FSAR. Qualification by validation is an approach where there is a transference of validation conclusions arrived at in the Waltz Mill assessments (Appendix H) to the demonstration calculation for short-term containment response. These two approaches are complementary, and actually differ only in terms of one input parameter, the multiplier on the ice bed Nusselt number for an ice column to account for interstitial flow and roughness.

Shown in Figure 4-7 are the CONTAIN pressurization profiles in a PWR ice condenser containment compared to results report in the Watts Bar FSAR obtained using the Westinghouse TMD code. A summary comparison of CONTAIN and TMD models is provided in Appendix B. The pressurization profiles in Figure 4-7 show that CONTAIN results are in good agreement with the TMD calculation, especially in the case of upper compartment pressurization. For example, Figure 4-8 shows that the upper compartment pressures calculated with CONTAIN are generally within a +/- 5% equivalency band centered on the TMD code results. More importantly, for the lower compartment comparisons, the CONTAIN predicted maximum average pressure is also within a +/- 5% equivalency band based on the TMD code results, see Figure 4-9. The shift of the lower compartment pressure profile between codes, CONTAIN profile slightly delayed, has been noted also in comparisons with TMD results reported for the Waltz Mill test and discussed in Appendix H. Those comparisons indicated that the shifted profile as calculated with CONTAIN was, in general, in better agreement with data than the profile calculated with TMD. The slight shift in the CONTAIN pressurization profile is believed not to be a concern for qualification; rather, we observe that the shift is consistent with a previous experimental study that favors CONTAIN predicted pressurization rise over TMD calculations. Furthermore, the

shift has no effect on the estimated maximum pressurization during the accident.

A design criterion for a PWR ice condenser is the limitation on the pressure differential across the containment operation deck that divides the lower and upper compartments. We show the pressure differential, difference between the pressure in a local region of the pipe rupture and the upper containment, in Figure 4-10. The profile of the CONTAIN pressure differential is compared in the figure with the maximum pressure differential reported in the Watts Bar FSAR. The comparison shows that the maximum pressure differential calculated with the CONTAIN code is reasonably within a +/-5% variation of the TMD maximum pressure differential.

The comparison of pressure calculations between CONTAIN and TMD codes are quite exceptional. Agreement is a reflection of the similarity within each code for key phenomena modeling and the relative insensitivity of key results to phenomena that is modeled differently. For instance, we note that condensation in the ice condenser is not an especially sensitive phenomenon as long as a limiting condensation rate is calculated that assures that most of the steam inflow is removed before reaching the upper containment. Even though the condensation models are quite different, this limit condition is realized by each code. However, we do note that a small variation in pressurization can be realized by adjusting the multiplier on the Nusselt number in the ice columns (cihtml). The CONTAIN results that are represented in Figures 4-7 through 4-10 have been obtained using a multiplier (cithml) of 40 for each ice bed cell (#4 - #7).

One of the key phenomena for the pressure predictions is the amount of entrained water transported from the lower compartment to the lower plenum and ice bed. A mechanistic model to determine this entrainment fraction is beyond the scope of both codes. However, through analysis, e.g., the sensitivity analysis performed in Appendix H, it has been shown that conservative pressure predictions will be obtained assuming 100% entrainment. In both the CONTAIN and TMD code results presented here, the entrainment is assumed to be 100%; and therefore, for this phenomenon the modeling is equivalent.

Due to the lower compartment rapid pressurization rate, there is a need to consider the possibility that flow exiting through the lower plenum doors may choke, that is, the flow may reach the critical two-phase flow limit.. In that case, the pressurization rate may increase even more rapidly than for unchoked flow as a result of the limitation on the rate of the escaping air/steam mixture from the lower compartment. To assess this possibility and account for the effect of critical flow, both the CONTAIN and TMD codes include two-phase critical flow models. The models are similar but not identical. For the CONTAIN code, a "frozen" homogeneous equilibrium model (FHEM) is used; whereas, the TMD code uses a homogeneous equilibrium model (HEM).[1] These models are compared in Figure 4-11, where the reservoir pressure may be related, in the case of an ice condenser containment, to the lower compartment pressure with flow represented as the mass flux exiting the lower compartment. There are a number of points to consider from

[1] An explanation of the the assumptions for the FHEM and HEM for critical flow is given in Reference [16].

Figure 4-11:

- For each model, critical flow increases as the upstream or reservoir pressure increases.
- The HEM produces lower critical flows than the FHEM.
- An experimentally derived correction factor for the HEM (as referred to as an augmented flow correction) applied to the HEM results for a flow quality x = 0.4, gives critical flows that are in very good agreement with the FHEM used in CONTAIN. (This conclusion is consistent with a similar conclusion from the literature that the FHEM more accurately represents experimentally measured critical flow rates.)
- Applying a multiplication factor F of 0.7 to the FHEM flows, reduces those flows well below the HEM results without augmentation.

The more conservative model for critical flow prediction is that model that calculates the lowest critical flow or limit flow exiting the lower compartment. Clearly, a fractional multiplier must be applied to the FHEM to produce such a critical flow. The CONTAIN calculations that have been reported in Figures 4-7 through 4-10 have been run using a multiplication factor F of 0.7. In the CONTAIN jargon used in the CONTAIN code manual, such a multiplication factor is referred to as the vena contracta factor, VCONTRA. An emphasis on critical flow modeling is important if the conditions of critical flow are satisfied. We note however, even with the disparity in the critical flow models, as shown in Figure 4-11, the CONTAIN and TMD code pressurization results are in good agreement. This can occur only in the case where conditions for critical flow have not been realized in either code model. It is concluded then that critical flow is not a factor in the demonstration calculation. Such an assessment is consistent with the analyses performed in the full-scale Waltz Mill tests, and is the basis for the conservative estimate for the multiplication factor F, as explained in the following discussion on model validation.

Model Validation.

The phenomena occurring in an ice condenser during the rapid pressurization phase of a LOCA event is very complex. There are issues regarding entrainment, two-phase choking, forced convective condensation in a time varying flow geometry, and drain-down effects of suspended or entrained liquid within channels in the ice bed and regions of the lower plenum, only to name a few. To assess the importance of these various processes, and to calibrate the modeling approaches, Westinghouse conducted a series of full-scale ice condenser blowdown tests in their Waltz Mill test facility. We have included in Appendix H an assessment of the CONTAIN code for modeling rapid pressurization in the Waltz Mill facility. From this assessment we were able to 1) calibrate the multiplier in the ice bed convection correlation used in the HMT analogy, and 2) set conservative bounds on the critical flow model used to limit two-phase flow in regions where pressure differentials across flow paths are large. These methods, can be misinterpreted as tuning, are appropriate only when there is a sufficient database of experimental information for tests that themselves are geometrically and temporally "scaled" to represent a full scale

containment event accurately. In the case of the Waltz Mill tests, distortions in the measured and containment conditions are minimized such that quantitative conclusions regarding the setting of parameters may be transferred directly from test to a containment event. We have this type of scaling with the Waltz Mill tests that allows transference of calibration parameters – for these tests, the geometry is full-scale and the rate processes are essentially identical with the postulated accident event. Two of the input parameters of special interest in the calibration of ice bed energy transfers are the liquid film thickness and multiplier on the Nusselt number in the ice columns. Both parameters affect the steam condensation process in the ice beds, and therefore also affect the inflows from the lower compartment to the ice bed. These flow rates directly determine pressurization rates. We have set the film thickness to a very small value to minimize liquid film resistance. This setting seems reasonable in the sense that surface water will be entrained by the high flow velocities within the ice bed where most of the condensation is occurring. The multiplier therefore becomes the main calibration parameter for the experiments. We have determined that a very good fit between calculations and measured pressurization occurs with a multiplier of 10. This value is less than that used above for establishing equivalency with the TMD code. Figures 4-12 through 4-14 show the comparison of CONTAIN results with the two choices of multipliers. In these figures we see that selecting a multiplier of 10, as compared to 40, produces a slightly more conservative pressurization profile; yet, either choice produces an equivalent pressure differential profile.

We also note that in the CONTAIN code application to the Waltz Mill tests, insights into the key phenomena and the appropriateness of various other modeling assumptions have been provided. For example, the conservatism associated with an assumed 100% entrainment model is demonstrated in the Waltz Mill assessments. The experiments also provide a needed justification for elimination of some modeling – like the inertia model for the lower and intermediate ice condenser doors in the CONTAIN code. Appendix H; therefore, provides validation of the CONTAIN methodology and corresponding user selection of input for ice condenser calculations, representing a valuable contribution for qualifying the CONTAIN code.

In the above discussion on comparisons with the TMD code, it was mentioned that critical flow is apparently not a modeling issue affecting the containment pressurization in the demonstration calculation – in either the CONTAIN or TMD applications. We would anticipate this conclusion based on the Waltz Mill analyses. Shown in Figure 4-15 are the lower compartment exit flows as calculated with the CONTAIN momentum equation and as would be predicted using the CONTAIN FHEM for critical flow (with and without a multiplication factor applied). For the demonstration calculation presented in Figures 4-12 through 4-14, a multiplication factor of 0.7 has been inputted to the code, as the vena contracta input VCONTRA. From Figure 4-15, we see that curve labeled "0.7 * G_{cnt}" just bounds the unchoked flow G. We have based our selection of the factor "0.7 " on experimental assessments of the Waltz Mill tests, as explained in Appendix H. The choice of this factor gives the most conservative critical flow modeling, that is also consistent with experimental analyses, where we have concluded critical flow was not attained in the Waltz Mill tests investigated.

A summary of the qualification of the CONTAIN code for short-term scenario is presented in Table 4-1; the summary includes information on the equivalency as well as the validation approach to qualification.

4.1.3 Modeling Recommendations

The model recommendations for a short-term LOCA analysis of a PWR ice condenser containment are developed in a manner that ensures conservative estimates of maximum pressure loads within the containment. These recommendations have been verified in full-scale tests, and have been found to provide conservative results also when compared to LOCA calculations obtained with a previously reviewed ice condenser containment code, TMD, referred to in the USNRC's Standard Review Plan for ice condenser containments.[2]

A summary of the model recommendations for the short-term LOCA scenario is presented in Table 4-2.

4.1.4 Input Preparation

Table 4-3 gives a summary of the input preparation for performing a short-term LOCA scenario analysis in an ice condenser containment with the CONTAIN code. In the section of the table dealing with ice bed input there are two sets of input specifications corresponding to the equivalency and validation argument as discussed in Section 4.1.1. We recommend the user select the ice bed parameter cihtml that gives the more conservative results, that is, the lower value; however, we recognize that the user may also be satisfied with an equivalency approach. In the latter case, the higher value of cihtml may be chosen.

Nodalization.

The complexity of an ice condenser containment, designed for pressure suppression, makes some challenging demands on code modeling and on the user for input preparation. Nodalization is one area where we depart from the simple single cell approach recommended for the large dry and subatmospheric containments. The adoption of multi-cell modeling in the case of ice condenser containments is a consequence of two facets associated with this unique containment type:

- The physical partitioning of major regions of containment that are coupled by well-defined flow paths suggests that we recognize the partitioning in a containment model to enable a prediction of realistic containment responses.

- The safety review of ice condenser containment systems emphasizes not only maximum internal pressure but also internal pressure differentials. Resolving these differentials requires a reasonable degree of containment partitioning by the user.

In the short-term scenario analysis, the containment model used for the demonstration calculation

---

[2] Standard Review Plan, NUREG-0800, Rev. 2, July 1981, Section 6.2.1.1.B, "Ice Condenser Containments."

is a 22 cell model of the containment, Figure 4-16, based on a compartmentalization described in the Watts Bar FSAR. The model, although similar to the FSAR containment nodalization, is not identical to that model. The FSAR containment model used for the TMD code calculations consisted of 50 cells. The added cells, that is, beyond the 22 cells of the CONTAIN model, were incorporated to circumferentially divide the ice condenser region. We do not recommend that level of detail in modeling the ice condenser; rather, we suggest a one-dimensional segmentation of the condenser that is similar to the level of detail used and verified in the CONTAIN assessment of the Waltz Mill tests. In the demonstration problem we have used four cells to model the ice bed and one cell each to model the ice condenser lower and upper plenums, respectively. Shown in Figures 4-17 and 4-18 are the cell partitioning described in the FSAR TMD model. In the open region of the lower compartment, consisting of cells 1 through 6 in the FSAR TMD model, the region of the pipe rupture is cell #1. This region is characterized by the highest local pressure following the break, and therefore is also an important region for establishing the maximum pressure differential across the operation deck that divides the lower and upper containment region. To resolve the pressure in the immediate vicinity of the pipe rupture from the rest of the open region, we collapse the FSAR partitioning into two regions, a large open region that excludes the pipe break and a smaller open region surrounding the break. The dead-ended rooms in the CONTAIN model remain as described in the FSAR, that is, each physical room is identified as a separate computational cell. The correspondence between the FSAR cell numbering and that used in the CONTAIN model is shown in Table 4-4.

We note that it is important to model the dead-ended rooms in the lower compartment since these compartments will trap air during the blowdown. Trapping air in these compartments will reduce the inventory of air transported to the upper compartment and therefore reduce the upper compartment pressurization. This effect is demonstrated in Figure 4-19, where pressurization with and without lower compartment dead-ended regions modeled are compared.

Ice Condenser.

A modeling approach for the ice condenser has been chosen that is very similar to that used in the Waltz Mill tests, as described in Appendix H. Because this modeling approach has been validated for an application, that is nearly identical to the DBA demonstration problem, we suggest a conservative combination of input parameters that set film liquid thickness and convection multiplier, that is, parameters ciflmx and cihtml, respectively. For the short-term scenario, these parameters are set as:

ciflmx = 5.0×10^{-6} meters, and

cihtml = 10.

The input parameters that correspond to the physical description of the ice bed, ice mass, initial ice surface area, and channel flow area, are all set according to the plant-specific geometrical specification of the ice bed.

We have noted that because of the exceptionally wet conditions that occur in the ice bed, the gas temperature in the bed is at the saturation temperature. In the CONTAIN code, the exit water temperature is limited to the saturation temperature when the ice bed is calculated to be saturated, irrespective of the set exit water temperature.

Structures.

Structural heat transfer is not modeled in the short-term LOCA input deck. Because the time frame for the short-term analysis is very brief, only a few seconds, heat transfer to structural material is not a significant contributor to energy removal from the containment atmosphere. For example, the lower compartment pressurization is essentially unaffected by excluding heat transfer to structures. There is a small effect in the case of the upper compartment pressurization, where a slight reduction in upper compartment pressurization can be observed with the inclusion of heat transfer to structures, as shown in Figure 4-20. Thus, by assuming no structural heat transfer, a slight conservative bias for maximum load analysis is provided.

Flow Path Characterization.

Characterizing the flow paths for the ice condenser is an important requirement for enabling a conservative determination of pressure maximums and pressure differentials. The most important parameter in this characterization is the loss coefficient, as demonstrated in the sensitivity analysis performed in the Waltz Mill test assessment.

Clearly, determining the loss coefficients for an ice condenser is a difficult matter, given the complicated geometry and the character of the flow stream. In this determination we turn to scaled flow tests conducted by Westinghouse for the Waltz Mill test facility. Shown in Table 4-5 are loss coefficients determined using 1/10 and 1/4 scaled models. We may apply these coefficients to the plant ice condensers by 1) observing the basis on which the coefficients' K are reported, and 2) adjusting the ice bed frictional coefficient to correspond to the plant ice bed length which is 1/3 greater in length than the Waltz Mill facility. We have adjusted the coefficients reported for the Waltz Mill facility to the plant ice condenser in the demonstration input [Appendix E]. Briefly, we show the steps in converting the loss coefficient used for the Waltz Mill facility to the demonstration ice condenser plant:

Door entrance (cell #1 to #3):

- change of basis – $K_{door} = K_{bed} \frac{A_{door}^2}{A_{bed}^2}$

- convert to CONTAIN flow coefficient (CFC)[3] – $\left[CFC = \frac{K_{door}}{2}\right]$

Turning and ice bed entrance (cell #3 to #4):

- no change in the basis – $K^{*}_{entrance} = 1.2$
- determine frictional loss for ½ of the downstream cell – $K^{**}_{ice} = 0.18$
- convert to CONTAIN flow coefficient (CFC) – $CFC = \frac{K^{*}_{entrance} + K^{**}_{ice}}{2}$

Ice bed (#4 to #5, #5 to #6, #6 to #7):

- frictional loss coefficient for ½ of ice bed cell (adjusted for added height) –

  total ice loss coefficient = (ice bed and exit loss - exit loss) * 1.33

  friction loss for ½ of ice bed cell = total ice loss coefficient / 8
- frictional loss coefficient for flow between ice bed cells –

  flow path loss coefficient = 2 x frictional loss for ½ of ice bed cell
- convert to CONTAIN flow coefficient (CFC) –

  CFC = flow path loss coefficient / 2

Ice bed exit (#7 to #8):

- frictional loss of ice bed exit = exit loss (K = 1) + friction loss for ½ of ice bed cell
- convert to CONTAIN flow coefficient (CFC)

  CFC = friction loss of ice bed exit / 2

Upper plenum exit (#8 to #2):

- frictional loss of plenum exit = exit loss (K=1)

---

[3] CONTAIN flow coefficient CFC is equal to loss coefficient / 2

- convert to CONTAIN flow coefficient (CFC)

  CFC = 1/2

For determining the loss coefficients for flow paths in the lower compartment cells, we have used the TMD loss coefficients as reported in the Watts Bar FSAR. For additional details on the flow path input, see the comments in the demonstration input deck listed in Appendix E.

As previously mentioned, we have relied on an analysis with the Waltz Mill tests to conclude that plenum door inertia modeling is not important for predicting containment pressurization during the short-term rapid pressurization phase of the postulated DBA. Consequently, we model the opening and closing of plenum doors with a static pressure versus area specification. This is accomplished in the CONTAIN code by using the reversible flow path input described in the CONTAIN manual [1]. The pressure versus area specification used in the demonstration calculation has been used in previous CONTAIN ice condenser analyses [17].

Table 4-1 Summary of the CONTAIN qualification for short-term LOCA calculations in a PWR ice condenser containment.

Modeling Area	TMD	CONTAIN	Comments	Reference
geometric nodalization:				
upper compartment	single cell	single cell	pressurization due mainly to air accumulation – stratification effects minimal importance due to the small effect of heat transfer in upper compartment during the short time period	pressure suppression design
ice condenser	3 vertical layers of ice bed cells – 6 circumferential divisions (total of 18 cells); 6 circumferential cells for each plenum	4, vertically stacked ice bed cells; single cell for each plenum	small circumferential flows, main pressure variation due to vertical flows	sensitivity calculations reported for TMD [13]
lower compartment	6 cells model open region; 13 cells model dead-ended rooms	2 cells model open region; 13 cells model dead-ended rooms	identical cell for pipe rupture located in open region – small variations in pressure within most of the open region (excluding break cell); equivalent nodalization for dead-ended rooms	TMD pressurization calculation [13]
two-phase steam injection	thermal equilibrium, homogeneous mixing, without dropout	thermal equilibrium, homogeneous mixing, with 100% entrainment	thermal equilibrium models are equivalent methods for partitioning steam and liquid water; no dropout of water (CONTAIN) and 100% entrainment (TMD) assumptions are essentially identical; thermal equilibrium and no dropout represent conservative assumptions	[Appendix H, pp. H-74, H-75]
heat transfer to structures	structures not modeled	structures not modeled	equivalent treatment, conservative	—
heat transfer to pools	pool interaction with atmosphere not modeled	pool interaction with atmosphere not modeled	equivalent treatment, conservative	—

Table 4-1 Summary of the CONTAIN qualification for short-term LOCA calculations in a PWR ice condenser containment (cont.)				
Modeling Area	TMD	CONTAIN	Comments	Reference
flow paths:				
equations	lumped parameter momentum equation, with acceleration terms; radial and hoop flow equations included	lumped parameter momentum equation (1-D), with acceleration terms	equivalent flow equations for vertical flows; sensitivity calculations with the TMD code for radial and hoop flows in the Watts Bar FSAR shows that pressurization is insensitive to these more sophisticated flow models	TMD [14] CONTAIN [1] Watt Bar FSAR [13]
loss coefficients (ice condenser)	based on experimental tests for scaled models; variable in time due to ice melting	based on experimental tests for scaled models	equivalent basis for time invariant loss coefficients as determined in the scaled model tests, conducted with air.	Waltz Mill test report [15]
critical flow	isentropic, homogeneous equilibrium model [HEM]	frozen, homogeneous equilibrium model [FHEM] with multiplier (0.7)	FHEM with a multiplication factor of 0.7 is shown to be more conservative than the HEM implemented in TMD; and, the FHEM with factor is additionally shown to be the most conservative critical flow model that is also consistent with experimental analyses, that is, the Waltz Mill assessments.	Watts Bar FSAR [13]; Appendix H
ice bed heat and mass transfer	semi-empirical model with calibration factor ELJAC	physically based HMT analogy method with calibration factor applied to Nusselt number calculated in ice column	Both the CONTAIN and TMD models are implemented using a calibration factor to account for the complexity of the ice bed flow geometry and convective correlation. These calibration factors are based on pressurization data for the Waltz Mill full-scale ice condenser tests.	Waltz Mill test report [15]; Appendix H
plenum door inertia (door dynamics)	door inertia, frictional resistance, and gravity forces included in a dynamic door motion model	static model; pressure versus area modeling	Investigation of pressurization sensitivity to door motion conducted for the Waltz Mill tests, with the CONTAIN and standalone dynamic door modeling, concluded that door response is so rapid as to not be a factor in pressurization calculations	Appendix H

Table 4-2 General modeling recommendations for a qualified CONTAIN short-term LOCA calculation in a PWR ice condenser containment.	
Phenomena	**Modeling Recommendations**
Multi-component gas compression	Nodalize the upper containment with a single cell; use multiple, vertical stacked cells for condenser (4 cells in the ice bed, single cells for lower and upper plenums); multiple cells in the lower compartment to resolve break region, open region, and dead-ended rooms
Two-phase water expansion	Use a thermal equilibrium method for water injection modeling (ATMOS SOURCE); no dropout of liquid water (default)
Two-phase inter-compartment flows	Gas loss coefficients (ice condenser scaled tests); critical flow model for all paths (default)
Plenum doors	Static opening under pressure -- pressure versus area (reversible, engineering vent option)
Ice bed heat and mass transfer	Geometrical specifications; minimum liquid film thickness; Nusselt multiplier
Structure heat transfer	Neglect (conservative assumption for obtaining maximum loads)
Pools	Include upper and lower compartment pools and lower plenum pools for gas volume displacement; no surface or bottom energy transfers
Ice melt and condensate	Divert to lower plenum with overflow to lower compartment; use default ice melt and condensate exit temperature

Table 4-3 Input guidance for modeling a short-term LOCA scenario in a PWR ice condenser containment.		
Input Section/Block	**Parameter(s)**	**Comment**
Global:		
Nodalization	ncells = M (multiple-cells) ncells = 22 (demonstration calculation)	Suggest single upper compartment, 4 cells for ice bed, single cell for each plenum, minimum of three cells for lower compartment (open region excluding break region, break region, and dead-ended rooms -- consult FSAR for region and room description)
Material properties	default properties	compound properties for nitrogen, oxygen, water vapor, and water liquid
Timesteps	~ 0.01 seconds	set to give accurate results for the time scale of interest (fractions of seconds)
Flow	—	no dropout of liquid water (default)
engineering vents		
plenum doors	RVAREA-P	reversible pressure versus area (see listing)
pool type paths	type = pool	liquid redistribution paths from lower plenum to lower compartment (set elevation for path at plenum floor level, set plenum gas path to lower compartment at elevation above pool path to avoid possible closing due to flooding)
loss coefficients	VCFC	gas loss coefficients (use FSAR specifications)
inertia mass	VAVL	area/length for paths (use FSAR specification as given for TMD; otherwise, in case of ice bed, use flow path area/ length between adjoining cell centers of mass)
vena contracta	VCONTRA	set for all paths, VCONTRA = 0.7
elevations	VELEVB, VELEVF	set according to specifications, use RESOLVE keyword
Upper compartment:		
Geometry	gasvol, cellhist	free volume for equivalency (FSAR specification), set to define pool
Atmosphere initial conditions	ATMOS block,	pressure, temperature, and humidity equivalency (FSAR specfication)
Structures	STRUC (omit), or HT-TRAN	neglect heat and mass transfer to structures

Table 4-3 Input guidance for modeling a short-term LOCA scenario in a PWR ice condenser containment (cont.).		
Input Section	**Block/Parameter(s)**	**Comment**
Upper compartment:		
Lower cell	low-cell	include with no heat or mass transfer (HT-TRAN off off off off off)
Lower compartments:		
Geometry	gasvol, cellhist	free volume for equivalency (FSAR specification), set to define pool
Atmosphere initial conditions and water injection	ATMOS block, SOURCE block	pressure, temperature, and humidity equivalency (FSAR specfication); blowdown injection in break region
Structures	STRUC (omit)	neglect heat and mass transfer to structures
Lower cell	low-cell	include with no heat or mass transfer (HT-TRAN off off off off off)
Ice condenser:		
Geometry	ICECOND (hitici, tmsici, ciarfl, arhtin)	set to FSAR geometric and initial condition specification
Heat and mass transfer	ICECOND (ciflmx, cihtml, citice)	ciflmx = 5×10^{-6}; cihtml = 10 (based on Waltz Mill assessment) cihtml = 40 (for equivalency to TMD code) citice (default)
lower plenum pool	low-cell	include with no heat or mass transfer (HT-TRAN off off off off off)

Table 4-4 Basis for CONTAIN lower compartment nodalization used for the ice condenser short-term demonstration calculation.		
CONTAIN cell #	**TMD cell # ***	**Volume, m^3**
Open region (excluding break region):		
1	2	1042.1
	3	1987.9
	4	1098.7
	5	1042.1
	6	711.2
		(Total = 5881.9)
Open region (break region):		
9	1	812.7
Dead-ended rooms:		
10	26	331.3
11	27	506.9
12	28	317.2
13	29	529.5
14	30	317.2
15	31	509.7
16	32	286
17	33	433.3
18	34	368.1
19	35	124.6
20	36	124.6
21	37	263.4
22	50	39.6

* Watts Bar FSAR [13]

Table 4-5 Ice condenser unrecoverable loss coefficients for Waltz Mill test facility (TMD model). *		
Location	**Loss coefficient (bed flow area basis)**	**Source**
Door entrance	1.8	1/10 scale model test
Turning and ice bed ** entrance	1.2	1/10 scale model test
Ice bed friction and exit	3.1	1/4 scale model test

* Waltz Mill final report [15]

** ice bed refers to region of ice condenser where ice columns are located

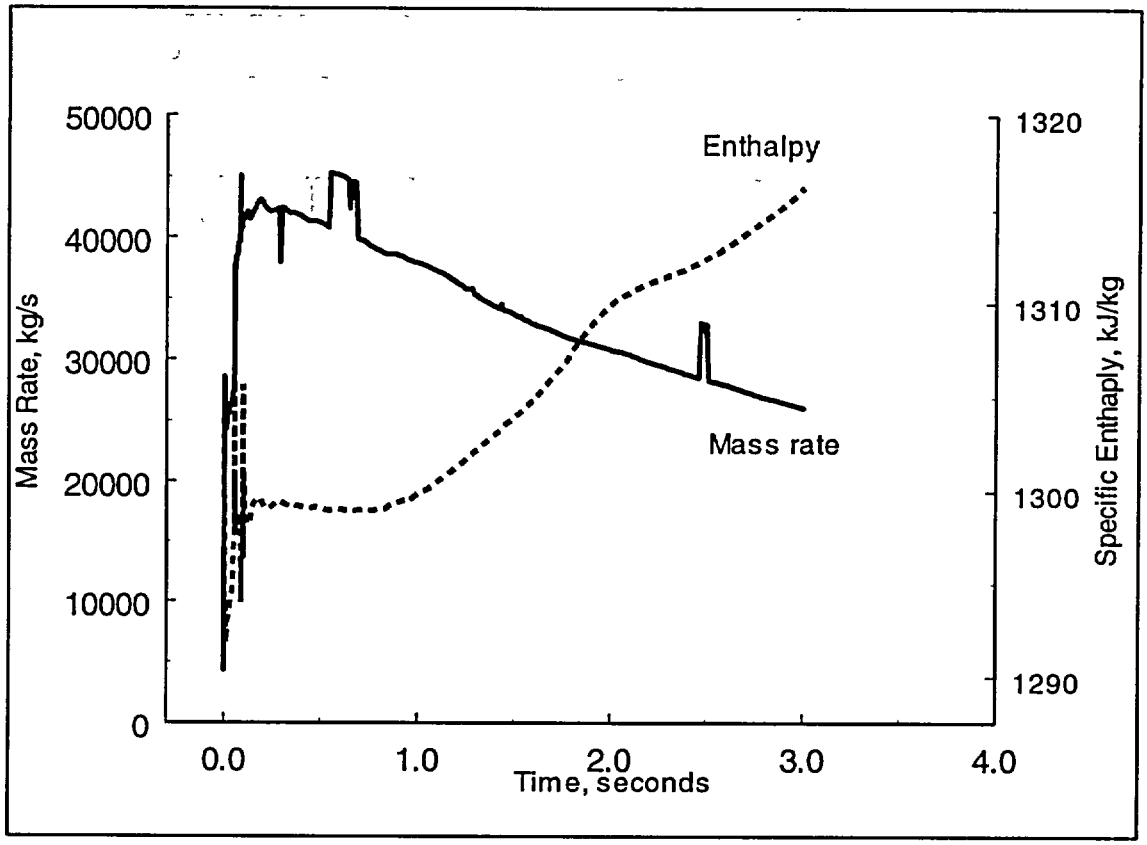

Figure 4-6 Break mass and energy flow from a double-ended cold leg break, Watts Bar FSAR [13].

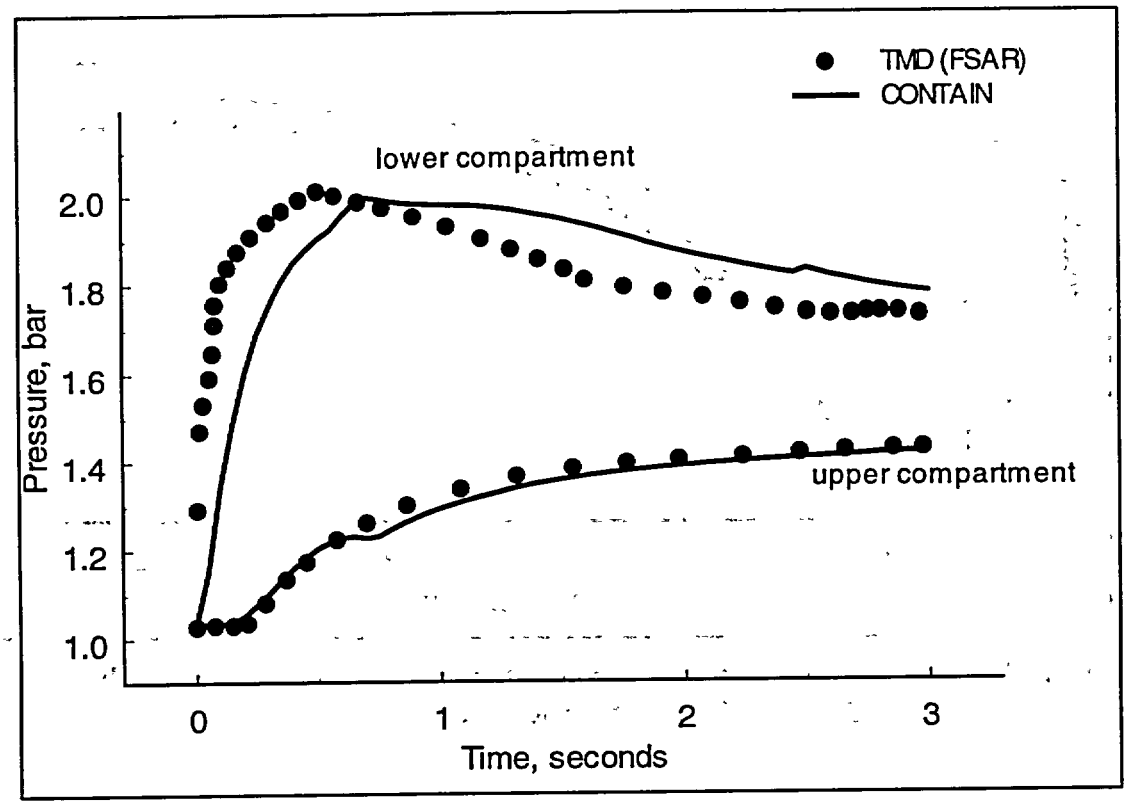

Figure 4-7 Comparison of short-term pressurization for ice condenser containment (double-ended cold leg break).

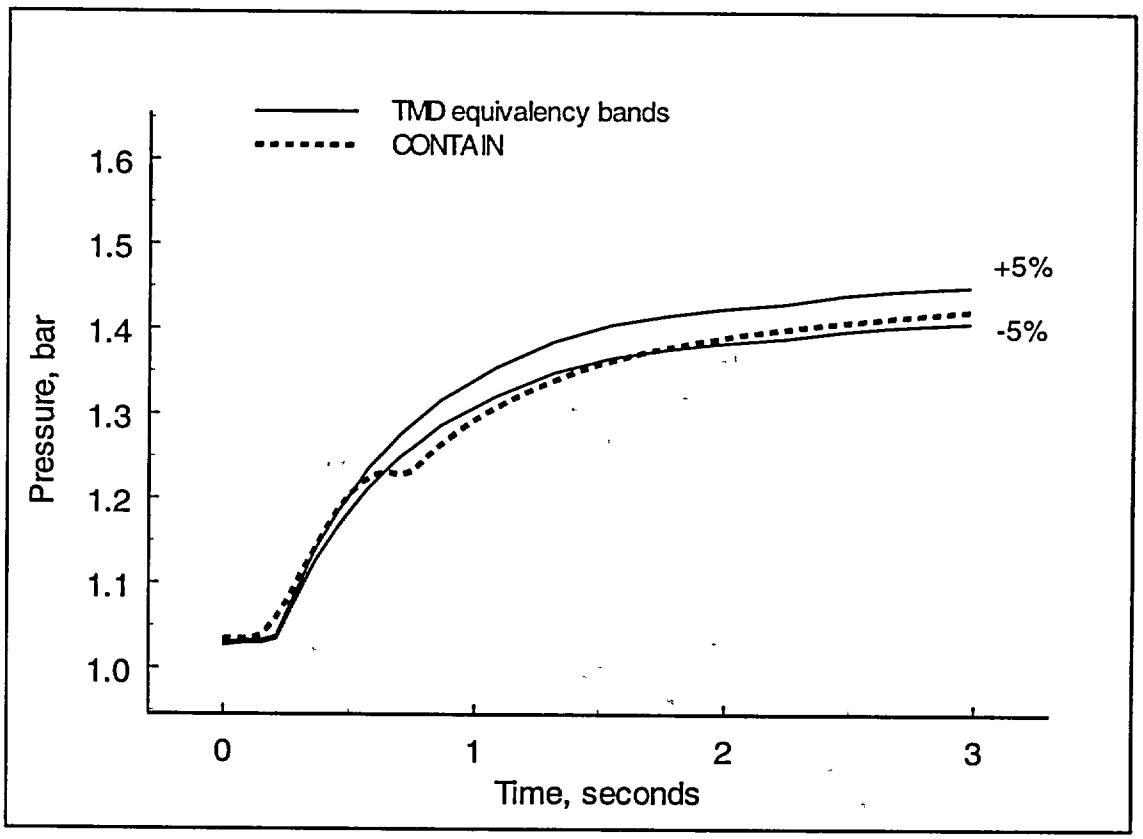

Figure 4-8 Upper compartment pressurization, showing the equivalency between the CONTAIN and TMD calculations.

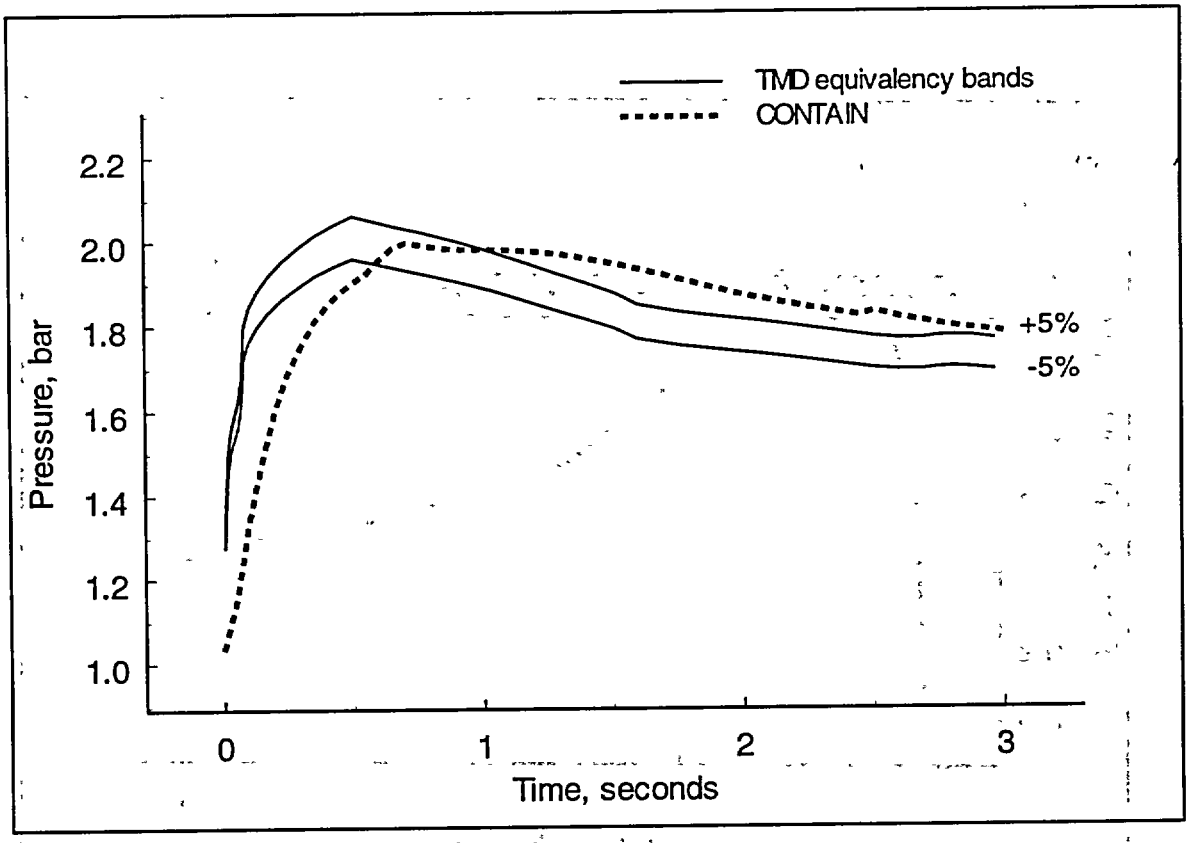

Figure 4-9 Lower compartment pressurization, showing the equivalency between the CONTAIN and TMD calculations

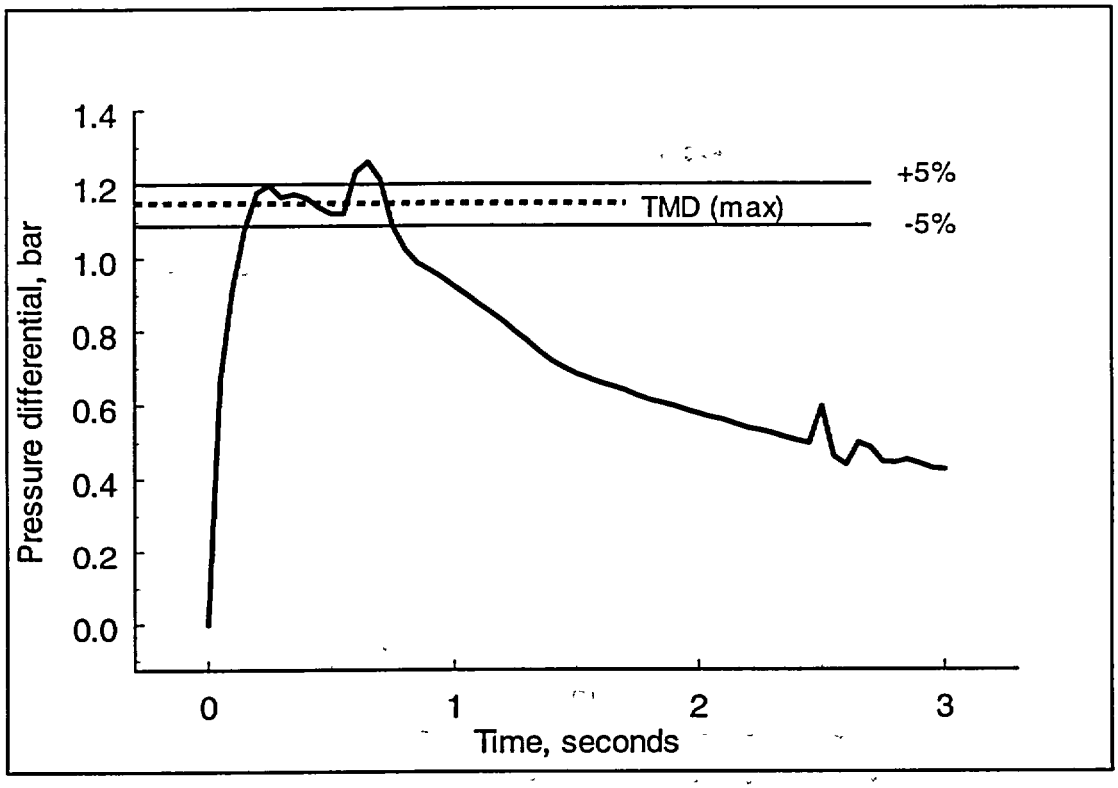

Figure 4-10 CONTAIN calculated maximum pressure differential across the containment operation deck in a ice condenser following a double-ended cold leg pipe rupture.

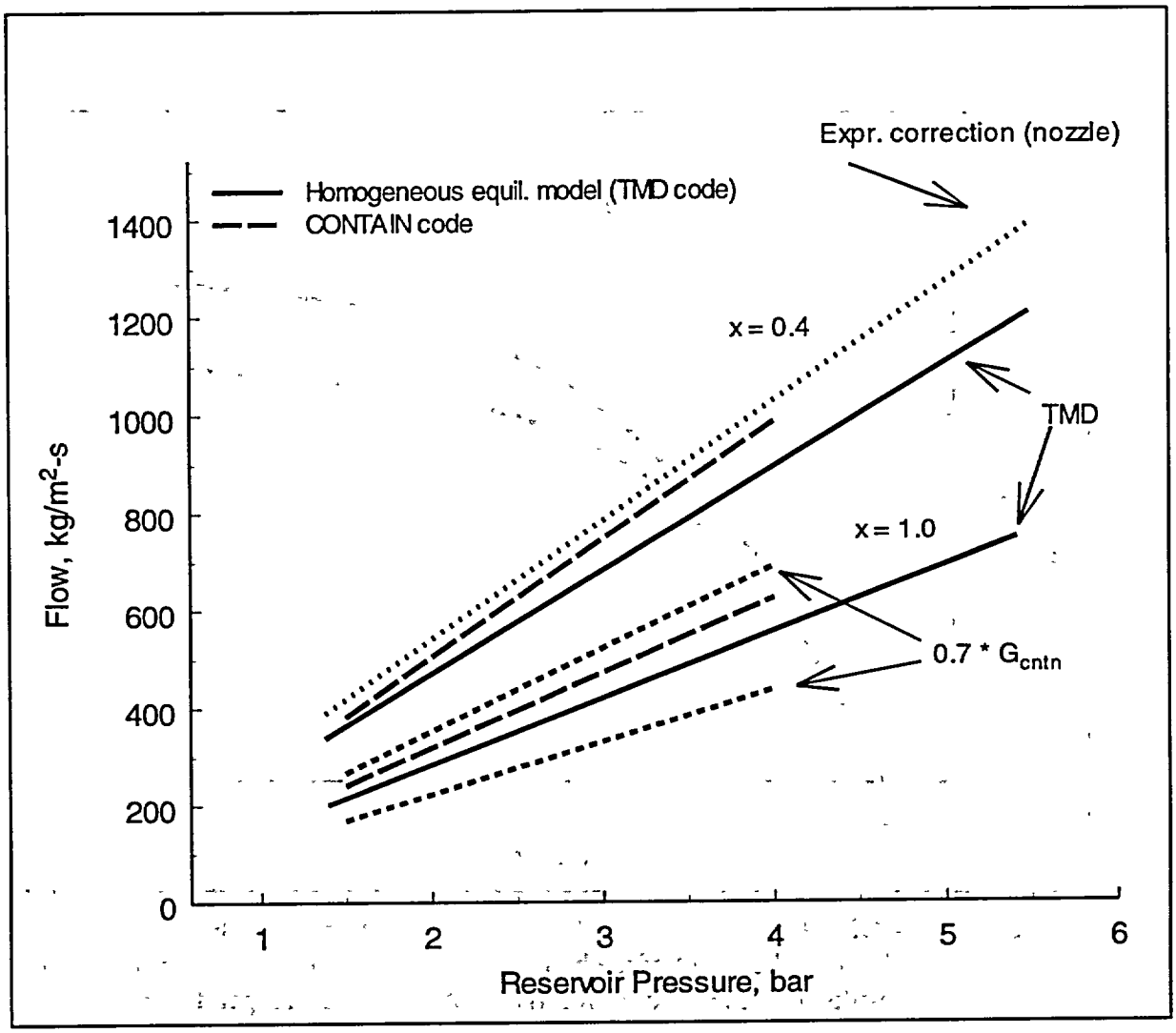

Figure 4-11 Two-phase critical flows calculated by CONTAIN and the TMD code for flow mixtures of quality x = 0.4 and 1.0 (steam). Curve labeled "Expr. correction" is an experimental correction applied to TMD results at x = 0.4; curves labeled "0.7 * G_{cnt}" apply to the CONTAIN results at x = 0.4 and 1.0.

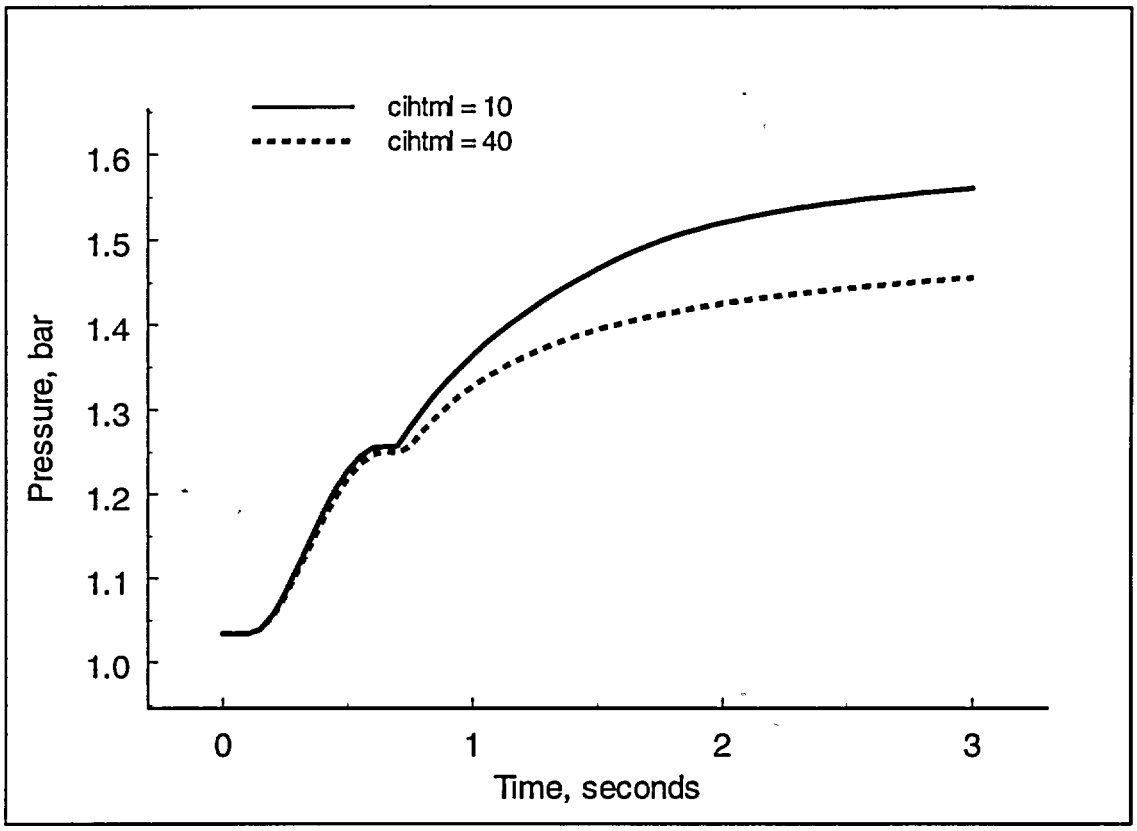

Figure 4-12 CONTAIN calculations of the upper compartment pressurization, showing the effect of ice bed Nusselt number multiplication factor on results (cihtml =10 used for Waltz Mill analysis, Appendix H).

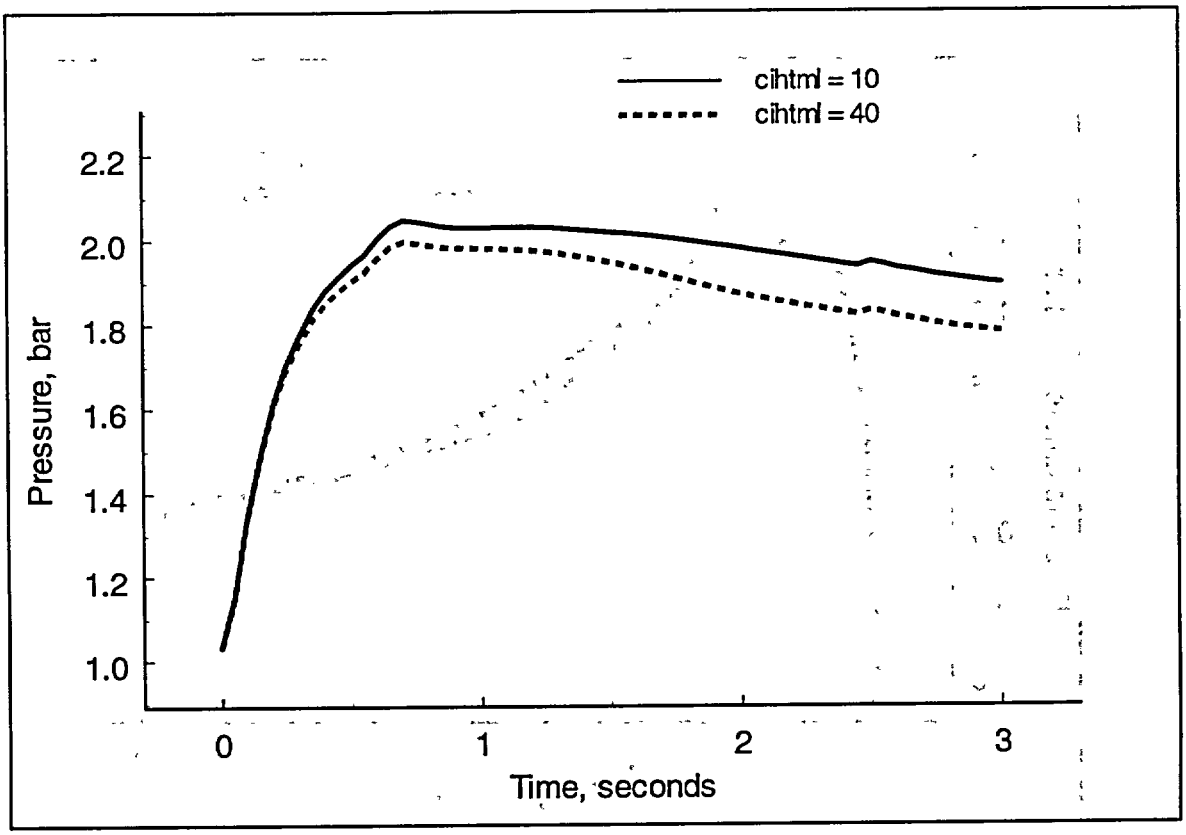

Figure 4-13 CONTAIN calculation of lower compartment pressurization, showing the effect of ice bed Nusselt number multiplication factor on results (cihtml =10 used for Waltz Mill analysis, Appendix H).

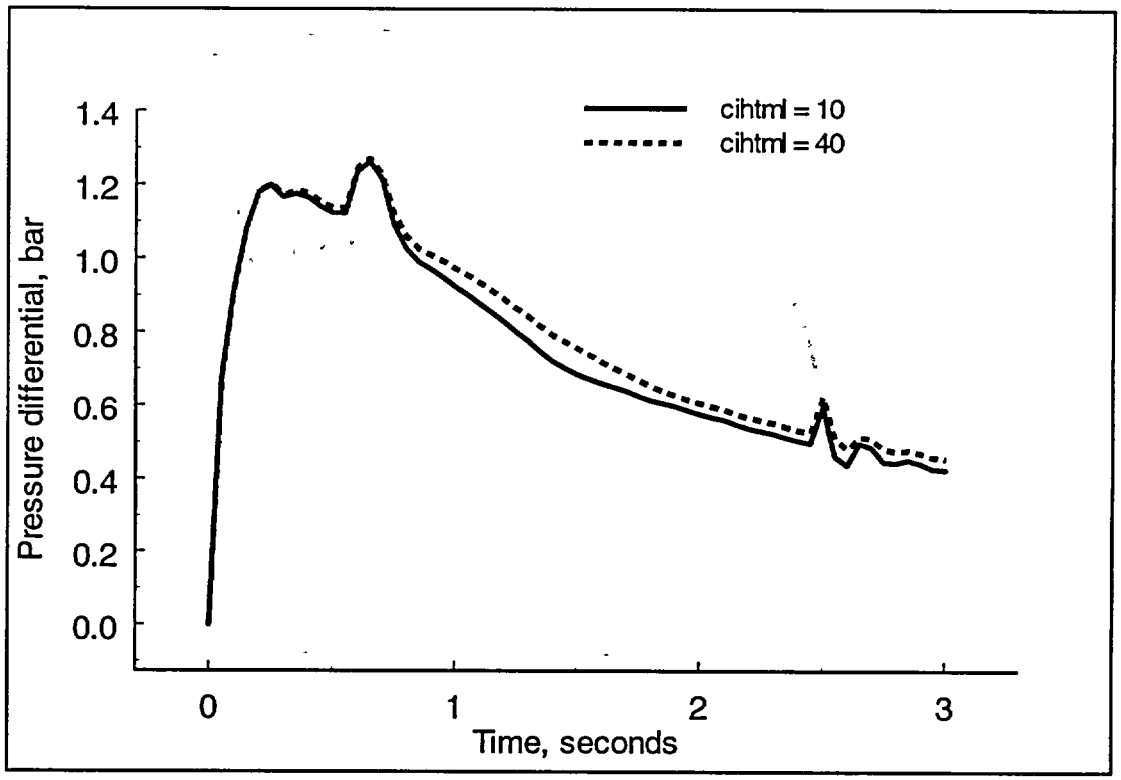

Figure 4-14 CONTAIN calculation of maximum differential pressure profile across the containment operation deck, showing the effect of ice bed Nusselt number multiplication factor on results (cihtml =10 used for Waltz Mill analysis, Appendix H).

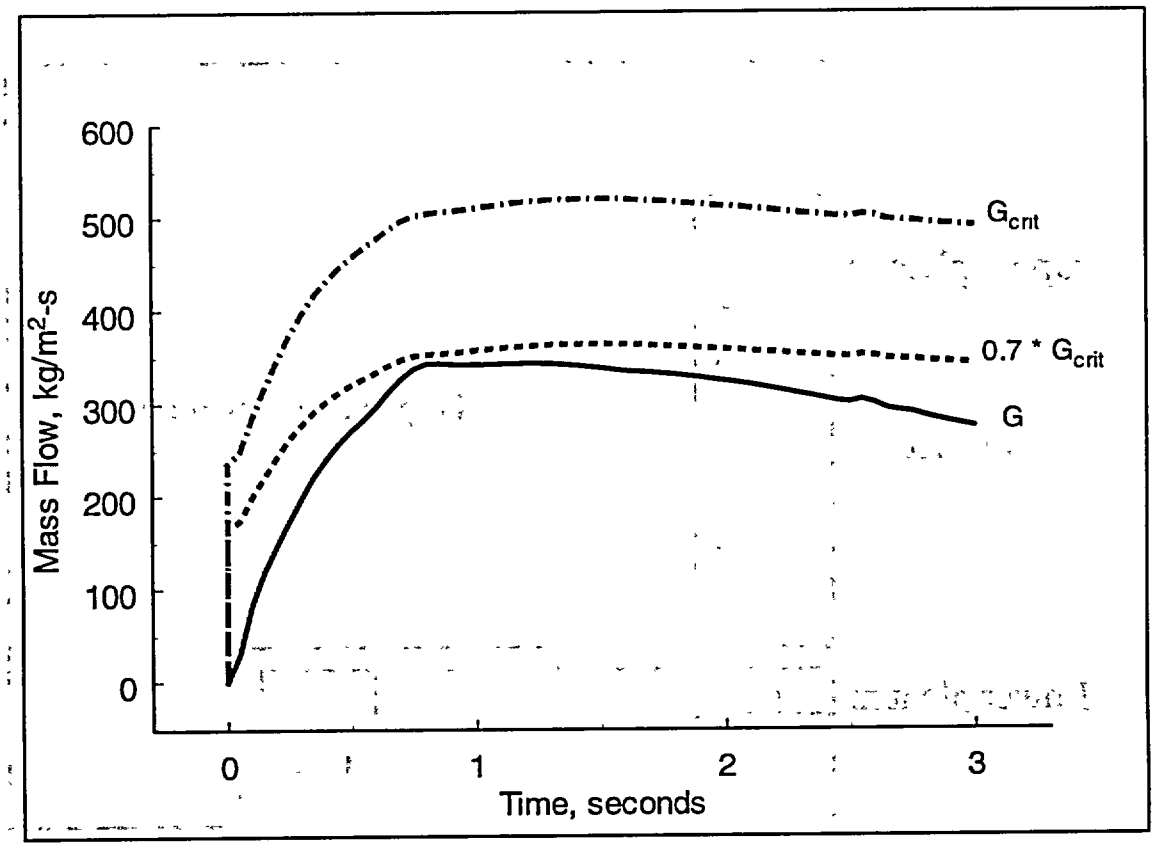

Figure 4-15 CONTAIN calculated vent flow (G) and critical flows for the lower plenum door path.

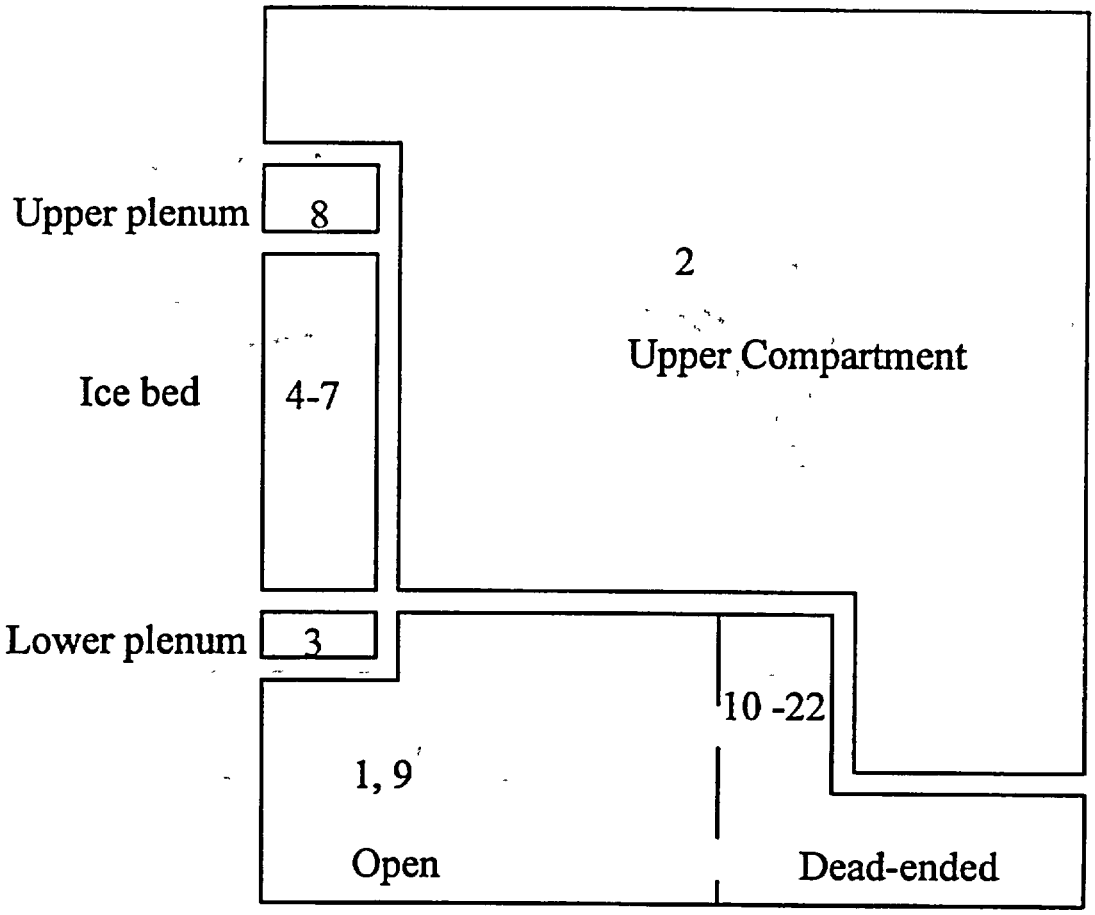

Figure 4-16 CONTAIN nodalization scheme for the short-term ice condenser plant demonstration calculation.

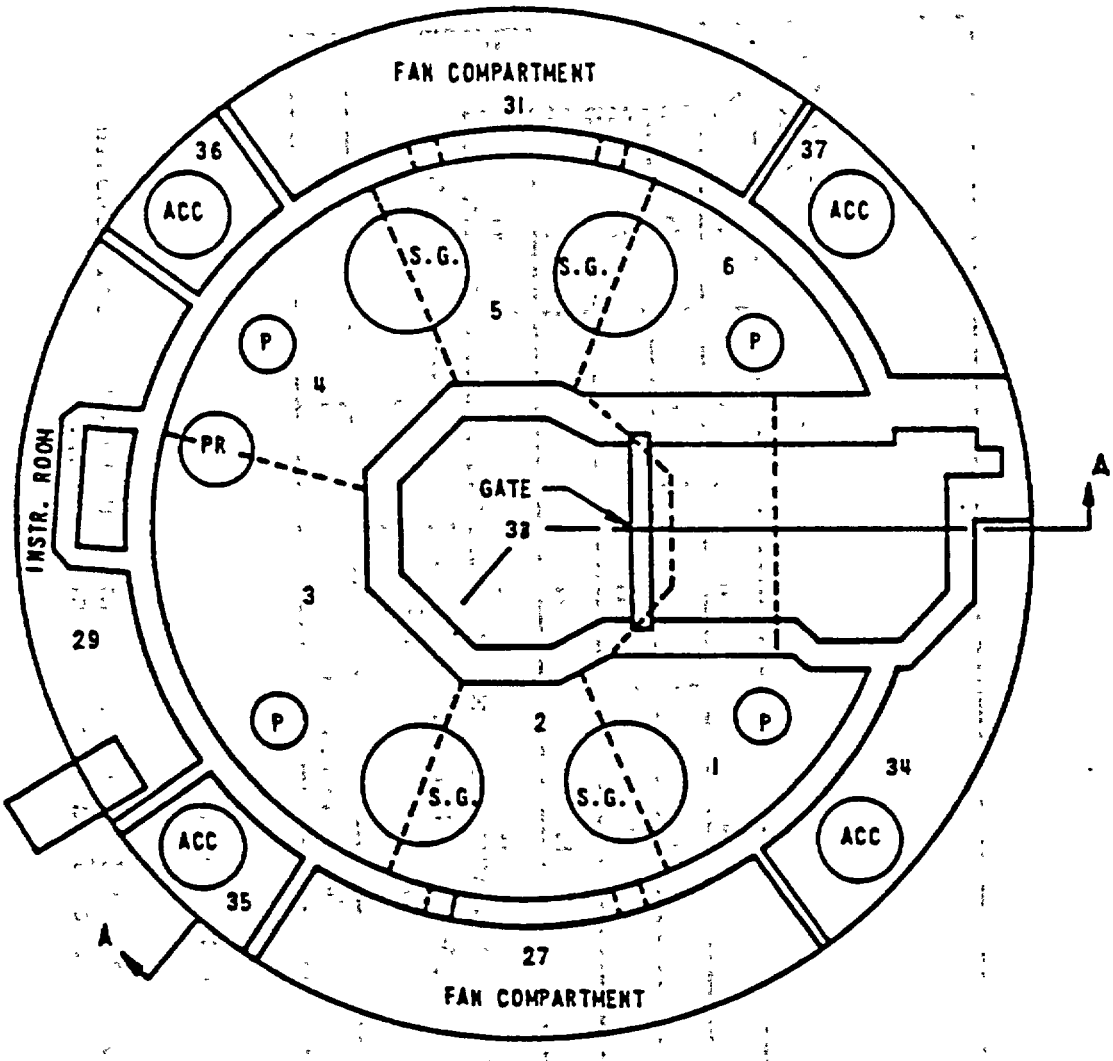

Figure 4-17 TMD model of equipment rooms in the lower compartment of the Watts Bar ice condenser plant [13].

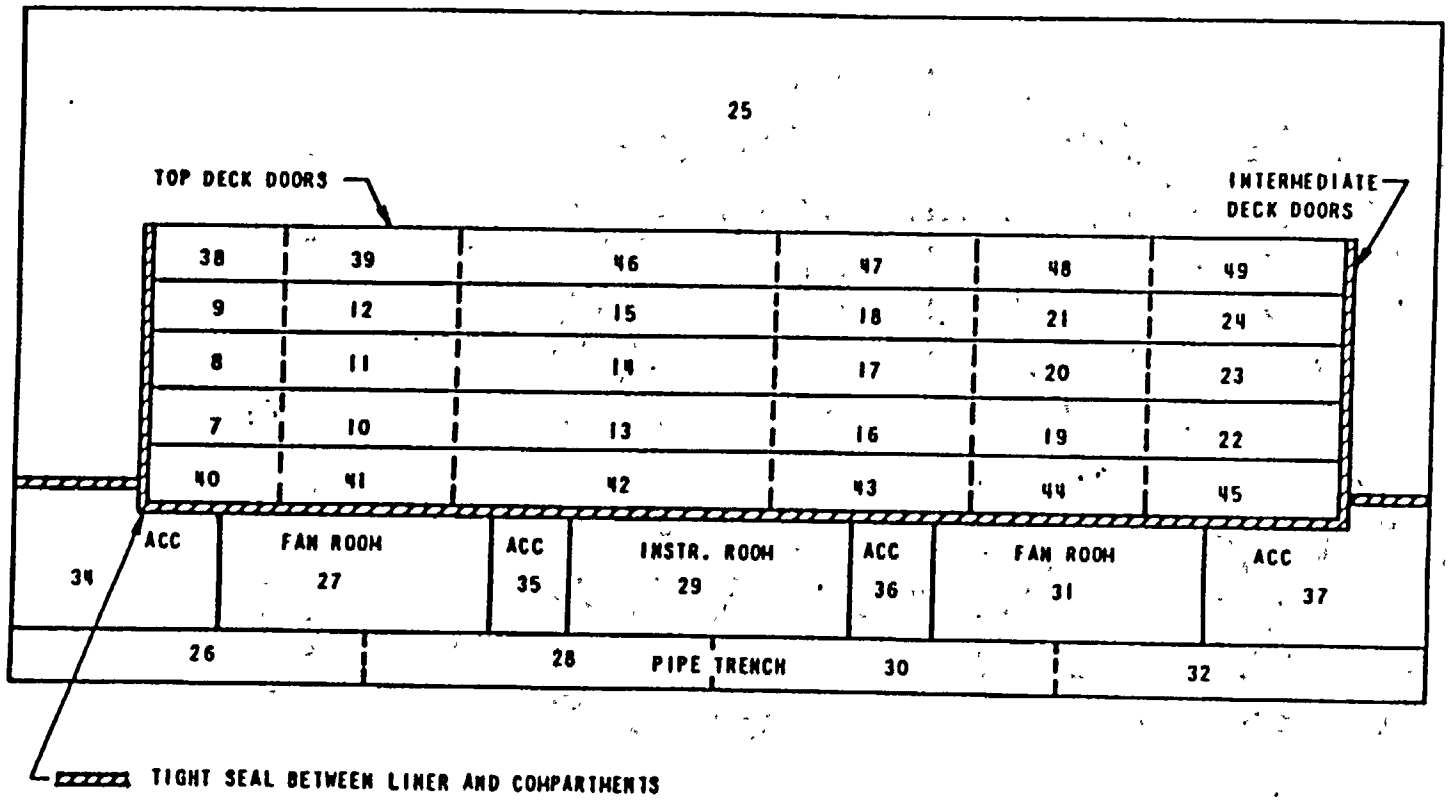

Figure 4-18 TMD model of lower compartment (specifically showing layout of the pipe trench region).

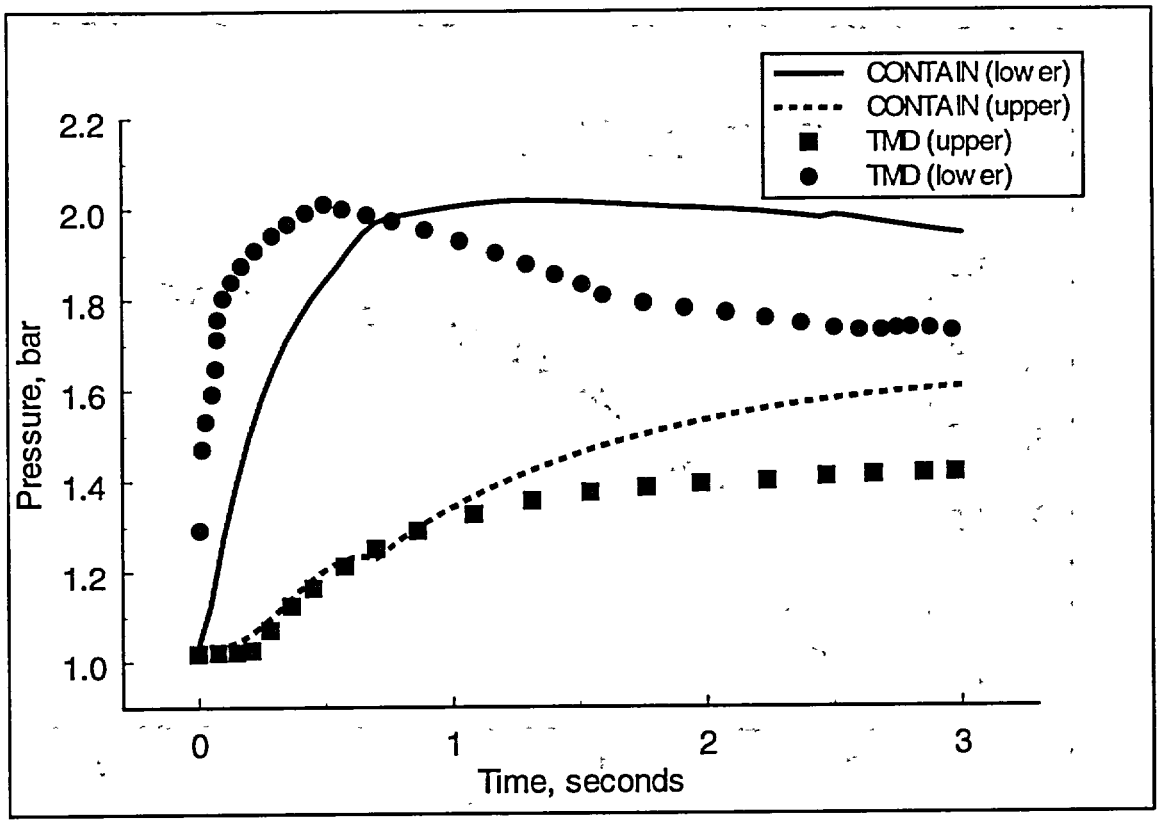

Figure 4-19 Comparison of CONTAIN and TMD pressurization profiles for a double-ended cold leg pipe rupture, where the CONTAIN model excludes modeling the dead-ended rooms in the lower compartment (Nusselt number multiplication factor, cihtml, set to 40 for an equivalent calculation comparison). The lower compartment over prediction by CONTAIN is due to the exhausting of the complete inventory of air in the lower compartment to the upper compartment during the blowdown.

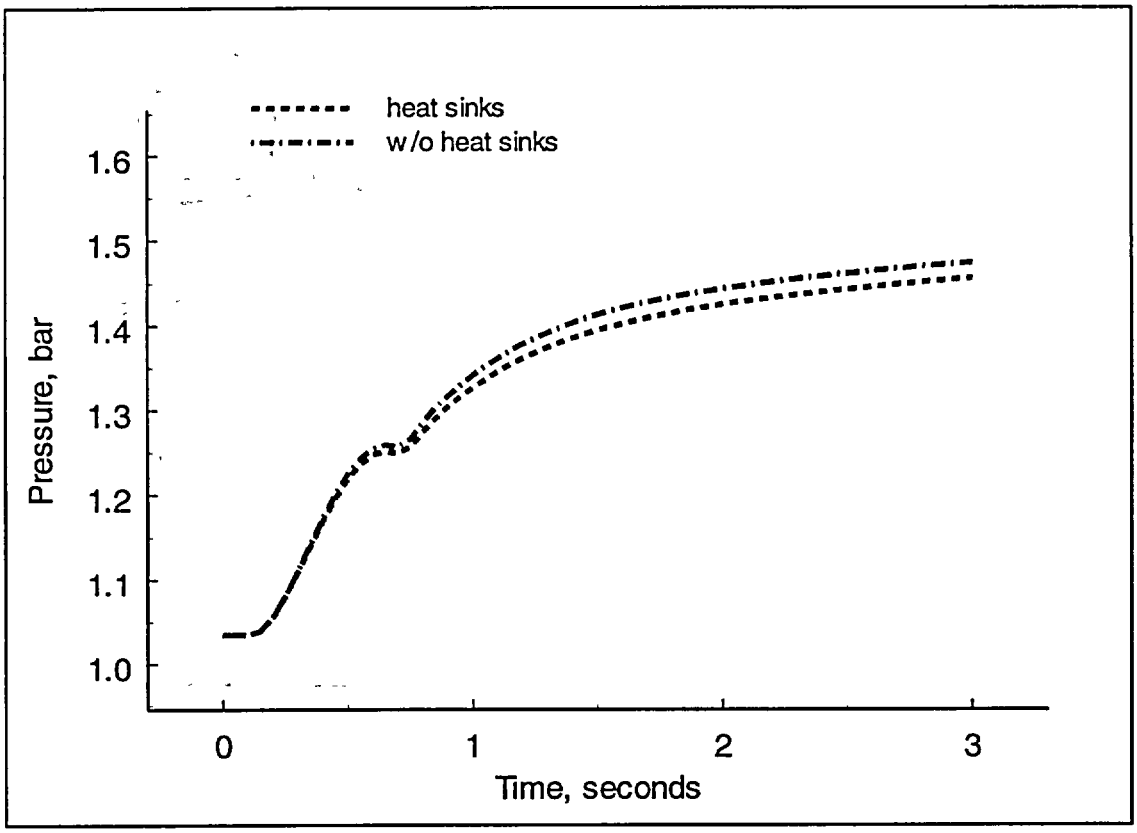

Figure 4-20 Upper compartment pressurization effect when including heat sinks in the short-term LOCA analysis (Nusselt number multiplication factor, cihtml, set to 40).

4.2 LOCA Long-term Accident Analysis

In the long-term accident analysis, we used the Watts Bar Final Safety Report (FSAR) [13] to obtain specific information for our demonstration calculation; this consists of information on the containment geometry, heat sinks, injection sources, and safety systems. We compare CONTAIN results to LOTIC code [18] calculations, as reported in the FSAR. The FSAR calculation serves as a guidepost for establishing an independent measure to support the qualification of the CONTAIN code, which may be differentiated from the claims of equivalency made in comparing CONTAIN results to other USNRC auditing calculations. The use of the term guidepost, a downgrading of our previous use of equivalency, reflects on our limited knowledge of the modeling details of the LOTIC code and input for the accident scenario. To address this concern, we have identified the key phenomena and included a number of sensitivity calculations in the qualification section that put into context comments regarding code qualification.

Furthermore, qualification for the CONTAIN code is supported by our validation efforts documented in Appendix H, where the CONTAIN code is exercised for a long-term test in the Waltz Mill test facility. From this validation work, we have established good evidence indicating phenomena important during the process of ice melt-out, and have shown that the CONTAIN modeling can be used to provide good estimates of ice melt-out times. However, there are no experimental data available to use as a basis to verify some of our calculational assumptions made during the pressurization period subsequent to ice melt-out. This pressurization phase is critical to establishing the peak pressure obtained in the long-term scenario.

It should be noted that the intent of these calculations, being demonstrative in nature, are intended only for qualification purposes and are not offered as a re-review of any conclusions found in Safety Evaluation Reports (SERs).

4.2.1 LOCA Long-term Scenario

The LOCA long-term scenario is initiated as a pump suction pipe rupture. This type of pipe rupture in the RCS results in the most severe post-blowdown injection into the containment that is expected to result in the highest late time pressurization of the containment when the ice melts out. In this case, core reflooding rate is high and all reflood water vented to the containment must past through the steam generators, becoming superheated before entering the lower compartment of the ice condenser containment. Shown in Figures 4.21 and 4.22 are the mass rate and energy of the injection into the lower compartment. The injection from the RCS is partitioned into four phases: blowdown, reflood, froth, and decay heating. We have shown in Figure 4.21 a band of some uncertainty for the decay heating portion of the injection. The uncertainty is the result of a lack of specificity in the Watts Bar FSAR concerning the injection mass rate during the decay heating period. In the qualification of the CONTAIN code, we will address what impact such an uncertainty in the injection has on containment loading, and how that uncertainty affects our perception of qualification based on comparisons with other code results.

In Section 4.1, we considered only the early portion of the blowdown phase when no active safety features of the plant were operational. However, during the long-term scenario not only must we be concerned with the pressure control provided by the ice condenser, which acts as a passive mitigator, but we must also consider the active safety features such as the quench and recirculation sprays activated after the blowdown phase. For the demonstration plant that we are using for code qualification, we have chosen a plant where the sprays are located in the upper compartment, as opposed to another configuration where sprays are located in both upper and lower compartments; this configuration was selected because it is the most common among ice condenser plants. Drains are placed in the upper compartment sump to return spray water to the lower compartment sump where spray water passes through recirculation spray pumps and heat exchangers. Shown in Table 4.6 is the accident chronology for a pump suction pipe rupture. This scenario is characterized as one with an assumed minimum safeguards condition; that is, a condition where there is one of two spray pumps, and one of two, spray heat exchangers operating; one of two RHR pumps and one of two RHR heat exchangers; one of two safety injection pumps and one of two centrifugal pumps; and, one of two air return fans available for mitigating the accident event.

4.2.2 Qualification

The qualification of CONTAIN for the long-term ice condenser analysis is based on an assessment of the code for predicting pressure suppression control. With our emphasis being placed on pressure response rather than both pressure and temperature means that we are less interested in our modeling assumption that will specifically affect lower compartment superheating. We will mention some of the processes that affect superheating but will not consider those processes in light of temperature estimations.

In qualifying the CONTAIN code for long-term ice condenser analysis, a corresponding calculation is extracted from the Watts Bar FSAR. Since the FSAR calculation was determined using a vendor's proprietary code, we will not consider the CONTAIN qualification basis to be one of equivalency as previously done when comparing other USNRC code results with CONTAIN. Rather, we use the FSAR results as a guidepost for discussing how results obtained with CONTAIN maybe contrasted with other codes, and specifically where modeling is or is not implemented in a mechanistic and consistent manner.

As in previous qualification sections for other plant types and scenarios, we will base much of our qualifying statements on CONTAIN validation studies. For long-term applications, the CONTAIN code has been compared to experimental data obtained by Westinghouse in the Waltz Mill test facility. Those comparisons for a long-term test, Test K, are documented in Appendix H. Test K represents a near prototypical test for evaluating the rate of ice melt-out during a long-term scenario that includes the effects of blowdown, frothing, and decay heating on the ice melt-out rate. Subsequent to melt-out, the pressurization phase is not addressed in the Waltz Mill testing because the facility does not include spray systems. However, the pressurization phase involves CONTAIN modeling and input options that have previously been qualified for other plant types. In this case, the phenomena of interest for modeling are the interaction of sprays

with steam/air mixtures (see Section 3.2).

Comparison with Watts Bar FSAR results.

The purpose of the ice condenser for long-term accidents is to provide pressure suppression control during those post-blowdown time periods (reflood and frothing) when steam injection rates are still relatively high. This means that ice melting must proceed at a rate that extends the time of melt-out beyond the frothing period, as in the case of the scenario considered here. Melting out too early may result in pressure increases above the design pressure, while melting out later during a less energetic injection period will allow the activated sprays to limit pressure increases to values below the containment design pressure, typically with some margin. In the following discussions we address modeling issues of melt-out and pressure control through a number of comparisons with results reported from the Westinghouse LOTIC code. Later in the discussion we also investigate how uncertainties in the decay heat steam injection can account for a range of CONTAIN pressure predictions that bound the FSAR long-term peak pressure estimate.

Shown in Figure 4.23 are the comparisons between the calculated long-term pressures as determined using the LOTIC and CONTAIN codes. Table 4.7 provides a summary of the inputs and assumptions for modeling used for each code. We note in the pressure profiles that the CONTAIN code predicts an early and delayed onset of pressurization depending on whether or not we assume in the CONTAIN modeling ice melt and condensate water interaction with the lower compartment atmosphere. The CONTAIN calculated ice melt-out times are compared in Figure 4.24 with the predictions from the LOTIC code. A comparison of containment atmospheric and sump temperatures are shown in Figures 4.25 and 4.26. We note those results from either code indicate that the condenser ice melts out at least 1000 seconds beyond the end of the frothing period. In the case where the extended melt-out is predicted by CONTAIN with drain-down interaction, modeled by assuming that the drain-down water forms a spray-like condition in the lower compartment, pressurization is minimized by the slightly reduced steam injection (reduced decay heat rate) and by the increase in the upper compartment spray flow rate that is caused by the start of the residual spray pumps at 3600 seconds.

In the LOTIC calculation, the atmospheric temperatures are constrained to the saturation line, however, this is not the case for the CONTAIN code. While the upper compartment temperatures are saturated for both code calculations, due to the introduction of sprays in that compartment, the lower compartment temperatures are calculated with CONTAIN do show a significant amount of superheating when no drain-down water interaction is assumed, and to a lesser degree when the ice melts out. Shown in Figure 4.27 are the lower compartment atmospheric and saturation temperatures calculated with CONTAIN compared to the LOTIC atmospheric temperature. Figure 4.28 presents a comparison of the CONTAIN calculated exit water temperature from the ice bed with the set value used for the LOTIC code. The code values may also be compared in this figure to the measured water temperature on the floor of the lower plenum in the Waltz Mill test facility during a long-term test.

Clearly, there are some significant inconsistencies between the CONTAIN and LOTIC results that may give rise to some concerns regarding validity of the comparisons, especially with regard to how saturation conditions in the lower compartment are arrived at. In an effort to resolve these concerns we note the following points concerning the LOTIC results as compared to CONTAIN:

- The LOTIC code restricts atmospheric temperatures to follow a saturation curve which we assume is suggested by the wet condition of the lower compartment, especially during periods of high rates of drain-down water that cascade from the lower plenum doors. Near saturated conditions in the lower compartment during the CONTAIN predictions can occur only if there is assumed a substantial thermal interaction between the drain-down water and lower compartment atmosphere; this interaction, however, substantially delays the rate of ice melt-out.

- The assumption to restrain the lower compartment atmospheric temperature to the saturation curve in LOTIC should be associated with an energy exchange between the atmosphere and liquid water in the lower compartment (suspended, on structures, or in the sump). We note however that the sump temperature (sole repository for lower compartment liquid water) predicted with the code is low, and in comparison to the CONTAIN results compares favorably only to estimates where drain-down water interaction is not accounted for.

- The LOTIC code predicts an early ice melt-out time that is consistent with the CONTAIN code only for a case where no drain-down water interaction is assumed.

These observations point to a conclusion that the LOTIC code invokes a restrictive condition in its modeling of the atmosphere (assumed saturation) that is not consistent with energy conservation rules that are adhered to with the CONTAIN code. As a result, it is not possible for the CONTAIN code to predict an early ice melt-out time while maintaining saturation conditions in the lower compartment. This is believed to be the reason for the inconsistencies between atmospheric and sump temperatures predicted by each code.

The CONTAIN pressure increases calculated after ice melt-out have been made using the lower bound decay heat steam injection rate shown in Figure 4.21. The upper bound on the decay heat steam injection is obtained from a tabulation in the Watts Bar FSAR. The lower bound steam rate is based on 1) a standard decay heat equation,[4] 2) the FSAR specified reactor power for decay heat prediction, and 3) 100% of decay heat directed to steam production. Our concern for uncertainty in this discussion of comparison calculations is that the pressure and temperature profiles in the LOTIC results do not appear consistent with the tabulated steam rate during the decay heat period, that is, a significant drop in pressure and temperature are noted in the LOTIC calculation at the end of frothing, whereas, the tabulated steam rates would suggest no reduction.

[4] Way and Wigner estimate of PWR decay heating given in Reference 19.

We show in Figure 4.29 the LOTIC and CONTAIN pressure comparisons with the tabulated decay heat steam rates listed in the Watts Bar FSAR used in the CONTAIN input. These results show that the CONTAIN results are significantly above the LOTIC prediction for either the early or delayed ice melt-out times. We believe from the CONTAIN sensitivity calculations (using the lower and upper bound decay heat steam rates) that the actual LOTIC input for the Watts Bar long-term containment pressurization most likely used a decay heat steam rate within the range inferred in Figure 4.21. We therefore observe that the CONTAIN predicted peak pressures for the long-term scenario would be in reasonable agreement with LOTIC predictions given a more definitive specification of decay heat steaming rates.

Model Validation.

As noted in the discussion on code comparisons that one of the items regarding ice melt-out was whether modeling of drain-down water interactions with the lower compartment atmosphere should be included. Additionally, if the interaction is included, to what extent should that interaction be assumed. Should we assume that 100% of the drain-down water interacts, and what amount of efficiency should be associated with the interaction? From our analysis of the Waltz Mill long-term testing we can attempt to answer these questions only to the extent that these facility tests are believed to be prototypical of the class of plant scenarios that are represented by our demonstration calculation. In terms of the prototypical aspects of the Waltz Mill tests, Westinghouse has stated that these tests are essentially full-scaled geometrical tests with appropriately scaled injections that represent long-term plant scenarios.[5] Our analysis of the Waltz Mill long-term test (Appendix H) has shown the following, with respect to ice melt-out:

- Using a facility nodalization similar to that of the plant demonstration calculation (single ice condenser cell), with ice condenser parameters set identically, the CONTAIN code predicted ice melt-out time earlier than measured.

- Invoking drain-down water interaction by use of spray modeling in the lower compartment resulted in a predicted ice melt-out time that was in better agreement yet still somewhat earlier than the measured ice melt-out time.

- Only in the case of the inclusion of drain-down water interaction could we calculate both an improved ice melt-out time along with a good estimate of the measured lower compartment sump temperatures (lower compartment atmospheric temperatures were not reported in the Waltz Mill Final Test Report).

The important points to be made in these observations are that 1) using the input configuration for nodalization and ice condenser parameters, CONTAIN predicts ice melt-out earlier than measured in the prototypical test, and 2) drain-down water interaction is an important process

---

[5] "Westinghouse Water Reactor Subcommittee Meeting on Ice Condensers," Advisory Committee on Reactor Safeguards, Monroeville, PA., 27 August 1974.

that, if modeled, will extend the period of ice-melt.

Another observation made in the CONTAIN assessment of the Waltz Mill long-term test, and consistent with the measurements, was that while there is even a small amount of ice in the condenser, the pressure suppression effect of the condenser is extremely good. Only, when essentially all of the ice melts out does the pressure begins to increase. As a result, we may view the pressurization phase during the long-term scenario as occurring subsequent to ice melt-out when the pressure suppression process is mainly the result of spray/atmosphere effects. In this case, we may rely on previous discussions where spray modeling validation was at issue. For those discussions we noted that pressure suppression by sprays has been investigated with very good results using the CONTAIN code. These validation studies have confirmed the CONTAIN modeling with both separate and integral test analyses. Specifically, the CONTAIN code spray modeling has been assessed using the JAERI and CVTR spray test results to verify the ability of code to predict accurately pressure suppression in a steam/air mixture.

A summary of the qualification of the CONTAIN code for a long-term scenario is presented in Table 4.8. This summary includes information on the code-to-code comparisons and the model validation approach to qualification.

4.2.3 Modeling Recommendations

The model recommendations for a long-term LOCA analysis of a PWR ice condenser containment are developed in a manner that ensures conservative estimates of maximum pressure loads within the containment. These recommendations have been verified in full-scale test of ice condensers and by comparisons with another NRC reviewed long-term ice condenser analysis code, LOTIC.[6]

A summary of the model recommendations for the long-term LOCA scenario is presented in Table 4-9.

4.2.4 Input Preparation

Table 4-10 gives a summary of the input preparation for performing a long-term LOCA scenario analysis in an ice condenser containment with the CONTAIN code. These input guidelines when followed should produce the type of long-term response result that are discussed in Section 4.2 with the most conservative ice melt-out time. These input guidelines, with respect to a neglect of ice melt and condensate water interactions with the lower compartment atmosphere are intended mainly for pressure suppression assessment. Should there be a requirement to investigate temperature loads in the lower compartment, an inclusion of drain-down water interaction via simulation with spray modeling would be recommended. In such a case, all water from the lower

---

[6] The LOTIC code is the Westinghouse long-term ice condenser code referenced in the USNRC's SRP for ice condenser containments [4].

plenum pool would be used to feed a lower compartment spray small spray droplets diameters (0.0007 meters).

Nodalization.

Shown in Figure 4-30 is a sketch of the nodalization used in the demonstration calculation discussed above. We include a "dummy" cell to receive excess sump water from the lower compartments. This is necessary for long-term scenario modeling where water injection rates are specified and no primary system or safety injection pumps are modeled to control the containment water inventory. The dummy cell with a connection to the lower compartment allows the user to limit at late times the active and inactive sump volumes that are approximately the volumes that would be present during the accident when water recirculation via safety injection pumping is occurring.

For simplicity and conservatism, we have selected a nodalization for the long-term scenario analysis that has the ice condenser modeled as a single cell. In the short-term scenario, we divided the ice condenser into four vertical sections. Shown in Figure 4-31 is the comparison of pressure profiles calculated with the ice condenser modeled with a single and multiple cells. As we see the single cell model results in a more conservative estimate of the late time peak pressure after ice melt-out. Since the single model is shown to be the more conservative model while representing a more simple and economical modeling approach, the single cell ice condenser scheme is used for qualification.

Sprays.

We have noted in various validation studies,[7] that pressure suppression by sprays is well represented by a modeling that simulates a high spray efficiency. To invoke the CONTAIN spray modeling with a high spray efficiency, we need to specify spray droplets of reasonably small size, in the range of the mean droplet size for most spray nozzles. Good results for comparisons with both pressure and temperature suppression profiles have been obtained using a spray droplet diameter of approximately 0.0007 meters.

We have arbitrarily selected the shell type heat exchanger to simulate the spray and residual spray heat exchangers that cool sump water recirculated to the upper compartment spray nozzles. In CONTAIN there are four types of heat exchangers that may be simulated (shell, cross flow, counter flow, or parallel). The method of modeling heat exchanger performance in the code is the well known effectiveness – NTU method, where heat exchanger performance can be modeled when only the inlet temperatures are known. A shell type exchanger has been used for the qualification of the code but other exchanger types could have been used with little impact on the calculated late time pressure profiles since the effectiveness between exchanger types is relatively

---

[7] NRC report, "An Assessment of CONTAIN 2.0: A Focus on Containment Thermal Hydraulics (Including Hydrogen Distribution)."

small. Figure 4-32 shows the importance of including the spray heat exchangers for limiting the late time pressurization. In this figure, we show the limiting cases where the spray temperature is 1) set at the ambient tank temperature, and 2) set at the sump temperature assuming no spray heat exchangers.

Lower Compartment Sumps.

The lower compartment sumps (active and inactive) are modeled with an exposed surface area that is equal approximately to the flooded floor area specified in the Watts Bar FSAR. The heat exchangers for the recirculating sprays are located in the active sump which is the pool in the open region of the lower compartment. The pool-type flow path that connects the two pools in the lower compartment (open and dead-ended regions) maintains a near equal pool level between each region. The inclusion of an overflow to the "dummy" cell functions to limit the maximum sump volumes at late times, as discussed above. It is important that the "dummy" cell be modeled in a manner that does not limit the flow of this overflowing water. This means that the "dummy" cell should be modeled as a large volume cell having a nearly constant pressure that is less than the containment – we chose a pressure condition for the "dummy" cell that is at the ambient atmospheric condition.

Table 4.6 Accident chronology for a double-ended pump suction LOCA, minimum safety injection.

Event	Time, sec	Comment
Rupture	0.	Lower compartment break location in the open region
Accumulator flow starts	15.5	Water driven into core by nitrogen pressurized accumulators (begin nitrogen injection)
Assumed initiation of ECCS	24.0	
End of blowdown	24.0	
Assumed initiation of quench spray system	55.0	Spray water from RWST; 135 seconds delay to reach full flow rate of ~ 253 kg/s
Accumulators empty	56.1	
End of reflood	195.0	
Froth injection from steam generators starts	195.0	Froth boiling in steam generator tubes after core has been quenched
Recirculating fans start	600.0	Flow rate of 18.88 m^3/s from upper to lower compartment
End of froth injection	1765	
Start of decay heating phase	1765	
End of quench spray water from RWST	2774	
Spray system begins to draw water from lower compartment sump	2894	Flow rate maintained at ~ 253 kg/s; flow from sump is cooled by the spray system heat exchangers
Residual spray begins	3600	Switch over of a residual heat removal pump from safety injection mode to recirculation spray mode, flow rate is ~ 126.5 kg/s

Table 4.7 Modeling and input selection for the Watts Bar demonstration calculation.		
Modeling/Input	**CONTAIN**	**LOTIC**
Input:		
Source injection (blowdown, reflood, frothing, and decay heat)	FSAR basis (tabulated values)	Same
Cooling water temperature for heat exchangers	302.6 K	
Steam flow to ice bed	no maldistribution of flow	
Ice condenser bypass	no bypass	
Spray pump flow	FSAR basis (~ 253 kg/s)	
Residual spray	FSAR basis (~ 126 kg/s)	
Structure heat sinks	FSAR basis for composition, geometry and location (forced convection for blowdown, free convection for post-blowdown)	FSAR basis for composition, geometry and location (Tagami correlation during blowdown)
Sump heat exchangers	FSAR basis for overall heat transfer coefficient X area	Same
Active sump volume	FSAR basis (1457 m^3)	
Air return fan rate	FSAR basis (18.88 kg/s)	
Modeling:		
Blowdown and post-blowdown ice condenser drain temperatures	Calculated (~ saturation temperature in ice condenser)	Set: blowdown (361 K) post-blowdown (328 K)
Pressure differentials	Calculated	Single pressure for entire containment
atmospheric temperatures	Calculated	Restricted to saturation
Ice melt and condensate drain-down interaction with lower compartment atmosphere	may be simulated using a spray-type modeling	Assumed not to occur (inferred from CONTAIN sensitivity analyses)

Table 4-8 Summary of the CONTAIN qualification for long-term LOCA calculations in a PWR ice condenser containment.

Modeling Area	LOTIC	CONTAIN	Comments	Reference
geometric nodalization:				
upper compartment	single cell	single cell	sprays in upper compartment result in a well mixed region, justifying a single cell model	CAR* [pp. 3-33, 3-64, 3-67, 4-15, 4-126]
ice condenser	single cell (subsections to account for local melt-out regions)	single cell	CONTAIN ice condenser single cell nodalization as used in the Waltz Mill long-term test assessment	Appendix H [H-58, H-90]
lower compartment	two cells (open and dead-ended regions)	two cells (open and dead-ended regions)	similar modeling approach; drain-down water and steam source maintains well mixed open region where the active sump and interactive atmosphere region is located	—
steam injections	—	thermal equilibrium, homogeneous mixing, with dropout	time period of interest is during the periods where the injection is single phase steam (thermal equilibrium homogeneous mixing is conservative), and when the injection rate is relatively low so that suspended or entrained liquid water is minimum	Appendix H [H-58]
heat transfer to structures	included – FSAR specification; Tagami correlation used during blowdown	included – FSAR specification; ramped forced convective condensation used during blowdown; natural convection condensation after blowdown	forced convective condensation velocity set to a velocity rate to simulate Tagami correlation; natural convective condensation represents a conservative assessment of condensation conditions	—
heat transfer to pools	pool interaction with atmosphere and basemat included	pool interaction with atmosphere and basmat included; natural convective conditions assumed	pool area specified in FSAR (floor structure in contact with pool); conservative model approach since evaporation of hot sump water will slightly retard the depressurization rate	CAR [pp. 4-22]

* CONTAIN assessment report (CAR) — NRC informal report, "An Assessment of CONTAIN 2.0: A Focus on Containment Thermal Hydraulics (Including Hydrogen Distribution)," March 1999.

Table 4-8 Summary of the CONTAIN qualification for long-term LOCA calculations in a PWR ice condenser containment (cont.).

Modeling Area	LOTIC	CONTAIN	Comments	Reference
flow paths:				
equations	uniform pressure	lumped parameter momentum equation (1-D), with acceleration terms	small pressure difference between cell due to the relatively low flow rates between cells	—
loss coefficients (ice condenser)	—	based on experimental tests for scaled models	minimum importance due to the small pressure differentials between cells	—
critical flow	—	frozen, homogeneous equilibrium model [FHEM] with multiplier (0.7)	no importance due to the small pressure differentials between cells	—
ice bed heat and mass transfer	semi-empirical model with calibration factor	physically based HMT analogy method with calibration factor applied to Nusselt number calculated for ice column	CONTAIN ice bed parameters are set according to the input selected for the Waltz Mill long-term test analysis	Appendix H [H-58]
plenum doors	not modeled	static model; pressure verses area modeling	CONTAIN door opening parameters based on plant specification obtained for TVA ice condenser plants; parameters set the same as CONTAIN input for Waltz Mill long-term test analysis	Appendix H [H-58], Reference 16
drain-down ice melt and condensate interaction	not modeled (assumed saturation temperature)	interaction by spray modeling in lower compartment fed by drain-down water	lower compartment spray modeling to simulate drain-down water cooling of atmosphere verified by Waltz Mill long-term CONTAIN calculations	Appendix H [H-58, H-90]
sprays	modeled (quench and recirculation sprays)	modeled (quench and recirculation sprays)	CONTAIN spray model validated in separate and integral effects tests (JAERI and CVTR)	CAR [pp. 3-33, 3-64, 3-67, 4-15]
spray heat exchangers	modeled	modeled (using overall heat transfer coefficient and area specified in FSAR)	CONTAIN analytical testing of heat exchanger modeling during code development used as validation of modeling	—

Table 4-9 General modeling recommendations for a qualified CONTAIN long-term LOCA calculation in a PWR ice condenser containment.

Phenomena	Modeling Recommendations
Multi-component gas compression	Nodalize upper containment with single cell; single cell model of ice condenser; multiple cells for lower compartment – resolving the open and dead-ended volumes.
Steam injection	Use a thermal equilibrium method for water injection modeling (ATMOS SOURCE); include dropout modeling of suspended liquid water (DROPOUT)
Inter-compartment flows	Gas loss coefficients (ice condenser scaled tests)
By-pass condenser flows	Neglect
Plenum doors	Static opening under pressure – pressure versus area (reversible or irreversible engineering vents)
Ice bed heat and mass transfer	Geometrical specifications; minimum liquid film thickness; Nusselt multiplier
Structure heat transfer	Include FSAR specifications for area and thickness; use adiabatic boundary conditions for outer shell surface; optional – to include forced convective heat transfer for blowdown; natural convective heat transfer for periods after blowdown
Pools	Include upper and lower compartment pools, diverting water from upper compartment to lower compartment; include pool/atmosphere heat and mass transfer; overflow lower compartment pool at set height to maintain active and inactive pool volumes – overflow to dummy cell; allow default basemat heat transfer
Ice melt and condensate	Divert to lower compartment without drain-down water interaction with lower compartment atmosphere; use default ice melt and condensate exit temperature
Sprays	Use spray droplet diameters of 0.0007 meters; simulate the delay of recirculating sprays with small tank mass and mass rate
Heat exchangers	Specify heat exchanger overall coefficient and area according to specification; use shell-type heat exchanger

Table 4-10 Input guidelines for modeling a long-term LOCA scenario in a PWR ice condenser containment.		
Input Section	**Block/Parameter(s)**	**Comment**
Global:		
Nodalization	ncells = M (multiple-cells) ncells = 7 (demonstration calculation)	suggest single upper compartment, single cell for ice condenser, single cell for each plenum, two cells for lower compartment (open and dead-ended regions) – consult FSAR for region and room description
Material properties	properties specification (rho, cond, and sph) – USERDAT	consult FSAR for specific properties values
Timesteps	TIMES	set to give accurate results for the time scale of interest (~ seconds); gradual increase from ~ 0.01 to 2 seconds over a 300 seconds period
Flow	DROPOUT	dropout of liquid water in atmosphere
engineering vents		
plenum doors	RVAREA-P or IRAREA-P	use static pressure vs. area tables (see listing)
pool type paths	type=pool	liquid redistribution path from lower plenum to lower compartment (set elevation for path at level just above plenum floor level, set plenum gas path to lower compartment at level above pool path to avoid possible closing due to flooding) liquid redistribution path from open to dead-ended cell in lower compartment, set path elevation below the open compartment overflow level to dummy cell that receives excess lower compartment sump water liquid redistribution path for upper to lower compartment sump
loss coefficients	VCFC	gas loss coefficients (see listing)
inertia mass	VAVL	area/length for paths (use FSAR specification; flow path area/length between adjoining cell center in ice condenser; otherwise, flow path area / volume ** 1/3, where the volume is the minimum volume connected to the path)

Table 4-10 Input guidelines for modeling a long-term LOCA scenario in a PWR ice condenser containment (cont.).

Input Section	Block/Parameter(s)	Comment
Flow		
vena contracta	VCONTRA	set for all paths, VCONTRA = 0.7
elevations	VELEVB, VELEVF	set according to specification, use RESOLVE keyword
fan flow rate	VFLOW-T	set volumetric flow vs. time according to FSAR specification
Upper compartment:		
Geometry	gasvol, cellhist	free volume and pool areas set to FSAR specification (assure that cellhist and free volume are consistent)
Atmosphere initial conditions	ATMOS block	pressure, temperature, and humidity (set according to FSAR specification)
Structures	STRUC	structure area, thickness, and composition (set according to FSAR specification)
Lower cell	low-cell	include with heat and mass transfer to atmosphere and basemat
Sprays (quench)	ENGINEER SPRAY	source and receiver cells to direct sprays (source and receiver cell is current cell, that is, upper compartment cell #) source table – mass rate and temperature vs. time (according to FSAR specification); spray droplet diamter = 0.0007 meters; spray height – distance from operation floor to spring-line
Sprays (recirculation)	ENGINEER SPRAY	source and receiver cells to direct sprays (sump in lower compartment, receiver cell is the current cell, that is, upper compartment cell #); include TANK, HEX, and PUMP keyword input in this sequence
tank	TANK	use to set effective time to begin recirulation; use small tank mass and mass flow rate to set time that tank empties and pump flow begins
spray heat exchanger	HEX, SHELL	use FSAR specifications for exchanger overall heat transfer coefficient, heat transfer area, coolant flow rate, and inlet coolant temperature
spray recirculation rate	PUMP	use FSAR specifications

Table 4-10 Input guidelines for modeling a long-term LOCA scenario in a PWR ice condenser containment (cont.).		
Input Section	**Block/Parameter(s)**	**Comment**
Lower compartment (open):		
Geometry	gasvol, cellhist	free volume and active sump area and volume (set to FSAR specification, using a two level cellhist input to define the (first level) active sump area and volume and remaining free volume using the second level height)
Atmosphere initial conditions and water injection	ATMOS block, SOURCE block	pressure, temperature, and humidity (FSAR specification); blowdown, reflood, frothing, and decay heat sources (FSAR specification)
Structures	STRUC	structure area, thickness, and composition (set according to FSAR specification)
Lower cell	low-cell	set area to sump area set in cellhist input; include basemat according to FSAR specification
Overflow excess water	ENGINEER OVERFLOW	source cell is low compartment cell #; divert water to dummy receiver cell set overflow height to correspond to active sump volume (~ first level height in cellhist input)
Ice condenser:		
Geometry	ENGINEER ICECOND (hitici, tmsici, ciarfl, arhtin)	source cell is current ice condenser cell #, divert water to set to FSAR geometric and initial condition specification
Heat and mass transfer	ICECOND (ciflmx, cihtml, citice, citlex)	ciflmx = 5×10^{-6}, cihtml = 10 (based on Waltz Mill assessment) citice (FSAR specification, or default), citlex (default)
Lower plenum pool	low-cell	include with no basemat heat transfer (HT-TRAN on off on on on)
Dummy compartment:		
Geometry	gasvol, cellhist	dummy large volume
Atmosphere initial conditions	ATMOS	set to atmospheric conditions
Lower cell	low-cell	dummy receiver pool

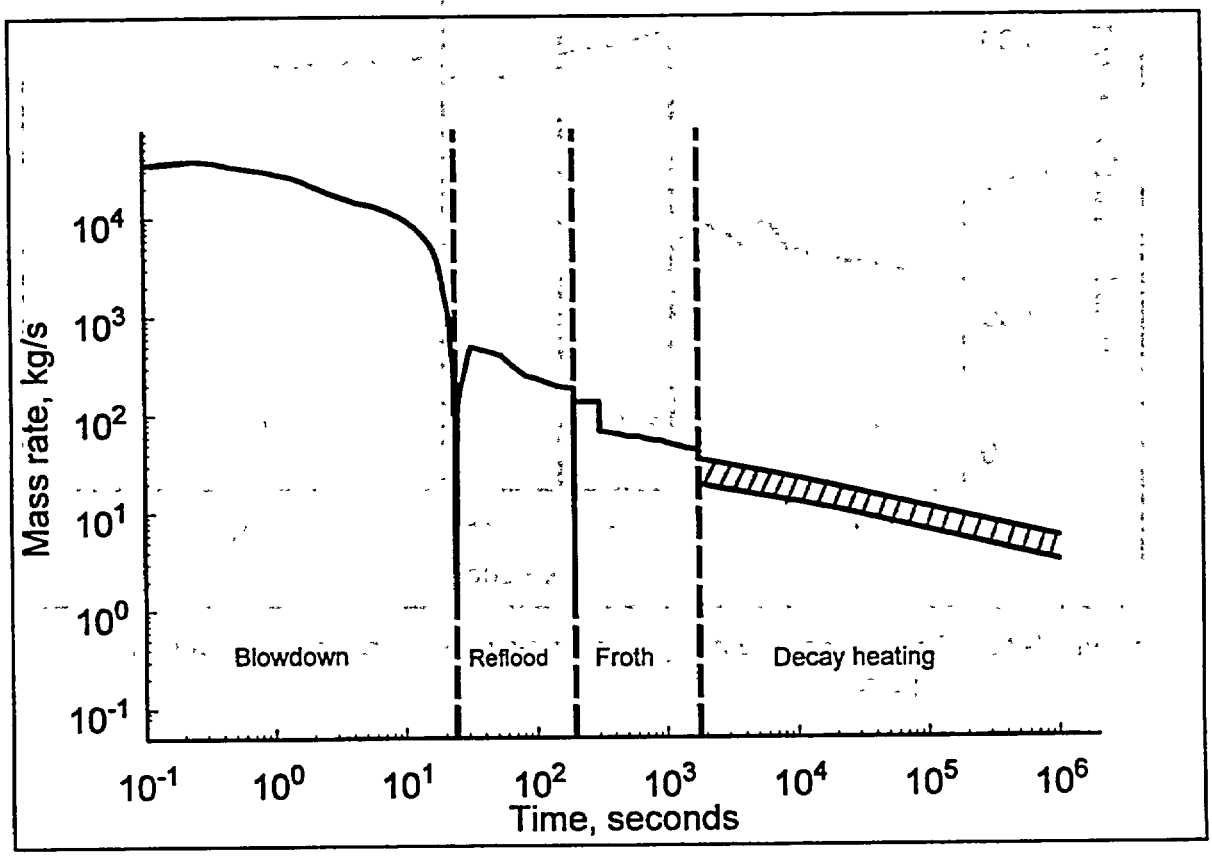

Figure 4-21. Break mass flow rate for long-term scenario (pump suction pipe rupture). Decay heating mass rates indicate the uncertainty in the projected rates.

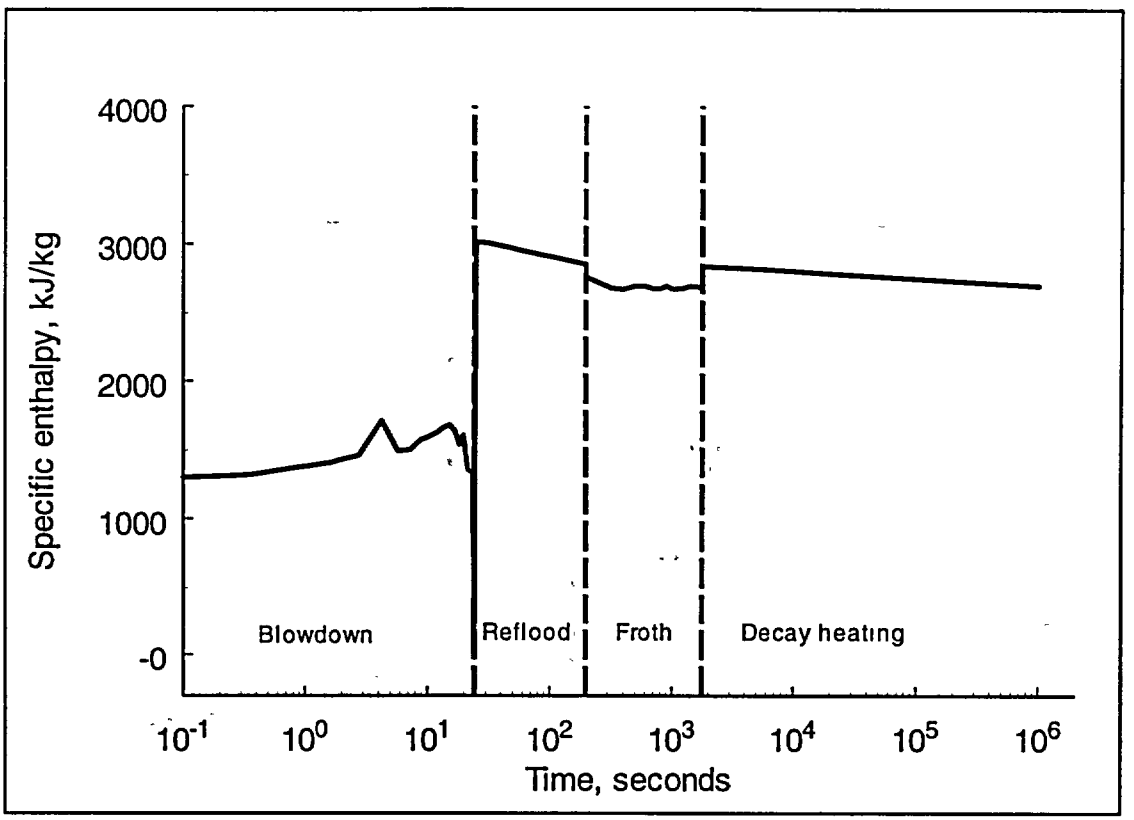

Figure 4-22. Break specific enthalpy for long-term scenario (pump suction pipe rupture).

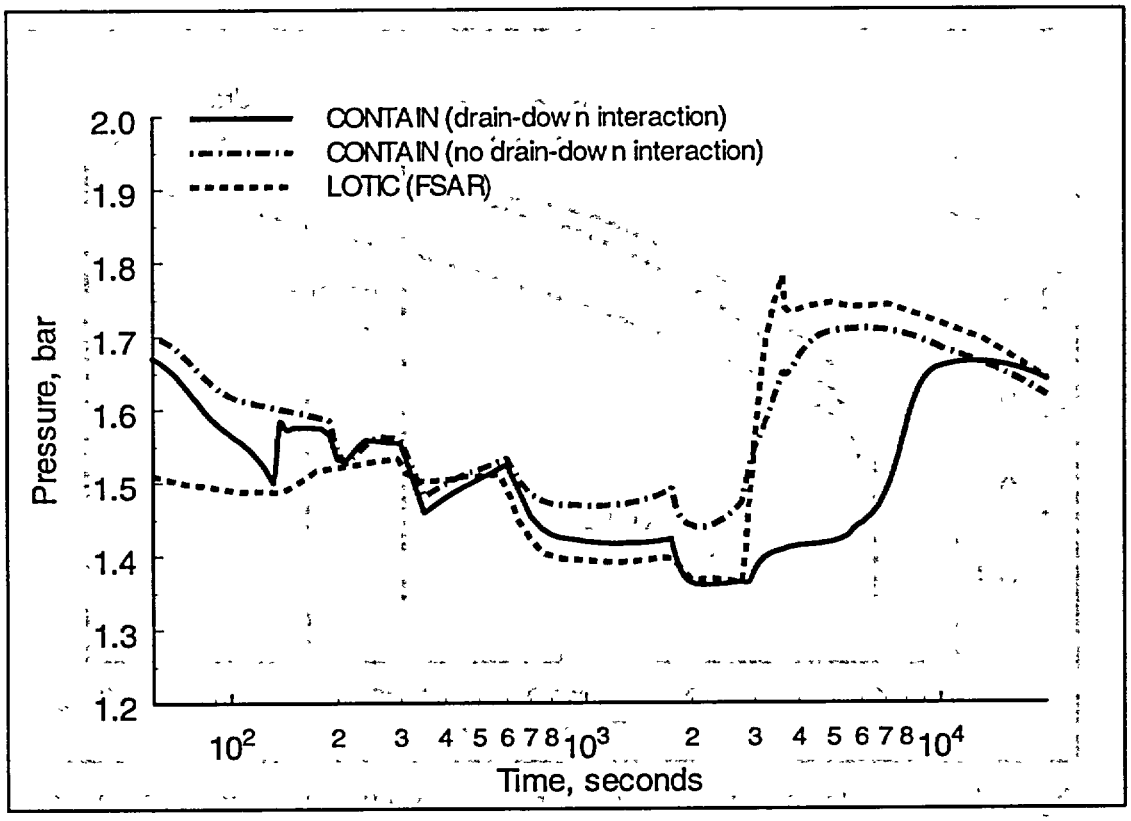

Figure 4.23 Calculated long-term pressures for a pump suction pipe rupture scenario in an ice condenser containment.

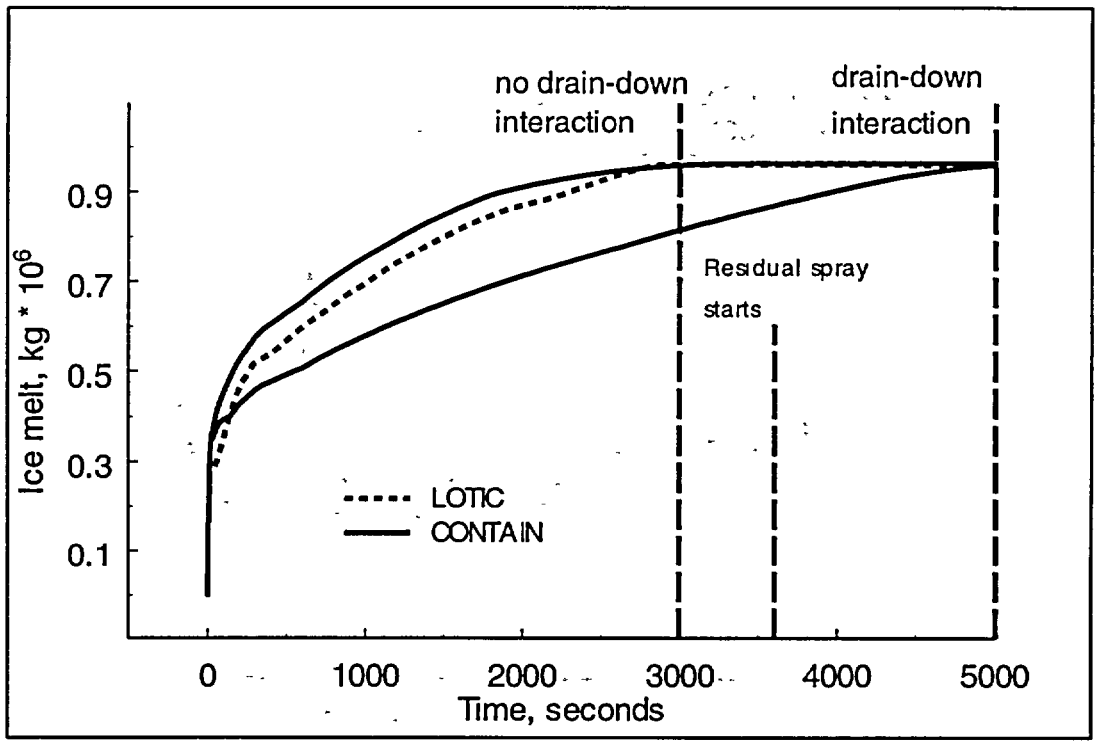

Figure 4-24 Calculated ice melt-out for a pump suction pipe rupture scenario, showing the effect of drain-down water interaction with lower compartment atmosphere.

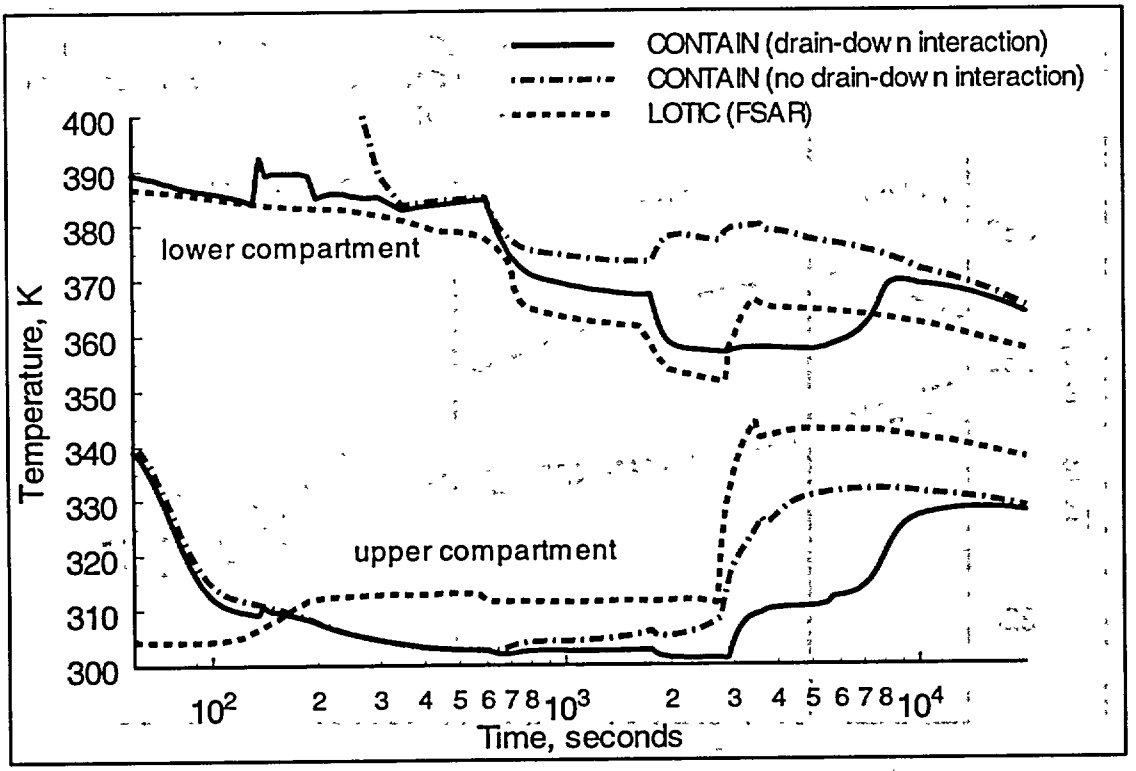

Figure 4-25 Calculated compartment atmospheric temperatures for a pump suction pipe rupture scenario.

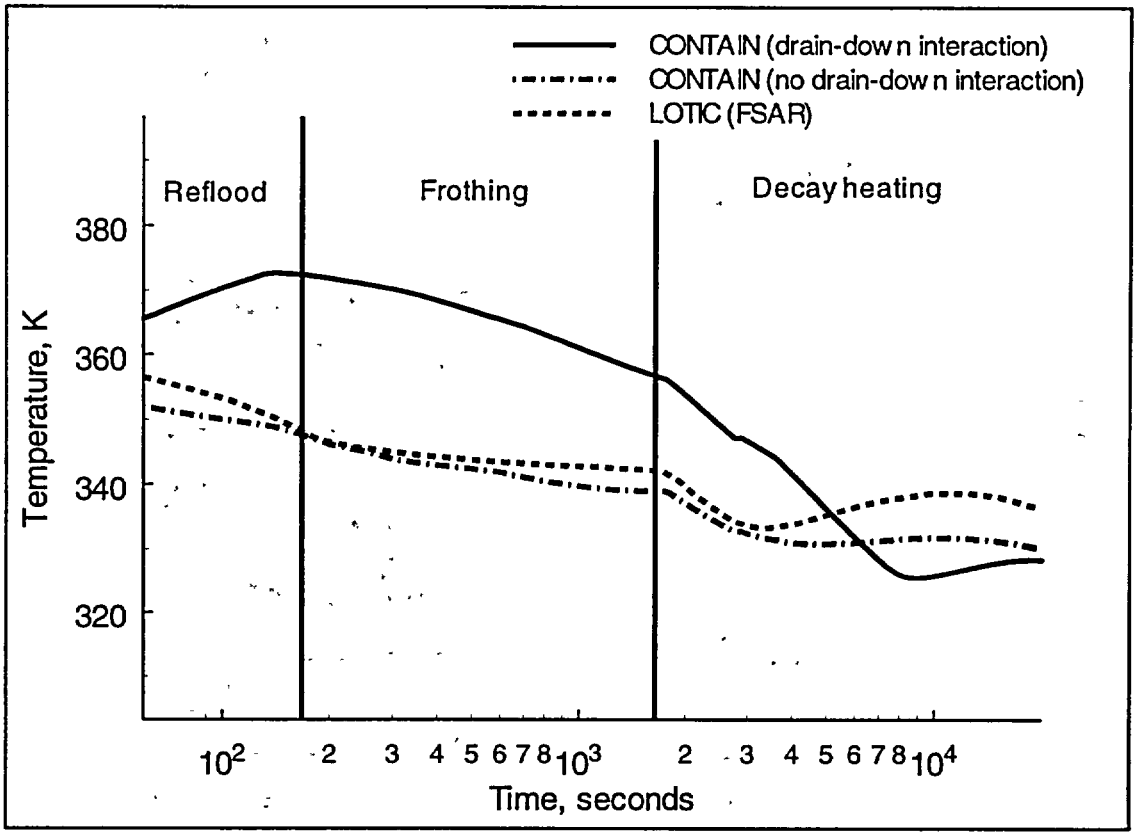

Figure 4-26 Calculated lower compartment active sump temperatures for a pump suction pipe rupture scenario.

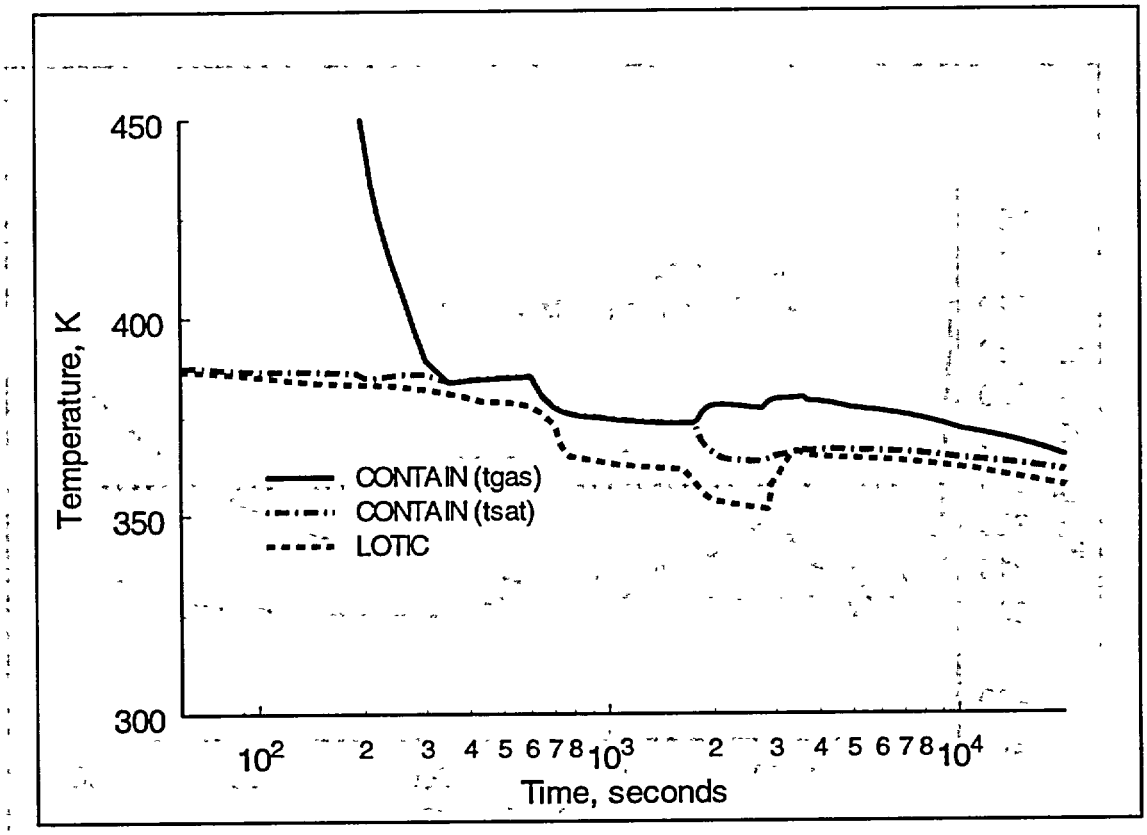

Figure 4-27 Calculated lower compartment atmospheric temperatures for a pump suction pipe rupture scenario (no drain-down water interaction for the CONTAIN calculation).

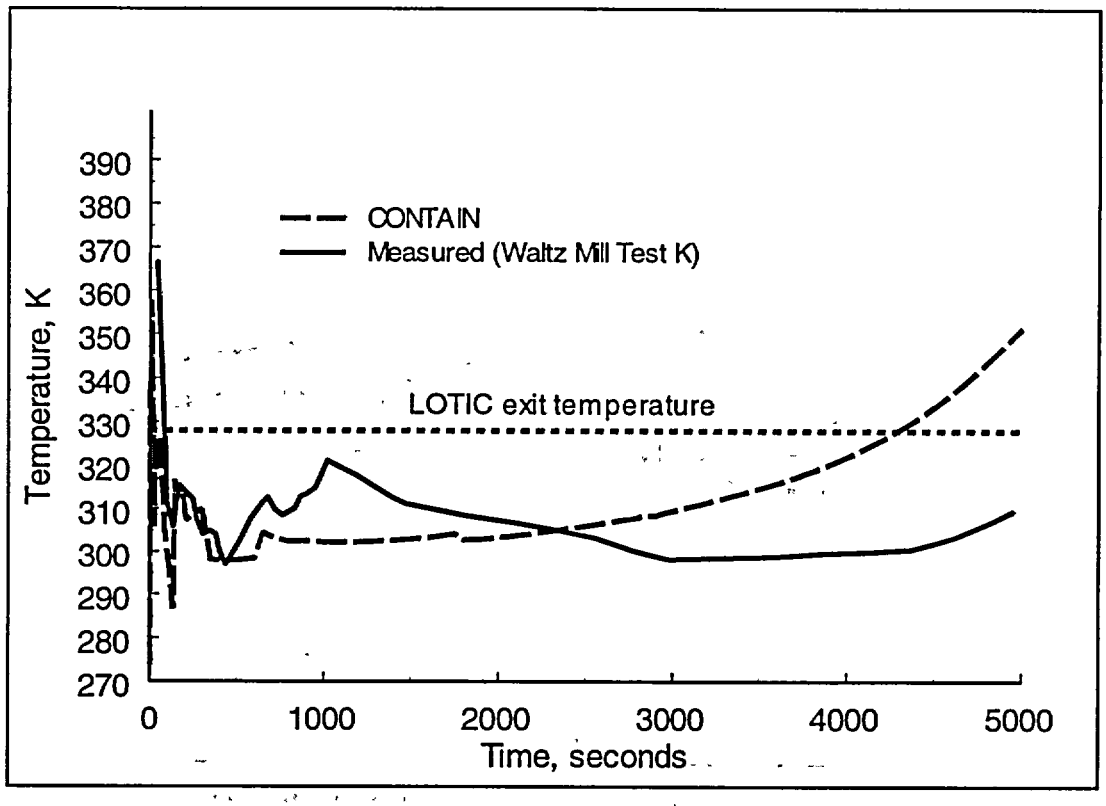

Figure 4-28 Ice bed melt water and condensate exit temperature for pump suction pipe rupture scenario.

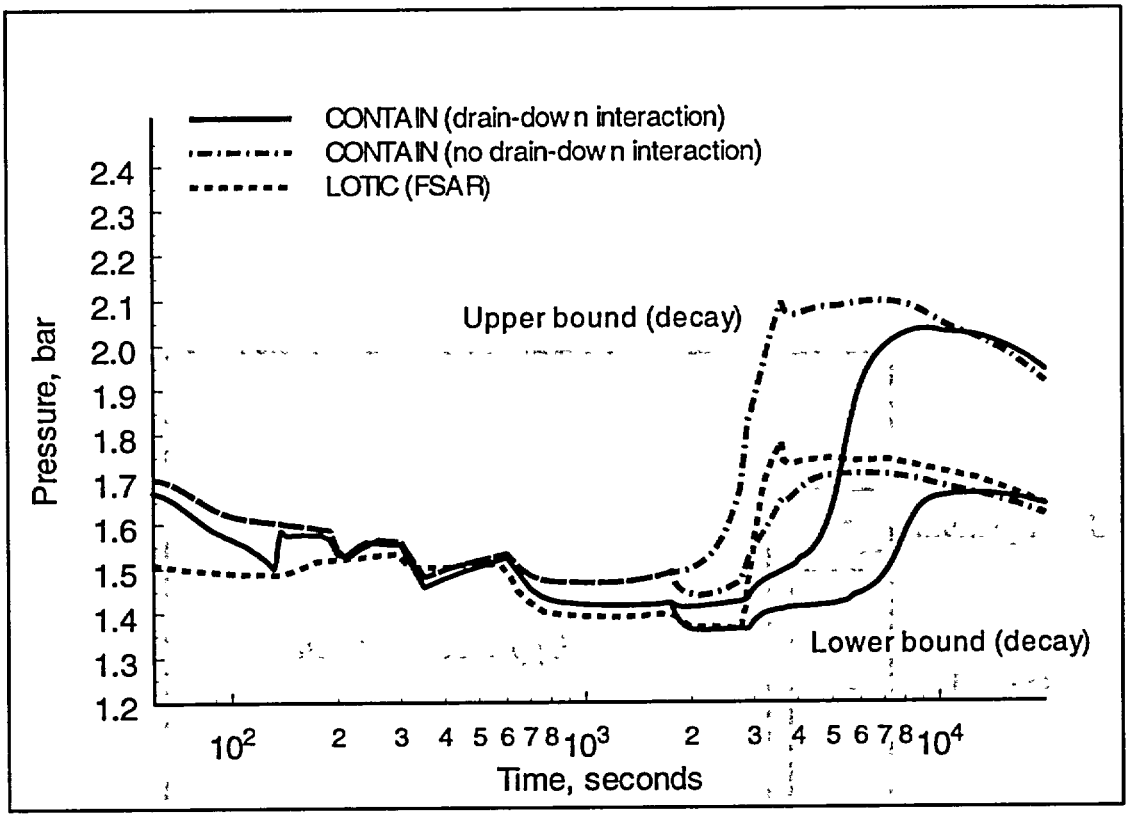

Figure 4-29 Calculated pressures for a pump suction pipe rupture, showing the sensitivity of the CONTAIN results to the range of upper and lower bounds on decay heating steam injection.

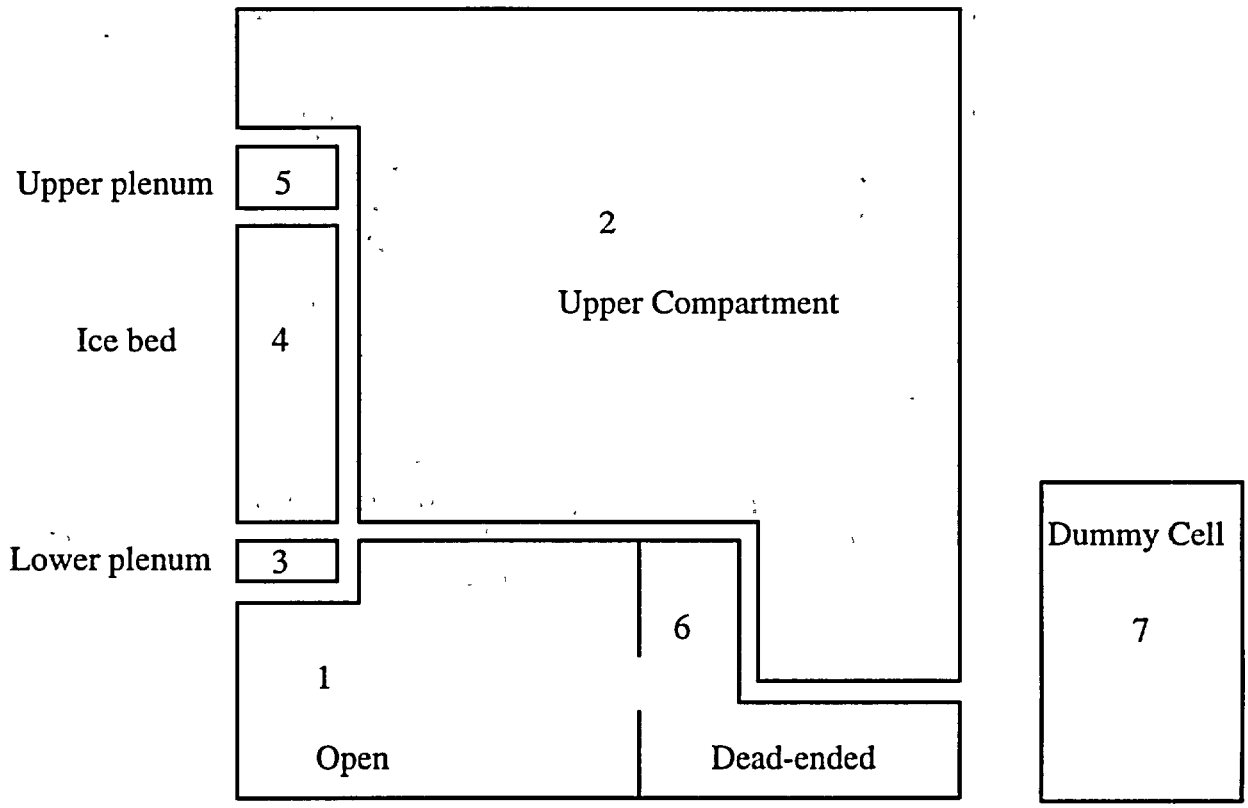

Figure 4-30 Sketch of the CONTAIN nodalization of an ice condenser containment recommended for long-term pressure analysis.

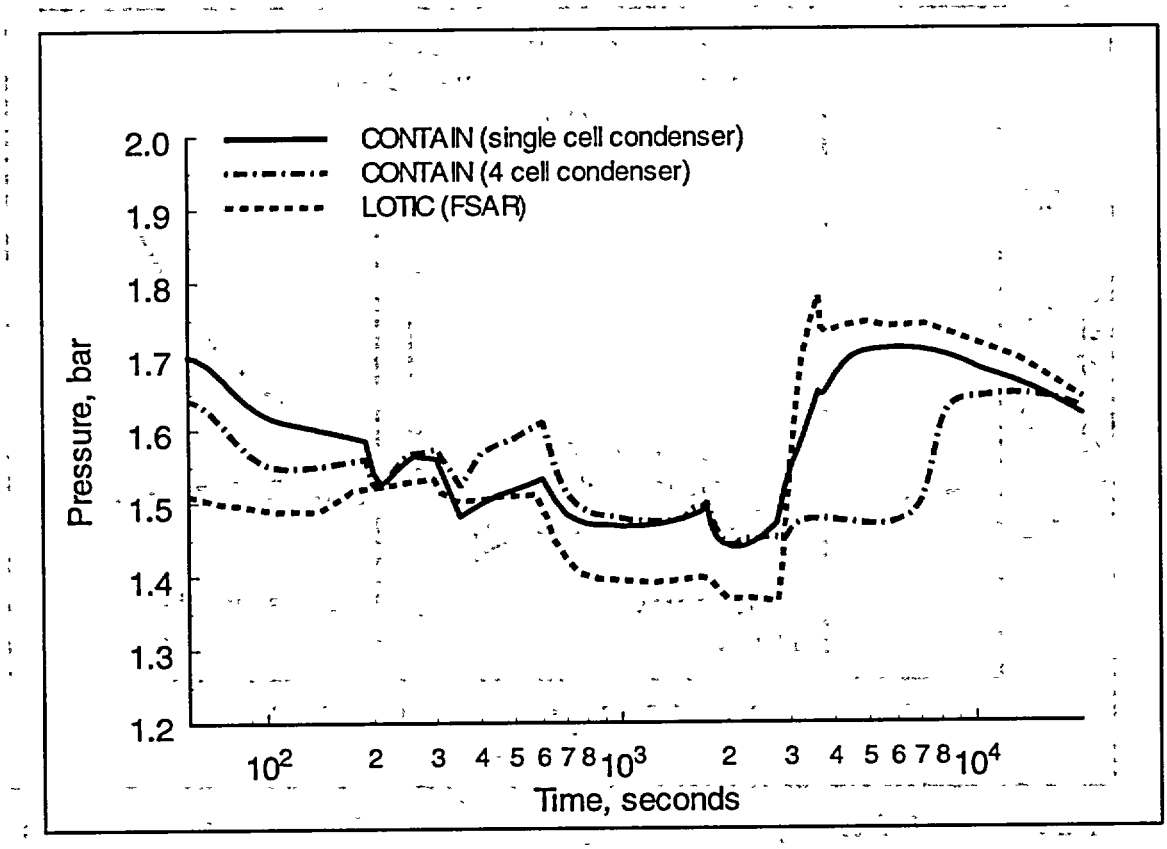

Figure 4-31 Calculated pressures for pump suction pipe rupture scenario, showing the effect of ice bed nodalization (no drain-down water interaction with lower compartment atmosphere).

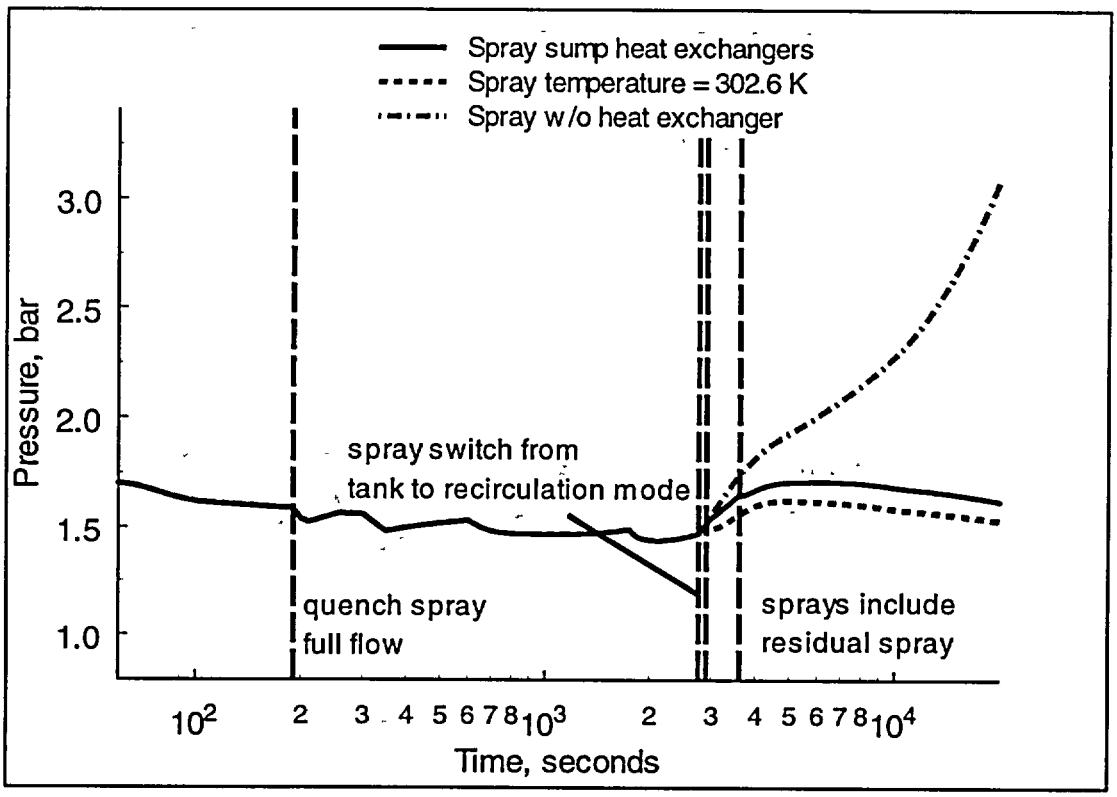

Figure 4-32 Effect of spray water temperature on CONTAIN calculated pressures for a pump suction pipe rupture scenario (no drain-down water interaction with lower compartment atmosphere).

5 Secondary Containment Analysis

In this chapter we discuss qualification and methods that can be used to evaluate the functional capability of a secondary containment system with CONTAIN [1]. The secondary containment system includes the outer containment structure of dual containment plants and the associated systems that mitigate the radiological consequences of postulated accidents. Figure 5-1 shows the shield building of an ice condenser plant. In this case, the primary containment building steel wall is included as a structure which is part of the secondary containment system. The region between the primary and shield building walls is referred to as the secondary containment. Secondary containment structures and supporting systems are provided to collect and process radioactive material that may leak from the primary containment following an accident. The supporting systems (e.g., fans and dampers) maintain a negative pressure[1] within the secondary containment and also collect and process radioactive material. The design-basis for the secondary containment is devised to assure that an effective barrier exists for airborne fission products that leak from the primary containment during a loss-of-coolant accident (LOCA). The Standard Review Plan 6.2.3, "Secondary Containment Functional Design" provides guidance and considerations that should be addressed in order to demonstrate the plant's design capabilities can maintain negative secondary containment pressure during a LOCA event.

The focus of this chapter is on the CONTAIN code's thermal hydraulic models for the secondary containment analysis; however, it should be noted that the CONTAIN code has sophisticated models to address fission product tracking and transport. These features of the code may be especially useful for a complete analysis of the secondary containment function. Examples of the fission product transport capability for the CONTAIN code can be found among numerous CONTAIN references that address source term issues. With respect to those issues related to fission product releases from stacks and ventilation systems, CONTAIN has been utilized by the Department of Energy for the analyses of production reactor confinements, such as the N-Reactor [20]. These applications required some modification to the code vent path logic to treat the complicated confinement ventilation system. The modifications are not included in the official CONTAIN 2.0 version of the code, and are not required for the secondary containment analysis discussed in this chapter.

5.1 Scenario Selected for Analysis

As a demonstration, we have chosen to analyze a plant that uses secondary containment systems similar to those used in the Watts Bar ice condenser plant. This plant was arbitrarily selected for purposes of demonstrating code capabilities for modeling a generic ice condenser problem which

---

[1] Secondary containment pressure is represented as a differential or gauge pressure in most cases in this chapter, where the reference environment pressure is assumed to be atmospheric (1.0×10^5 Pa). The common unit for indicating small pressure differentials in secondary containment analyses is in inches of water. Gauge pressure units are therefore denoted as "in. w. g." in the figures.

tends to be more difficult than other containment types. Hence, in some areas actual plant specific information was not used because further clarification was needed. In this regard, the long-term LOCA scenario discussed in section 4.2 of the previous chapter is used as the basis for the analysis. Shown in Figures 5-2 and 5-3 are the profiles of the primary containment pressure and temperature loading profile for a LOCA scenario. These profiles were discussed in the previous chapter, where the specific calculation was denoted as "drain-down interaction" profiles (Figures 4-23 and 4-25).

As noted with the ice condenser LOCA, there are four phases to the accident, as described in Chapter 4. From the standpoint of the secondary containment analyses, the concern is with all phases – the blowdown, reflood, frothing, and decay heat portion of the accident. However, with respect to our review and code qualification, we have restricted our analysis to the first 2000 seconds of an accident scenario, which is prior to ice melt-out.

The accident scenario therefore begins with a very rapid pressurization of the primary containment due to a high energy line rupture and then continues during the period of significant ice melting when the primary containment pressure is partially reduced. Pressure in the secondary containment rapidly increases as a result of the 1) secondary volume decrease when the primary containment shell expands due to pressure and thermal loading, 2) heating of the secondary containment atmosphere as the primary containment shell temperature increases, and 3) post-accident secondary containment in-leakage. As the safety grade emergency gas treatment system (EGTS) is activated, gas from the secondary containment is exhausted to maintain a negative pressure differential. Of special importance to our analysis is the ability of the EGTS to keep the air pressure within the secondary containment below atmospheric pressure at all times in which the integrity of the secondary containment is required.

5.2 Modeling Requirements

Shown in Figure 5-4 is a sketch of a primary and secondary containment, where the primary containment pressure and temperature loads Pp(t) and Tp(t), as well as, the secondary containment loads Ps(t) and Ts(t) are indicated as functions of time. Due to the large range of primary containment loads, there will be an expansion of the primary containment steel shell into the secondary containment enclosure due to pressure and thermal loads on the shell from the primary containment side. In the sketch, this is indicated by the dashed line around the primary containment initial boundary and the designation dV(t). As a result of the "flexing" of the primary containment boundary during the accident, the secondary containment volume varies with time, Vs(t).

To keep the secondary containment pressure below atmospheric pressure, the EGTS activates during an accident to maintain negative pressure that was also maintained during normal operation by another control subsystem. The EGTS is a complicated ventilation system that pulls secondary containment air from the top of the containment ($\dot{V}_{out}(t)$) and returns a portion of the air (after filtering) to the lower elevation of the secondary containment ($\dot{V}_{in}(t)$). A portion of

the air taken from the secondary containment is not returned;

$$\dot{V}ex(t) \sim \dot{V}out(t) - \dot{V}in(t) ,$$

is exhausted from the secondary containment. Dampers in the EGTS control the amount of exhaust gas to keep the secondary containment air pressure below a post-accident set point (~ - 0.5 inches of water, or -124.4 Pa below atmospheric pressure). Whether this pressure control is capable of maintaining a negative pressure in the secondary containment is the objective of this analysis.

To model the secondary containment system during a LOCA we require modeling in four important areas:

- containment volume change;
- atmospheric heating;
- in-leakage; and,
- ventilation.

Additionally, we require that the containment model be able to resolve the hydrostatic pressure variation within the containment space. Resolution of the hydrostatic pressure variation is needed to analyze the potential for leakage at various elevations into the containment from the surrounding environment.[2]

The driving functions for the containment volume change are based on the primary containment pressure and thermal loads. The pressure load is determined from a decoupled primary to secondary containment calculation, such as presented in Figure 5-2. The atmospheric heating of the primary containment shell and the secondary containment gases are based also on a decoupled calculation, Figure 5-3, where now the driving function for the calculation is the primary containment gas temperature determined as discussed in Chapter 4. In this case, the primary gas temperature, as a boundary condition for this analysis, provides a conservative estimate of the actual gas temperature since the temperature is based on a calculation where the primary containment shell outer boundary condition is assumed adiabatic. Using this gas temperature boundary condition for the primary shell, and a conservative gas to wall heat transfer coefficient, the thermal loading of the shell and sensible heat transfer to the secondary containment is determined in a conservative manner.

In-leakage results from the negative pressure being maintained in the secondary containment air space, resulting from leakage occurring around penetrations in the primary containment shell and shield building. The ventilation system that maintains pressure control during an accident consists of a network of fans, filters, and dampers that operate on feedback from measured pressure differentials between the secondary containment and environment. This functional

---

[2] Note, the hydrostatic head in the secondary containment is approximately 2.2 inches.

control is designed into the EGTS.

5.3 Qualification

In qualifying the CONTAIN code, a secondary containment demonstration calculation is described and some results are compared to information presented in the Watts Bar FSAR. In our approach, we assure that the key modeling requirements are met by the various modeling and input features of the code, as shown in Table 5-1. In the following subsections we discuss how each key phenomenon or design feature may be modeled by the code. These models are then combined in the final subsection that presents a CONTAIN secondary containment demonstration calculation.

5.3.1 Containment Volumetric Change

In the CONTAIN code, atmosphere gases in a volume can be displaced by water in a pool. As the water rises or falls, the volume of gas is compressed or expanded. To simulate the secondary containment volume change due to the movement of the primary containment shell, we use a time varying pool volume to represent a function $dV(t)$. The pool input is setup so that there are no heat or mass transfer interactions between the pool and secondary containment atmosphere. Since the primary containment shell expansion and contraction is decoupled from the secondary containment analysis, so that in order to derive the function $dV(t)$, we may devise some simple methods. For instance, if we assume that the primary containment is a pressure vessel with a thin shell wall, then we can use simple quasi-static equations for the deformation due to an internal pressure, or pressure differential p and wall temperature change ΔT.

Pressure. The deformation or dilation of the primary containment due only to pressure, is as follows:

$$\delta_{cyl} = \frac{pr^2}{2hE}(2-\mu), \qquad 5\text{-}1$$

for the cylinder portion of the primary containment wall; and, for the hemispherical portion

$$\delta_{sph} = \frac{pr2}{2hE}(1-\mu). \qquad 5\text{-}2$$

In these equations, p is the pressure differential across the wall, r is the cylinder or spherical dome radius (17.5 m), and h is the thickness of the wall (~0.02 m). E and μ are the wall modulus of elasticity and Poisson's ratio, respectively. The volume change as a result of dilation may be given by

$$dV_{cyl}^{press}(t) = \pi L\left[(r+\delta_{cyl}(t))^2 - r^2\right], \qquad 5\text{-}3$$

for the cylinder portion, where L is the height of the cylinder (34 m). For the dome, assumed to be hemispherical, the change in volume is

$$dV_{sph}^{press}(t) = \frac{2\pi}{3}\left[(r + \delta_{sph}(t))^3 - r^3\right]. \qquad 5\text{-}4$$

The total volume change of the secondary containment due to pressure loading on the primary containment shell is

$$dV^{press}(t) = dV_{cyl}^{press}(t) + dV_{sph}^{press}(t). \qquad 5\text{-}6$$

Using the pressure profiles shown in Figure 5-2, the secondary containment volume changes are calculated as shown in Figure 5-5. The maximum volume change due to pressure loading is approximately 21 m^3, which compares favorably to the total volume change listed in the Watts Bar FSAR; 21.7 m^3.

Temperature. The dilation of the lower compartment and upper compartment is determined approximately by calculating an average primary wall temperature T_{avg} during the transient, and estimating the dilation as;

$$\delta_{low}^{temp}(t) = R_{cyl}\alpha(T_{avg}^{low}(t) - T_{avg}^{low}(0)) \text{ , and} \qquad 5\text{-}7$$

$$\delta_{up}^{temp}(t) = R_{cyl}\alpha(T_{avg}^{up}(t) - T_{avg}^{up}(0)) \qquad 5\text{-}8$$

where α is the thermal expansion coefficient for the primary containment steel wall. Additionally, there will be a vertical expansion of the primary containment steel cylinder, based on the vertical section heated (which would be the lower compartment section), and the volume change is

$$dV_{vert,\,cyl}^{temp} = \pi R_{cyl}^2 \alpha L_{low}(T_{avg}^{low}(t) - T_{avg}^{low}(0)) \qquad 5\text{-}9$$

where L_{low} is the portion of the lower compartment primary containment shell that is heated.

The average wall temperatures are based on heat transfer calculations for the secondary containment air space, and that calculation includes heat transfer to the primary containment shell as a bounding structure. The basis for the secondary containment heat transfer calculation is addressed in the following subsection. Once the dilation of the lower and upper compartment regions are determined, the volume changes may be calculated using equations similar to those used above for the volume change due to pressure. However, in the case of the lower compartment, we estimate that only a portion of the vertical cylinder height will expand; since the ice bed region does not experience a significant temperature change, the containment

expansion in this region is neglected. Shown in Figure 5-6 is the secondary containment volume change due to temperature expansion of the primary containment shell. The total expansion maximum is about 38 m^3, which also compares favorably with the 34.9 m^3 listed in the Watts Bar FSAR.

Secondary pressure change due to dilation effects. To calculate the secondary pressure change as a result of volume changes due to dilation of the primary containment shell, we first construct a profile of the total volume change for the transient, and from that profile calculate a rate of volume change. Next, the volume rate of change is formulated as a liquid volumetric inflow and outflow to a pool modeled in the secondary containment. The pool is modeled such that there is no heat or mass exchange with the secondary containment atmosphere (HT-TRAN keyword). The purpose of the pool is to displace air in the secondary containment, thereby simulating the movement of the primary containment shell.

Shown in Figure 5-7 is the total volume change for the secondary containment. The CONTAIN engineered vent input for volumetric rates of liquid between a dummy pool (cell 5) and the pool modeled in the secondary containment (cell 4) is

```
&& pool flow for volume compression
 from 5 to 4
  type=pool
   vflow-t
    flag=1
   x=54
   0.0000E+00  5.3650E-01  3.3070E+00  6.1858E+00  9.9004E+00
   1.2426E+01  1.3413E+01  1.5518E+01  1.7494E+01  1.8747E+01
   2.1445E+01  2.3816E+01  2.5726E+01  2.8617E+01  3.3340E+01
   3.8591E+01  4.4960E+01  4.9296E+01  6.1253E+01  7.5617E+01
   9.0727E+01  1.0535E+02  1.1901E+02  1.2902E+02  1.3511E+02
   1.3997E+02  1.5266E+02  1.6704E+02  1.8191E+02  1.9265E+02
   1.9850E+02  2.1100E+02  2.2634E+02  2.4029E+02  2.6823E+02
   2.9476E+02  3.4237E+02  5.9506E+02  6.2583E+02  6.7756E+02
   7.5861E+02  8.4382E+02  9.0388E+02  9.8628E+02  1.0229E+03
   1.2075E+03  1.5404E+03  1.7502E+03  1.7950E+03  1.8650E+03
   1.9546E+03  2.1364E+03  2.3574E+03  2.4860E+03
   y=54
   3.8316E+01  5.5773E-01  5.3793E-01  5.9834E-01
   9.1103E-01  8.5124E-03  6.1951E-02 -5.0443E-01 -8.9033E-01
  -1.1674E-01 -4.1900E-01 -4.6320E-01  4.7587E-01  1.1291E+00
   9.0925E-01  7.1563E-01  5.5388E-01  3.4150E-01  1.8789E-01
   8.3596E-02  4.4169E-02  2.0500E-03 -4.9256E-02  1.5382E-01
   2.1296E-01  1.0149E-02  5.2020E-02  2.9670E-02 -7.5190E-03
  -8.5567E-02 -3.2985E-02  2.6854E-02  1.4817E-02 -1.0873E-02
  -3.7310E-03 -5.1527E-02  5.3380E-04 -2.9844E-02 -2.5621E-02
  -1.6305E-02 -8.2910E-03 -6.6950E-03 -7.3320E-03 -1.3390E-03
  -1.9370E-03 -1.6600E-04  5.7110E-04 -1.6809E-02 -9.3700E-03
  -4.1190E-03 -9.2400E-04  9.7710E-04  8.5580E-04  0.0
    eoi
 eoi
```

The pressure change in a secondary containment, which is initially at an average negative pressure of -5 inches of water, due to dilation effects is shown in Figure 5-8. We see from this calculation that the effect of dilation is significant, but that by itself the dilation effect will not result in pressure changes that challenge the requirement to maintain a negative pressure in the secondary containment.

5.3.2 Containment Atmospheric Heating

Sensible and latent heat transfer to the primary containment wall from the primary containment atmosphere will have two consequences for the secondary containment pressure response. The first has been discussed above; it concerns the thermal expansion of the primary containment wall and the compression of the secondary containment gas space. The other effect of concern here is the heating of the secondary containment air as the primary containment shell temperature increases, causing sensible energy to be transferred via free convection from the hot shell surface to the air. Because we are concerned with small variations in secondary containment pressure, only a small change in the secondary containment air temperature (i.e., a few degrees) will be important.

The procedure for performing a secondary atmospheric heating calculation has been described in the Watts Bar FSAR. We have adopted this procedure as a demonstration to show that the CONTAIN code can address these types of modeling issues. As mentioned previously, the forcing functions for the calculation are containment loads (gas temperatures) obtained in the DBA analysis for the Watts Bar containment (Figure 5-3). To formulate the heat transfer problem, consistent with the FSAR specifications, we require the following:

Heat transfer coefficients —

- primary containment atmosphere to primary containment wall = 2274 W/m^2-K
- primary containment atmosphere to secondary containment atmosphere = $1.3 * \Delta T^{1/3}$ W/m^2-K
- secondary containment wall to secondary containment atmosphere = $1.3 * \Delta T^{1/3}$ W/m^2-K

Wall thermal radiation emissivity —

- primary containment emissivity = 0.9
- secondary containment emissivity = 0.9.

The high value for the primary containment atmosphere to primary containment wall heat transfer coefficient is used to assure a conservative estimate for the heat transfer to the primary containment wall. The convective coefficient formulas specified for the secondary containment air space are simplified forms of free convection for a vertical surface where the fluid is air at conditions near ambient. The emissivity specifications indicate the need to include a thermal radiation model for structure-to-structure heat transfer.

The CONTAIN models for surface-to-atmosphere and structure-to-structure heat transfers are well suited to address the specification listed above. In terms of the heat transfer from the primary atmosphere to the primary wall, the CONTAIN structure outer boundary conditions can model a temperature dependent gas temperature with a specified heat transfer coefficient. The convection formulas, being a free convective correlation, are simulated directly using the CONTAIN default convective models for vertical surfaces. The structure-to-structure heat transfer by thermal radiation is treated in the code through a radiation enclosure model.

Shown in Figure 5-9 is a CONTAIN model of the secondary containment, showing four vertically stacked cells. The use of four cells as opposed to a single cell is preferred for a number of reasons:

- vertically stacked cells allow a determination of the hydrostatic pressure in the containment, which can be important for determining potentials for leakage at various penetration locations.

- vertically stacked cells provide a more accurate representation of the regional gas volumes that are in contact with the containment primary shell whose temperature varies according to its vertical location.

- ventilation inflows and outflows are separated by significant elevation differences; meaning that gases removed or introduced in the containment will be transported at the local average temperature of the containment gas.

- dividing the secondary containment space into cells simplifies the specification of view factors for the radiation enclosure model.

In reporting pressure differentials for this demonstration calculation, we give only the average pressure differential ΔP_{avg} where

$$\Delta P_{avg} = \frac{P_1V_1 + P_2V_2 + P_3V_3 + P_4V_4}{V_1 + V_3 + V_3 + V_4} - P_{env} \qquad 5\text{-}10$$

In referencing calculated pressure differentials to atmospheric pressure, an environmental pressure P_{env} of 1.0×10^5 Pa is assumed. Therefore, an initial pressure differential of -5 inches translates into an average secondary containment pressure differential of 1244 Pa, and an average pressure in the secondary containment of 9.876×10^4 Pa.

An example of the type of structure heat transfer input used for a portion of the primary containment wall in cell 3 (lower compartment region) is:

```
&& primary shell
```

```
name=slab5 tunif=310.92
type=wall shape=slab nslab=14 chrlen=10.0
slarea=549.78
bcinner hpaint=1.0e4 hmxmul=1.0 hydarea=1.0e6 eoi
bcouter hcoef=2271.0
 var-parm
  flag=2 name=tlow
  var-x=time
  x=13 0.0 0.6 10.0 25.0 40.0 60.0 100.0 132.0
     170.0 200.0 1000.0 2000.0 2500.0
  var-y=tgas
  y=13 310.92 374.7 359.47 345.25 369.59 374.22
     367.76 363.5 369.16 366.46 360.01 359.33 359.73
 eoi
eoi
compound
cs5 cs5 cs5 cs5 cs5 cs5 cs5
cs5 cs5 cs5 cs5 cs5 cs5 cs5
x=
0.0 1.0e-3 2.0e-3 3.0e-3 4.0e-3 6.0e-3 8.0e-3
0.01 0.012 0.014 0.016 0.017 0.018 0.019 0.02
eoi
```

The enclosure radiation is simply treated in an approximate fashion for cells 1 through 3 (dome, ice condenser, and lower compartment regions) by assuming that the gas space is totally enclosed by the primary and secondary walls. For cell 4 (pool region), there is no convection or thermal radiation modeled. An example of the enclosure input for cell 3 (lower compartment region) is

```
rad-heat
 emsvt 0.9 0.9
 enclos
  vufac 0.0 1.0
            0.54005
 eoi
eoi
```

where the reciprocity relation and summation rule for view factors are used to determine the values following the keyword "vufac."

Shown in Figure 5-10 is the pressure differential for the secondary containment based only on a consideration of atmospheric heating. Atmospheric heating is clearly seen as a significant, and requiring intervention (ventilation) to maintain a negative pressure differential.

5.3.3 In-leakage

In-leakage refers to the flow of gas into the secondary containment space as a result of penetrations in the walls, and the negative pressure differential between the air space and surrounding gas volumes connected by these penetrations. For the purpose of this demonstration,

we use the in-leakage rate specified in the Watts Bar FSAR for the secondary containment wall, 250 cfm (or 0.118 m^3/s). To model this inflow, we specified a volumetric flow rate from an environmental cell (cell 6) to the secondary containment air space (for example, cell 3):

```
from 6 to 3
 type=gas
 vvflow=0.118
eoi
```

Shown in Figure 5-11 is the pressure differential for the secondary containment based only on a consideration of in-leakage. For this ice condenser plant case, unlike the volume change or temperature effect phenomena which can change the pressure differential by 5 inches of water within ~ 100 seconds, in-leakage is a slower process taking nearly 1000 seconds to change the pressure differential by the same amount.

In-leakage has been treated here in a simple manner, mainly because the specification for the process (that is, in terms of a constant volumetric rate) was first order, in that the rate was independent of the pressure differential. A more sophisticated modeling approach would assume some dependence on the pressure differential between the source volume and the secondary containment air volume. In most cases, the flow may not resemble the type of turbulent flow modeling for flow paths that is treated directly by the CONTAIN orifice type flow model. In those cases, that is, where flow is dependent on pressure differential and an equational form different from a turbulent orifice equation, a different approach to flow modeling must be considered. This is similar to that discussed in the next section that deals with ventilation; it involves the use of flow path area versus pressure differentials, and can offer some generality with respect to in-leakage and ventilation.

5.3.4 Ventilation

Especially for conditions of atmospheric heating and in-leakage, a ventilation system must be operating to maintain pressure control for the secondary containment. This is the purpose of the EGTS. In auditing licensee's calculations, we can take a couple of approaches: the first one is the easiest in terms of modeling and requires that we model a specified exhaust rate; the second approach is more difficult, requiring that we simulate the system feedback so as to specify the exhaust rate based on the secondary containment pressure with respect to the environment or another reference pressure. We will demonstrate how each approach can be modeled with the CONTAIN code in this subsection. It should be noted, however, that direct comparisons with FSAR results are not possible with these demonstration calculations since more information regarding the licensee's calculation for the FSAR results would be required. Yet the information that is available provides input for a reasonable demonstration calculation, at least for the first approach.

Filtered air from the secondary containment is removed from containment and exhausted to the environment through the secondary containment exhaust stack. We assume that the EGTS

begins operation shortly after accident initiation. Shown in Figure 5-12 is a specified exhaust volumetric flow rate $\dot{V}_{exhaust}$ for the secondary containment. The intake of the EGTS is at the top of the containment (cell 3); the intake rate $\dot{V}_{out}$ is 1.8878 m^3/s. The portion of $\dot{V}_{out}$ that is returned to the containment (cell 1) is

$$\dot{V}_{in} = \dot{V}_{out} - \left|\dot{V}_{exhaust}\right|. \qquad 5\text{-}11$$

We can model the behavior of the EGTS by providing two engineered vents that specifies 1) the air extracted from the dome region and returned to the lower compartment region ($\dot{V}_{in}$) and 2) the exhaust rate $\dot{V}_{exhaust}$. For example, the exhaust rate is model as follows:

```
&& stack exhaust
 from 1 to 6
  type=gas
  vflow-t
   flag=2
   x=31
   0.0000E+00  1.0000E+01  8.8274E+01  1.0221E+02  1.0686E+02
   1.2312E+02  1.3009E+02  1.4635E+02  1.5796E+02  1.7423E+02
   1.9746E+02  2.2301E+02  2.4392E+02  2.8573E+02  3.3219E+02
   3.6704E+02  4.0653E+02  4.5299E+02  5.0874E+02  5.4823E+02
   5.9701E+02  6.0631E+02  1.0000E+03  1.0001E+03  1.7004E+03
   1.7167E+03  1.8003E+03  1.9049E+03  1.9931E+03  2.0698E+03
   2.0977E+03
   y=31
   0.0000E+00  0.0000E+00  1.6831E+00  1.6897E+00  1.2049E+00
   1.2661E+00  1.3014E+00  1.3305E+00  1.3499E+00  1.3532E+00
   1.3470E+00  1.3119E+00  1.2672E+00  1.1616E+00  1.0400E+00
   9.3440E-01  8.3845E-01  7.0725E-01  5.8578E-01  5.1871E-01
   4.5816E-01  3.5000E-01  3.5000E-01  4.0178E-02  5.0178E-02
   9.3156E-02  9.3586E-02  1.0175E-01  1.0175E-01  1.0246E-01
   1.0269E-01
  eoi
 eoi
```

The designated cell 6 is a dummy cell that represents the environment. Redistribution of the portion of air removed from the dome region and returned to the lower compartment region of the containment is given as

```
&& redistributed air from secondary containment
 from 1 to 3
  type=gas
   vflow-t
    flag=2
    x=31
    0.0000E+00  1.0000E+01  8.8274E+01  1.0221E+02  1.0686E+02
    1.2312E+02  1.3009E+02  1.4635E+02  1.5796E+02  1.7423E+02
```

```
 1.9746E+02  2.2301E+02  2.4392E+02  2.8573E+02  3.3219E+02
 3.6704E+02  4.0653E+02  4.5299E+02  5.0874E+02  5.4823E+02
 5.9701E+02  6.0631E+02  1.0000E+03  1.0001E+03  1.7004E+03
 1.7167E+03  1.8003E+03  1.9049E+03  1.9931E+03  2.0698E+03
 2.0977E+03
 y=31
 1.8878E+00  1.8878E+00  2.0468E-01  1.9812E-01  6 8285E-01
 6.2169E-01  5.8634E-01  5.5727E-01  5.3792E-01  5.3457E-01
 5.4075E-01  5.7586E-01  6.2061E-01  7.2618E-01  8.4775E-01
 9.5337E-01  1.0493E+00  1.1805E+00  1.3020E+00  1.3691E+00
 1.4296E+00  1.5370E+00  1.5370E+00  1.77E+00   1.77E+00
 1.77E+00    1.77E+00    1.77E+00    1.77E+00   1.77E+00
 1.77E+00
 eoi
eoi
```

Shown in Figure 5-13 is the secondary containment pressure differential obtained with the exhaust rate specification. The CONTAIN input used to generate this calculation is listed in Appendix E.

In the case where an exhaust rate is given as a function of secondary containment pressure differential, we can utilize the CONTAIN vent flow tables for area versus pressure differential to construct a flow rate versus pressure differential. Once a table is constructed for $\dot{V}_{exhaust}$ as a function of pressure differential, we may use that table in an exhaust path connected to the secondary containment and the reference pressure (or exhaust cell) that is specified as a constant pressure cell with a pressure that is expected to remain below the secondary containment cell connected to the vent path. As an example, suppose that we intend the exhaust rate, $\dot{V}_{exhaust}$ is a function of the pressure differential ΔP as shown in Figure 5-14. The pressure in the secondary containment is given as $P_s = 10^5 - \Delta P$. We include a reference cell in the CONTAIN input with a constant pressure $P_{ref} = 9.5 \times 10^4$ Pa. The exhaust is from the secondary containment cell at pressure P_s to the reference cell at pressure P_{ref}. To approximate the exhaust function, a variable area is calculated as

$$A(\Delta P) = \frac{\dot{V}_{exhaust}}{\sqrt{\frac{(10^5 - \Delta P) - P_{ref}}{\overline{\rho}_s}}}. \qquad 5\text{-}12$$

Because we are concerned with only small changes in the secondary containment pressure, the air density $\overline{\rho}_s$ may be assumed to be a constant average density for the containment atmosphere. Following the above method, the vent path input for an exhaust rate (Figure 5-14) from cell 1 in the secondary containment to reference cell 6 is given as

```
from 1 to 6
vavl=1.0 vcfc=1.0 type=gas
resolvhd
 rvarea-p flag=2
 x=6 0.0 3756.0 4751.0 5000. 5124.0 5249.0
 y=6 0.0 0.0 0.02951 0.02877 0.02842 0.02808
 eoi
eoi
```

Note that in this development the CONTAIN loss coefficient "vcfc" is specified as unity as implied by Equation 5-11.

5.4 Modeling Recommendations

The modeling recommendations for secondary containment analysis are developed to ensure a conservative estimate of containment pressure that could be used to assess the release of radioactivity to the environment during a postulated accident event. Conservatism is built into the modeling in a number of ways:

- Volumetric change is determined based on a conservative decoupled primary containment calculation of a LOCA event, meaning that pressure and gas temperature loads are calculated higher than actual loads. From these conservative loads, the primary containment shell pressure expansion is determined. Additionally, the gas temperature in the primary containment analysis (with an adiabatic outer boundary condition on the primary shell) is used to drive the thermal calculation of the primary containment shell as well as the secondary containment atmospheric heating calculation. Assumptions made in the thermal calculation produce a conservative thermal expansion of the shell. The sum of the pressure and thermal expansions of the shell translate into a transient secondary containment volumetric change that is expected to be greater than the actual change during the accident.

- Atmospheric heating is conservatively calculated through the use of the conservative primary atmospheric gas temperature, as a boundary condition for the secondary containment calculation, along with a conservative assumption regarding the primary containment gas to shell heat transfer coefficient. For times greater than a few seconds after the initial blowdown, the primary containment heat transfer coefficient used is believed to be approximately 4 to 5 times higher than a coefficient based on free convective heat transfer.

- In-leakage through the shield building wall is specified as a constant value throughout the secondary containment calculation. The value is the rated in-leakage amount during normal operation conditions. Using a constant value when the secondary containment pressure is rising is a conservative assumption, since increased secondary containment pressure would be expected to reduce the in-leakage rate.

The modeling of the secondary containment ventilation is somewhat problematical in that the EGTS is a complicated system that functions on a set of sophisticated dampering, filtering, and cooling controls. Because audit reviews are not intended as design calculations, the complexity of the EGTS can be avoided by using the licensee's estimate of exhaust rates versus time. A conservative aspect of the secondary containment calculation is that returning air removed from the top of the containment is returned to the lower containment space without cooling. The startup of the EGTS and the in-leakage to this system can introduce additional air mass into the containment. An approximation for this additional air injection into the containment is included in the demonstration calculation. Audit calculations would need to assess and quantify rates of any additional air or primary containment gases that enter into the secondary containment air space.

Shown in Table 5-2 is a summary of the recommendations for a CONTAIN model for secondary containment analysis.

5.5 Input Preparation

Shown in Table 5-3 is a summary of the input guidance for a secondary containment analysis. The guidance relates to the construction of the CONTAIN input for calculating secondary containment pressurization during a DBA. Most of the specific guidance has been demonstrated in the previous subsections that reduced the problem into separate effects modeling for volumetric change, atmospheric heating and in-leakage. In addition to a review of those subsections, the user is directed to the subsection on ventilation where the overall CONTAIN input deck was exercised (containing all models) to predict the secondary containment pressure response. The input for that calculation is listed in Appendix E (subsection E.3), and discussed below is guidance for specific categories of input preparation.

Primary containment calculation. In order to setup the secondary containment calculation, a primary containment analysis of the LOCA event must be made first. Guidance for that analysis is given in the previous chapters for PWR containment types, for instance, the ice condenser plant. In general, a coupled calculation both the primary and secondary containment is possible, however, only to the extent that volumetric changes in the secondary air space are determined independently. Volumetric changes must be determined independently because there is no implicit modeling of volume changes due to pressure and temperature expansion of the primary containment shell. These changes had to be calculated separately and added to the CONTAIN calculation through air displacement by a variable level pool surface.

We have followed a procedure here for demonstration that completely decouples the primary from the secondary containment calculation. In this case, a conservative primary containment calculation, as discussed in previous calculations forms the boundary conditions for the secondary containment analysis. The long-term ice condenser plant calculations as discussed in the previous chapter may be used directly; for other containment types, the short-term inputs can be used to extend the calculation to longer time periods by adjusting the time inputs in the TIMES block.

The pressure and gas temperature profiles calculated for the primary containment LOCA may be extracted from the CONTAIN plot file and output as time history vectors. The pressure vector is used in standalone calculations to determine the primary shell expansion due to pressurization (Equations 5-1 through 5-6). This calculation does not involve the CONTAIN code. For estimating the thermal expansion of the primary shell, a separate CONTAIN secondary atmosphere and primary shell heating calculation will be required. In this calculation the secondary containment is modeled for atmospheric heating (including conservative heat transfer coefficients for the primary gas to shell surface, and thermal radiation within the secondary air space), yet without volumetric change effects. Since volume changes in the secondary containment gas space are small and those changes have a minor effect on secondary containment gas temperatures, then the decoupling of a thermal expansion calculation from a secondary containment calculation that implicitly includes all volumetric changes is justified.

Thermal expansion. Once the primary shell temperature calculation is available, the thermal expansion calculation is made using an average shell temperature. Various methods for determining the shell average temperature may be suggested. For the demonstration calculation we have used a three point averaging scheme that uses the inner, middle, and outer structure node temperature of the shell to form an average,

$$T_{avg} = \frac{T_{inner} + 2T_{middle} + T_{outer}}{4}.$$

The node temperatures are obtained from the CONTAIN plot file. The regional average temperatures of the shell (Equations 5-7 through 5-9) are then used to estimate the dilation of the shell due to thermal expansion.

Volumetric change modeling. After the total (pressure and temperature) volumetric change history of the secondary containment is determined. The profile must be differentiated to obtain a volumetric rate profile. That rate is then used to specify a volumetric liquid water flow rate into and out of the secondary containment air space. A dummy pool is defined with no heat or mass transfer to the overlying atmosphere. Because the atmospheric heating requires modeling of thermal radiation from the primary shell to the secondary containment shield wall, all atmosphere heat transfer cells need to include input for modeling thermal enclosure radiation. If a cell has a pool surface, this surface must also be included as a component surface in the radiation enclosure modeling, by a requirement of the code. CONTAIN cannot run with the enclosure modeling active and no heat or mass transfer to the atmosphere from the pool surface. Therefore, the only way to include a pool with air displacement is to place the pool in a small cell with no structure-to-structure thermal radiation. As a result of this restriction, the displacement or volume change cell is a cell (cell #4 in the demonstration calculation) that has no structures defined. In this way, heat and mass transfer from the pool to atmosphere can be completely deactivated using the keyword HT-TRAN.

Thermal radiation enclosure. In the demonstration calculation we have modeled a simple radiation enclosure model having two surfaces (concave and convex). In this case the convex

primary containment shell (surface #1) radiates all energy to the secondary containment wall (surface #2). The reciprocity relation and summation rule are applied to determine the radiation view factors:

$F_{11} = 0, F_{12} = 1$; and,

$$F_{21} = \frac{A_1}{A_2}, F_{22} = 1 - F_{21}.$$

View factor input is specified with the "vufac" input, where only the upper triangle of the view factor matrix is input; that is,

F_{11} F_{12}
F_{22}

Pressure initialization. The setup of the vertically stacked cells is according to the geometry and elevations of the various regions of the secondary containment. In the case of the ice condenser plant, these regions are defined by the three major compartmental regions of the plant adjacent to the primary containment wall. The lower compartment regions that are in contact with the primary containment shell are mainly the dead-ended equipment rooms. Gas temperatures used for atmospheric heating calculations will use these regional gas temperatures as boundary conditions. For the ice condenser region, the primary containment shell is assumed to be insulated on the condenser side, and therefore an adiabatic thermal boundary condition is used for the outer boundary condition on the primary containment shell for this region. In the upper compartment, the air temperature is generally calculated to be near ambient due to the cooling effect of the ice. This low gas temperature region is in contact with the upper or dome portion of the primary containment shell.

When initializing the vertically stacked cells, we specify for each cell the average secondary containment pressure and temperature at the beginning of the accident event, before the operational ventilation system is switch to the EGTS. The code will calculate the relative pressures in the containment as a result of cell elevation ("cellhist" input). After time zero (initialization time), the pressure reported in the CONTAIN output will reflect the hydrostatic contribution to the total pressure. The average pressure of the containment however, after the first time step, will equal the initial pressure specified in the CONTAIN ATMOS input block. (This assumes that the secondary containment pressure and temperature are specified with a single pressure and temperature value.) Note, in all references to secondary containment pressure, we have used the volume averaged pressure for the containment (Equation 5-10).

Table 5-1 Modeling and input features of the CONTAIN code to enable an evaluation of secondary containment performance during postulated accidents.

Key phenomenon/design feature	Code model/input feature	Code input keywords/parameter
containment volumetric change, $V_s(t)$	atmospheric gas displacement due to lower-cell pool volume	cellhist lower-cell flows [pool volumetric flow tables]
atmospheric heating	convective heat transfer from structures to atmosphere; thermal radiation heat transfer from structure to structure	struc bcinner [default free conv] bcouter [tables for tgas, and hcoef] rad-heat [enclos, emsvt, vufac]
inleakage	flow path specification	flows vvflow [volumetric flow from environment cell
ventilation	flow path specification	flows vflow-t [volumetric flow vs. time table] rvarea-p [flow area vs. differential pressure table]

Table 5-2 General modeling recommendations for a CONTAIN qualified secondary containment analysis.	
Phenomena / Process	Modeling recommendation
Volumetric change	Simulate with variable pool volume; level control via pool flow path; no heat or mass transfer with surrounding atmosphere Volume change based on de-coupled primary containment LOCA calculation; primary containment pressure used to generate pressure dilation of primary containment; primary containment volume change due to thermal expansion of containment wall heating – where the primary containment wall temperatures are determined based on a conservative secondary containment thermal calculation (see atmospheric heating phenomena)
Atmospheric heating	Primary containment gas temperature obtained from decoupled LOCA calculation; conservative gas-to-wall heat transfer coefficient used for primary containment atmosphere to wall heat transfer; free convective heat transfer for secondary containment wall structures; thermal radiation heat transfer between primary and secondary wall using enclosure radiation model
Inleakage	Specified leakage rate via engineering vent model
Ventilation	Time rate of exhaust modeled using a variable volumetric flow table with engineering vent model; alternative ETGS feedback exhaust based on pressure differential modeled using variable area versus pressure differential table in the engineering vent model

Table 5-3 Input guidance for modeling secondary containment pressure response during a long-term LOCA.		
Input Section / Block	**Parameter(s)**	**Comment**
Global:		
Nodalization	ncells = n+2	"n" vertically stack cells model the secondary containment; example, 4 vertical cells for ice condenser plant (three cells corresponding to the regions of upper or dome compartment, ice condenser, and lower compartment; small pool cell at the bottom of the containment having a volume of approximately three times the maximum volume change); two environmental cells for 1) exhausting air and reserve pool volume to transfer to containment pool; and, 2) reserve cell for specified inleakage
Material properties	user defined properties	concrete and primary containment steel thermal conductivity, density, and specific heat
Timesteps	0.1 - 2.0 seconds	problem relatively insensitive to reasonable timestep settings
Flow	implicit = n+2; engvent (vvflow, rarea); type = pool and gas	vvflow option for constant (inleakage) and time tables (for pool and exhaust flows); alternative reversible area versus pressure differential to specify exhaust flow rate
Upper Cell:		
Geometry	gasvol; cellhist	cell lower and upper elevation boundary specified in cellhist keyword for secondary containment cells; environment cells use large volume (1.0e10), height of secondary containment
Atmospheric initial conditions	ATMOS block (tgas, pgas)	average temperature and pressure in secondary containment
Structure	Struc block (hcoef, tgas);	Primary containment side specified as outer boundary with constant heat transfer coefficient, hcoef; time dependent gas temperature for outer boundary using primary containment temperatures obtain in LOCA calculation; inner boundary condition uses default free convective model

Table 5-3 Input guidance for modeling secondary containment pressure response during a long-term LOCA (cont.)		
Input Section / Block	Parameter(s)	Comment
Upper Cell:		
Thermal radition between structures	rad-heat block emsvt enclos vufac	two surface radiation enclosure; inner structure – primary containment shell (1), outer structure – secondary containment wall (2); $F_{11} = 0$; emissivity = 0.9
Lower Cell:		
Low-cell (secondary containment)	geometry pool	pool surface area equal to area of secondary containment floor (cellhist); no heat or mass transfer to pool (ht-tran off off off off off); no structures in pool cell; height of secondary containment pool cell ~ 1 meter
Low-cell (environment)	geometry pool	dummy pool with approximately three times the total volume change (pressure and temperature expansion of primary containment) in initial water

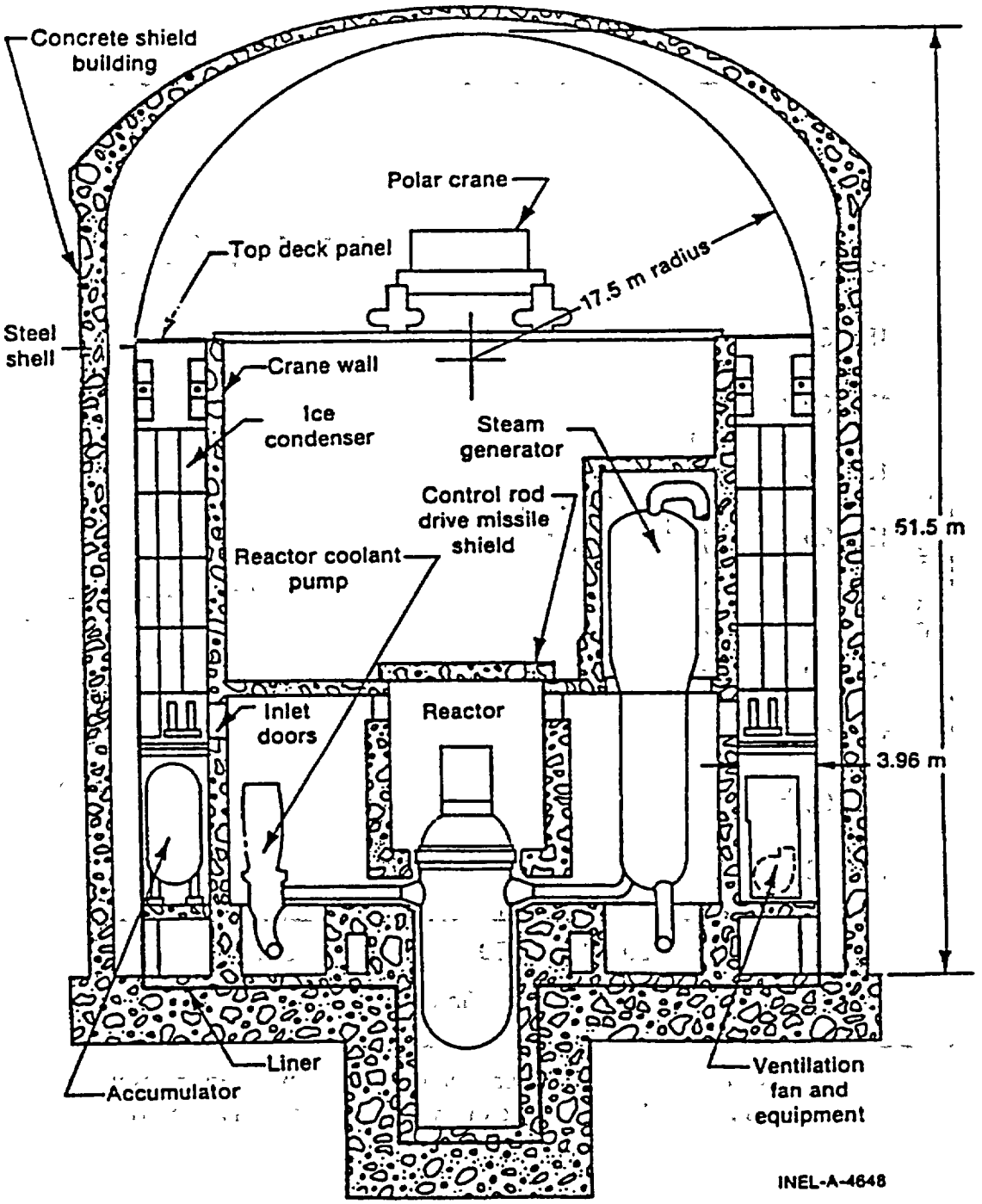

Figure 5-1 Dual-containment ice condenser plant

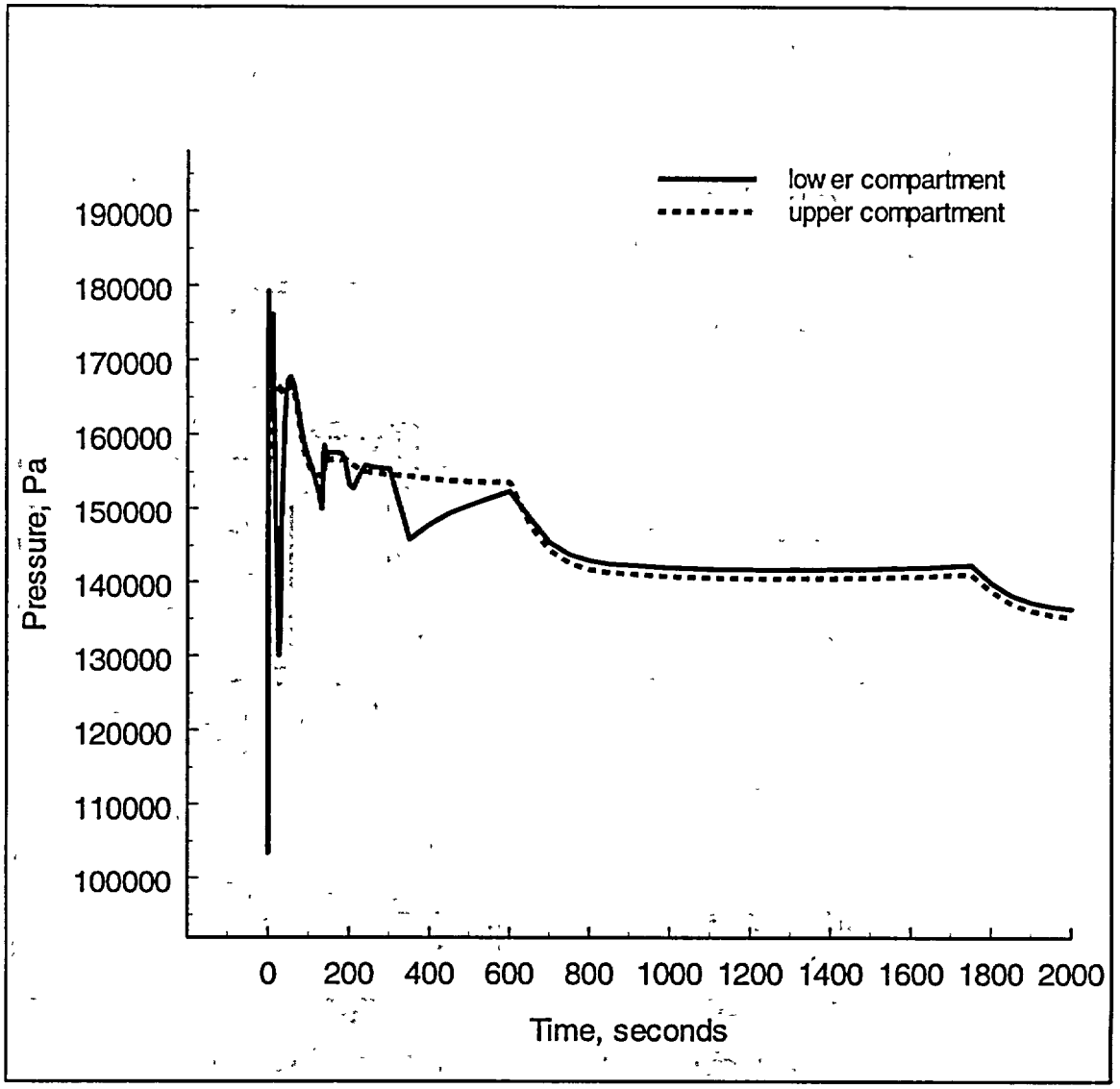

Figure 5-2 CONTAIN calculated upper and lower compartment pressure for an ice condenser plant (assumed drain-down interaction as described in Chapter 4).

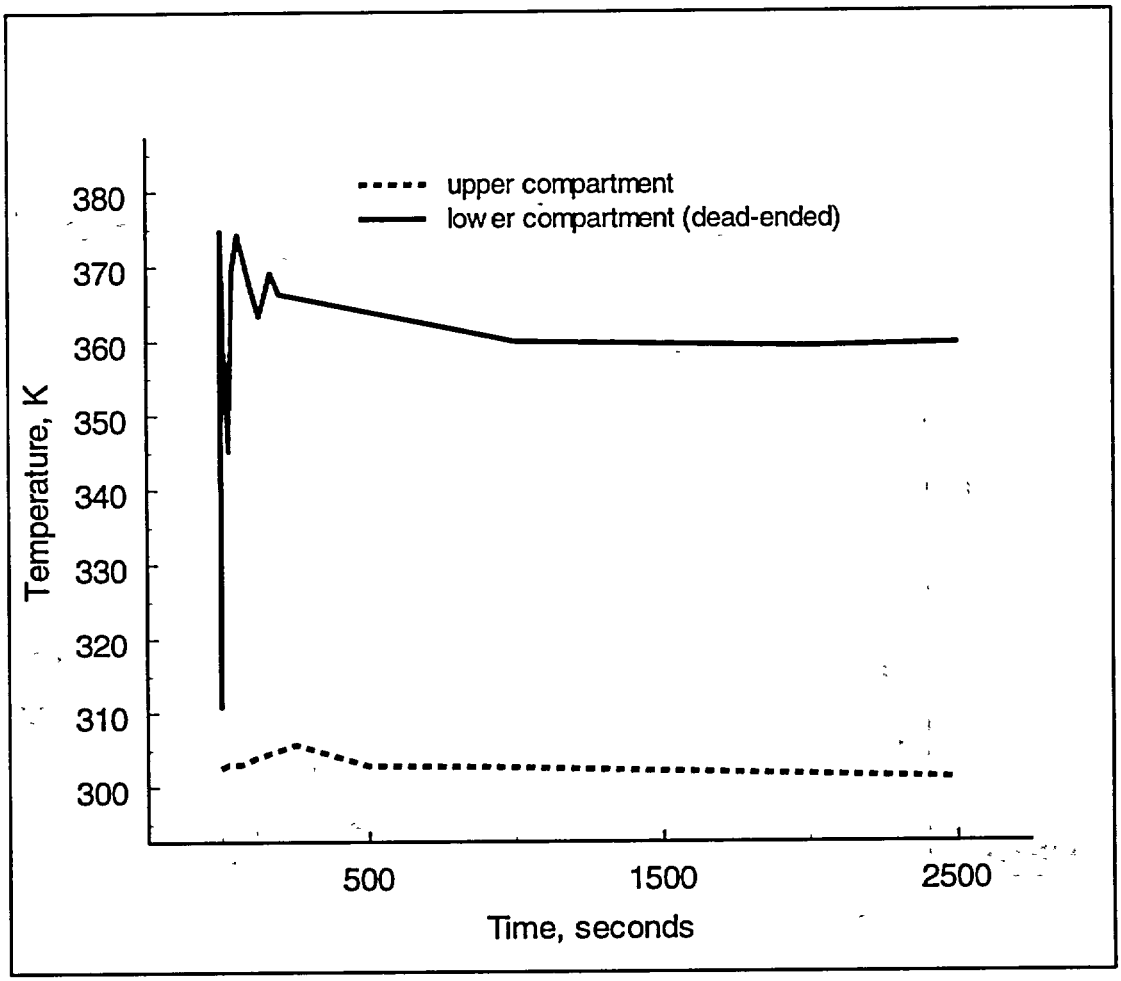

Figure 5-3 CONTAIN calculated upper and lower compartment gas temperature for an ice condenser plant (assumed drain-down interaction as described in Chapter 4).

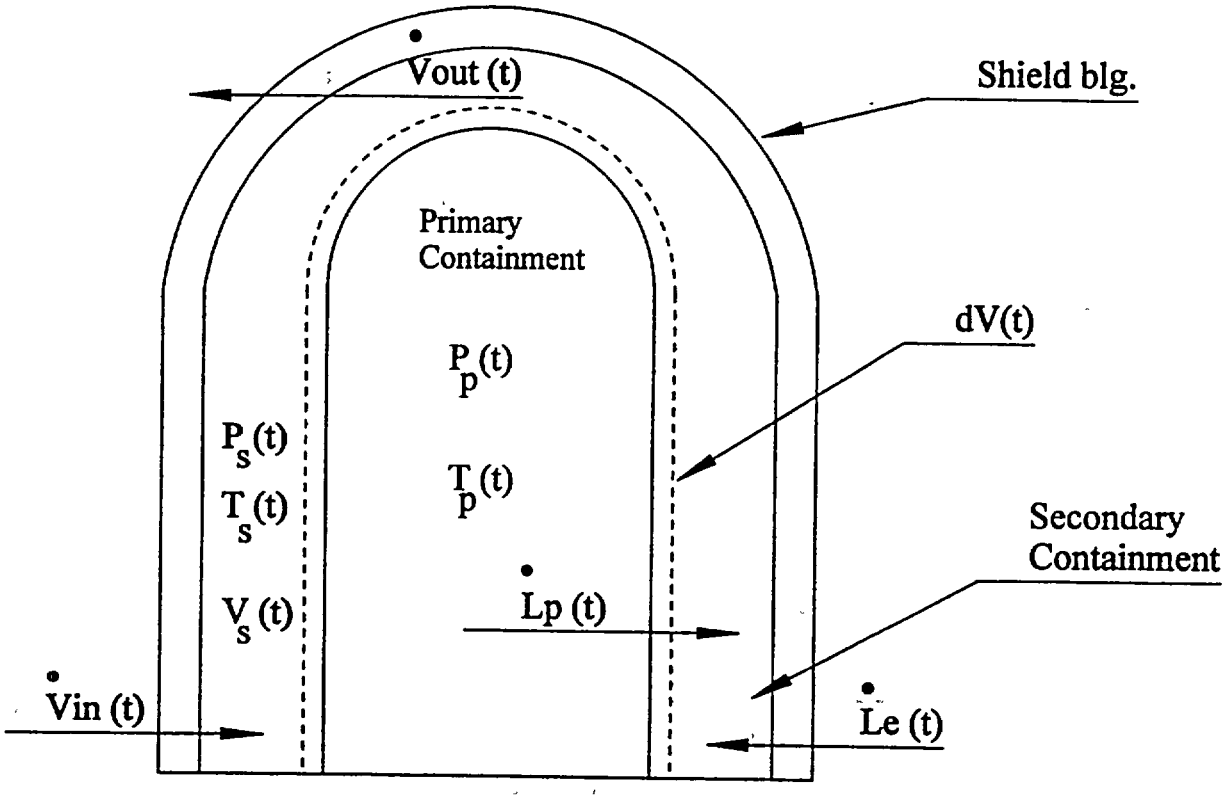

Figure 5-4 Sketch of dual-containment plant showing various phenomena and features important for secondary containment pressure evaluation.

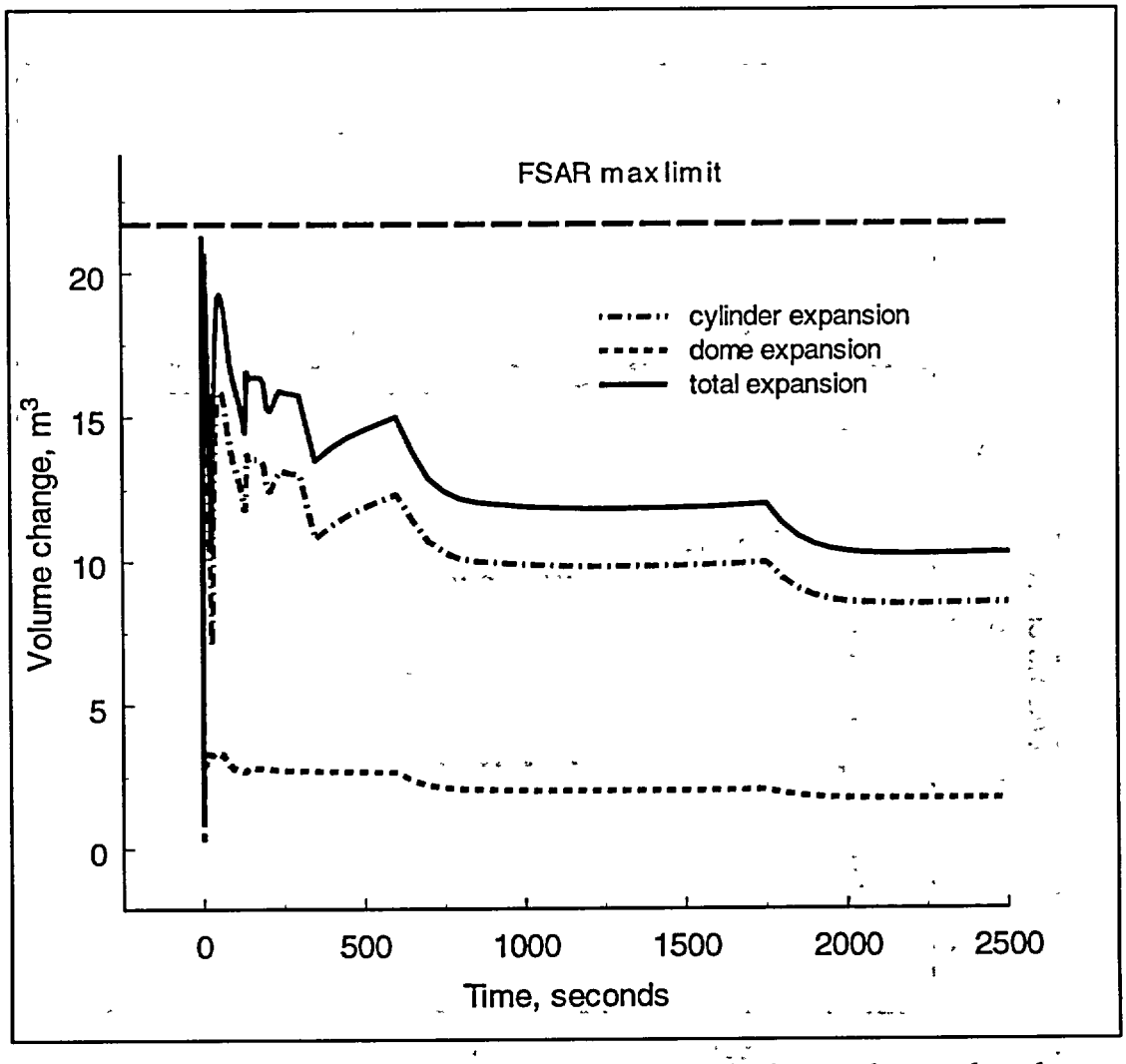

Figure 5-5 Secondary containment volume change for ice condenser plant due to pressure loading on the primary containment dome and cylinder shell. [Watts Bar plant containment volume change due to pressure expansion is shown as FSAR max limit, Reference 13.]

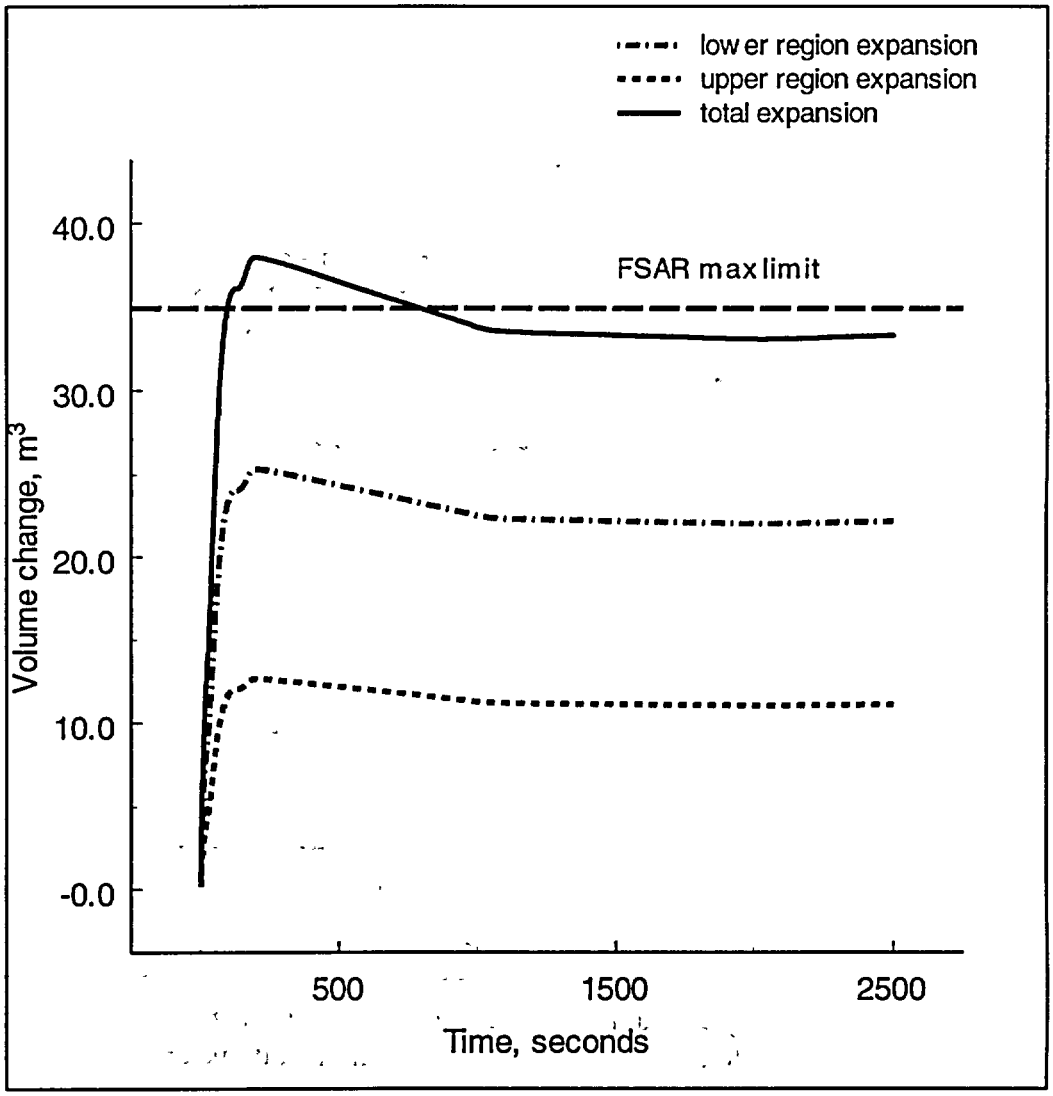

Figure 5-6 Secondary containment volume change for ice condenser plant due to thermal expansion of primary containment shell (LOCA long-term calculation primary containment gas temperatures and secondary containment thermal calculation using conservative primary gas to containment wall heat transfer coefficient = 2271 W/m^2-K). [Watts Bar plant containment volume change due to pressure expansion is shown as FSAR max limit, Reference 13.]

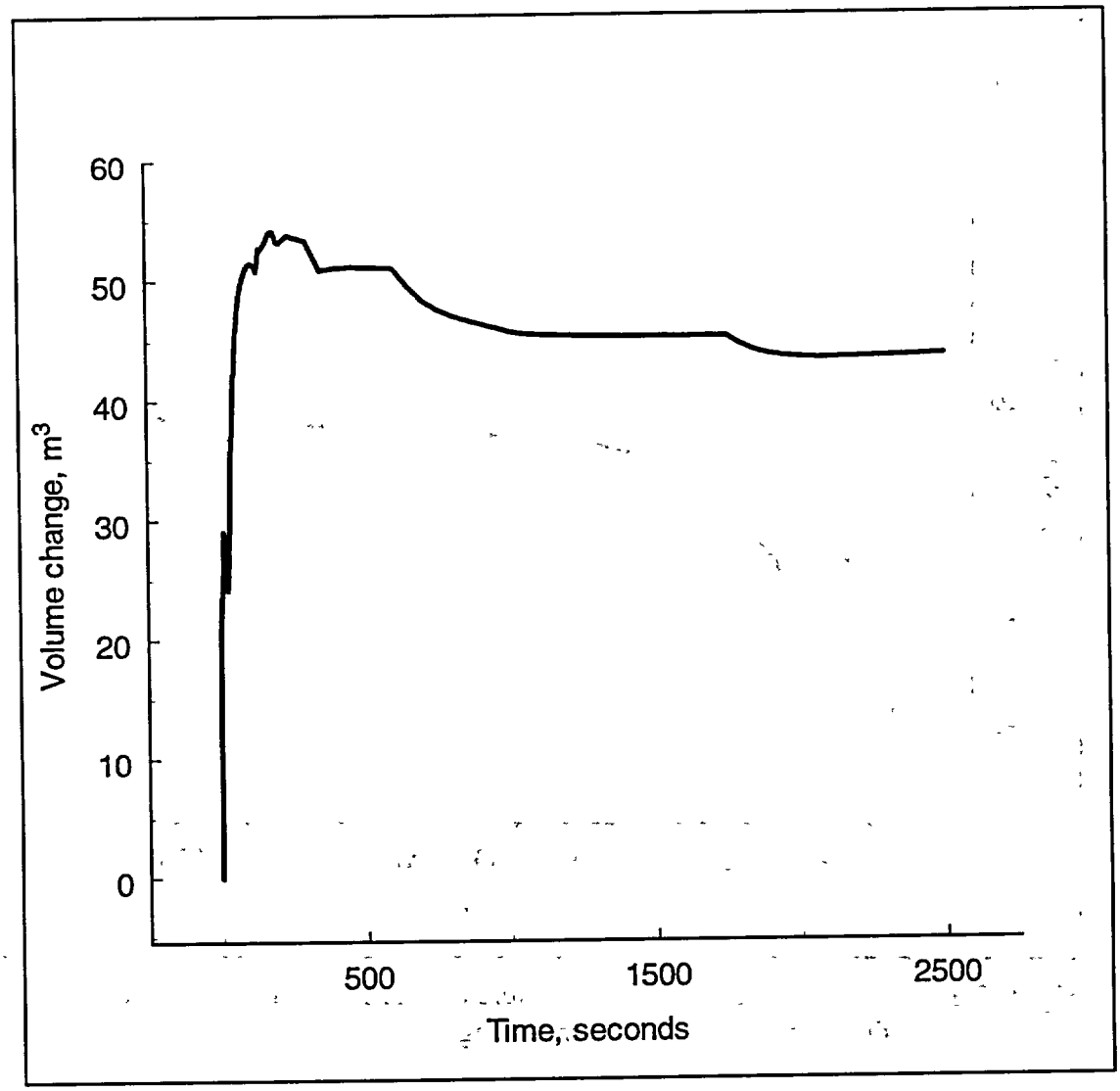

Figure 5-7 Total secondary containment volume change for the ice condenser plant due to pressure and thermal expansion of primary containment shell.

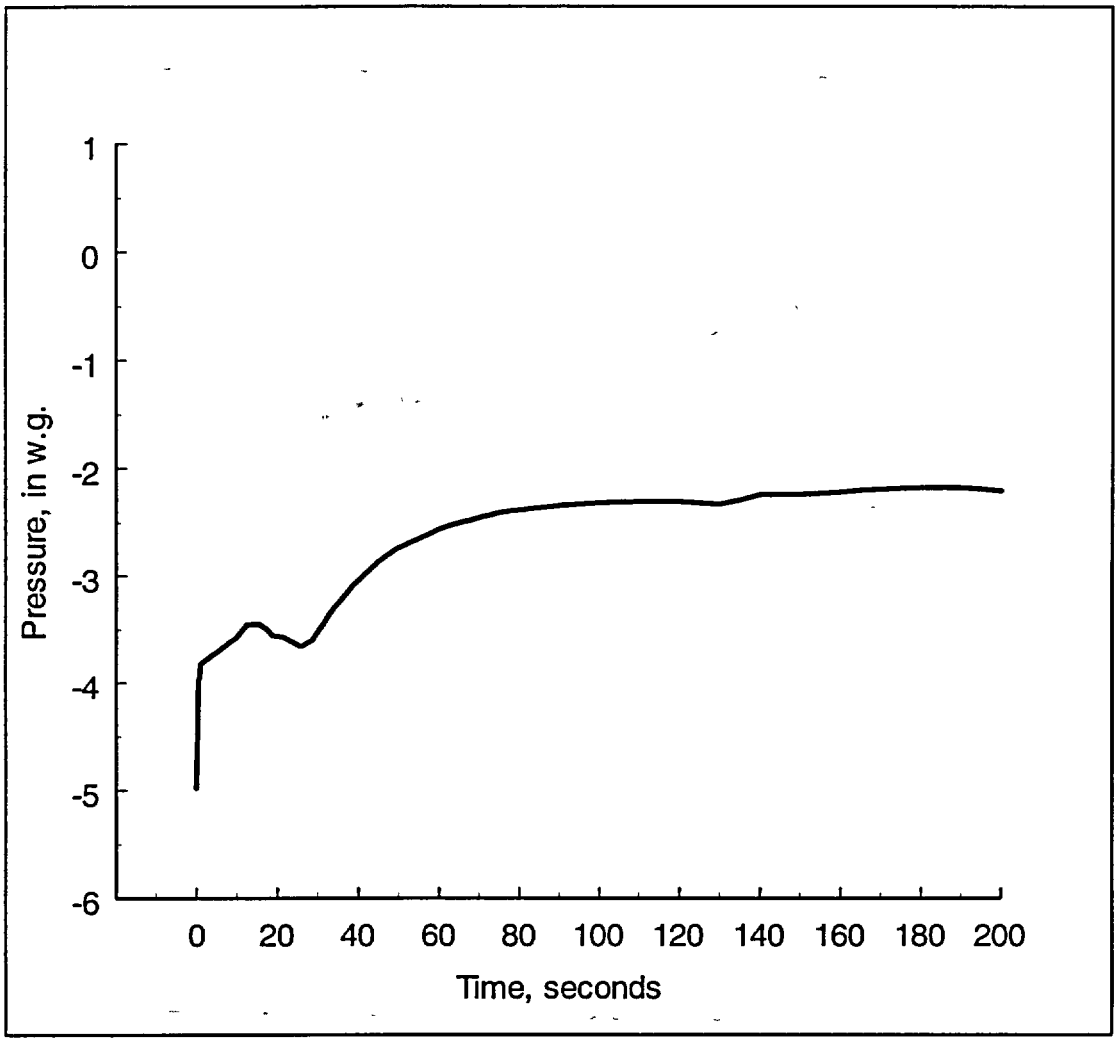

Figure 5-8 Secondary containment pressure change for the ice condenser plant due to containment volume change.

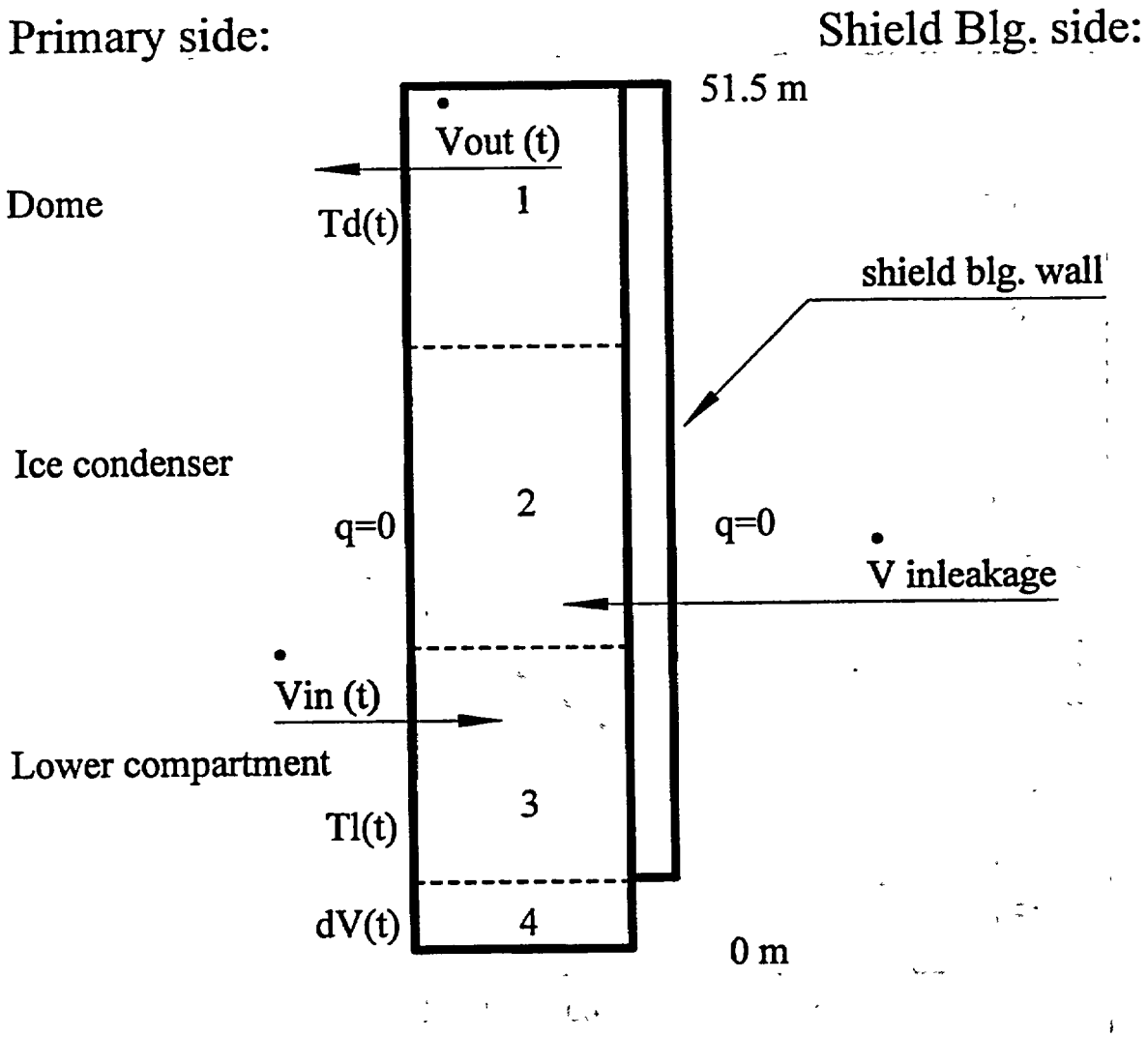

Figure 5-9 Sketch of the secondary containment nodalization for the ice condenser plant. The primary containment gas temperatures for the upper (dome) compartment and lower compartment are shown as Td(t) and Tl(t), respectively. Primary containment shell in the ice condenser section is assumed insulated. Bottom cell 4 is used for a "pool" that is used to vary the secondary containment volume change.

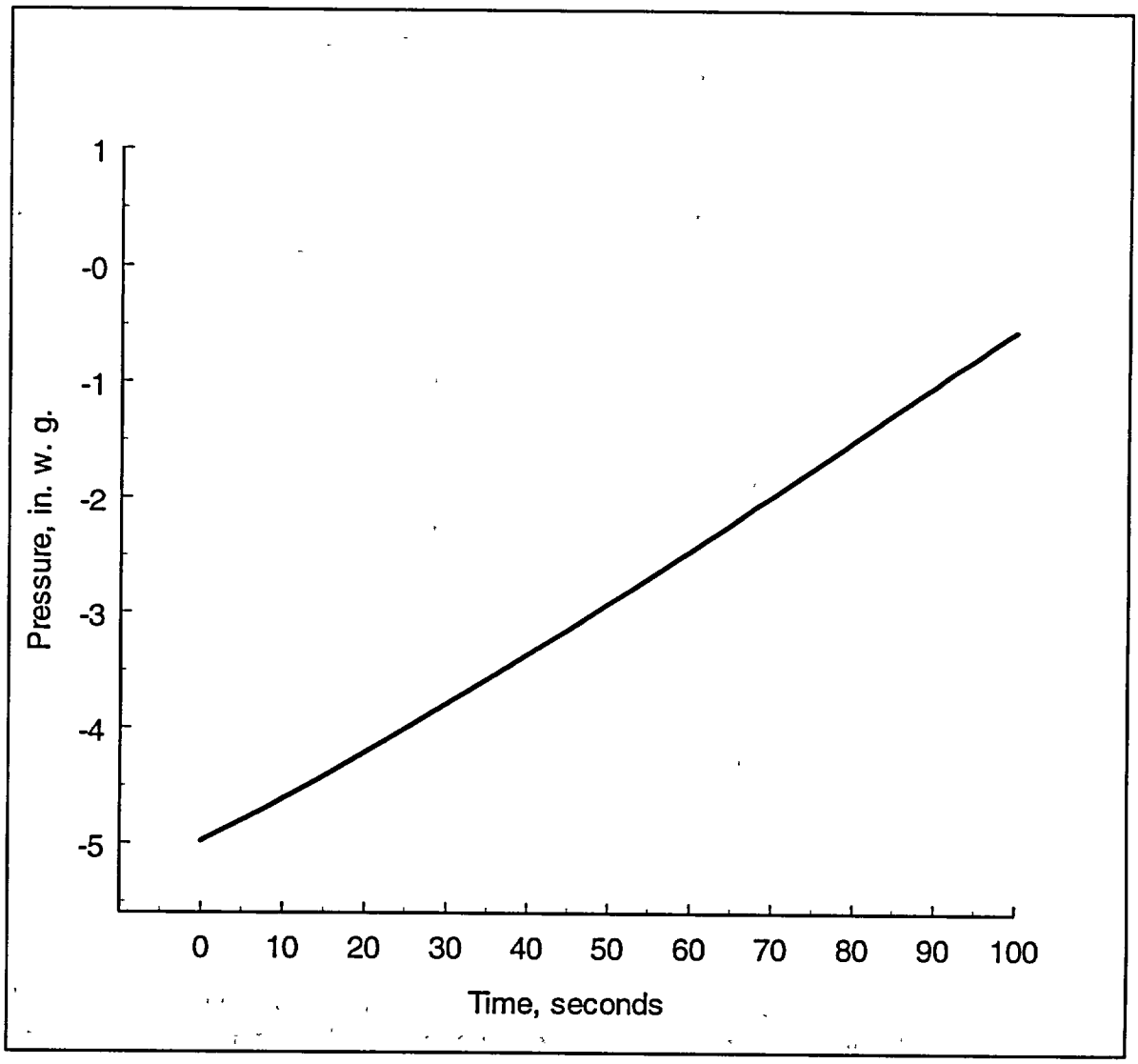

Figure 5-10 Secondary containment pressure change for the ice condenser plant due to atmospheric heating.

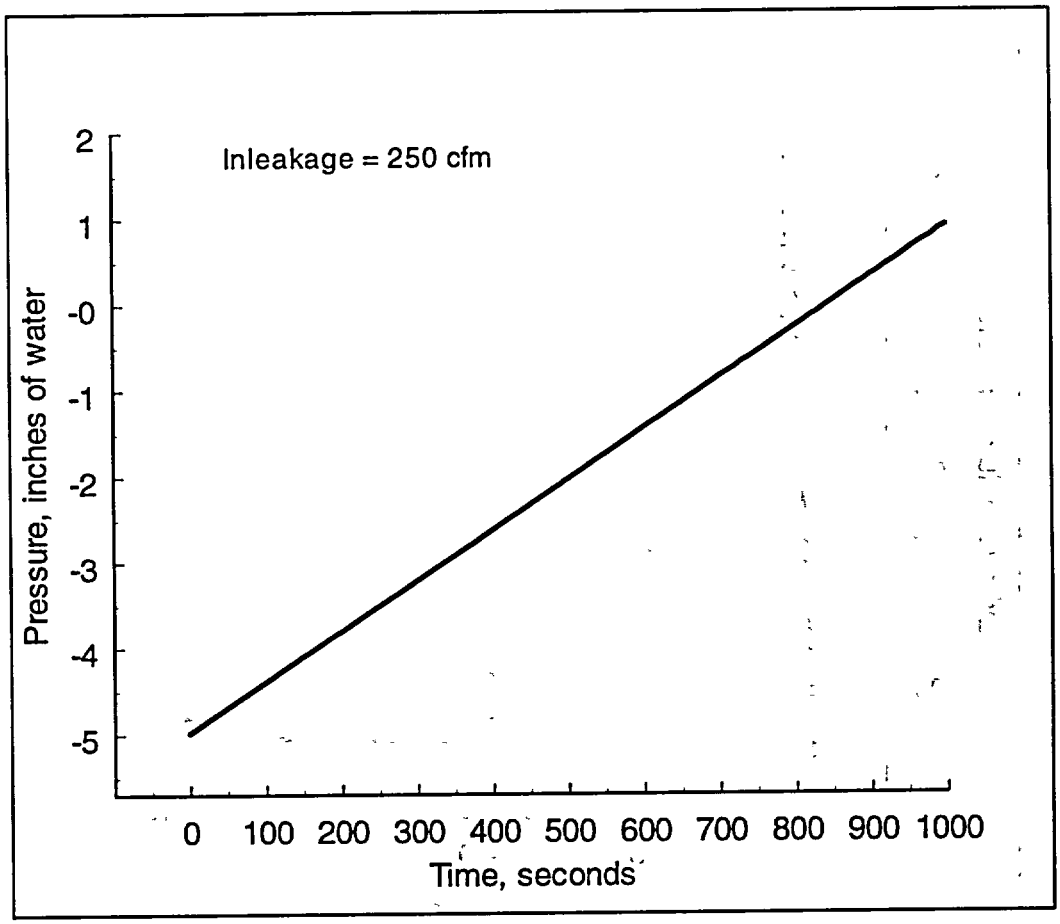

Figure 5-11 Secondary containment pressure change for the ice condenser plant due to inleakage.

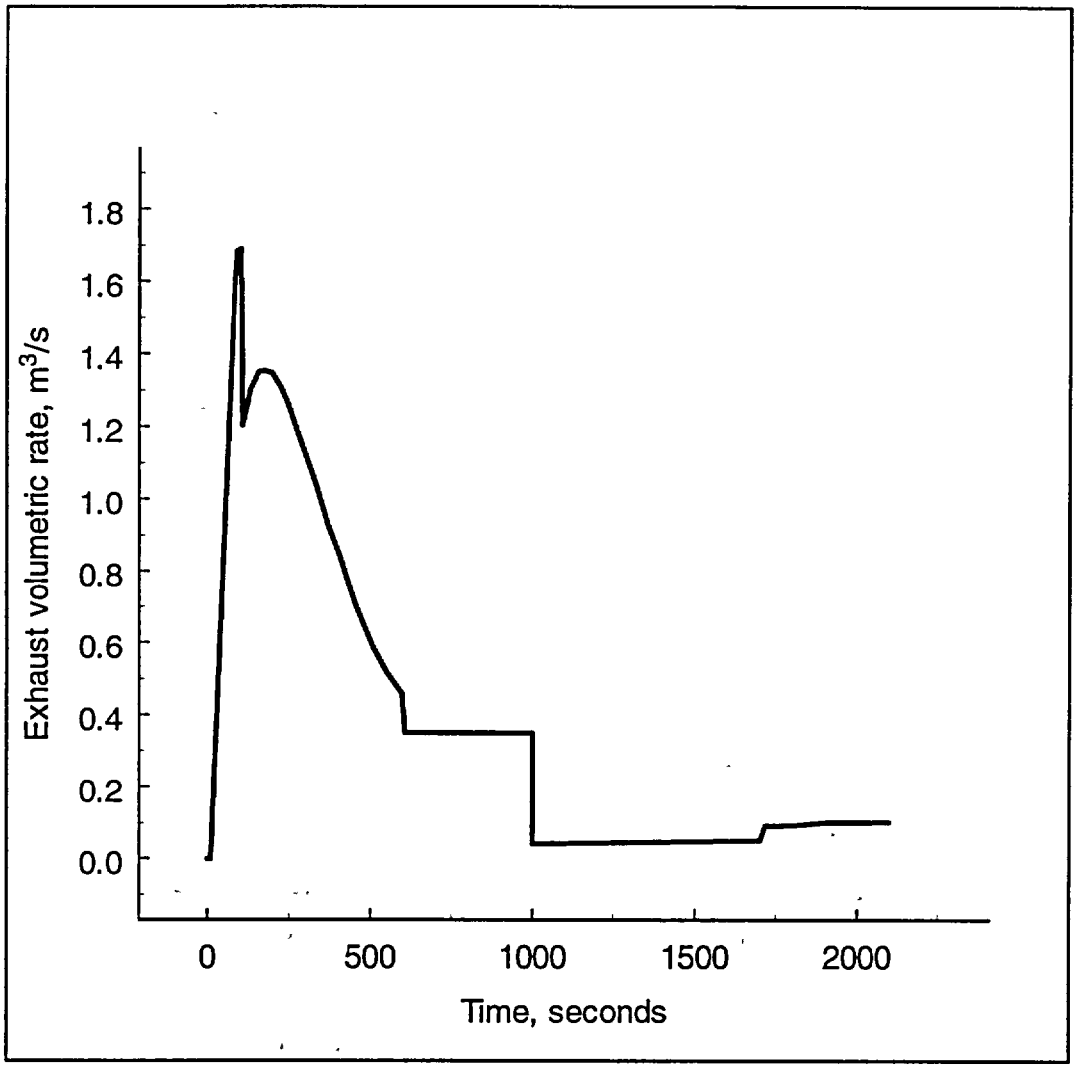

Figure 5-12 Stack exhaust volumetric flow rate for ice condenser plant demonstration calculation.

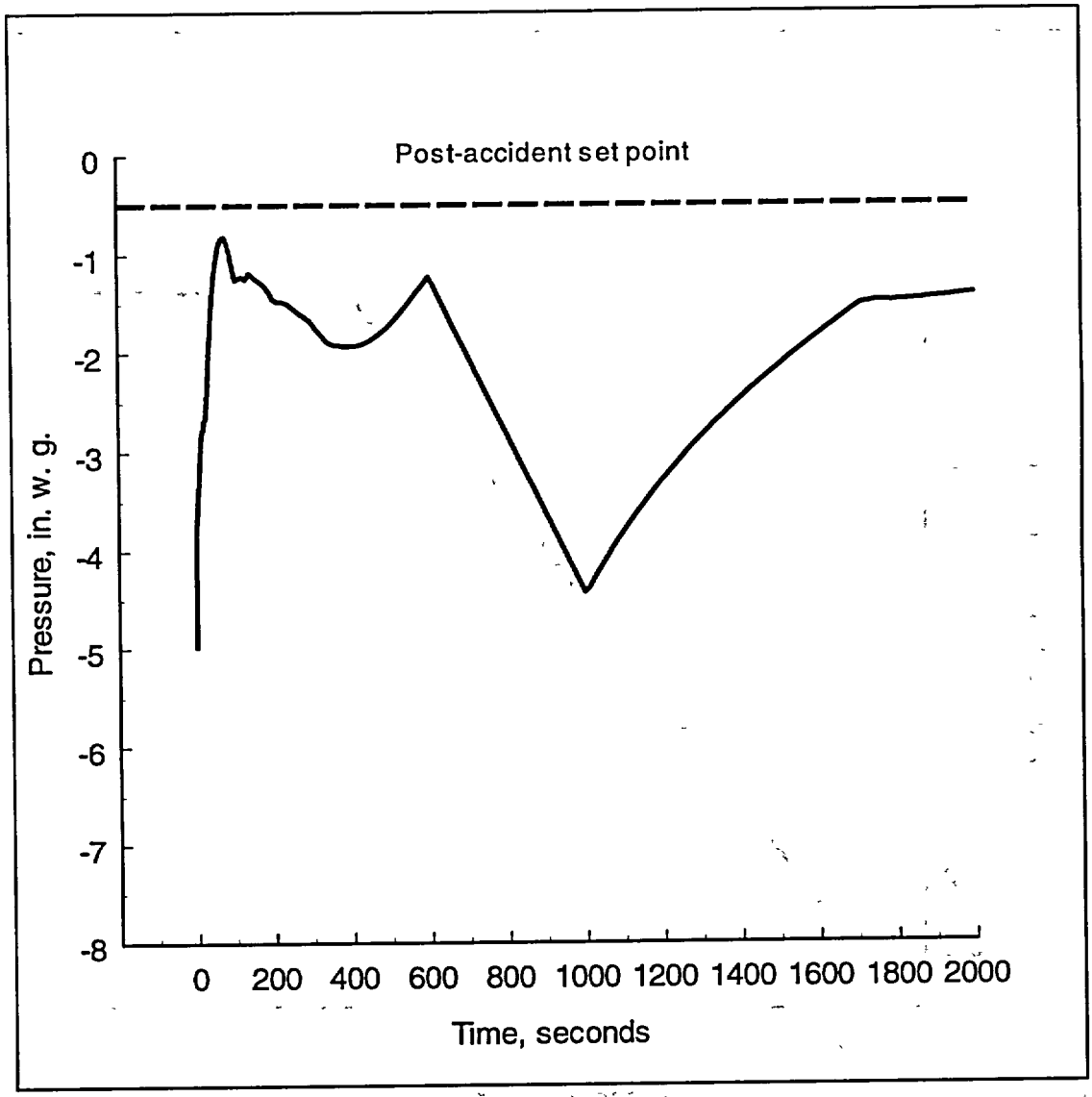

Figure 5-13 CONTAIN calculated secondary containment pressure response for a demonstration ice condenser plant.

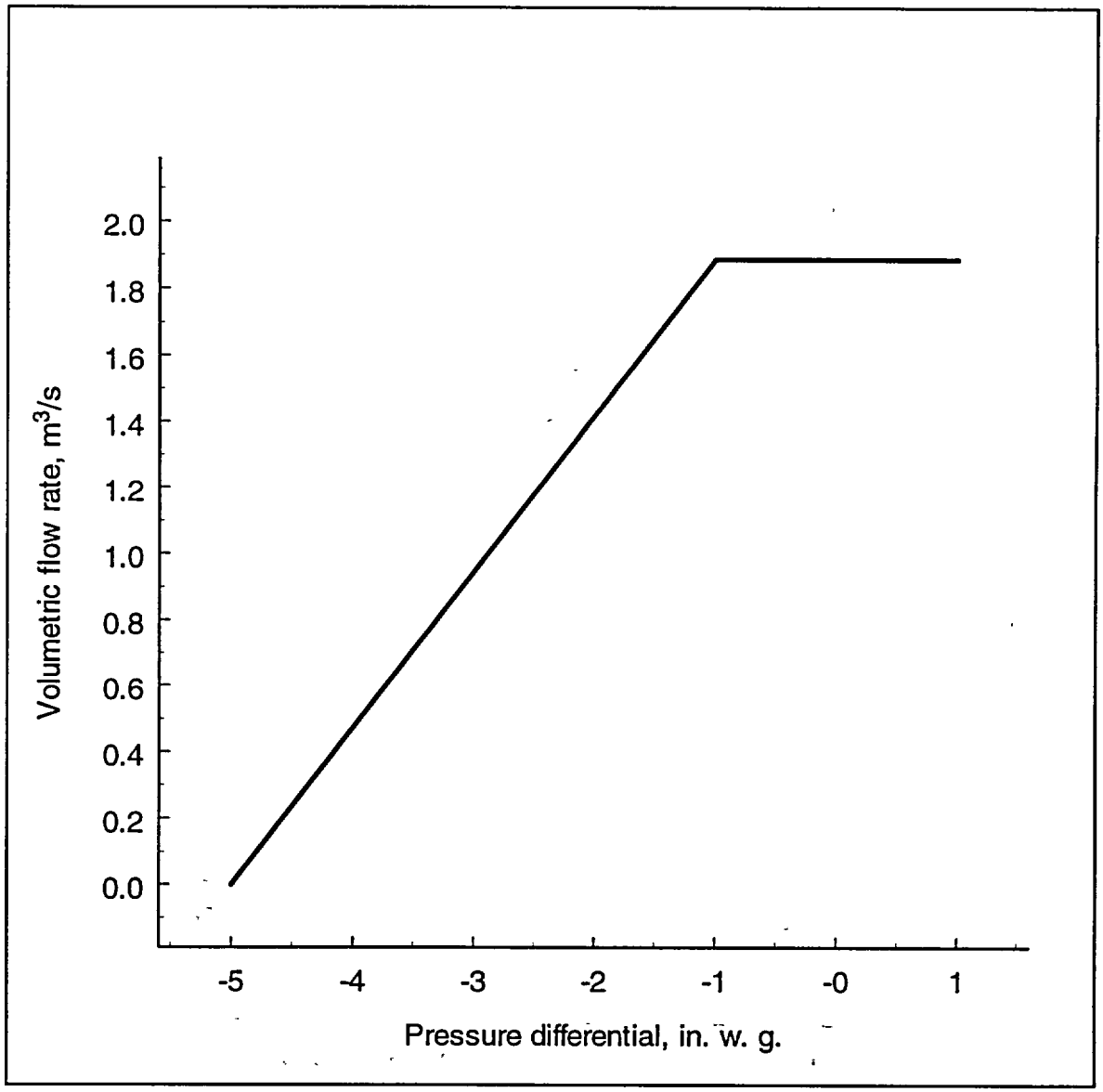

Figure 5-14 Example of an exhaust volumetric flow rate profile as a function of secondary containment pressure differential.

6 References

1. Murata, K. K., et al., "Code Manual for CONTAIN 2.0: A Computer Code for Nuclear Reactor Containment Analysis," NUREG/CR-6533, SAND97-1735, Sandia National Laboratories, Albuquerque, NM, December 1997.

2. Tills J., et al., "User Guidance on the CONTAIN Code for Advanced Light Water Reactors," SAND96-0947, (Proprietary), Sandia National Laboratories, Albuquerque, NM, April 1996.

3. Murata, K. K., and Stamps, D. W., "Development and Assessment of the CONTAIN Hybrid Flow Solver," SAND96-2792, UC-610, Sandia National Laboratories, Albuquerque, NM, November 1996.

4. USNRC Standard Review Plan (SRP), NUREG-0800, Rev. 2, July 1981.

5. "Interim Staff Position on Environmental Qualification of Safety-Related Electrical Equipment," Appendix B, NUREG-0588, Rev. 1, July 1981.

6. Hargroves, D. W., et al., "CONTEMPT-LT/028 – A Computer Program for Predicting Containment Pressure-Temperature Response to a Loss-Of-Coolant Accident," NUREG/CR-0255, March 1979.

7. Almenas, K., "Heat Transfer for Saturated and Superheated Atmospheres for Containment Analysis," Nucl. Engr. Des., 71, pp. 1-14, 1982.

8. Peterson, P. F., Shrock, V. E., Kageyama, T., "Diffusion Layer Theory for Turbulent Vapor Condensation with Noncondensable Gases," J. Heat Transfer, 115, pp. 998-1003, 1993.

9. Herranz, L. E., et al., "A Diffusion Layer Model for Steam Condensation within the AP600 Containment," Nucl. Engr. Des., 183, pp. 133-150, 1998.

10. Green, J., and Almenas, K., "Modeling of the HDR E11.4 Experiment using CONTAIN 1.12," College of Engr., University of Maryland, College Park, Maryland, Report submitted to USNRC, March 1992.

11. Tills, J., "Calculations and Analyses for the Large-Scale Passive Containment Cooling System (PCS) Tests," SAND96-1089, (Proprietary), Sandia National Laboratories, Albuquerque, NM, May, 1996.

12. North Anna Power Station Units 1 & 2 (Docket Nos. 50-338/9)- UFSAR

13. Watts Bar Nuclear Plant (Docket No. 50-390)- FSAR

14. Westinghouse Electric Corporation, "Ice Condenser Containment Pressure Transient Analysis Methods," WCAP-8077, (Proprietary), Pittsburgh, Pa., March 1973.

15. Westinghouse Electric Corporation, "Final Report: Ice Condenser Full-Scale Section Tests at the Waltz Mill Facility," WCAP-8282, (Proprietary), Pittsburgh, Pa., February 1974.

16. Henry, R. E., and Fauske, H. K., "The Two-Phase Critical Flow of One-Component Mixtures in Nozzles, Orifices, and Short Tubes," Journal of Heat Transfer, pp. 179-187, May 1971.

17. Williams, D. C., and Gregory, J. J., "Mitigation of Direct Containment Heating and Hydrogen Combustion Events in Ice Condenser Plants," NUREG/CR-5586, SAND90-1102, Sandia National Laboratories, Albuquerque, NM, October 1990.

18. "Long-term Ice Condenser Containment Code – LOTIC Code," WCAP-8355, Westinghouse Electric Corporation, April 1976, (Non-Proprietary).

19. Way, K. and Wigner, E. P., "The Rate of Decay of Fission Products," Phys. Rev., 73, 1318-1330, 1948.

20. Tills, J. L., "The CONTAIN Code Severe Accident Confinement Analysis for the N-Reactor Phase 1 and 2," SAND88-7010, Sandia National Laboratories, Albuquerque, NM, November 1988.

Appendix A

Modeling Comparison between the CONTEMPT and CONTAIN Codes

To understand the implications of using CONTAIN for DBA auditing calculations in place of traditional DBA codes, like CONTEMPT, it is important to compare the specific models in the codes. It is not expected that the models would be the same — on the contrary, the benefits of making the transition to CONTAIN arises from the differences in the models. But an understanding of the differences, and their implications, will illuminate the degree of continuity in code predictions that is possible under various accident and plant conditions. It is sometimes possible to predict with confidence the implications of certain types of model differences (e.g., degree of conservatism) in the results predicted by the codes. However, it is more often the case that general statements about the direction of differences may not be possible due to the integrated influences that various models have on results. That is why it is important to carry out specific comparisons of code results, as in the main body of this report, and in this appendix where the code results are compared for a few integral and separate effects tests.

In this appendix, the CONTAIN modeling [A-1] as applied to PWR containments and safety systems is discussed and compared to models in the CONTEMPT-LT/028 code [A-2]. The comparisons are summarized in Tables A-1 and A-4, and assumes that the user guidelines in the main body of this report are being followed, e.g., single-cell representations of the large dry containments.

A.1 Containment Modeling

We note that the CONTEMPT code is applicable to PWR large dry containments, and that in this domain the user, by code design, is limited to single-cell representations of the containment (i.e., the drywell model). While not limited to single-cell representations, the CONTAIN code is applied to containments in this report using only single-cell models. This choice, which also allows for a direct comparison to the CONTEMPT code, was selected as a result of an assessment of both CONTAIN single and multi-cell calculations that showed, for maximum containment loads during DBAs, single-cell models tend to give more conservative results than multiple-cell models. With the selection of a single-cell containment representation, model reviews of flow equations including buoyancy and stratification modeling are eliminated from the discussion here; rather, we focus on issues of atmospheric thermodynamics, two-phase water injection, and heat and mass transfers to pools and passive heat sinks. Shown in Table A-1 is a listing of the comparisons of CONTAIN and CONTEMPT code specific models in these areas.

One area showing significant difference in the modeling approach between the codes is in the

modeling of heat and mass transfer to passive heat sinks. Here the CONTAIN code uses a physically based heat and mass transfer analogy [HMTA] method while the CONTEMPT code uses an empirical correlation method. The empirical method is characteristic of an approach used by most containment analysis codes developed for DBA-type analysis in the early 1970's. Codes based on the HMTA or the diffusion layer method represent a more recent modeling approach that is now used in state-of-the-art containment codes. Shown in Tables A-2 and A-3 are some of the modeling issues related to a comparison of each modeling method under near stagnant and turbulent atmospheric conditions, respectively.

In the case of the near stagnant atmospheres, which are also characterized by natural convective conditions, the CONTEMPT and CONTAIN mass transfer models show near equivalent condensation heat transfers, as indicated by the similar trends in condensation heat transfer coefficients, as shown in Figure A-1. The CONTEMPT tabulation of Uchida's data follows the measurements made for experiments conducted at relatively high initial air pressures. Peterson [A-3] made note of the importance of initial air pressure for air/steam condensation coefficient estimation using a diffusion layer modeling method. The CONTAIN HMTA model similarly shows such an effect, which is also noted in the Uchida data, as well as more recently obtained results for condensation in stagnant atmospheres [A-4]. For a single-cell representation of a containment, an initial pressure of approximately one bar is appropriate. In applications where pressures predictions during blowdown periods are required, the variations indicated in Figure A-1 have only a small effect on calculations. For example, in Figure A-2 the similarity between condensation models for an assumed near stagnant atmosphere is demonstrated by a comparison of each code's pressure prediction for the integral blowdown Test #3 performed in the CVTR facility, without spray injection [A-5].

An improvement in the CVTR pressure prediction for each code can be realized by trying to account for the enhancing effects of forced turbulence on atmosphere-to-structure heat and mass transfer. In the case of CONTAIN, a forced convective velocity profile may be used to reproduce measured pressures. For the CONTEMPT code, selection of the Tagami correlation may also be used to account for enhancement of heat and mass transfer due to turbulence. However, in the case of the CVTR test, use of the Tagami correlation still results in a significant over prediction of CVTR pressures; and in fact, the Tagami coefficients must be multiplied by a factor of four to give a pressure calculation that reproduces the maximum pressure in the CVTR facility [A-6]. Use of a multiplication factor for the Tagami correlation points to a difficulty known to exist with this correlation, i.e., the correlation is not directly scalable to large containment configurations with scaled blowdowns. In this sense, that is, having a modeling method to perform "best-estimate" pressure predictions during periods of high turbulence, we note that both CONTAIN and CONTEMPT have limitations. Fortunately, most actual blowdown periods are of such short duration, heat and mass transfers to structures are but a small factor in determining atmospheric energies, and either the stagnant (natural convection) or turbulent (forced convection) modeling method will provide good, yet slightly conservative containment loads predictions. The CVTR facility blowdown tests, being of relatively long duration tend to over emphasize the importance of turbulent heat and mass transfer modeling used for performing DBA auditing calculations.

In some DBA scenarios where the injected steam is superheated, the containment gases may also become superheated. The CONTEMPT code has an ad hoc method for treating condensation during superheated conditions, where a condensation coefficient derived from saturated condensing experiments is assumed applicable to superheated environments through a simple adjustment in the driving potential for condensation.[1] When an adjustment in the driving potential is not performed, applications where the Uchida correlation coefficients are used will significantly over predict condensation rates and result in non-conservative pressure and temperature predictions, as noted in the Phebus FPT0 test program [A-7]. Even with the ad hoc correction, a prediction of superheat temperatures is problematic, as shown in Figure A-3. We also note in the comparisons in Figure A-3 that the CONTEMPT input for partitioning sensible and latent energy transfers (FAC) must be adjusted to improve superheated temperature predictions. CONTAIN, on the other hand, includes this partitioning within the physical modeling for both heat and mass transfers, and the good agreement with measurements shows the advantage of this approach. (For a description of the Phebus FPT0 test, and more detail on the CONTAIN calculations, see the CONTAIN 2.0 assessment report (CAR).[2])

A.2 Containment Safety Systems Modeling

There are two types of containment safety systems activated during DBAs that are designed to limit containment loads. These systems are the containment sprays (quench or recirculation) and fan coolers. Of the two, the more effective system for both short and long-term pressure suppression is the spray systems. In the case of long-term analyses, pressure suppression is provided by the recirculation spray system, where the water is taken from the containment sump. To effectively use sump water, safety grade heat exchangers serviced by external chill water are used to cool the sump water before the water reaches the spray nozzles. Shown in Table A-4 is a summary of modeling comparisons for the containment safety systems and component heat exchanger.

We note in Figure A-2, that the CONTAIN and CONTEMPT quench spray modeling provides a similar degree of pressure suppression during short-term periods in the CVTR facility (Test #4). For a long-term, separate effects pressure suppression spray test comparison we use data obtained by JAERI [A-9] which is discussed in the CAR. For this test, the CONTAIN and CONTEMPT

---

[1] During saturated atmospheric conditions condensation mass rate $\dot{m}_c$ is given by $\dot{m}_c = h_c A\left(T_g - T_w\right)$, where h_c is the condensation coefficient (Uchida or Tagami), A is surface area, T_g and T_w are the atmospheric gas and structure surface temperature. Under superheated conditions, condensation is given by $\dot{m}_c = h_c A\left(T_{sat} - T_w\right)$, where T_{sat} is the atmosphere saturation temperature.

[2] "An Assessment of CONTAIN 2.0: A Focus on Containment Thermal-Hydraulics (Including Hydrogen Distributions)"

models are compared to pressure and temperature data in Figures A-4 and A-5. The comparisons are reasonably good, with the CONTAIN code spray model giving a slightly better prediction than the CONTEMPT code.

A.3 References

A-1 Murata, K. K. et al., "Code Manual for CONTAIN 2.0: A Computer Code for Nuclear Reactor Containment Analysis," NUREG/CR-6533, SAND97-1735, Sandia National Laboratories, Albuquerque, NM, December, 1997.

A-2 Hargroves, D. W. et al., "CONTEMPT-LT/028 — A Computer Program for Predicting Containment Pressure-Temperature Response to a Loss-of-Coolant Accident," NUREG/CR-0255, TREE-1279 R4, Idaho National Engineering Laboratory, Idaho Falls, Idaho, March 1979.

A-3 Peterson, P.F., "Theoretical Basis for the Uchida Correlation for Condensation in Reactor Containments," Nuclear Engineering and Design 162, pp. 301-306, 1996.

A-4 Kataoka, Y. et al., "Experiments on Convection Heat Transfer Along a Vertical Flat Plate between Pools with Different Temperatures," Nucl. Tech., Vol. 99, pp. 386-395, 1992.

A-5 Schmitt, R.C., Bingham, G.E., and Norberg, J.A., "Simulated Design Basis Accident Tests of the Carolinas Virginia Tube Reactor Containment – Final Report," IN-1403, UC-80, Idaho Nuclear Corporation, National Reactor Testing Station, Idaho Falls, Idaho, December 1970.

A-6 Carbajo, J.J., "Heat Transfer Coefficients Under LOCA Conditions in Containment Buildings," Nuclear Engineering and Design 65, pp. 369-386, 1981.

A-7 "Phebus-FP Information Meeting – Proceeding," Phebus Report No. IP/94/224, Institut de Protection et de Surete Nucleaire, CEA, France, November 1994.

A-8 "Phebus PF FPT0 Preliminary Report, Part C – Degradation Phase," Phebus Report No. IP/94/211, Institut de Protection et de Surete Nucleaire, CEA, France, May 1994.

A-9 Kitani, S., "Containment Spray Experiments for Pressure Suppression," presentation at 1st International Conference on Liquid Atomization and Spray Systems, Tokyo, Japan, August 27-31, 1978.

Table A-1. Modeling Comparisons between CONTAIN and CONTEMPT for Containment Conditions.

Modeling Item	CONTAIN	CONTEMPT
Atmosphere thermodynamics	Homogeneous mixture,① thermal equilibrium	Homogeneous mixture, thermal equilibrium
Bulk condensation of liquid water (excluding water injection)	Choice of either leaving suspended in atmosphere (default), or dropping out, into pool, at end of global timestep	Dropout, into pool, at end of timestep
Two-phase water injection	Temperature and pressure flash models (mass rate and specific enthalpy source tables)	Temperature and pressure flash models (mass rate and specific enthalpy source tables)
Free volume displacement	Pool water displacement of free volume gases	Not modeled
Atmosphere to structure heat (sensible) transfer	Convective correlation (natural and forced convection); thermal radiation modeling	Parametric model (re-vaporation factor, fraction of total heat and mass transfer); constant throughout calculation
Atmosphere to structure mass (latent) transfer	Heat and mass transfer analogy [HMTA] — diffusion layer model (natural and forced convection)	Empirical correlation (Uchida tabulated data / Tagami correlation)
Condensate mass accounting	Condensate film on structures, runoff directed to pool	Condensate directed to pool
Structure heat transfer	1-D, implicit conduction algorithm (composite materials, default and user supplied thermal properties); temperature defined at mesh nodes	1-D, implicit conduction algorithm (composite materials with user supplied thermal properties); temperature defined at mesh gridlines
Pool heat (sensible) transfer	Natural convective correlation for atmosphere/pool interface	Natural convective correlation
	Pool to basemat heat transfer	Pool to basemat not modeled
Pool mass (latent) transfer		
Boiling	Instantaneous mass transfer model (assumed saturated pool conditions)	Instantaneous mass transfer model (assumed saturated pool conditions)
Evaporation/condensation	HMTA, (natural convection) for saturated interface and saturated or superheated bulk atmosphere conditions	HMTA (natural convection) for saturated interface and bulk atmosphere conditions

① Refers to the steam, air, and suspended blowdown water present in the containment.

Table A-2. Comparison of heat and mass transfer modeling methods for near stagnant atmospheres in the CONTEMPT and CONTAIN codes.

Phenomena/ effect / process	CONTAIN Heat and Mass Transfer Analogy [HMTA]:	CONTEMPT Uchida Tabulated Correlation:
Surface orientation	Vertical, horizontal (roof and floor)	No explicit orientation in method, database from vertical surface implies an implicit applicability to vertical surfaces
Film resistance	Parametric ① and simple laminar film model	No explicit accounting; database from small dimension plates implies applicability to small vertically dimensioned surfaces.
Air/steam effects	Diffusion layer model	Empirical data for stagnant air/steam atmosphere
Atmospheric-to-surface temperature dependency	Modeled (physical basis)	Not modeled
Superheated conditions	Modeled (physical basis)	Ad hoc model (no physical basis)
High mass transfer rates	Modeled (film theory)	Unclear, database lacks information on mass transfer rates investigated
Evaporation/condensation	Each modeled	Condensation only

① User selectable film thickness

Table A-3. Comparison of heat and mass transfer modeling methods for turbulent atmospheres in the CONTEMPT and CONTAIN codes.

Phenomena/ effect / process	CONTAIN Heat and Mass Transfer Analogy [HMTA]:	CONTEMPT Tagami Correlation:
Surface orientation	N/A	N/A
Film resistance	Parametric ① and simple laminar film model	No explicit accounting; database from small dimension plates implies applicability to small vertically dimensioned surfaces.
Air/steam effects	Diffusion layer model; Time dependent forced velocity or Nusselt number table specification	Empirical data for turbulent air/steam atmosphere ②
Atmospheric-to-surface temperature dependency	Modeled (physical basis)	Not modeled
Superheated conditions	Modeled (physical basis)	Ad hoc model (no physical basis)
High mass transfer rates	Modeled (film theory)	Unclear, database lacks information on mass transfer rates investigated
Evaporation/condensation	Each modeled	Condensation only

① User selectable film thickness
② Degree of turbulence not characterized

Table A-4. Modeling Comparisons between CONTAIN and CONTEMPT for Containment Safety Systems.

Modeling System	CONTAIN	CONTEMPT
Sprays:	Heat and mass transfer analogy with rate effects; single drop fall model with drag equation Time dependent spray rate and temperature specification for external source (quench spray) Heat exchanger for internal (recirculation spray)	Steady state with user input efficiency for variable atmospheric and spray water thermal equilibrium calculation Time dependent spray rate and temperature specification for external source (quench spray) Heat exchanger for internal (recirculation spray)
Fan Cooler:	Two modeling options: MARCH code fan cooler model Energy removed from atmosphere, without condensate mass removal Mechanistic model using heat and mass transfer analogy Energy (sensible and latent) and condensate mass removal from atmosphere	Energy versus saturation temperature table Energy and condensate mass removal from atmosphere Ratio of sensible to latent heat determined by user input
Sump heat exhangers:	Four types modeled (parallel, cross-flow, counter-flow, and shell) Effectiveness approach — NTU method	Four types modeled (parallel, cross-flow, counter-flow, and shell) Effectiveness approach — NTU method

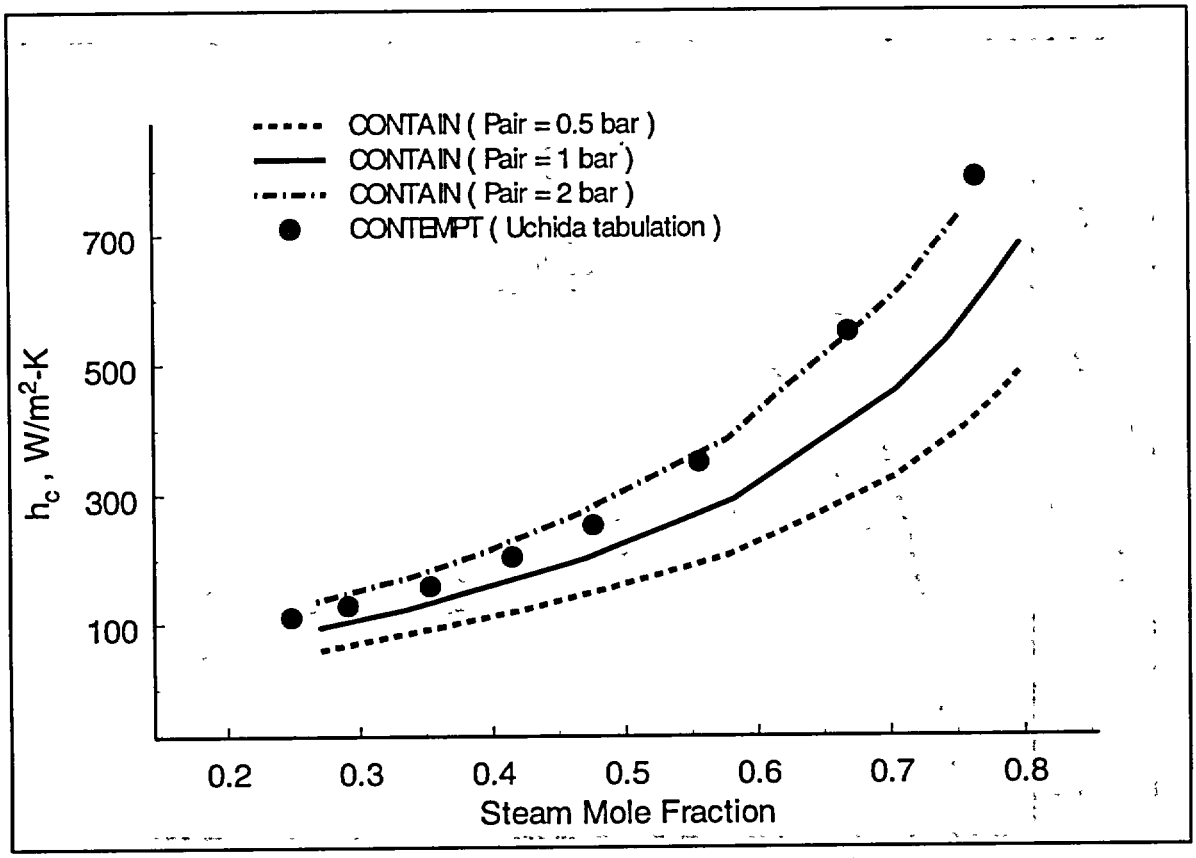

Figure A-1. Condensation heat transfer coefficient determined using the CONTAIN heat and mass transfer model for various initial air pressures and compared to the CONTEMPT Uchida tabulation. The CONTAIN calculations were made for saturated atmospheres, 30 degree temperature difference between atmosphere and condensing surface, and no paint layer or liquid film modeled for the condensing surface.

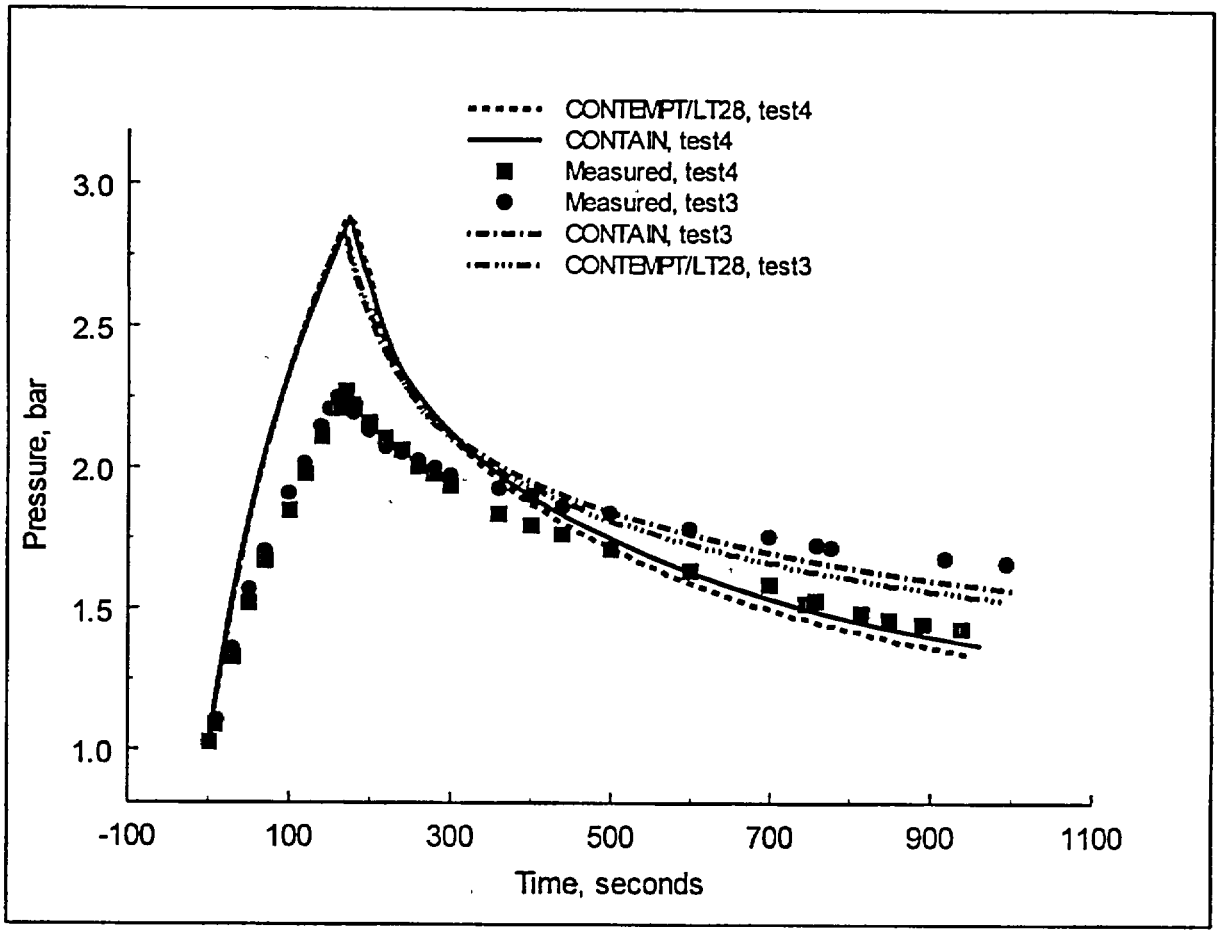

Figure A-2 Comparison of measure and calculated pressures in the CVTR facility for blowdown tests #3 and #4. Test #3 was conducted without sprays and test #4 included sprays. The CONTAIN calculations were made with natural convective heat and mass transfer modeling, and the CONTEMPT calculations were made using the CONTEMPT Uchida tabulation for condensation coefficients.

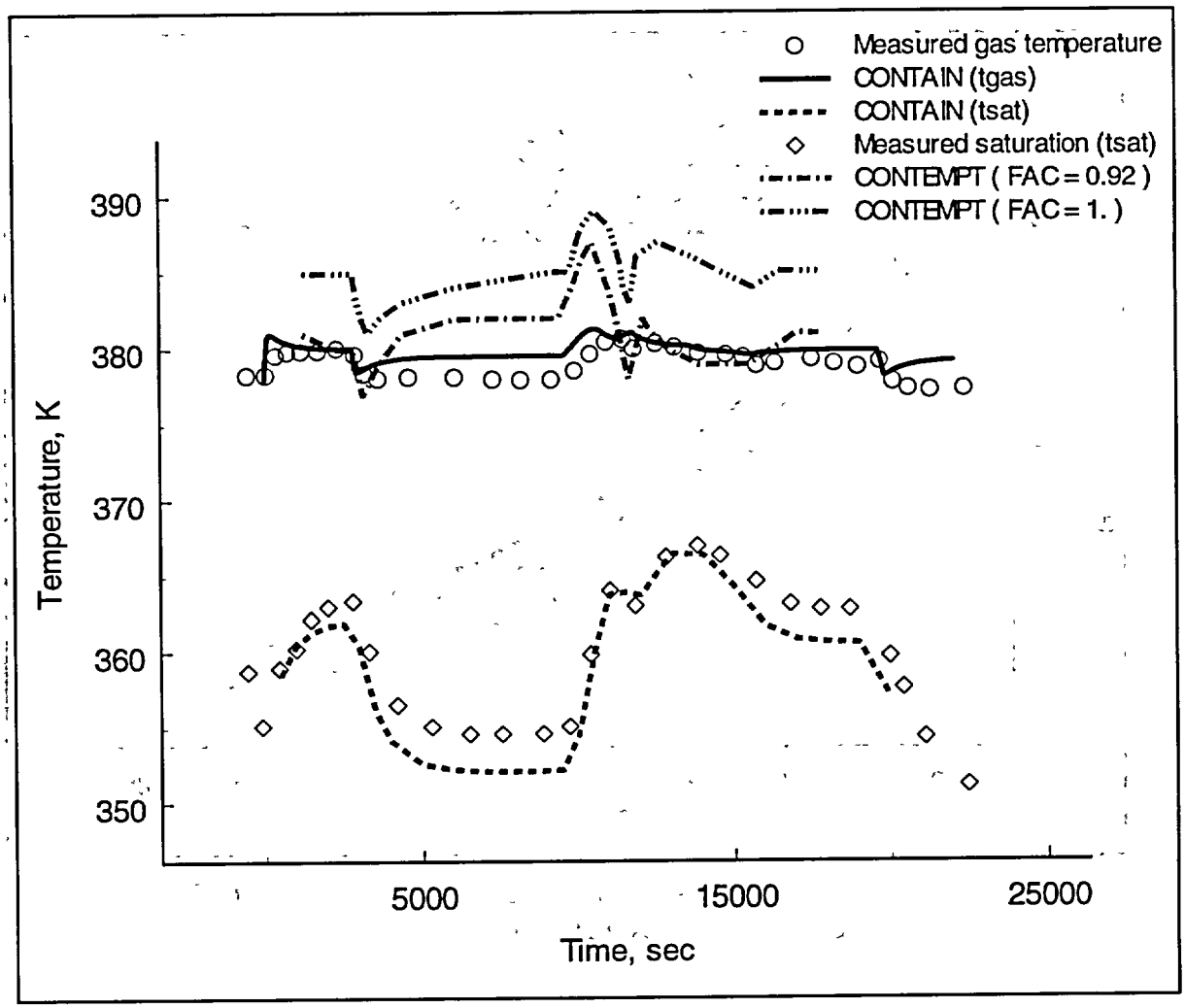

Figure A-3. Comparison of measured and calculated vessel gas temperatures for the Phebus FPT0 test [A-8]. The CONTEMPT calculations represent temperature variations resulting from inputs that change the fraction of total energy transfer that is assumed to be sensible energy transfer. Parameter FAC is often associated with a "re-vaporation percentage," where the re-vaporation percentage is (1-FAC) X 100.

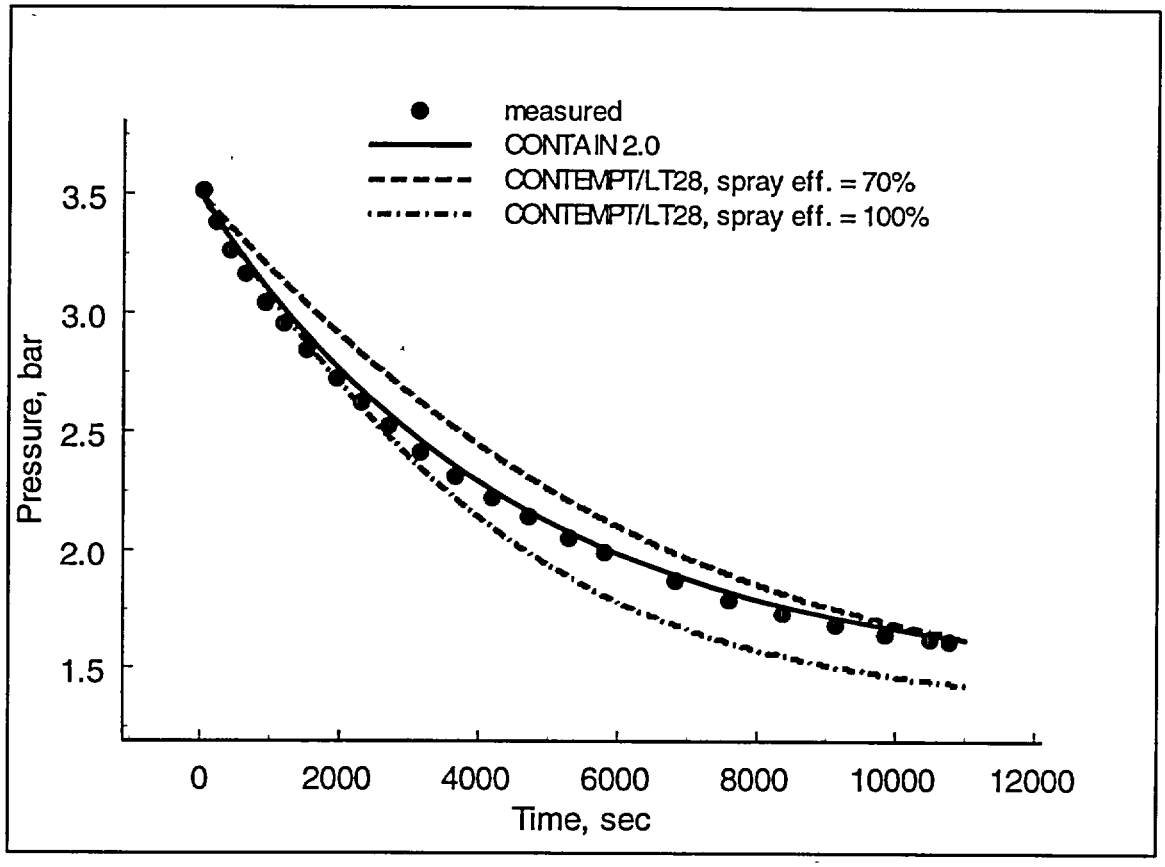

Figure A-4. Comparison of measured and calculated pressures for the JAERI spray pressure suppression test PHS-6 [A-9].

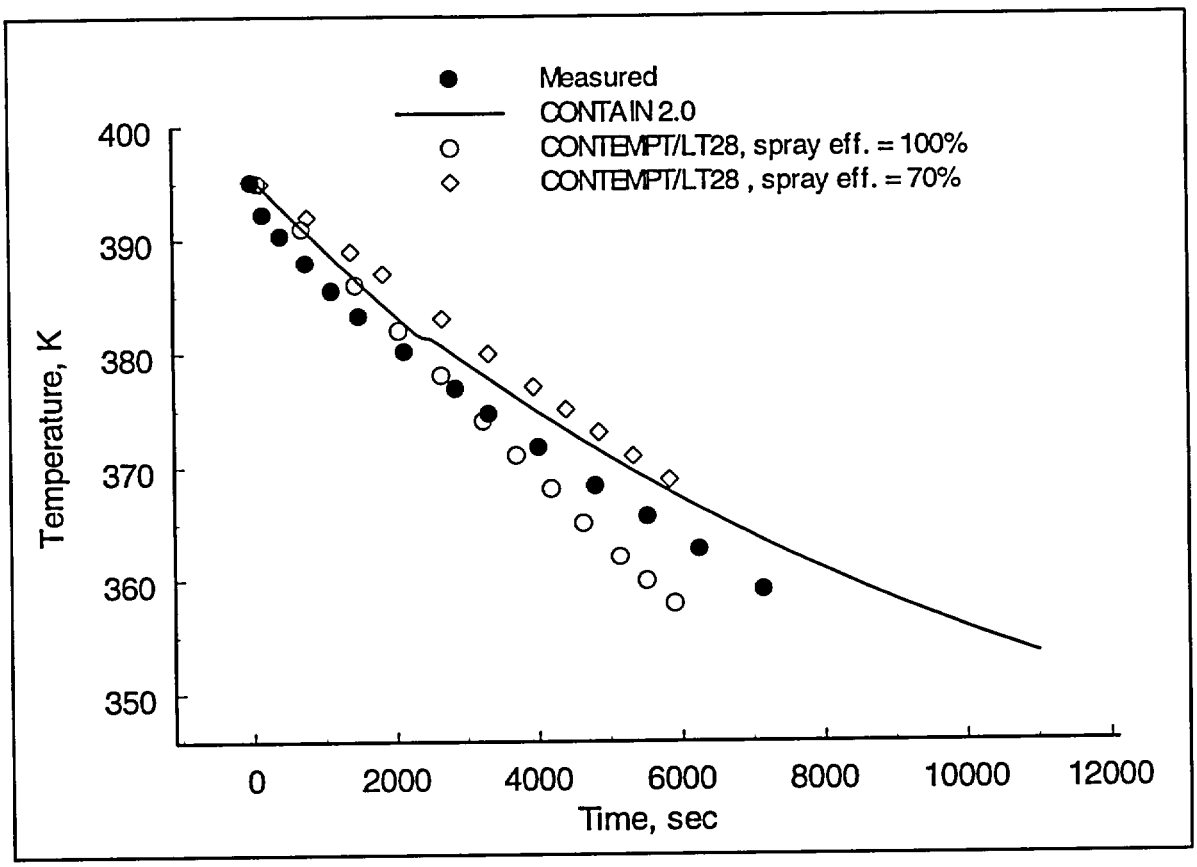

Figure A-5. Comparison of measured and calculated gas temperatures for the JAERI pressure suppression spray test PHS-6 [A-9].